Adhesion.   II. Relationships between Viscoelasticity, Interfacial Equilibrium, and the Temperature Dependence of Adhesion

J. R. HUNTSBERGER, *Fabrics and Finishes Department,*
E. I. du Pont de Nemours & Company, Inc., Wilmington, Delaware

Synopsis

The temperature dependence of adhesion is investigated by two different techniques. Data are given for several polymers.   An hypothesis is presented which appears to provide a satisfactory explanation for the observed performance, and which attributes a major role to the extent of interfacial contact (or proximity to interfacial equilibrium). Striking differences are shown in the temperature dependence of adhesion for samples of a given pair of materials which were prepared under different bonding conditions. The behavior is believed to be established by the relationships between the viscoelastic response of the adhesive, the temperature and effective strain rate of the adhesion test, and the concentration of stress at interfacial discontinuities.

Introduction

Progress in the study of adhesion has been greatly retarded because of the inability to achieve quantitative data providing correlations between adhesion and the nature of the materials involved.   The difficulty lies largely in the extreme complexity of the tests employed to appraise the adhesion.

No satisfactory nondestructive test has been devised which can measure adhesion, and all of the destructive tests involve several factors which cannot be quantitatively defined.   Probably the only absolute measure of adhesion is the energy of interaction between the adhesive and the substrate when these are at equilibrium.   There is presently no way to measure the interfacial energy between two solid materials, nor can the relative proximity to equilibrium be assessed.

In view of the difficulty in obtaining absolute values, the most attractive approach to the adhesion problem lies in determining quantitative relationships between changes in the performance with changes in temperature, strain rate, sample geometry, composition, sample preparation, etc.

In recent years, considerable progress has been made through recognition of the importance of the viscoelastic response of polymeric adhesives in establishing the performance.   Meisner and Merrill[1] observed an apparent relationship between the second order transition temperature and a maximum in the adhesion as a function of temperature.   McLaren and

Seiler[2] also observed a maximum in the adhesion versus temperature.
They noted interfacial separation at temperatures below the maximum and
cohesive failure within the polymeric adhesive at higher temperatures.
Bright[3] observed similar behavior for pressure sensitive tapes adhered to a
variety of substrates. At temperatures above the maximum, the failure
was cohesive and was coincident for all substrates. At temperatures be-
low the maximum, failure was at the interface and was different for differ-
ent substrate materials. No apparent relationship was reported between
performance and any characteristic of the substrate. Bright also noted
the shift of the temperature at which the maximum occurred when the test
rate was varied, and suggested that the viscoelastic response of the poly-
mer was involved. Kaelble[4] showed that the time–temperature super-
position principle[5] can be applied to peel adhesion data. He has reported
maxima for samples exhibiting only interfacial separation as well as for
samples showing a transition from interfacial to cohesive failure.

The objective of this paper is to provide further data which introduce new
factors into the adhesion versus temperature performance, and to present
an hypothesis which appears to provide a satisfactory explanation for the
observed behavior.

Experimental Procedures and Results

Adhesion as a function of temperature was determined for a variety of
polymer–substrate pairs using two methods. The first comprised breaking
lap joints through application of tension as indicated in Figure 1. This
method was adopted because it provided a convenient means for forming
bonds under known loads and testing *in situ* with no history of thermal
cycling. This was accomplished by using the apparatus shown diagram-
matically in Figure 2. (The sample holding device has been omitted for
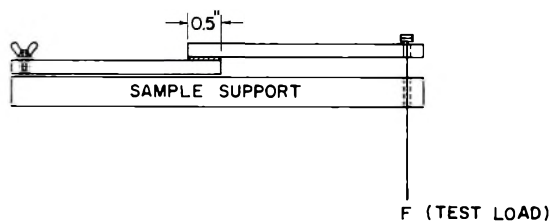clarity.)

Fig. 1. Schematic diagram of "tensile" adhesion test.

The 0.5 × 0.5 in. lap area was bonded by holding for three hours at
150°C. under a 10-lb. load applied at the end of the load line (L). After
formation of the bond, the load was removed and the temperature of the
oven lowered slowly. Samples were tested at the desired temperatures by
applying shot at a rate of 100 g./sec. to the test line. The apparatus pro-
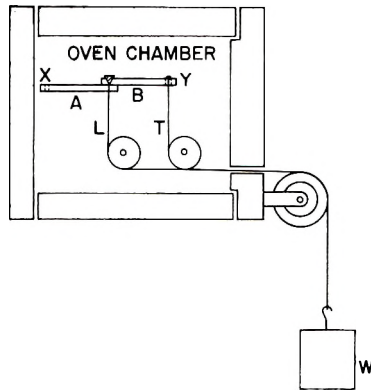vided twelve samples for each experiment.

Fig. 2. Schematic diagram of "tensile" adhesion apparatus.   (L), line for application of load for bond formation; (T), line for application of test load.
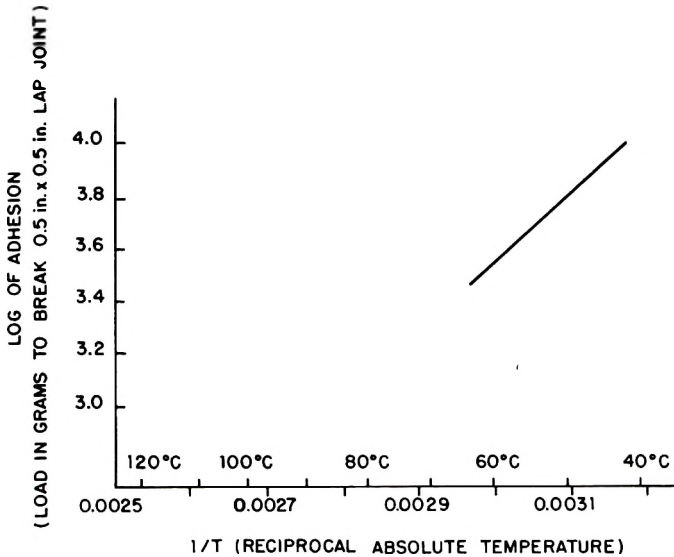

Fig. 3. Adhesion to steel vs. temperature for poly(vinyl acetate).

The samples were prepared by casting films on the clean surfaces of the $0.25 \times 0.5 \times 5$ in. bars using fixed clearance applicators and removing residual solvent by heating for one hour at 120°C. prior to use.

Using this apparatus and technique, data were obtained for steel bars bonded with poly(vinyl acetate).   These are shown in Figure 3 in which the log of the load at failure is plotted versus reciprocal absolute temperature. For convenience the temperature is also given in centigrade degrees.

Data for a low molecular weight polyethylene (Epolene C) are given in Figure 4 and those for poly(n-butyl methacrylate) in Figure 5.

Figure 6 shows the behavior for aluminum bars bonded with poly(n-butyl methacrylate).   The performance is virtually identical for the two differ-
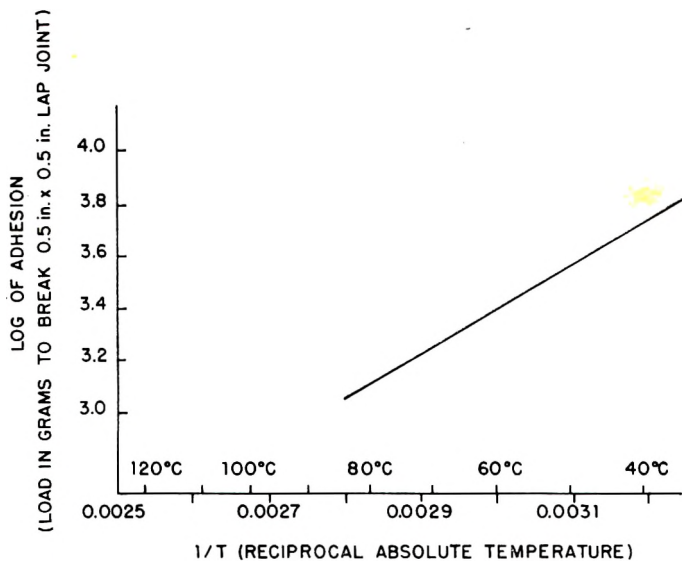
Fig. 4. Adhesion to steel vs. temperature for low molecular weight polyethylene.
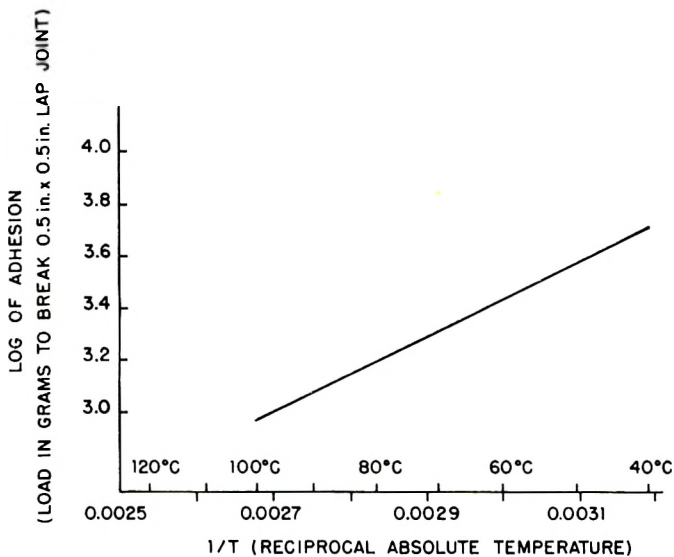
Fig. 5. Adhesion to steel vs. temperature for poly(n-butyl methacrylate).

ent substrates. The failure mechanism for these samples was cohesive separation within the polymeric adhesive layers.

Steel bars bonded with polystyrene and with poly(methyl methacrylate) (Figs. 7 and 8) have shown behavior which is reminiscent of that reported by Bright[3] for pressure-sensitive adhesives. The failure at temperatures above that at which the adhesion is maximum was cohesive. At lower
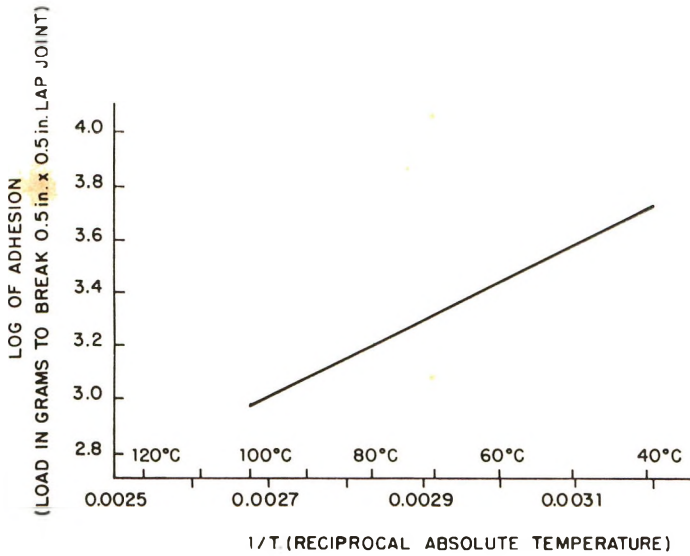
Fig. 6. Adhesion to aluminum vs. temperature for poly(n-butyl methacrylate).
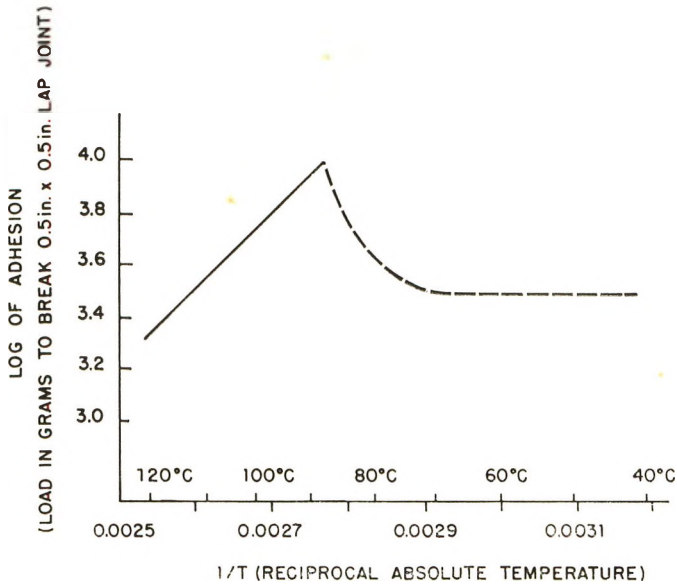
Fig. 7. Adhesion to steel vs. temperature for polystyrene.

temperatures, the separation appeared to occur at the interface. In these and in subsequent figures, a dotted line is used to indicate interfacial separation, a solid line indicates cohesive failure.

The performance of poly(methyl methacrylate) plasticized with benzyl butyl phthalate is shown in Figure 9. The shift of the position of the maximum to lower temperatures with increasing plasticizer content is that
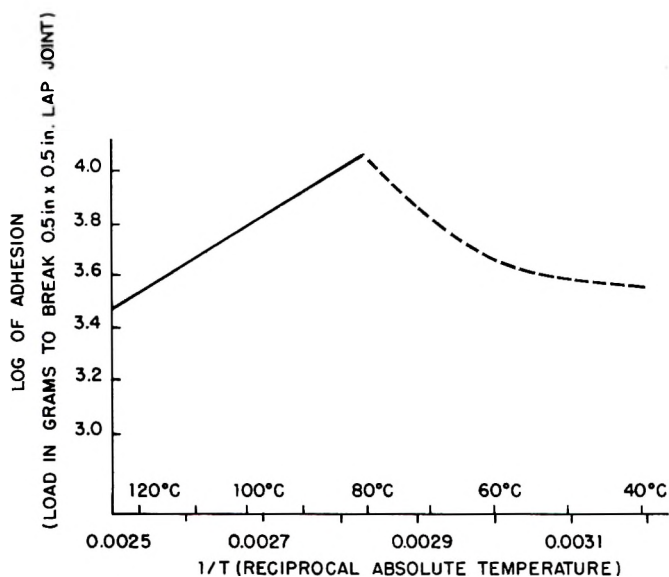
Fig. 8. Adhesion to steel vs. temperature for poly(methyl methacrylate).
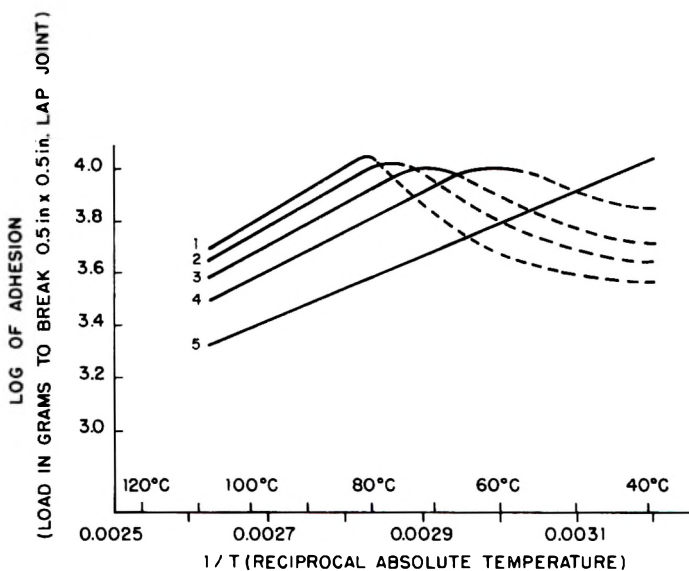
Fig. 9. Adhesion to steel vs. temperature for poly(methyl methacrylate) plasticized with benzyl butyl phthalate (BBP): (*1*), PMMA; (*2*), PMMA/BBP = 95/5; (*3*) PMMA/BBP = 90/10; (*4*), PMMA/BBP = 80/20; (*5*), PMMA/BBP = 70/30.

expected through the influence of the plasticizer on the viscoelastic response of the polymer.

Further tests of the influence of temperature on adhesion were carried out using a peel test. This was done in an effort to determine the effect of

SIDE VIEW
(SHOWING LOAD LINE ATTACHED)

TOP VIEW
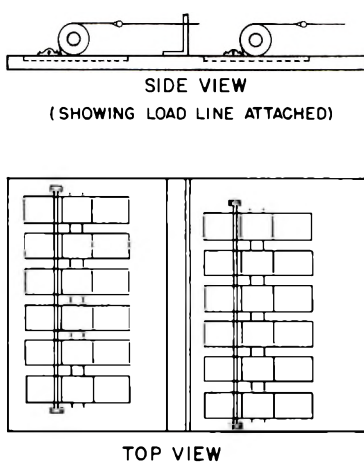
Fig. 10. Schematic diagram of peel adhesion apparatus.
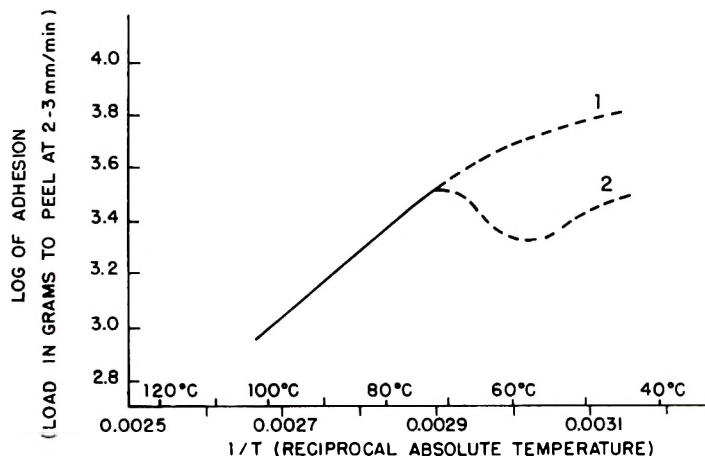
Fig. 11. Peel adhesion vs. temperature for poly(n-butyl methacrylate) adhered to steel: (1) baked 1 hr. at 150°C., (2) baked 1 hr. at 100°C.; (—) cohesive failure; (--) apparently interfacial failure.

gross changes in the physical character of the sample and in the strain rate. Peeling even at slow rates corresponds to relatively high effective strain rates in the deformed adhesive layer. The preceding test involved slow rates of strain.

The apparatus shown diagrammatically in Figure 10 was used in conjunction with the modified oven to carry out the peel tests. Substrate panels 1 in. wide slid in Teflon-lined tracks as the films were peeled slowly from their substrates. Tests were carried out by applying shot slowly to the test line until peeling proceeded at a rate of 2–3 mm./min. In order to obviate stretching and tearing of the films, two mil thick glass fabric was
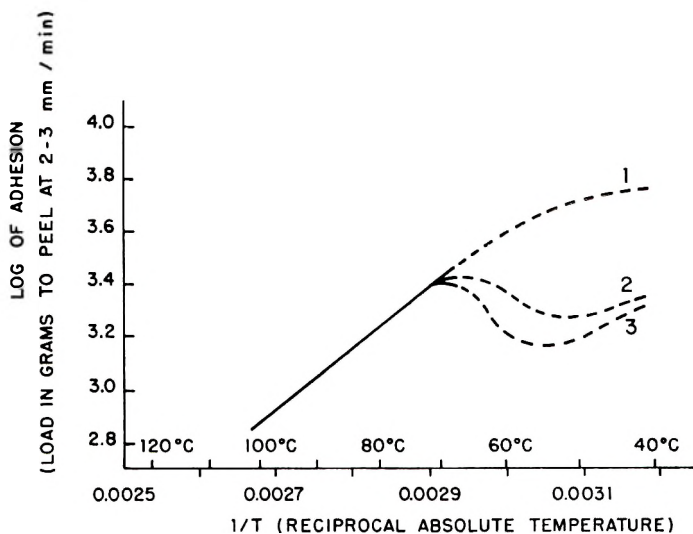
Fig. 12. Peel adhesion vs. temperature for poly(*n*-butyl methacrylate) adhered to an alkyd resin: (*1*) was baked 1 hr. at 180°C., (*2*) baked 1 hr. at 150°C., (*3*) baked 1 hr. at 120°C.; (—) cohesive force; (--) apparently interfacial failure.

embedded within the polymer by casting the films in two layers pressing the glass fabric into the second layer.

Since sample preparation as well as the mechanical aspects of the test methods had been varied, investigation of the influence of sample preparation was included in subsequent studies. The most important aspects of sample preparation are the cleaning of the substrate and the time and temperature of bond formation. The technique employed to prepare the substrates was not changed. The time and temperature of bonding were chosen for study.

The data for poly(*n*-butyl methacrylate) adhered to steel are presented in Figure 11. The log of the load required to peel the film at 2–3 mm./min. is plotted versus reciprocal absolute temperature. These data show a very striking and enlightening influence of sample preparation on the performance. At temperatures above ∼72°C. the samples behaved identically, and failure was cohesive. The sample held for 1 hr. at 100°C. exhibited a maximum at 72°C. At lower temperatures, the failure occurred at the interface. The adhesion of the sample prepared by holding for 1 hr. at 150°C. continued to increase with diminishing temperature below 72°C., but at a slower rate than at higher temperatures where failure was cohesive.

The performance has thus far been observed only for relatively high energy substrates. In order to appraise the effect of changing to a low energy substrate, a set of experiments was carried out using poly(*n*-butyl methacrylate) adhered to a crosslinked alkyd resin. A 52% soya oil resin, exhibiting an acid number of 6, was coated on a steel panel and was cured by baking for 0.5 hr. at 200°C. Poly(*n*-butyl methacrylate) films were

cast on the alkyd surface. Three sets of samples were prepared using bonding temperatures of 120°C., 150°C., and 180°C. The data are given in Figure 12. The performance is very similar to that exhibited with steel substrates, the most interesting difference being that higher temperatures were required to reach equivalent performance in the same time with the low energy substrate. The slightly lower adhesion values may result from a small change in the relative position of the glass fabric in these samples, and this is probably not significant.

Discussion

The experimental behavior appears to be satisfactorily explainable. The two major factors influencing the performance are the viscoelastic response of the polymer and the extent of interfacial contact. Taylor and Rutzler[6] have proposed that the maximum possible number of molecular contacts between an adhesive and its substrate may be greatly restricted by virtue of the steric aspects of molecular geometry. This has also been discussed by the present author[7] as an important consideration in establishing the locus of adhesive failure. Very frequently in practice, however, the maximum or equilibrium interfacial contact is not achieved under the conditions and procedures employed in formation of the adhesive bond. Under these circumstances, there exist discontinuities in the interface of such magnitude that relatively high local stresses are met at these "microedges" when the polymer is strained at a rate sufficiently fast that relaxation cannot occur.

For example, examine the curves of Figure 11. The sample held for 1 hr. at 100°C. had not achieved interfacial equilibrium. At temperatures above 72°C., the relaxation rate was faster than the effective strain rate of the test, and cohesive failure occurred. When the temperature fell below 72°C., however, the relaxation rate was slower than the test rate, consequently stress concentration occurred at the edges of the interfacial discontinuities as well as at the physical edges of the sample. As the temperature was lowered further, the relaxation rates became slower, and the modulus increased leading to higher stress concentration and to lower "adhesion" values. Failure occurs when these concentrated stresses exceed either the cohesive strength of the material or the interfacial bond strength depending upon the locus of failure.

At temperatures below about 58°C., the stress concentration did not increase appreciably, but the bond strength continued to increase, and the measured adhesion increased again. The sample held for 1 hr. at 150°C. had attained or at least closely approached interfacial equilibrium, and consequently at temperatures below 72°C., the stress concentration occurred only at the sample edges and had a much smaller effect on the performance. However, the stress was maximum at or near the interface; therefore, the locus of failure shifted to or very close to the interface.

Looking again at Figure 9, the smaller lowering of adhesion at temperatures below the maxima for the plasticized samples may be interpreted as

being due to closer approach to equilibrium with increasing plasticizer content, since all of the samples were prepared using the same time and temperature for bond formation.

Conclusions

Experimentally determined adhesion values are markedly dependent upon the viscoelastic response of the adhesive and the effective strain rate and temperature of the test employed. The extent of interfacial contact is a major factor in establishing the performance. If correlations between adhesion and composition are sought, it is mandatory that interfacial equilibrium be achieved.

References

1. Meisner, H. P., and E. W. Merrill, *ASTM Bull.*, No. 151, 80 (1948).
2. McLaren, A. D., and C. J. Seiler, *J. Polymer Sci.*, **4**, 63 (1949).
3. Bright, W. M., *Adhesion and Adhesives*, J. Clark, J. E. Rutzler, Jr., and R. L. Savage, Eds., Wiley, New York, 1954, p. 130.
4. Kaelble, D. H., Paper No. 5, Division of Paint, Plastics and Printing Ink Chemistry, Cleveland Meeting American Chemical Society, April 1960.
5. Tobolsky, A. V., *Properties and Structure of Polymers*, Wiley, New York, 1960.
6. Taylor, D., Jr., and J. E. Rutzler, Jr., *Ind. Eng. Chem.*, **50**, 928 (1958).
7. Huntsberger, J. R., *J. Polymer Sci.*, **A1**, 1339 (1963).

Résumé

On a étudié l'influence de la température sur l'adhésion en utilisant deux techniques différentes. On donne les résultats pour différents polymères. On propose une hypothèse qui semble fournir une explication satisfaisante et attribue un rôle prépondérant au degré de contact interfacial (ou voisin de l'équilibre interfacial). De nettes différences sont mises en évidence sur la dépendance, en fonction de la température, de l'adhésion pour des échantillons d'une paire définie de matériaux qui ont été préparés dans différentes conditions de liaisons. Le comportement est supposé être établi par les relations entre la réponse viscoélastique de l'adhésif, la température et la vitesse de tension effective du test d'adhésion, et la concentration des tensions aux discontinuités interfaciales.

Zusammenfassung

Die Temperaturabhängigkeit der Adhäsion wird nach zwei verschiedenen Verfahren untersucht. Ergebnisse für mehrere Polymere werden angeführt. Eine Hypothese wird aufgestellt, die eine befriedigende Erklärung für das beobachtete Verhalten zu liefern scheint und die dem Ausmass des Grenzflächenkontakts (oder der Nähe zum Grenzflächengleichgewicht) eine ausschlaggebende Rolle zuschreibt. Auffallende Unterschiede treten in der Temperaturabhängigkeit der Adhäsion bei Proben eines gegebenen Stoffpaares auf, wenn diese unter verschiedenen Bindungsbedingungen hergestellt wurden. Für das Verhalten werden als massgebend die Beziehungen zwischen den viskoelastischen Eigenschaften des Klebstoffes, der Temperatur und der effektiven Verformungsgeschwindigkeit beim Adhäsionstest, sowie die Spannungskonzentration an Grenzflächendiskontinuitäten angenommen.

Electron Spin Resonance of Polypropylene

B. R. LOY, *Physical Research Laboratory, The Dow Chemical Company, Midland, Michigan*

Synopsis

Radicals produced in Co^{60} irradiated normal and $1,1d_2$-polypropylene have been examined by electron spin resonance. It is concluded that 80% of the radicals are $-CH_2-CH(CH_2.)-$ and 20% are $-CH_2-C(CH_3)-CH_2$ in both atactic and isotactic polymer. In the isotactic, but not in the atactic material, the primary radical disappears much faster than the secondary one when heated. Interpretation of the spectra of polybutylene and polyisobutylene is also given.

Introduction

The identification of radicals produced in polypropylene by ionizing radiation and the nature of their possible rearrangement has been the subject of investigation in this laboratory at different intervals during the past two years. In short, the problem has revolved around the fact that the spectrum of irradiated polypropylene, principally a four-line spectrum when initially observed at 77°K., changes after heat treatment to a nine-line spectrum. Attempts were made to correlate these observations with scission mechanisms proposed for irradiated polymers of the type $-(CX-CH_2)-$. The results will be reported in the order of occurrence.
$$\overset{|}{CH_3}$$
Some of the data did not answer questions regarding polypropylene but will be recorded here since it is relative to polymers of this type.

Experimental

Almost all of the samples were prepared as previously described[1] receiving 8 Mrad. of Co^{60} radiation at 77°K. Recently the spectrometer was modified to use a 50-kc. modulation system which made it difficult to use the low temperature cavity, previously described.[1] A cavity, using a Dewar insert, is now in use. The sample tubes are made from Suprasil,* which is a very highly purified form of silica. Relatively few unpaired electrons are produced by ionizing radiation in this material.

Results and Discussions

The primary spectrum of gamma-irradiated isotactic polypropylene as shown in Figure 1a is seen to consist principally of four lines. Assuming

---

* Registered trademark of the Englehard Industries.

(a)

(b)

(c)

(d)

Fig. 1. Isotactic polypropylene: (b) heat treated 15 min. at 78°C., (c) heat treated 15 min. at 41°C.

that this is the result of equal interaction with three protons, three possible radical structures are

$$-CH_2-CH-CH_2-, \quad -CH-\overset{\cdot}{C}H-CH-, \quad \text{and} \quad \overset{\overset{\displaystyle CH_2}{\displaystyle \|}}{-CH-CH_2\cdot}$$
$$\underset{\displaystyle CH_2\cdot}{|} \qquad\qquad \underset{\displaystyle CH_3}{|} \quad \underset{\displaystyle CH_3}{|}$$
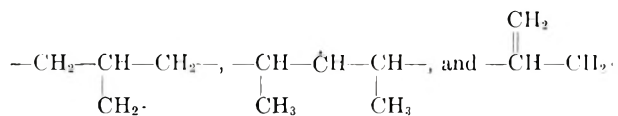
The first two possibilities result from the loss of a hydrogen atom, either in the primary event or abstraction by free H atoms produced in the primary event. The third is the scission product from the reaction suggested by Wall,[2]

$$\underset{\displaystyle -CH-CH_2-CH-}{\overset{\displaystyle CH_3 \quad\quad CH_2\cdot \quad\quad CH_3}{|\qquad\quad |\qquad\quad |}} = \underset{\displaystyle -CH-CH_2\cdot}{\overset{\displaystyle CH_3}{|}} + \overset{\overset{\displaystyle CH_2}{\displaystyle \|}}{CH-}$$
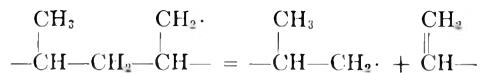
The secondary spectrum after 15 min. heat treatment at 41°C. as shown in Figure 1c consists of nine lines. Jones[3] suggested that these could be the result of equal interaction of the unpaired electron with the protons of the

$$CH_3-\overset{\displaystyle |}{\underset{\displaystyle CH_3}{C}}-CH_2-$$
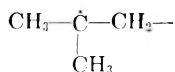
radical. This radical presumably results from the rearrangement of the

$$\underset{\displaystyle -CH-CH_2\cdot}{\overset{\displaystyle CH_3}{|}}$$
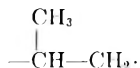
radical considered above.

Opposed to the above interpretation is the treatment given by Buch[4] in his doctorial dissertation. Briefly, the primary spectrum is considered to be a combination of all possible radical species that can be obtained by the removal of hydrogen atoms. The origin of the nine-line spectrum is unexplained but it is thought to be

$$-CH_2-\overset{\displaystyle |}{\underset{\displaystyle CH_3}{C}}-CH_2-$$
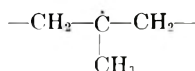
radical. The nine-line spectrum is explained by assuming that the methyl group is not freely rotating at 77°K. but frozen in such a position that two of its hydrogens are equivalent to the methylene hydrogens and the interaction with the third hydrogen is twice as great. The plausibility of this argument is shown by a rigorous mathematical treatment of the problem. Buch also states that the secondary spectrum is present only in the isotactic material.

The remainder of this paper is devoted to resolving the conflicts of the above interpretation with those of this laboratory.

Figure 1b is the −195°C. spectrum of the same material as Figure 1a after 15 min. of heat treatment at −78°C. An increase in resolution is noted at the high and low field portions of the spectrum along with a decrease in the center. The decrease in resolution is obviously due to the fact that the nine- and four-line spectrum, having nearly equal hyperfine splitting are 180° out of phase with each other. Figure 1d is the theoretical spectrum of nine Gaussian lines with a binomial distribution of intensities and a ratio of hyperfine separation linewidth of 1.4. This is not a good fit; however, it has been pointed out that a small amount of residual four-line spectrum will distort the center.

Figure 2 shows spectra of irradiated atactic polypropylene before and after heat treatment for varying times at −28°C. This verifies Buch's observations; however, it is noted that resolution decreases in the center and increases in the outer portions as the heat treatment is increased. This fact is pointed out here because of observations later noted in the deuterated material.
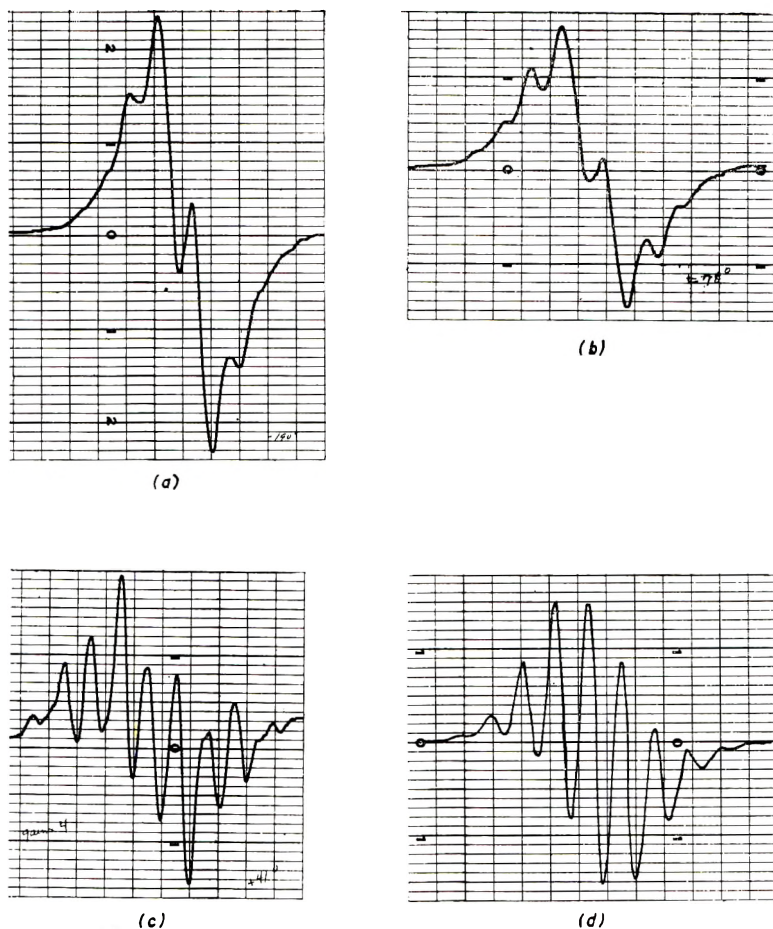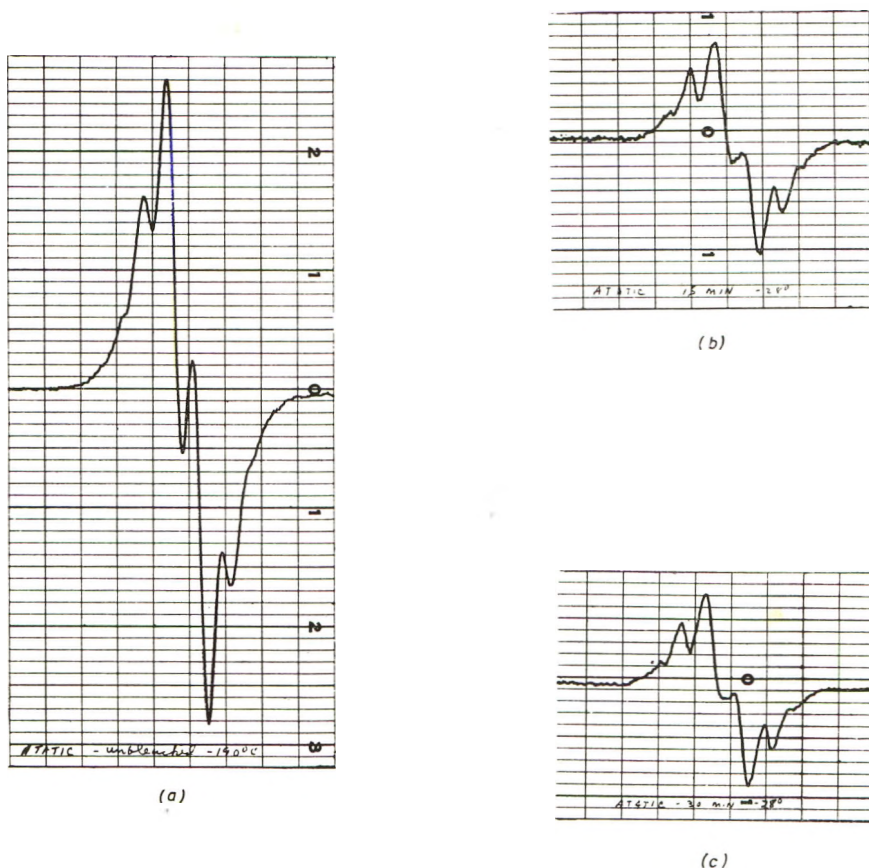
Fig. 2. Atactic polypropylene: (b) heat treated 15 min. at 28°C., (c) heat treated 30 min. at 28°C.

Several experiments were suggested by Jones in an effort to solve the problem. One was to prepare the radical

$$
\begin{array}{c}
CH_3 \\
| \\
-CH_2-C-CH_2-
\end{array}
$$
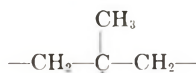
by irradiating a mixture of polypropylene and some photosensitive materials with ultraviolet light. Other suggestions were to irradiate polybutylene (from butene-1) and polyisobutylene with Co^{60} to see if the analogous scission radicals could be detected:

$$
\begin{array}{c}
-CH-CH_2 \cdot \ \text{and} \ -C(CH_3)_2-CH_2 \cdot \\
| \\
CH_2-CH_3
\end{array}
$$
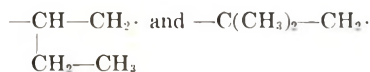
With the former we might expect to see an eight-line secondary spectrum, but in the latter there should be no change.

The first approach failed because proper experimental conditions were
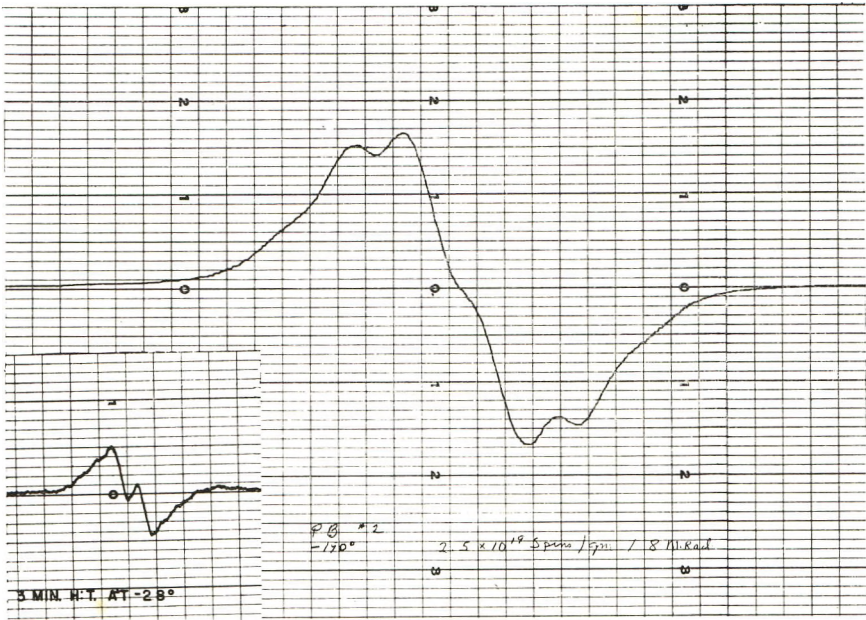
Fig. 3. Polybutylene.

−190°

−150°

−107°

−82°

−55°

−190° AFTER H.T.
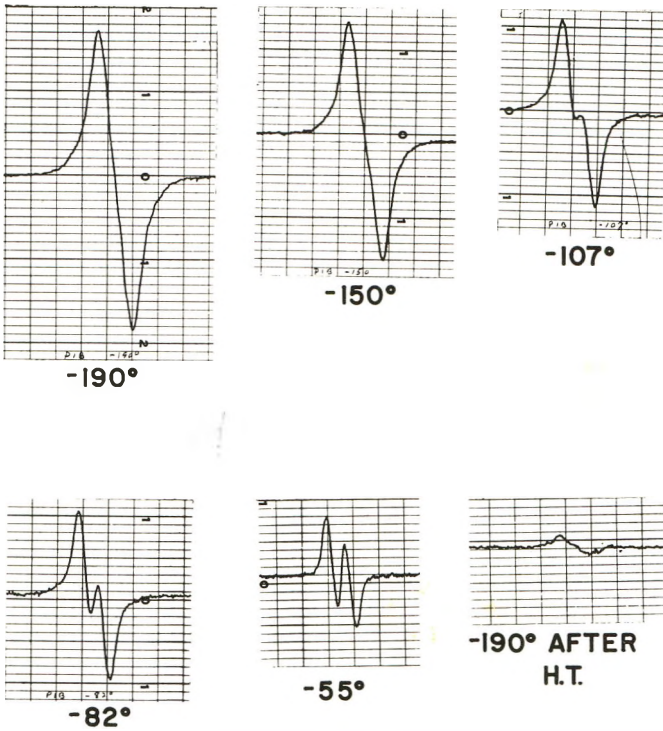
Fig. 4. Polyisobutylene.

not found where the reaction would proceed with the matrix still stable enough to trap the polymer radical.

Figure 3 is the spectrum of Co^{60} irradiated (from butene-1) polybutylene which was recorded at $-190°C$. The resolution is poor but there appear to be six lines, with a splitting constant of about 21 gauss indicating the

$$-CH-CH_2-$$
$$\cdot CH-CH_3$$
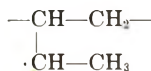
radical. After 3 min. of heat treatment at $-28°C$, only the doublet shown in the insert remains.

Figure 4 shows a series of spectra of Co^{60} irradiated polyisobutylene

(a)

(b)

(c)

(d)
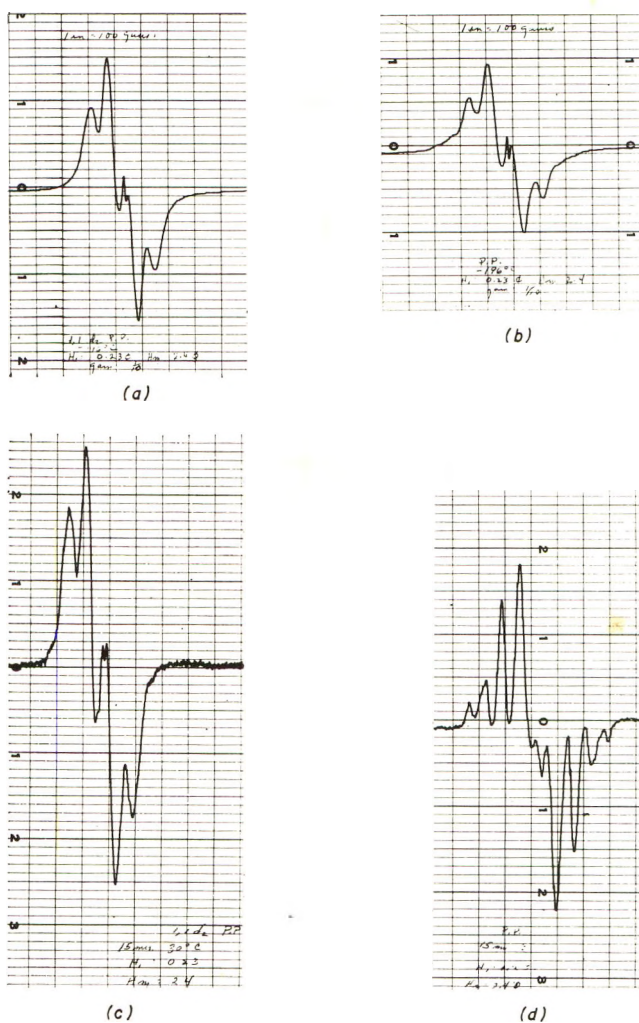
Fig. 5. Polypropylene: (c) deuterated, heat treated 15 min. at 30°C.; (d) regular, heat treated 15 min. at 30°C.

(Vistanex 200C) recorded at $-190°$C. and increasing temperatures. This is a doublet, indicating that for practical purposes the $—C(CH_3)_2—\dot{C}H—C(CH_3)_2—$ radical is the only one trapped. The broad line at $-190°$C. indicates that the methyl groups have ceased to rotate fast enough to average out some of the anisotropic splitting, which in an amorphous polymer serves to broaden the line. These results do not appear to support either interpretation; however, they do show that one is not justified in assuming that all possible radicals will be stabilized at liquid nitrogen temperature in quantities proportional to the number of hydrogen atoms at each position. Consider, for example, the 6/1 ratio of methyl to tertiary hydrogens in polyisobutylene.

The next approach, suggested by Szwarc,[5] was to use deuterated polypropylene. Deuterium has a magnetic moment about one-third that of hydrogen and a spin of one. The hyperfine splitting, therefore, is expected to be one-sixth of the hydrogen splitting constant. Linewidths in irradiated polymers are of the order of 11–15 gauss. Hyperfine splittings for hydrogen are usually 20–25 gauss. When the ratio of the hyperfine separation to the linewidth is 0.9 or less, the hyperfine splitting will not be resolved. Therefore one does not expect to see any splitting from the deuterium atom in deuterated polypropylene.

Raich of the Dow Styrene Polymerization Laboratory polymerized $CD_2{=}CH—CH_3$ by using a method which had in the past produced high molecular weight isotactic polypropylene. Regular propylene was prepared in the same apparatus so that the two could be irradiated and compared simultaneously.

Figure 5 shows the spectra of both compounds before and after heat treatment at 30°C. for 15 min. The amplifier gain has been changed by a factor of 10 to compensate for the 80% loss in radicals. The fact that principal portion of the spectrum is still a quartet identifies the principal radical in the primary spectrum as

$$CH_2\cdot$$
$$|$$
$$—CD_2—CH—$$
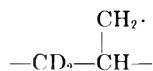
since the other possibilities were

$$CH_3 \qquad CH_3$$
$$| $$
$$—CH—\dot{C}D—CH—$$
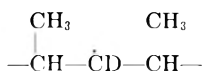
which would be a triplet, and

$$CH_3$$
$$|$$
$$—CH—CD_2\cdot$$
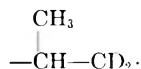
which would be a doublet.

A comparison of the secondary spectra reveals that the methylene hydrogens and the methyl hydrogens contribute to the hyperfine splitting.

REGULAR   DEUTERATED
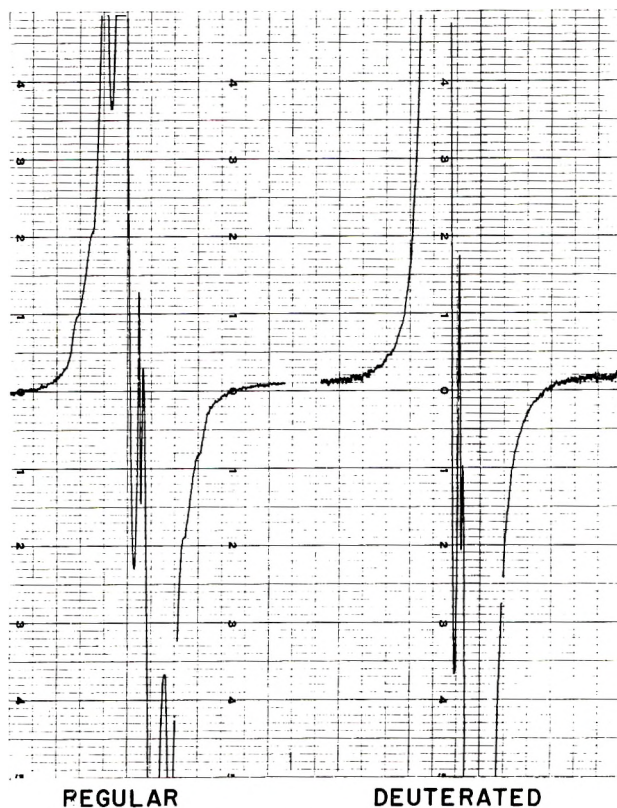
Fig. 6. Polypropylene.

This almost certainly places the unpaired electron on the tertiary carbon. The four-line spectrum of Figure 5c representing the

$$-CD_2-\overset{.}{C}-CD_2-$$
$$\underset{CH_3}{|}$$
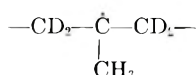
radical, tells us that the methyl group is freely rotating. This is perhaps more in harmony with the quality of resolution shown in Figure 5d. Compare with Figure 4 where the anisotropic splitting has broadened the line so that the hyperfine separation is not resolved.

Figure 6 shows enlarged primary spectra of both compounds. The extra lines that appear in the high and low field extremities of the regular polypropylene spectrum and not in the other correspond to the outer lines of the nine-line spectrum. While it is difficult to subtract the one spectrum from the other, one can say that, within a factor of two, the nine-line spectrum has resisted the heat treatment at 30°C. If the primary spectrum of the atactic polymer in Figure 2a is re-evaluated in the light of this development, one recognizes the probability that there is also 20% of the nine-line spectrum there. The difference in stability between the atactic and isotactic material is probably coincident with the rigidity of the

substrate. It was attempted to verify this by irradiating some high molecular weight atactic polypropylene, but the spectrum was not sufficiently resolved to make any identification.

Although the secondary radical has been identified by deuterium substitution, the splitting pattern remains a subject for speculation. Perhaps one should use an approach such as employed by Buch in which three methyl and three methylene hydrogens are equivalent, the odd one having twice the overlap. The difficulty still remains of reconciling the motional narrowing of the dipolar term with the hindered rotation assumption required for nonequivalence.

The fact that the primary radical is stable as

$$
\begin{array}{c}
CH_2\cdot \\
| \\
-CH-
\end{array}
$$

casts considerable doubt on the proposed scission mechanism

$$
\begin{array}{ccc}
CH_2\cdot & & CH_2 \\
| & & \| \\
-CH-CH_2- & = & -CH + \cdot CH_2-{}^2
\end{array}
$$

since this reaction requires only a rearrangement of electrons.

References

1. Loy, B. R., *J. Phys. Chem.*, **65** (1961).

2. Wall, L. A., *J. Polymer Sci.*, **17,** 141 (1955).

3. Jones, G. D., private communication.

4. Buch, T., Ph.D. thesis, Northwestern Univ. 1960, Univ. Microfilms, MIC 60–4761, Ann Arbor, Mich.

5. Szwarc, M., private communication.

Résumé

On a étudié par résonance de spin électronique les radicaux produits par irradiation au Co-60 de polypropylène normal et 1,1d_2-. On conclut que 80% des radicaux sont —CH$_2$—CH(CH$_2\cdot$)— et 20% sont —CH$_2$—$\dot{C}$(CH$_3$)—CH$_2$ dans les deux polymères atactique et isotactique. Dans l'échantillon isotactique, mais non dans l'atactique soumis au chauffage, le radical primaire disparait beaucoup plus vite que le secondaire. On donne l'interprétation du spectre du polybutène et du polyisobutène.

Zusammenfassung

In Co-60-bestrahltem, normalen und 1,1 d_2-Polypropylen erzeugte Radikale wurden mittels Elektronspinresonanz untersucht. Es ergibt sich der Schluss, dass im ataktischen und isotaktischen Polymeren 80% der Radikale —CH$_2$—CH(CH$_2\cdot$)— und 20% —CH$_2$—$\dot{C}$(CH$_3$)—CH$_2$—Radikale sind. Im isotaktischen Polymeren, aber nicht im ataktischen, verschwindet das primäre Radikal beim Erhitzen viel rascher als das sekundäre. Eine Interpretation der Spektren von Polybutylen und Polyisobutylen wird ebenfalls gegeben.

The Mastication of Elastomers.   Part III.   The Solution Properties of Masticated Synthetic *cis*-Polyisoprene

G. M. BRISTOW, *The Natural Rubber Producers' Research Association, Welwyn Garden City, Herts., England*

Synopsis

Data are reported on the light scattering, osmotic, and viscometric properties of solutions of masticated synthetic *cis*-polyisoprene.   Mastication produces a sharpening of the molecular weight distribution and this is consistent with the hypothesis that degradation proceeds by a nonrandom process.

Much work has been published recently on the mastication behavior of high polymers, in particular of natural and synthetic rubbers.   Most of this has been concerned with the mechanism of the breakdown process[1] and the chemical consequences, both in the absence of other materials, and in the presence of various reactive species such as oxygen,[2] carbon black,[3] and polymerizable monomers.[4]   Little detailed work has been reported on the solution properties of masticated rubbers.   Mastication is believed to be a nonrandom degradation process, in that scission does not occur at random along the chains, but only in those molecules greater than a certain critical chain length.   Angier et al.[5] have adduced evidence for this both from the variation of the rate of degradation with time and from the form of the viscosity-molecular weight relation for masticated natural rubber.

The preferential rupture of large molecules is also indicated in a theoretical treatment of mastication developed by Bueche.[6]   Data are reported here for the light scattering, osmotic, and viscometric properties of masticated polyisoprene rubber.   Synthetic *cis*-polyisoprene was chosen since this elastomer, like natural rubber but unlike many synthetic rubbers, shows well-defined breakdown behavior and further, light scattering behavior which is not complicated by the presence of a microgel component as is that of its natural counterpart.[7]   These solution measurements are interpreted in terms of a nonrandom degradation process.

Experimental

Materials

Polyisoprene (*ca.* 93% *cis*-1,4-isomer) was obtained from the Shell Development Co.   After sheeting on a warm mill, the material was ex-

tracted with hot acetone for 24 hr. This process reduced, but did not completely remove, the pale pink coloration which is presumably due to the presence of antioxidants.* The extracted material still contained 0.02% nitrogen, 0.04% phosphorus, and 0.4% ash. After drying *in vacuo* at 40°C. the rubber was stored in the dark at $-20°C$. Under these conditions no degradation, as indicated by a decrease in solution viscosity, was observed over a period of several months.

Solvents were either of A.R. grade or redistilled laboratory grade. Solvent mixtures were made up by volume.

Mastication

The masticator and its operation have been described previously.[2,9] All mastications were carried out in a stream of oxygen and with the masticator head cooled with cold water.

Light Scattering

After clarification of the solutions by filtration through a range of sintered glass filters (grades 2–5) light-scattering measurements were made using a Brice Phoenix series 1000 photometer employing light of wavelength 4358 A. Measurements at ambient temperature, 20–21°C., were carried out at angles of observation (θ) in 10° intervals over the range of 30 to 100° and at a range of concentrations from 3 to 5×10^{-3} g./ml. down to *ca.* 0.5×10^{-3} g./ml. Tetrahydrofuran (peroxide free) was used as a "good" solvent and 60:40 di-*n*-butyl ether:*n*-butanol as a theta solvent. At this temperature (20–21°C.) the latter mixture gave solutions having $A_2 = 0$, and since the refractive indices of the solvents are almost identical, no complications in light scattering behavior were produced by the selective absorption of one component by the dissolved polymer.[10] Values for the refractive index increments were interpolated from the data of Altgelt and Schulz.[11]

In accordance with the Flory "dilute solution theory"[12] as modified by Stockmayer and Casassa,[13] values of A_2 and $\langle M \rangle_w$ were determined from the slopes and intercepts of linear plots of $(c/\tau)_{\theta=0}^{1/2}$ versus c, where τ is the turbidity and c the concentration in grams per milliliter, correction to $\theta = 0$ being made by the Zimm diagram method. Similarly, from the slopes of linear plots of $(c/\tau)_{c=0}$ versus $\sin^2 \theta/2$, values of $\langle S^2 \rangle_z$, the mean square radius of gyration, were deduced. In a theta solvent, where the chains are unextended by polymer-solvent interaction this latter quantity will be denoted by $\langle S_0^2 \rangle_z$. Measurements in the two solvents confirmed the identity $\langle M \rangle_w = \langle M_0 \rangle_w$.

Osmometry

The osmometers were of the Zimm-Myerson type fitted with Ultracella *feinst* membranes. Measurements were made in toluene at 25°C. at four

---

* Prolonged extraction almost completely removes the coloration. Similar difficulties in removal of antioxidants have been reported by Morton et al.[8]

or five concentrations in the range 0.1 to 1.5% and values of $\langle M \rangle_n$ and A_2 deduced from linear plots of $(\pi/c)^{1/2}$ versus c.[14]

Viscometry

Measurements were made in Ubbelohde viscometers at 25°C. and values of $[\eta]$ or $[\eta]_0$ (theta solvent) obtained by extrapolation using the Huggins equation. For the theta solvent the error involved in the use of 25°C. rather than the theta temperature (20-21°C.) was very slight and this temperature differential served as a safeguard against polymer precipitation in the viscometer. Some measurements were also made in a second theta solvent, 68:32 toluene:n-propanol; no significant differences were noted between values of $[\eta]_0$ in the two solvent mixtures.

Results and Discussion

Table I records the observed data for a range of masticated samples. For convenience, the viscosities in toluene have been taken as the primary data and smoothed plots of the other parameters drawn (Figs. 1–5). Data for given values of $[\eta]$ derived from these smoothed plots are given in Table II. Where appropriate, linear relations have been derived by the method of least squares. The linear relation between $\langle M \rangle_n$ and $[\eta]_{\phi CH_3}$ (Fig. 1)

$$[\eta] = 9.00 \times 10^{-6} \, (\langle M \rangle_n)^{1.026}$$

differs somewhat from that published by Mullins and Watson[15] for masticated natural rubber. They derive

$$[\eta] = 2.29 \times 10^{-7} \, (\langle M \rangle_n)^{1.33}$$
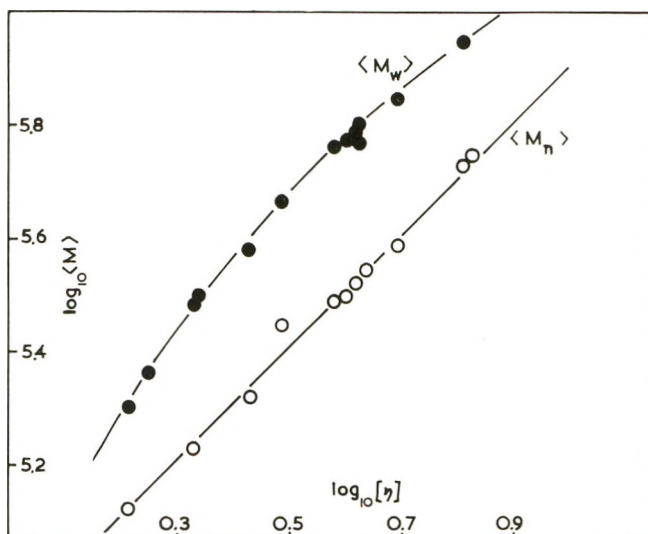
Fig. 1. Relations between the viscosity in toluene and the weight and number average molecular weights.

TABLE I

Solution Properties of Masticated Rubbers

Light scattering				Osmometry		Viscometry			
	Tetrahydrofuran		Theta A.ᵃ		Toluene	Toluene		Theta Aᵃ	Theta Bᵇ
$\langle M\rangle_\omega$ $\times 10^{-6}$	$A_2 \times 10^4$, ml. mole g.$^{-2}$	$\langle S^2\rangle_z$, cm.$^2 \times 10^{11}$	$\langle S_0^2\rangle_z$, cm.$^2 \times 10^{11}$	$\langle M\rangle_n$ $\times 10^{-5}$	$A_2 \times 10^4$, ml. mole g.$^{-2}$	$[\eta]$, dl. g.$^{-1}$	k', g. dl.$^{-1}$	$[\eta]_0$, dl. g.$^{-1}$	$[\eta]_0$ dl. g.$^{-1}$
8.76	6.28	4.46	2.74	5.57	5.64	6.74	0.34		2.22
4.58	7.51	1.90	0.82	5.31	6.04	6.50	0.38	1.04	1.13
2.29	8.45	0.74	0.36	2.80	7.38	3.08	0.27	0.72	0.82
			1.63			1.86	0.36	0.77	
5.84	5.49	3.13		1.75	8.09	1.78	0.35	1.49	
				4.88	5.96	4.59	0.35	1.41	
6.28	6.52	2.86				4.26	0.41		1.30
						1.42	0.44		1.53
5.89	5.19	2.62	1.18	3.14	6.79	4.25	0.32	1.44	0.55
						3.59	0.33	1.26	0.78
3.04	6.91	1.11		1.70	8.64	4.03	0.24	1.42	
6.94	5.83	3.94		3.87	6.62	1.06			1.53
				3.49	6.91	2.15			
6.06	5.64	2.67		3.31	6.83	4.97			1.40
5.73	7.06	2.79	1.02	3.09	6.91	4.34			0.68
2.00	8.59	0.63		1.33	9.25	4.18			1.03
3.77	7.30	1.37	0.70	2.09	8.04	3.84			
3.15	8.07	0.97				1.64			
			2.28			2.70			
			5.24			2.19			
						2.70			
						5.60			
						9.24			

ᵃ Theta A—60:40 butyl ether:butanol.

ᵇ Theta B—68:32 toluene:propanol.

Fig. 2. Second virial coefficient in THF as a function of the viscosity in toluene.
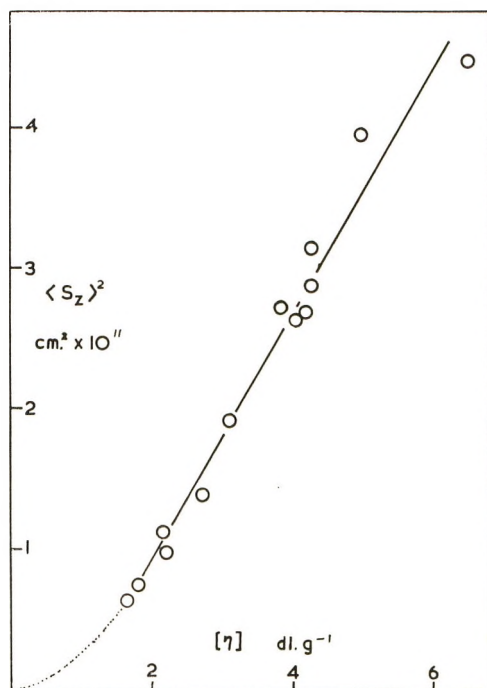
Fig. 3. Radius of gyration in THF as a function of the viscosity in toluene.

for viscosities measured in benzene.* (No difference can, however, be attributed to this change in solvent since polyisoprenes have almost identical limiting viscosity numbers in both solvents.) While in the absence of detailed measurements of the solution properties of masticated natural rubber, no definite conclusion can be drawn as to the source of this difference

* More extensive measurements in these laboratories have recently yielded a substantially identical relation.[16]

$[\eta]$ toluene, dl. g.$^{-1}$	$\langle M \rangle_w$ $\times 10^{-5}$	$\langle M \rangle_n$ $\times 10^{-5}$	$\dfrac{\langle M \rangle_\omega}{\langle M \rangle_n}$	$[\eta]_0$ dl. g.$^{-1}$	$K = [\eta] / \langle M \rangle_n^{0.67}$ $\times 10^4$	$K_0 = [\eta]_0 / \langle M \rangle_n^{1/2}$ $\times 10^3$
1.5	1.66	1.23	1.35	0.68	6.08	1.94
1.75	2.23	1.42	1.57	0.75	6.42	1.99
2	2.75	1.62	1.70	0.83	6.73	2.06
2.25	3.23	1.82	1.77$_5$	0.90	6.98	2.10
2.5	3.67	2.01	1.83	0.98	7.29	2.19
3	4.52	2.41	1.88	1.13	7.75	2.30
3.5	5.24	2.80	1.87	1.28	8.17	2.42
4	5.90	3.18	1.85$_5$	1.44	8.58	2.55
5	7.18	3.96	1.81	1.86	9.27	2.95
6	8.22	4.74	1.73$_5$	2.04	9.86	2.96

in the $[\eta]$ versus $\langle M \rangle_n$ relation it seems likely to reflect the much broader molecular weight distribution of natural rubber as compared with the synthetic *cis*-polyisoprene. This feature implies that for a given initial viscosity, natural rubber will possess a lower osmotic molecular weight and thus for mastication to a state in which the molecular weight distributions of the two materials are more or less comparable, the slope of the $[\eta]$ versus $\langle M \rangle_n$ relation will be greater than that for synthetic *cis*-polyisoprene.

The data for A_2 are rather scattered (Fig. 2). Similar values were obtained osmotically in toluene and by light scattering in tetrahydrofuran
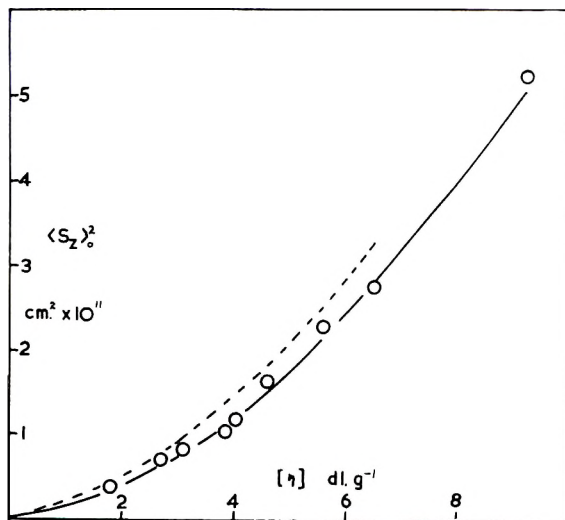

Fig. 4. Radius of gyration in a theta solvent: (O) observed; (- - -) calculated from the equation of Krigbaum (see ref. 17).

II
Rubber (Smoothed Data)

$A_2{}^a$ $\times 10^4$ ml. mole g.$^{-2}$	$\langle S^2 \rangle_z$ cm.$^2 \times 10^{11}$	$\langle S_0^2 \rangle_z$ cm.$^2 \times 10^{11}$	$Q(y)$	$\langle S_0^2 \rangle_z$ calc. cm.$^2 \times 10^{11}$	$\langle S_0^2 \rangle_n$ cm.$^2 \times 10^{11}$	$\langle S_0^2 \rangle_z / \langle S_0^2 \rangle_n$	$\langle S_0^2 \rangle_{z\,(calc).} / \langle S_0^2 \rangle_n$
8.50	0.54	0.29	1.73	0.36	0.19	1.5$_2$	1.8$_9$
8.25	0.75	0.35	2.03	0.43	0.23	1.5$_2$	1.8$_7$
8.01	0.95	0.43	2.19	0.48	0.27	1.6$_0$	1.7$_8$
7.81	1.16	0.48	2.27	0.56	0.30	1.6$_0$	1.8$_7$
7.63	1.39	0.56	2.34	0.69	0.34	1.6$_5$	2.0$_3$
7.30	1.81	0.73	2.40	0.89	0.43	1.7$_0$	2.0$_7$
7.05	2.24	0.94	2.38	1.18	0.51	1.8$_4$	2.3$_1$
6.85	2.68	1.16	2.37	1.52	0.60	1.9$_3$	2.5$_4$
6.55	3.53	1.76	2.32	2.14	0.83	2.1$_2$	2.5$_8$
6.34	4.40	2.46	2.23	2.91	0.99	2.4$_9$	2.9$_5$

^{a} Value from light scattering in THF.

(THF), this being consistent with the comparable solvent power of both solvents. As expected from the Flory theory[12] A_2 decreases with increase in molecular weight but in view of the difficulties in interpretation of this theory for polydisperse polymers little quantitative significance can be attached to the decrease. Values of $\langle S^2 \rangle_z$ in tetrahydrofuran are given in
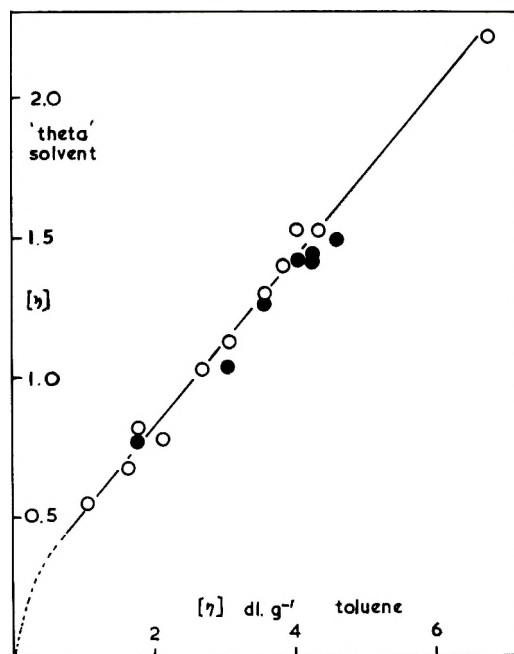

Fig. 5. Relation between the viscosity in toluene and that in a theta solvent. (O) In 60:40 n-butyl ether-n-butanol; (●) in 68:32 toluene-n-propanol.

Figure 3. The experimental measurement of $\langle S_0^2 \rangle_z$ in a theta solvent is somewhat inaccurate due to the rather small dependence of τ on $\sin^2 \theta/2$. Good confirmation of the experimental values has been obtained by use of the semiempirical relation between $\langle S^2 \rangle_z$ and $\langle S_0^2 \rangle_z$ suggested by Krigbaum.[11] For a polydisperse polymer this may be written:

$$(\langle S^2 \rangle_z)^{3/2} = (\langle S_0^2 \rangle_z)^{3/2} + 1.41 \times 10^{-25} \, (\langle M \rangle_w)^2 \, Q(y)A_2$$

Here polydispersity is measured by $y = [(\langle M \rangle_w/\langle M \rangle_n)-1]^{-1}$ and $Q(y) = [(y+2)^{1/2} \, \Gamma(y+3.5)]/[(y+1)^2 \, \Gamma(y+2)]$. In general, in view of the order of magnitude of the various terms involved, the *exact* value of $Q(y)$ is not very important. Using the values of $\langle M \rangle_w$, A_2, and $\langle S^2 \rangle_z$ obtained in tetrahydrofuran solution, values of $\langle S_0^2 \rangle_z$ have been deduced. These compare favorably with those measured in the theta solvent; the variation with $[\eta]$ is similar, the calculated values being some 20% greater than those observed throughout the range (Fig. 4). In Figure 5 the linear relation between the intrinsic viscosity in toluene and that in a theta solvent is shown.

The data of Tables I and II allow changes in molecular weight distribution as mastication proceeds to be estimated in three ways. Firstly there is the approach adopted by Angier et al.[5] from changes in the parameter K of the Mark-Houwink equation

$$[\eta] = K\langle M \rangle_n{}^a$$

In this expression, α is constant for a given polymer-solvent system, while K is similarly constant but dependent on the molecular weight distribution, the sharpening of which causes a decrease in K. In particular, K for a monodisperse polymer is related to K' for a polymer having a random molecular weight distribution by

$$K' = K \, \Gamma(\alpha+2)$$

Carter et al.[18] have shown that for solutions of fractionated natural rubber in toluene

$$[\eta] = 5.02 \times 10^{-4} \, (\langle M \rangle_n)^{0.67}$$

whence, for a random distribution,

$$[\eta] = 7.55 \times 10^{-4} \, (\langle M \rangle_n)^{0.67}$$

In Table II apparent values of K have been deduced as $[\eta]_{\phi CH_3}/\langle M \rangle_n{}^{0.67}$ and these show a monotonic decrease from 9.9 to 6.1 $\times 10^{-4}$ as mastication proceeds, a change consistent with a steady sharpening of the distribution. The absolute numerical value of K is in reasonable agreement with that found by Carter et al.[18] For solutions in a theta solvent $\alpha = 0.5$ so the Mark-Houwink equation becomes

$$[\eta]_0 = K_0 \, \langle M \rangle_n{}^{1/2}$$

Values of K_0 have been deduced as $[\eta]_0/\langle M \rangle_n{}^{1/2}$, and these too show a steady decrease from 3 to 2 $\times 10^{-3}$. These values are in fair agreement

with that of 1.2×10^{-3} found by Flory and Wagner[19] for fractionated natural rubber in methyl n-propyl ketone at 14.5°C. (The value for a random distribution would be 1.8×10^{-3}.)

A more direct measure of molecular weight distribution is given by the ratio $\langle M \rangle_w / \langle M \rangle_n$. This has the value 2 for a random distribution decreasing to 1 for a monodisperse polymer. Values of this ratio are given in Table II. The initial, virtually unmasticated, polymer has $\langle M \rangle_w / \langle M \rangle_n \simeq 1.7$ characterizing a rather sharper than random distribution. On mastication this ratio increases initially then falls rapidly, indicating an initial broadening followed by a rapid sharpening of the distribution.

As a third method of detecting distribution changes the ratio $\langle S_0^2 \rangle_z / \langle S_0^2 \rangle_n$ has been studied. Since providing Gaussian statistics apply, $\langle M \rangle_z \propto \langle S_0^2 \rangle_z$ this is the equivalent to $\langle M \rangle_z / \langle M \rangle_n$. Values of $\langle S_0^2 \rangle_n$ have been deduced from $[\eta]_0$ using the Flory[20] relation *for linear chains*.

$$^1/_6 \langle S_0^2 \rangle_n = [\langle M \rangle_n \, [\eta]_0 / \Phi]^{2/3}$$

where $\Phi = 2.1 \times 10^{21}$ (for $[\eta]$ in dl. g.$^{-1}$) is a universal constant. Since the samples studied were not sharp fractions Φ should probably be assigned a somewhat greater value[20] and hence the values for $\langle S_0^2 \rangle_n$ are probably minimum values. The ratios $\langle S_0^2 \rangle_z / \langle S_0^2 \rangle_n$ are included in Table II. A monotonic decrease is again observed. As indicated above the absolute value of this ratio is probably too low and indeed a comparison with the values of $\langle M \rangle_w / \langle M \rangle_n$ shows that this must be so since it is a theoretical requisite that $\langle S_0^2 \rangle_z / \langle S_0^2 \rangle_n$ (or $\langle M \rangle_z / \langle M \rangle_n$) exceeds $\langle M \rangle_w / \langle M \rangle_n$. However, the general trends are probably substantially correct.

These trends in $\langle M \rangle_z / \langle M \rangle_n$ and $\langle M \rangle_w / \langle M \rangle_n$ can be explained in terms of the preferential rupture of large molecules by mastication. Initially, the scission of very high molecular weight species causes a rapid reduction in $\langle M \rangle_z / \langle M \rangle_n$, but the creation of a large number of shorter chains broadens the distribution in terms of the $\langle M \rangle_w / \langle M \rangle_z$ ratio. As mastication proceeds and shorter chains are ruptured a low molecular weight "tail" is produce and $\langle M \rangle_w / \langle M \rangle_n$ then decreases. At the same time the decrease in $\langle M \rangle_z / \langle M \rangle_n$ is somewhat arrested since the largest molecules which contribute most to $\langle M \rangle_z$ have been destroyed and this parameter is insensitive to changes in the low molecular weight end of the distribution.

It is clear therefore that the changes in solution properties of the rubber as mastication proceeds are consistent with the hypothesis that mastication is not a random process but occurs by the rupture of chains exceeding a certain critical value. In this instance, however, the situation is somewhat complicated by the rather narrow molecular weight distribution of the initial unmasticated rubber. It is interesting to note that the theory of Bueche[6] predicts that the mastication of such narrow distribution polymers will result initially in a broadening of the distribution.

No mention has been made above of the possible occurrence of branching during mastication, which could vitiate some of the conclusions. The *cis*-polyisoprene used here contained appreciable quantities of antioxidant

and such a material in reacting rapidly with the RO_2 radicals produced during mastication will effectively inhibit branching processes. Recently, results have been presented which support this conclusion.[21] Since the unmasticated rubber is believed to be a linear polymer it may be concluded that the masticated rubbers studied here are also essentially linear materials.

References

1. Watson, W. F., and M. Pike, *J. Polymer Sci.*, **9**, 229 (1952); G. Ayrey, C. G. Moore, and W. F. Watson, *J. Polymer Sci.*, **19**, 1 (1956).

2. Bristow, G. M., *Trans. Inst. Rubber Ind.*, **38**, T104–114 (1962).

3. Watson, W. F., *Proc. Rubber Technol. Conf. 3rd, London*, **1954**, 553.

4. Angier, D. J., R. J. Ceresa, and W. F. Watson, *J. Polymer Sci.*, **34**, 699 (1959).

5. Angier, D. J., W. T. Chambers, and W. F. Watson, *J. Polymer Sci.*, **25**, 129 (1957).

6. Bueche, F., *J. Appl Polymer Sci.*, **4**, 101 (1960).

7. Allen, P. W., and G. M. Bristow, *J. Appl. Polymer Sci.*, **4**, 237 (1960).

8. Morton, M., I. Piirma, R. J. Stein, and J. F. Meier, *Proc. Rubber Technol. Conf. 4th London*, **1962,** in press.

9. Watson, W. F., and D. Wilson, *Rubber Age (London)*, **38**, 982 (1957).

10. Ewart, R. H., C. P. Roe, P. Debye, and J. R. McCartney, *J. Chem. Phys.*, **14**, 687 (1946).

11. Altgelt, K., and G. V. Schulz, *Makromol. Chem.*, **36**, 209 (1960).

12. Flory, P., and W. R. Krigbaum, *Ann. Rev. Phys. Chem.* **2**, 383 (1951).

13. Stockmayer, W. H., and E. F. Casassa, *J. Chem. Phys.*, **20**, 1560 (1952).

14. Bristow, G. M., and M. R. Place, *J. Polymer Sci.*, **60**, S21 (1962).

15. Mullins, L., and W. F. Watson, *J. Appl. Polymer Sci.*, **1**, 245 (1959).

16. Bristow, G. M., and B. Westall, to be published.

17. Krigbaum, W. R., *J. Polymer Sci.*, **18**, 315 (1955).

18. Carter, W. C., R. L. Scott, and M. Magat, *J. Am. Chem. Soc.*, **68**, 1480 (1946).

19. Wagner, H. L., and P. Flory, *J. Am. Chem. Soc.*, **74**, 195 (1952).

20. Flory, P., *Principles of Polymer Chemistry*, Cornell Univ. Press, Ithaca, N. Y., 1953, p. 612.

21. Bristow, G. M., *J. Polymer Sci.*, **62**, S168 (1962).

Résumé

On donne des résultats obtenus par l'étude de la diffusion lumineuse, des propriétés osmotiques et viscométriques de solutions de polyisoprène-*cis* synthétique après mastication. La mastication produit un retrécissement de la distribution du poids moléculaire et cela concorde avec l'hypothèse que la dégradation a lieu par un processus nonstatisque.

Zusammenfassung

Es werden Angaben über Lichtstreuung, sowie osmotische und viskosimetrische Eigenschaften von Lösungen von mastiziertem synthetischen *cis*-Polyisopren gemacht. Die Mastizierung führt zu einer Verengung der Molekulargewichtsverteilung; das stimmt mit der Annahme überein, dass es sich beim Abbau um einen nichtstatistischen Prozess handelt.

Organic Reactions under High Pressure.
IX. The Effect of Pressure on the Stereochemistry
of Methyl Methacrylate Polymerization

CHEVES WALLING and DENNIS D. TANNER, *Department of Chemistry, Columbia University, New York, New York*

Synopsis

The radical polymerization of methyl methacrylate has been carried out at 51°C. over a pressure range of 1–8000 kg./cm.², and the stereochemistry of the polymer analyzed by NMR spectroscopy. Over the entire pressure range, the stereochemistry of addition is independent of the stereochemistry of the growing polymer chain. The percentage of syndiotactic linkages decreases from about 75% to 62%, and the change in the resulting distribution of stereoseqeuences is calculated. It is concluded that the transition state for syndiotactic addition is slightly larger than that for isotactic addition to the growing chain.

Current interest in the stereochemistry of vinyl polymerization has prompted us to investigate the effect of pressure on polymer stereochemistry as part of our program of study of the effect of high pressures on the rates and course of organic reactions. As far as we know, only two such investigations have been reported previously: a study of styrene polymerization which indicated no detectable difference in properties between polymer prepared at atmospheric and high pressure,[1] and a more recent Russian investigation of methyl methacrylate[2] with results qualitatively in agreement with those reported here. As a suitable system we selected the radical polymerization of methyl methacrylate, since it shows detectable, but incomplete, stereoselectivity at atmospheric pressure, and because an elegant method of analysis of polymer structure by NMR spectra is available through the work of Bovey and Tiers.[3]

Experimental

High pressure experiments were carried out in our high pressure apparatus[4] thermostated at 51°C., in collapsable Teflon internal reaction vessels of the sort described previously.[5] Degassed solutions of freshly distilled methyl methacrylate containing 1% benzoyl peroxide and 1% 1-pentanethiol (to reduce polymer molecular weight for the subsequent analysis) were transferred under nitrogen to the Teflon vessels, placed in the pressure apparatus, and allowed to react for 16 hr. As judged by the small pressure changes observed in the system, reactions were smooth
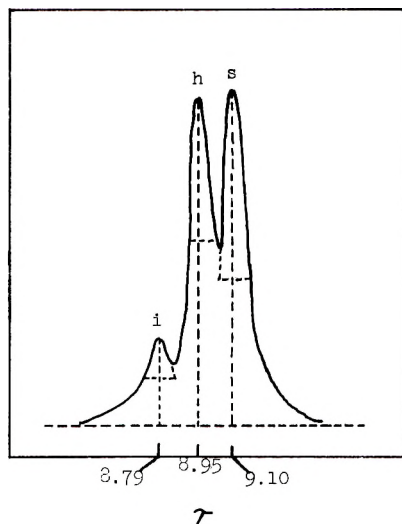
Fig. 1. NMR spectra of methyl methacrylate polymer prepared at 6850 kg./cm.^{2} pressure.

and essentially isothermal. After reaction the solid polymer was removed, dissolved in benzene, precipitated with methanol, allowed to settle overnight, and the solvent decanted. The residual polymer was ground to a fine powder and dried overnight under vacuum with the aid of an infrared lamp.

NMR spectra were obtained on 15% solutions (w/v) of polymer in purified chloroform using a model HR 60 Varian spectrometer equipped with a probe heated to 94°C. with tetramethylsilane as an internal standard. Polymer structure was determined from the areas of i, s, and h peaks (discussed further below) as described by Bovey and Tiers.[3] A typical spectrum is shown in Figure 1, and gives an idea of the resolution attained and the precision of the analysis. Several spectra were obtained on each sample, and the results averaged to give the values listed in Table I.

TABLE I
Effect of Pressure on the Stereochemistry of Methyl Methacrylate Polymerization

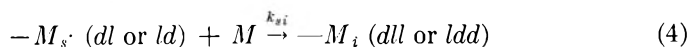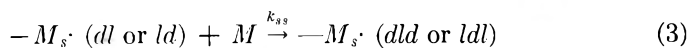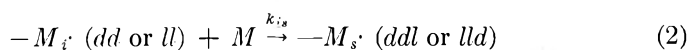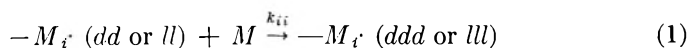| P, kg./cm.^{2}	i, %	h, %	s, %
1	4.2 ± 0.4	38 ± 1.3	57 ± 1.0
2380	4.5 ± 0.1	37 ± 0.7	58 ± 0.8
4750	8.4 ± 1.3	38 ± 1.4	54 ± 1.6
6300	8.8 ± 0.5	40 ± 2.2	51 ± 2.3
6850	9.8 ± 0.5	44 ± 1.2	46 ± 1.6
7960	11.4 ± 0.1	49 ± 3.0	40 ± 3.4

Results

The NMR technique of Bovey and Tiers permits the analysis of polymethyl methacrylate structure in terms of pairs of linkages or triads of

monomer units, and distinguishes three types of stereochemistry for the central unit: isotactic, i (*ddd* or *lll*), syndiotactic, s (*dld* or *ldl*), and heterotactic, h (*ddl*, *dll*, *ldd*, or *lld*). Our results in these terms are summarized in Table I, and it is evident that pressure significantly increases the number of isotactic links (*dd* or *ll*), while decreasing those which are syndiotactic. Our result at atmospheric pressure is in reasonable agreement with Bovey's,[6] and, judging from his published NMR spectrum, we may have achieved somewhat better resolution. Our conclusions concerning the effect of pressure also agree with those of Zubov, Kabanov, Kargin, and Shchetinin[2] in that they deduce from measurements of the density and thermomechanical properties of their polymers that the number of syndiotactic linkages decrease with pressure.

Discussion

As several workers have shown,[3,7-9] the development of the stereochemical relations between successive monomer units in a vinyl polymer may be conveniently treated as a problem in copolymerization. Although the general expressions have all been given, we here present a short derivation which shows clearly the relation to "classical" copolymerization theory[11] and leads directly to an expression for the relative amounts of i, s, and h units in the polymer. If we assume that the tendency of a growing chain to add the next monomer unit via an isotactic or syndiotactic linkage is influenced by the stereochemistry of the preceding linkage, but not by more remote chain structure, two types of growing ends, and four reactions, will determine polymer structure

$$-M_i \cdot (dd \text{ or } ll) + M \xrightarrow{k_{ii}} -M_i \cdot (ddd \text{ or } lll) \tag{1}$$

$$-M_i \cdot (dd \text{ or } ll) + M \xrightarrow{k_{is}} -M_s \cdot (ddl \text{ or } lld) \tag{2}$$

$$-M_s \cdot (dl \text{ or } ld) + M \xrightarrow{k_{ss}} -M_s \cdot (dld \text{ or } ldl) \tag{3}$$

$$-M_s \cdot (dl \text{ or } ld) + M \xrightarrow{k_{si}} -M_i (dll \text{ or } ldd) \tag{4}$$

It is evident that eqs. (1–4) are identical with the propagation steps in a normal copolymerization, subscripts i and s replacing the conventional 1 and 2. If we now add the usual "steady-state" expression,

$$k_{is}[M_i \cdot][M] = k_{si}[M_s \cdot][M] \tag{5}$$

and note that i units are produced by reaction (1), s units by (3) and h units by (2) and (4) we obtain

$$d[s]/d[i] = s/i = r_s/r_i \tag{6}$$

$$d[h]/d[i] = h/i = 2/r_i \tag{7}$$

where $r_i = k_{ii}/k_{is}$, $r_s = k_{ss}/k_{si}$, ratios of rate constants analogous to the usual monomer reactivity ratios r_1 and r_2. In the special case that the stereochemistry of the preceding linkage has no effect upon the stereo-

chemistry of the link being formed (analogous to an "ideal" copolymer[12]) $r_s = 1/r_i$ and

$$s/i = r_s^2 \tag{8}$$

$$h/i = 2r_s$$

A relation analogous to eq. (8) was developed by Bovey and Tiers[3] and shown to be consistent with their data on the radical polymerization of methyl methacrylate at atmospheric pressure. Their conclusion was originally criticized by Miller and Nielsen,[9] but, in a subsequent paper[10] Miller has recognized that the two independent ratios s/i and h/i provide the necessary information to uniquely determine r_i and r_s. The situation is, in fact, analogous to the determination of two monomer reactivity ratios from the analysis of two copolymer samples prepared from two different monomer feeds.

Since i, s, and h are expressed as fractions of total linkages,

$$i + h + s = 1 \tag{9}$$

and, for case (8)

$$i + 2r_s i + r_s^2 i = 1 \tag{10}$$

whence

$$i^{1/2} + s^{1/2} = 1 \tag{11}$$

Equation (11) provides a convenient test of the condition $r_s = 1/r_i$, and in Table II this sum is calculated for each of our experiments. It will be seen that eq. (11) is satisfied within the experimental error of our measurements, and we conclude that the tendency of a growing chain to add isotactic or syndiotactic linkages is independent of its previous stereochemistry over the entire pressure range. With this established, r_s may be calculated from the relation $r_s = 2s/h$, which is probably more accurate than using the other ratios of eq. (8), since i is determined from rather a small NMR peak with a large percentage uncertainty. Values are listed in Table II, and indicate that the percentage of syndiotactic linkages, $100 (1 + r_s)/r_s$, decreases from 75% at atmospheric pressure to 62% at 7960 kg./cm.² (or approximately 8000 atm.) The net effect on the distribution of syndiotactic linkages may be calculated from Miller and Nielsen's equations[9] and

TABLE II
Effect of Pressure on r_s

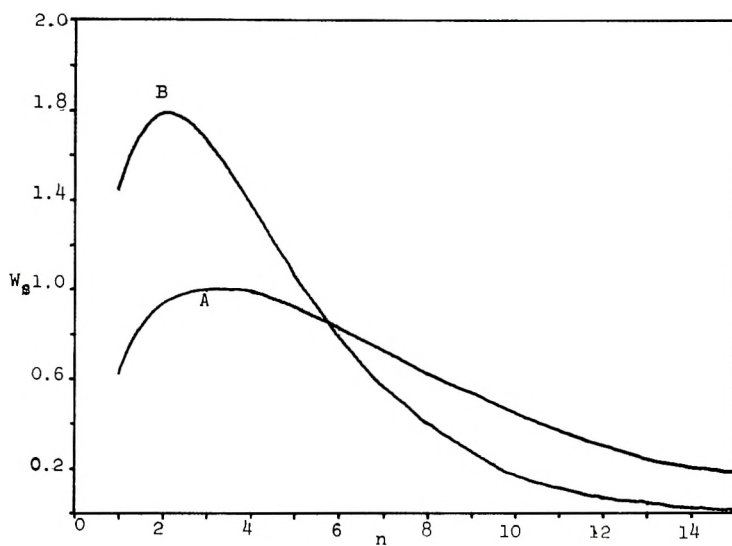| P, kg./cm.²	$(i^{1/2} + s^{1/2})$	r_s
1	0.984	3.00
2300	0.976	3.13
4750	0.986	2.84
6300	1.013	2.55
6850	1.053	2.09
7960	0.970	1.63

Fig. 2. Weight fraction, W_s, of syndiotactic sequences n monomer units in length for polymethyl methacrylate prepared at (A) atmospheric pressure (B) 7960 kg./cm.².
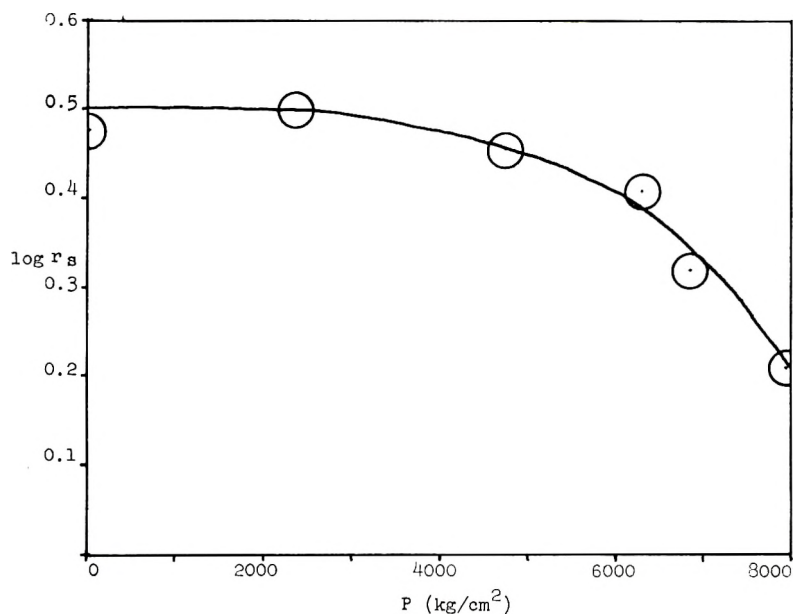

Fig. 3. Effect of pressure on r_s for the polymerization of methyl methacrylate.

are shown in Figure 2. At high pressures there is a very significant decrease in long syndiotactic sequences.

The difference in volumes of the transition states for adding isotactic and syndiotactic units to the growing chain may be obtained from the relation[13]

$$d \ln r_s / dP = (\Delta V_i^{\ddagger} - \Delta V_s^{\ddagger}) / RT. \tag{12}$$

The slope of the curve obtained by plotting log r_s vs. pressure is proportional to $\Delta V_i^{\ddagger} - \Delta V_s^{\ddagger}$. Such a plot is shown in Figure 3, and is rather surprising in that it is concave downward, indicating that the difference in volume is very small in the range 1–4750 kg./cm.^{2}, but amounts to 5.5 cc./mole between 4750 and 7960 kg./cm.^{2}.

Finally we may compare our results with those of Zubov et al.[2] These workers estimated the fraction of syndiotactic links by measurement of polymer density, using known densities of pure isotactic and syndiotactic polymer (1.230 and 1.180, respectively) and assuming a linear variation of density with the fraction of syndiotactic links. On this basis they calculate 80% syndiotactic linkages at 1 atm. and 65% at 7500 atm., in good agreement with our results. However, at intermediate pressures their percentages are higher than ours, and their estimate of $\Delta V_i^{\ddagger} - \Delta V_s^{\ddagger}$ decreases with pressure. In either case, $\Delta V_s^{\ddagger} > \Delta V_i^{\ddagger}$, paralleling the fact that the syndiotactic polymer has the lower density.

References

1. Trementozzi, G. A., and R. Buchdahl, *J. Polymer Sci.*, **12**, 149 (1954).

2. Zubov, V. P., V. A. Kabanov, V. A. Kargin, and A. A. Shchetinin, *Vysokomol. Soedin.*, **2**, 1722 (1960).

3. Bovey, J. A., and G. V. D. Tiers, *J. Polymer Sci.*, **44**, 173 (1960).

4. Walling, C., and J. Pellon, *J. Am. Chem. Soc.*, **79**, 4776 (1957).

5. Walling, C., and J. Pellon, *J. Am. Chem. Soc.*, **79**, 4786 (1957).

6. Bovey, H. A., *J. Polymer Sci.*, **46**, 59 (1960).

7. Coleman, B. D., *J. Polymer Sci.*, **31**, 156 (1958).

8. Fordham, J. W. L., *J. Polymer Sci.*, **39**, 321 (1959).

9. Miller, R. L., and L. E. Nielsen, *J. Polymer Sci.*, **46**, 303 (1960).

10. Miller, R. L., *J. Polymer Sci.*, **57**, 975 (1962).

11. Mayo, F. R., and C. Walling, *Chem. Revs.*, **46**, 191 (1950).

12. Wall, F. T.. *J. Am. Chem. Soc.*, **66**, 2050 (1944).

13. Evans, M. G., and M. Polanyi, *Trans. Faraday Soc.*, **31**, 875 (1935).

Résumé

On polymérise par voie radicalaire des méthacrylates de méthyle à 51 °C sous une pression de 1–8000 Kg/cm^2, et on détermine la stéréochimie du polymère par spectroscopie NMR. Dans le domaine entier de pression, la stéréochimie d'addition est indépendante de la stéréochimie de la chaîne polymérique en corissance. Le pourcentage de liaison syndiotactique diminue de 75% à 62%, et la diminution dans la distribution des stéréo-

séquences résultantes est calculée.   On en conclut que l'énergie de l'etat de transition de l'addition syndiotactique à la chaine en croissance est légèrement supérieur à celle de l'addition isotactique.

Zusammenfassung

Die radikalische Polymerisation von Methylmethacrylat wurde bei 51°C im Druckbereich von 1–8000 kg/cm² durchgeführt und der sterische Bau der Polymeren mittels NMR-Spektroskopie untersucht.   Im ganzen Druckbereich ist die Stereochemie der Addition von der Stereochemie der wachsenden Polymerkette unabhängig.   Der Prozentsatz an syndiotaktischen Verknüpfungen nimmt von etwa 75% auf 62% ab, die Änderung der erhaltenen Verteilung der Stereosequenzen wird berechnet.   Man kommt zu dem Schluss, dass der Übefgangszustand bei der syndiotaktischen Addition etwas grösser als bei der isotaktischen Addition an die wachsende Kette ist.

Nuclear Magnetic Resonance in Solid Polypyrrolidone

G. FILIPOVICH, *Central Research Department, Minnesota Mining and Manufacturing Company, St. Paul, Minnesota*

Synopsis

Nuclear magnetic resonance in solid poly-2-pyrrolidone has been studied over the temperature range 77–450°K. Experimental evidence concerning the differently ordered regions that contribute to the composite NMR curves has been obtained. Experimental techniques and results are described in detail. A detailed comparative interpretation of two-component NMR curves as a function of temperature is offered in terms of motion in differently ordered regions. The width of the component corresponding to the crystalline regions was found to be independent of temperature over a certain range above that of liquid nitrogen; this is taken to indicate a rigid structure. At higher temperatures there is a gradual decrease in line width indicating increasing segmental molecular motion. The NMR line width representing amorphous regions was found not to change over approximately the same range of low temperatures; it then decreases faster with increasing temperature than that of the crystalline regions; it finally decreased sharply and became the narrow component above the glass transition temperature. The glass transition temperature in polypyrrolidone appears to decrease with increasing water content. Comparison of the temperature of glass transition of dry polypyrrolidone with those of other polyamides supports the observation that the temperature of this transition is lower, the smaller is the ratio of NH groups to methylene groups in a polyamide. Empirical second moment values at liquid nitrogen temperature and at room temperature, as well as an estimate of theoretical second moment for an assumed sheet model, are reported.

Introduction

Nuclear magnetic resonance in a number of polyamides has been studied over a wide range of temperatures by Slichter,[1] by Woodward et al.,[2,3] by Illers and Kosfeld,[4] by Jones,[5] by Gupta,[6] and by Shaw and Dunel.[7] To our knowledge NMR studies of polypyrrolidone (also termed nylon 4) have not previously been reported. This material is a polyamide having a relatively short repeating unit in the polymer chain. It has remarkable physical properties. The mechanism of accelerated polymerization of 2-pyrrolidone (γ-butyrolactam) was first disclosed by Ney and Crowther[8] and has been described in detail.[9]

It is of interest to compare the NMR behavior of polypyrrolidone with that of other members of the polyamide series, and also to correlate its broad line NMR characteristics, which represent molecular motion, with its mechanical, dielectric, and thermal properties. The present study pro-

vides NMR information on predominantly crystalline and predominantly amorphous polypyrrolidone in the 77–450°K. temperature range. By "predominantly crystalline" it is meant that the ordered regions, contained in a spherulitic structure, constitute a substantial part of the sample. In predominantly amorphous samples, the disordered regions, as evidenced by x-ray diffraction and density, constitute most of the sample. A comparison is made between the theoretically estimated second moment for "rigid structure" of an assumed as reasonable model of this material, with the value experimentally obtained at the temperature of liquid nitrogen.

Experimental

The NMR curves were obtained with a Varian V-4300-2, 40 mcycle/sec, dual-purpose spectrometer equipped with a V-4340 variable temperature probe accessory. The V-4331-TWL probe insert was modified by us to accommodate solid polymer samples up to $1/2$ in. in diameter, thus gaining in signal-to-noise ratio by a factor of 2. This design also made it possible to obtain wide-line curves of samples still immersed in liquid nitrogen. Precooled (or preheated) dry nitrogen was circulated at controlled rates of flow inside the Dewar insert along the periphery and through the hole along the axis of the cylindrical sample to vary its temperature. Enough time was allowed to stabilize the temperature of the samples in most cases to within ±1°C. before recording the NMR curves. Considerable difficulties in stabilizing the temperature as well as additional noise problems due to vibration of the samples were encountered when maximal rates of gas flow had to be used, these being at lowest and highest temperatures. In most cases the modulation amplitude was kept low enough to prevent modulation broadening of the broad component of the curves. Saturation broadening of the line width was investigated by recording sets of curves at different power levels at most of the temperatures; erroneous (saturation broadened) data were readily eliminated by this procedure. Generally the signal-to-noise ratio was high enough to yield reasonably reproducible curves with definite maximal and minimal points. Four to eight recordings were made at every choice of conditions, the average line width values being used for plotting. The reproducibility of width data for the broad line was ±0.15 gauss at most temperatures, but became less, namely ±0.3 gauss for those runs requiring high gas flow rates. The narrow components of the curves were in some cases recorded by means of instrumental arrangements used for high resolution NMR work. This is useful procedure when one wants to determine the true line width for a liquid component in the sample, or for example when it becomes necessary to determine whether water or monomer is responsible for the narrow component.

Samples were prepared from polymer made in these laboratories by the method of Ney et al.[8,9] The crystalline samples were obtained by pressing small polymer crumbs into cylindrical form. The amorphous samples were prepared from fibers held tightly together by glass sample holders. In most cases the samples were handled under moisture-free conditions to

keep their water content at a minimum. The relative crystallinity of the samples was established by means of their x-ray diffraction patterns and also by their measured densities.

Results

Prior to the detailed broadline NMR studies on solid samples of polypyrrolidone the material was dissolved in trifluoroacetic acid, and, by the use of Me_4Si as internal reference, the high resolution spectrum of the polymer was compared with that of the monomer in the same solvent. Good agreement in spectral peak positions and the observation of broadened spectral lines for the polymer confirmed the chemical structure of the material.

Preliminary broad line spectra of solid polypyrrolidone indicated its hygroscopic nature. A narrow line of relatively low intensity superimposed on the broad one was shown, by the procedure described before,[10] to represent water absorbed during exposure of the samples to the air. Another source of narrow line impurity was degradation of the solid polymer into highly mobile monomer. That this occurred at temperatures above $550°K$. was confirmed by the observation of NMR curves having multiple peak structure that was shown to agree well with the NMR spectrum of the monomer. The thermal degradation was carried out on dry samples protected by glass tubes that were sealed under vacuum. It was also established that the presence of liquid monomer in the solid sample can decrease the measured line width for the broad component (which is produced by the solid part of the sample) by as much as 10% at the temperatures above the freezing point of the monomer.

Some NMR curves (upper halves of the derivative curves) of solid polypyrrolidone recorded at room temperature and at elevated temperatures are shown in Figures 1–3. In these figures the curves recorded at different temperatures are superimposed on each other to show the relative changes in their broad and narrow components. The curves have been redrawn to eliminate noise, which is far from negligible. The narrow components are modulation-broadened due to the necessity of using a modulation amplitude high enough to obtain a reasonably good signal-to-noise ratio for the broad component. Some inconsistency in the peak heights of the curves was introduced by changes in gain. Figure 1 represents the characteristic NMR behavior of a polypyrrolidone sample made of randomly pressed fibers having predominantly an amorphous structure and containing less than 5% water and monomer. Figure 2 shows the changes of the NMR curves with temperature for this sample after it had been crystallized by heating in a stream of dry nitrogen. Some water and monomer were removed by this treatment. Figure 3 displays similar curves obtained on a highly crystalline polypyrrolidone sample pressed from small polymer crumbs. The water and monomer were thoroughly removed from the sample by drying it in a vacuum oven at $393°K$. for 16 hr. While in other cases the low-temperature NMR spectra were obtained first in
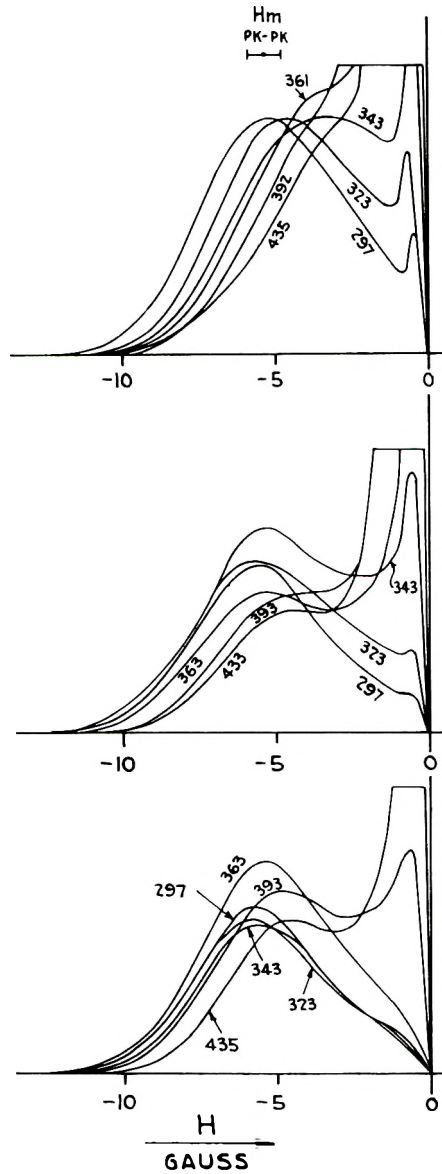
Fig. 1. (top) Relative changes with temperature in broad and narrow components of NMR curves for predominantly amorphous polypyrrolidone fibers with some water and monomer.

Fig. 2. (middle) Relative changes with temperature in broad and narrow components for crystallized polypyrrolidone fibers with water and monomer contents lower than those for fibers in Fig. 1.

Fig. 3. (bottom) Relative changes with temperature in broad and narrow components for crystalline dry polypyrrolidone.
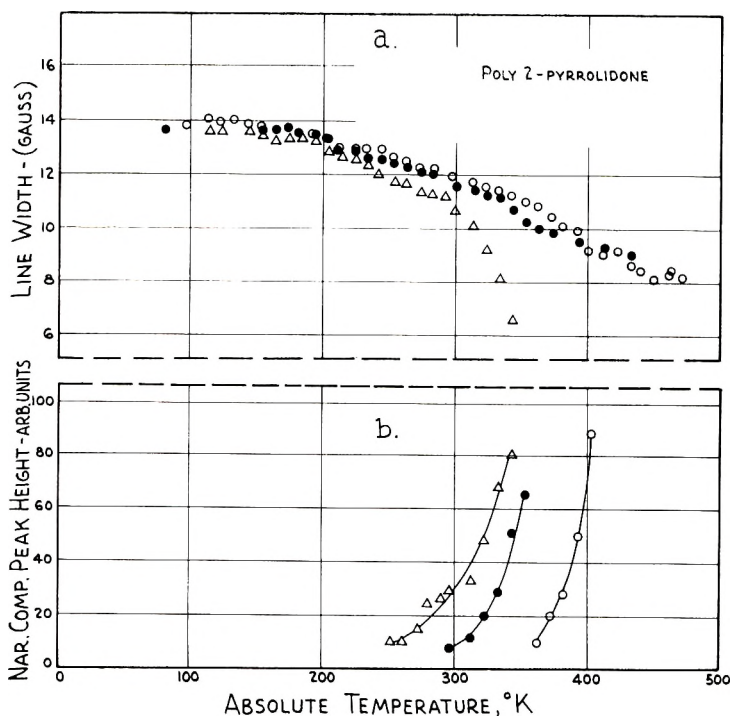
Fig. 4. (a) Line width of the broad component (measured directly from the composite curve) as a function of temperature: (Δ) predominantly amorphous fibers (as in Fig. 1); (●) crystalline fibers; (○) crystalline dry polypyrrolidone. (b) Rise of peak height of the narrow component with temperature. Notation as in Fig. 4a.

order to minimize changes due to annealing, the sample of Figure 3 was first heated to the highest temperature in order rapidly to eliminate any water still remaining, then the recordings of the curves were made as the sample was cooled in stepwise fashion. All three kinds of samples were prepared from the same original lot of material.

The variation of the width of the broad component (the horizontal distance between the maximum and minimum of the derivative of the NMR absorption curve) as a function of temperature, as well as the relative increase of peak height of the narrow component (in arbitrary units) are shown in Figure 4. It should be pointed out that the line width data plotted there were obtained directly from the composite curves representing the sum of the broad and narrow components. No attempt at resolving the curves into two separate components was made. For the predominantly amorphous fibers (Fig. 4) the line width data were plotted only up to 343°K. because at higher temperatures the broad component was no longer easily distinguished from the narrow one.

Other NMR runs on predominantly amorphous and predominantly crystalline polypyrrolidone were made in certain temperature ranges with reasonably reproducible results. The line width of the narrow component

invariably decreased with increasing temperature. The lowest value found for the line width of the narrow component was less than 0.1 gauss. This was observed at 452°K. by direct measurement of the width at half-height of the NMR absorption peak; the latter had been obtained by the high resolution method, which is more appropriate for narrow peaks.

Discussion

The results obtained provide additional evidence that broad line NMR curves having two components differing greatly in width can be correlated with the presence of differently ordered regions in samples of polymeric materials. The changes with temperature of the NMR second moment (and of the line width) can be better correlated with certain modes of molecular motion when the separate contributions to the composite NMR curves from the ordered and disordered regions are known. This means that the composite NMR curves must first be resolved and the separate components ascribed to the proper regions of the samples. Polypyrrolidone, like other polyamides, poses this problem. In addition to differently ordered regions, the water and monomer often present in samples influence the shape of the composite NMR curve. Polypyrrolidone samples having different degrees of crystallinity were compared in this study to show as far as possible the changes with temperature of the NMR characteristics that represent the ordered and disordered regions. The narrow component of the NMR curve obtained at 297°K. (room temperature) in Figure 1 represents monomer left in the sample after its melting, plus some water absorbed during brief exposures to the air. This was proved by actually pumping out and trapping the liquid component, and subsequently analyzing it by high resolution NMR. The width of the broad component for this predominantly amorphous sample decreases above room temperature (and the broad component essentially turns into a narrow one) at much lower temperatures than in case of crystalline fibers (Fig. 2). This difference is even more apparent on comparison of the amorphous fibers having some liquid component (Fig. 1) and the crystalline polymer (Fig. 3), from which the water and monomer had been carefully removed. In amorphous fibers as the temperature is raised the broad component becomes much more narrow and is hardly distinguishable at 435°K.; in contrast to this, in the case of the crystalline fibers, and especially in the crystalline dry polymer, it is clearly seen even at the highest temperature. Also from comparison of all three cases one can see that the peak height of the narrow component rises more rapidly with temperature, the more amorphous is the sample. Any contribution due to the liquid component in the samples should, of course, be taken into consideration. The curves representing the temperature variation of the broad component's width (shown in Figure 4a) for amorphous and crystalline samples do not differ much at low temperatures, but at higher temperatures significant deviations occur. Additional NMR runs made on carefully dried partially crystalline samples showed that the first growth of the narrow component occurs at the

higher temperatures, the more crystalline the sample, and the more thoroughly water and monomer are removed from it. The polymer most extreme in this respect was a highly crystalline sample of fibers, oriented by drawing and dried in vacuum at 383°K. No growth of a narrow component for this sample was observed until the temperature reached 403°K. The formation and growth of the narrow component in dry samples is entirely reversible and shows no hysteresis. The detailed comparative analysis of broad line NMR data obtained on polypyrrolidone leads to the following conclusions.

(1) At room and lower temperatures both ordered and disordered regions contribute to the broad component of the NMR curve. Any narrow component, if observed, at these temperatures is due to the presence of liquids in the samples. The observed curve is essentially a superposition of a broad line representing the crystalline regions and of a somewhat narrower one representing the amorphous regions.

(2) As the temperature is raised the molecular motion increases earlier in the amorphous regions, especially if liquids are present, and the line width of the broad composite curve decreases primarily as a direct result of the contributions from these regions.

(3) With further elevation of temperature, a sharp narrow component appears and rapidly rises as the system goes above the glass transition temperature of the amorphous regions of the sample. It is interesting that the glass transition apparently does not take place as an abrupt process throughout the whole sample. The disordered regions must differ in their degree of order, because the rise in relative intensity of the narrow component and the corresponding decrease in intensity of the broad component continues over a rather wide range of temperatures.

(4) The narrow component's line width above the glass transition temperatures is a measure of highly intensified molecular motion of molecular chains in amorphous regions. The possibility that at higher temperatures (not exceeding 453°K.) the strong narrow component may represent the products of degradation of the polymer, e.g., monomer, is excluded by the fact that upon partial cooling it again disappears. This disappearance cannot result from evaporation of the decomposition products in the stream of dry nitrogen, as no additional loss of weight (beyond the 2% water and monomer originally present in the polymer) was observed, even during very extended runs.

(5) It appears that the glass transition temperature of polypyrrolidone depends strongly on the amount of water present in the specimen, being lower the higher the water content. In the sample having behavior illustrated by Figure 1, the glass transition appears to take place at 300 ± 10°K., being accompanied by a sharp change in the correlation frequency of molecular motion. Judging by the appearance and the rise of the narrow component (Fig. 4b) in the NMR curves for the samples having NMR behavior illustrated in Figures 2 and 3, the glass transitions in the amorphous parts of these samples take place at 330 ± 10°K. (Fig. 2) and 380 ± 10°K. (Fig. 3).

(6) Above the glass transition temperature the broad component represents the crystalline regions of the samples. The broad component's line width proceeds to decrease gradually, presumably until the melting temperature of the crystallites is reached. It should be noted that the plot of the broad component line width above the glass transition temperature (the narrow component is very strong) may become misleading if the line width data is still measured directly from the composite curve, as is generally done. This is thought to be the case for the crystalline samples in Figure 4, for which it is believed that the line width would be greater in the temperature range above 370°K. if the measurements were made only on the broad component. (For the moment we are assuming that it could be resolved from the narrow component.) The evaluation of relative intensities of the broad and narrow component is complicated by experimental difficulty in keeping both components on the same recorder scale and to resolve them without making large errors. The decrease in intensity of the broad component with temperature takes place not only because the amorphous regions switch their contribution from the broad to the narrow component above the glass transition but also because of the general decrease in the excess number of nuclei (according to the Boltzmann distribution) that are available for NMR detection. The latter fact has to be considered if one wants to compare the "absolute" intensities of the broad components over the wide temperature ranges.

(7) To judge by the leveling off of the line width versus temperature curves of amorphous and crystalline polypyrrolidone it appears that the molecular chains approach the rigid structure in the 77–150°K. temperature range. Above 150–160°K., segmental motion appears to begin, and with further increases in temperature it becomes relatively more important in the disordered regions than it does in the crystallites.

(8) It would be difficult and perhaps of little value to make any detailed comparison of the NMR data on polypyrrolidone obtained in this study with the results obtained by other workers on other polyamides. In addition to the difference in chemical structure the materials investigated may differ in molecular weight, molecular weight distribution, crystallinity, dryness, etc. The instrumental techniques and the methods of presentation of data also vary considerably. It should be stated, however, that with respect to the general trend of the motional narrowing of the NMR curves as well as the dependence of the data on water content polypyrrolidone does resemble poly(hexamethylene adipamide). The glass transition in dry polypyrrolidone appears to be at a higher temperature than that of poly(hexamethylene adipamide).[3] This means that, as one might expect, polypyrrolidone (nylon 4) should be put ahead of nylon 66 in the series:[3] nylon 66 > nylon 610 > nylon 1010 > 17% N-methylated nylon 1010 > 58% N-methylated nylon 1010. This series shows the shift of the principal NMR line width transition of polyamides to higher temperatures as the ratio of NH groups to methylene groups is increased.[1]

Second Moment Evaluation

The empirical second moment values were obtained from the low temperature NMR curves for crystalline thoroughly dry polymer. The values ranged from 21.5 ± 1 gauss^2 at the temperature of liquid nitrogen down to about 14 gauss^2 at room temperature. The crystal structure of polypyrrolidone is not known. For this reason no exact comparison of theoretical and experimental values of second moments can be made.

A theoretical estimate of the second moment of the rigid structure was made on the basis of an assumed and reasonable model, in which the fully extended chains in the crystallites are linked together by hydrogen bonds in a closest packed manner to form sheets. This assumed structure is similar to that of polycaprolactam and poly(hexamethylene adipamide) as determined by Bunn et al.[11,12] The second moment calculation was made by the use of the Van Vleck formula[13] applicable to powdered samples. The fact that, at least at liquid nitrogen temperature, $T_1 >> T_2$ in polypyrrolidone (as established by saturation curve method[14]), was taken into consideration.[15] The detailed geometry of the model was worked out on the basis of the usual tetrahedral bond structure and generally known bond lengths.[16] The estimated part of the second moment due to intramolecular contributions is 13.5 gauss^2. By taking into account all intramolecular contributions as well as those contributions from the two neighboring chains in the sheet model, the second moment is estimated as 18.5 gauss^2. This calculation does not include the contributions from the molecules in the neighboring sheets. These contributions are expected to be smaller than those from the neighboring molecules in the sheets.

References

1. Slichter, W. P., *J. Appl. Phys.*, **26**, 1099 (1955).

2. Glick, R. E., R. P. Gupta, J. A. Sauer, and A. E. Woodward, *J. Polymer Sci.*, **42**, 271 (1960).

3. Woodward, A. E., R. E. Glick, J. A. Sauer, and R. P. Gupta, *J. Polymer Sci.*, **45**, 367 (1960).

4. Illers, K. H., and R. Kosfeld, *Makromol. Chem.*, **42**, 44 (1960).

5. Jones, D. W., *Polymer*, **2**, 203 (1961).

6. Gupta, R. P., *J. Phys. Chem.*, **65**, 1128 (1961).

7. Shaw, D. J., and B. A. Dunel, *Can. J. Chem.*, **39**, 1154 (1961).

8. Ney, W. O., Jr., and M. Crowther, U. S. Pat. 2,739,959 (1956).

9. Nummy, W. R., C. E. Barnes, and W. O. Ney, *Abstracts of Papers, 133rd Am. Chem. Soc. Meet.*, San Francisco, California, April 1958, p. 22R.

10. Filipovich, G., *J. Polymer Sci.*, **60**, S37 (1962).

11. Bunn, C. W., and E. V. Garner, *Proc. Roy. Soc. (London)*, **A189**, 39 (1947).

12. Holmes, D. R., C. W. Bunn, and D. J. Smith, *J. Polymer Sci.*, **17**, 159 (1955).

13. Van Vleck, J. H., *Phys. Rev.*, **74**, 1168 (1948).

14. McCall, D. M., and D. C. Douglass, *J. Chem. Phys.*, **33**, 777 (1960).

15. Miyake, A., *J. Phys. Soc. Japan*, **15**, 1057 (1959).

16. Billmeyer, F. W., Jr., *Textbook of Polymer Chemistry*, Interscience, New York, 1957, pp. 15–17.

Résumé

On a étudié la résonance magnétique nucléaire dans la poly-2-vinylpyrrolidone solide dans un domaine de température allant de 77° à 450°K. On a obtenu des résultats expérimentaux au sujet des régions différemment organisées qui donnent lieu à des courbes complexes NMR. On décrit en détail les techniques expérimentales et les résultats obtenus. On propose une interprétation comparative détaillée des courbes NMR à deux composants en fonction de la température, en terme de mouvement dans les régions différemment organisées. La largeur de la composante correspondant aux régions cristallines ne dépend pas de la température dans un certain domaine au-dessus de la température de l'azote liquide; ceci est considéré comme indiquant une structure rigide. Aux températures plus élevées il y a une diminution graduelle de la largeur de la ligne indiquant un mouvement moléculaire segmentaire. La largeur de la ligne NMR représentant les régions amorphes ne change pas dans un domaine de basses températures à peu près semblable; lorsque la température augmente, la diminution ultérieure est plus forte que celle observée pour les régions cristallines; finalement elle décroît fortement et devient le composant étroit au-dessus de la température de transition vitreuse. La température de transition vitreuse de la polypyrrolidone semble décroître avec l'augmentation de la teneur en eau. Une comparaison entre la température de transition vitreuse de la poly yrrolidone sèche et de celles d'autres polyamides confirme l'observation que cette température de transition est d'autant plus basse que le rapport entre les groupes NH et CH_2 dans les polyamides est plus petit. On rapporte des valeurs empiriques du second moment à la température de l'azote liquide et à température de chambre de même qu' une estimation du second moment théorique pour un modèle en feuilles hypothétique.

Zusammenfassung

Die kernmagnetische Resonanz von festem Poly-2-pyrrolidon wurde im Temperatur-bereich von 77–450°K untersucht. Experimentelle Hinweise auf die verschieden geordneten Bereiche, die zu den zusammengesetzten NMR-Kurven beitragen, wurden erhalten. Versuchsmethodik und Ergebnisse werden im einzelnen beschrieben. Eine detaillierte, vergleichende Interpretierung von Zwei-Komponenten-NMR-Kurven als Funktion der Temperatur wird anhand der Bewegung in verschieden geordneten Berei-chen gegeben. Die Breite der den kristallinen Bereichen entsprechenden Komponente erwies sich in einem gewissen Temperaturbereich oberhalb von flüssigem Stickstoff als unabhängig von der Temperatur; dieses Verhalten wird als Hinweis auf eine starre Struktur betrachtet. Bei höheren Temperaturen besteht eine graduelle Abnahme der Linienbreite, was eine zunehmende Bewegung von Molekülsegmenten erkennen lässt. Die NMR-Linienbreite der amorphen Bereiche zeigte im angenähert gleichen Bereich niedriger Temperaturen keine Änderung; dann nahm sie mit steigender Temperatur rascher ab als diejenige der kristallinen Bereiche; schliesslich fiel sie scharf ab und wurde oberhalb der Glasumwandlungstemperatur zur engen Komponente. Die Glasumwand-lungstemperatur scheint bei Polypyrrolidon mit steigendem Wassergehalt niedriger zu werden. Ein Vergleich der Glasumwandlungstemperatur von trockenem Polypyrroli-don mit der anderer Polyamide liefert eine Bestätigung für die Beobachtung, dass die Temperatur dieser Umwandlung um so niedriger ist, je kleiner das Verhältnis von NH— zu Methylengruppen in einem Polyamid ist. Empirische Werte für das zweite Moment bei der Temperatur von flüssigem Stickstoff und bei Raumtemperatur sowie das für ein angenommenes Schichtenmodell erhaltene theoretische zweite Moment werden mitge-teilt.

Synthesis of Vinyl Polymers Containing α-Substituted γ-Butyrolactone Groups in Their Backbones

N. L. ZUTTY and F. J. WELCH, *Research and Development Department, Union Carbide Chemicals Company, South Charleston, West Virginia*

Synopsis

When vinyl chloride–methyl methacrylate copolymers having a uniform chain-to-chain composition, are pyrolyzed at temperatures around 150°C., an intramolecular lactonization occurs forming α-methyl-γ-butyrolactone groups in the polymer backbone concomitant with the quantitative elimination of methyl chloride. This reaction has been shown to be a general reaction for copolymers containing α-substituted γ-haloester groups in their backbone. The formation of the lactone groups in these polymers leads to increased chain rigidity and higher polymer softening points. Advantage has been taken of the gaseous alkyl halide elimination to produce rigid vinyl foams of good compressive strengths.

INTRODUCTION

The anomalous thermal behavior of vinyl halide–methyl methacrylate copolymers has puzzled several workers in past years. Blauer and Goldstein[1] noted that poly(vinyl bromide) was more thermally stable than a copolymer of vinyl bromide and methyl methacrylate, while Alfrey and co-workers[2] showed that vinyl chloride–methyl methacrylate copolymers gave off abnormally large amounts of chlorinated products upon reaction with zinc.

In studying uniform* methyl methacrylate–vinyl chloride copolymers we noted that, although these polymers evolved a gas above their softening points, they otherwise seemed quite stable and did not undergo the color change usually associated with the degradation of vinyl chloride copolymers. Examination of this phenomenon showed the evolved gas to be pure methyl chloride and the resulting polymer to contain lactone groups. Subsequent work showed the reaction to be as given in eq. (1).

$$
\left[\begin{array}{c} \text{CH}_3 \\ | \\ \text{-CH}_2\text{--CH--CH}_2\text{--C----} \\ | \qquad\quad | \\ \text{Cl} \qquad \text{C=O} \\ \quad\quad / \\ \text{CH}_3\text{--O} \end{array}\right]_{2}
\;\rightarrow\;
\left[\begin{array}{c} \text{CH}_3 \\ | \\ \text{-CH}_2\text{--CH--CH}_2\text{--C----} \\ | \qquad\quad | \\ \text{O--------C=O} \end{array}\right]_{x}
+ \text{CH}_3\text{Cl} \uparrow \quad (1)
$$

* By uniform copolymers it is meant copolymers that have been prepared by continuously feeding the faster copolymerizing monomer throughout the duration of the reaction so as to keep the ratio of polymerizing comonomers constant. This will lead to polymer chains having the highest ratios of adjacent comonomers. Polymer uniformity can also be achieved by running the reaction to low conversion so that the polymerizing comonomer ratio is not altered appreciably.

Although this is the first report of this lactonization reaction in copolymer systems, Marberg,[3] Wolff and co-workers,[4,5] and Perkin and Stone[6] all showed that α-substituted γ-bromoesters lactonized upon heating with the elimination of an alkyl halide. The homopolymeric poly(alkyl α-chloroacrylate) resins have been shown[7-9] to undergo lactonization upon heating with a variety of reagents, and the gaseous decomposition products from this pyrolysis reaction with no added reagents have been utilized to prepare foamed polymers.[10]

We have examined the applicability of this lactonization reaction and have shown it to be quite general. Unlike the pyrolysis of poly(alkyl α-chloroacrylates) which also dehydrohalogenate, the lactonization reaction is in some cases statistically quantitative for many γ-haloester-containing copolymers.

RESULTS AND DISCUSSION

The Lactonization Reaction

The specificity of the pyrolytic reaction occurring with vinyl chloride–methyl methacrylate copolymers is shown in Table I where it is compared to the pyrolysis of a blend of two homopolymers.

From these data it can be seen that the reaction was smooth and rapid when uniform copolymers were pyrolyzed. This is opposed to the polymer blend which, although yielding a small amount of methyl chloride, decomposed to give the expected pyrolysis products of homopolymer decomposition: benzene and hydrogen chloride from poly(vinyl chloride) and methyl methacrylate from poly(methyl methacrylate). A nonuniform copolymer, prepared by polymerizing a mixture of methyl methacrylate and vinyl chloride to complete conversion, behaved, upon pyrolysis, much like the mixture of two homopolymers, and not at all like the uniform copoly-

TABLE I
Pyrolysis of Vinyl Chloride Copolymers
Containing 12.1 Mole-% Methyl Methacrylate[a]

Resin type	Temp., °C.	Time, min.	% of theoretical CH_3Cl evolved	Gas analyses, mole-%[b]		
				CH_3Cl	HCl	Others
Uniform copolymer	150	287	74.4	99.8	0.2	Trace
"	175	77	76.2	99.8	0.2	Trace
"	193	43	82.2	100.0	—	—
Homopolymer blend	193	110	—	5.5	54.1	MMA, 35.7 benzene, 5.4

[a] All copolymer compositions via elemental halide analysis.

[b] All gas analyses via mass spectrometry.

TABLE II
Pyrolysis of Uniform Vinyl Chloride–Methyl Methacrylate (VCl–MMA)
Copolymers to about 75% Lactonization[a]

Resin composition		Pyrolysis temp., °C.	Time, min.	$\eta_{red\ (after)}$[b] $\overline{\eta_{red\ (before)}}$	Gas analysis, mole-%		
VCl, mole-%	MMA, mole-%				CH_3Cl	HCl	Other
29	71	150	353	0.83	100.0	—	—
88	12	175	77	1.24	99.8	0.2	Trace
88	12	193	43	1.25	100.0	—	—
80	20	200	15	1.07	99.9	0.1	Trace

[a] 75% of the theoretically contained methyl chloride, assuming that all possible vinyl chloride and methyl methacrylate units are adjacent in the polymer chain.

[b] Reduced viscosity after and before pyrolysis, (dl./g.).

mers. This is further demonstrated below in utilizing these resins to make polymeric foams (Fig. 3).

Table II presents some representative data showing the rapidity, specificity, and the intramolecular nature of the reaction.

From the data in Table II it is evident that uniform vinyl chloride–methyl methacrylate copolymers, upon pyrolysis, smoothly and quantitatively eliminate methyl chloride at a rapid rate which seems to be independent of polymer composition. It is also evident that the reaction is quite intramolecular in nature as is shown by the reasonable constancy of the reduced viscosity measurements before and after pyrolysis.

For comparison purposes Table III reports data on the pyrolysis of poly-(methyl α-chloroacrylate).
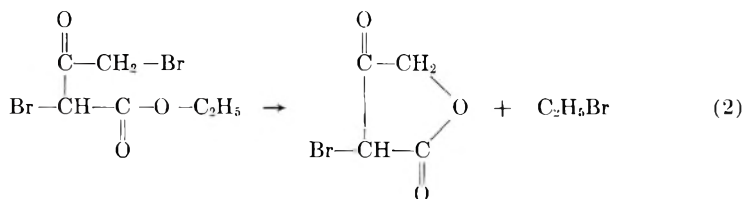
From the data in Table III it can be seen that poly(methyl α-chloroacrylate), when pyrolyzed, yields products from reactions other than lactonization. It was also evident during these experiments that the rate of lactonization of the α-chloroacrylate polymer was slower than that for the vinyl chloride–methyl methacrylate copolymers. Poly(methyl α-chloroacrylate) also degrades badly in molecular weight upon pyrolysis, again unlike the vinyl chloride–methyl methacrylate copolymers.

Other uniform γ-haloester copolymers were examined qualitatively for their ease of alkyl halide elimination. Pyrolyzing a series of copolymers con-

TABLE III
Pyrolysis of Poly(methyl α-Chloroacrylate) to about 75% Lactonization

Pyrolysis temp., °C.	Time, min.	$\eta_{red\ (after)}$ $\overline{\eta_{red\ (before)}}$	Gas analysis, mole-%			
			CH_3Cl	HCl	Benzene	Other
150	403	0.46	59.2	3.7	10.3	MeOH, 26.8
175	271	0.13	89.0	3.8	1.7	CO_2, 5.5
200	309	0.04	81.0	16.0	0.7	CO_2, 2.3

taining the same methacrylate comonomer but varying halogen containing comonomers led to results which showed, as expected, that bromine was more reactive than chlorine (vinyl bromide versus vinyl chloride) and that vinylidene chloride was more reactive than vinyl chloride. In a similar set of experiments, varying the ester group in the methacrylate series showed no effect on the rate or efficiency of lactonization. It was also found that α-substitution in the ester comonomer is necessary for lactonization. Although electron-withdrawing or electron-repelling groups on the α-carbon atom have some effect on the ability of the copolymers to lactonize (e.g., methyl α-chloroacrylate versus methyl methacrylate), ester comonomers containing no α-substituent form little, if any, lactone upon pyrolysis (e.g., ethyl acrylate copolymers). These results were in agreement with those of Perkin and Stone,[6] who performed the synthesis shown in eq. (2) at 120°C. in 2 hr.:

$$
\begin{array}{ccc}
\underset{\substack{\parallel \\ \text{C--CH}_2\text{--Br} \\ | \\ \text{Br--CH--C--O--C}_2\text{H}_5 \\ \parallel \\ \text{O}}}{\text{O}} & \rightarrow & \underset{\substack{\parallel \\ \text{C--CH}_2 \\ | \quad \backslash \\ | \quad \quad \text{O} \\ \text{Br--CH--C} \\ \parallel \\ \text{O}}}{\text{O}} + \text{C}_2\text{H}_5\text{Br}
\end{array} \qquad (2)
$$

It was noted that when the α-bromo atom was replaced with chlorine the reactant was stable under the experimental conditions, but when it was replaced by a methyl group the reaction proceeded normally and led to the expected α-methyl-β-ketobutyrolactone. The fact that the bulkier bromine and methyl groups promoted this reaction while the smaller chlorine atom did not is explainable only on steric, and not electronic, grounds.
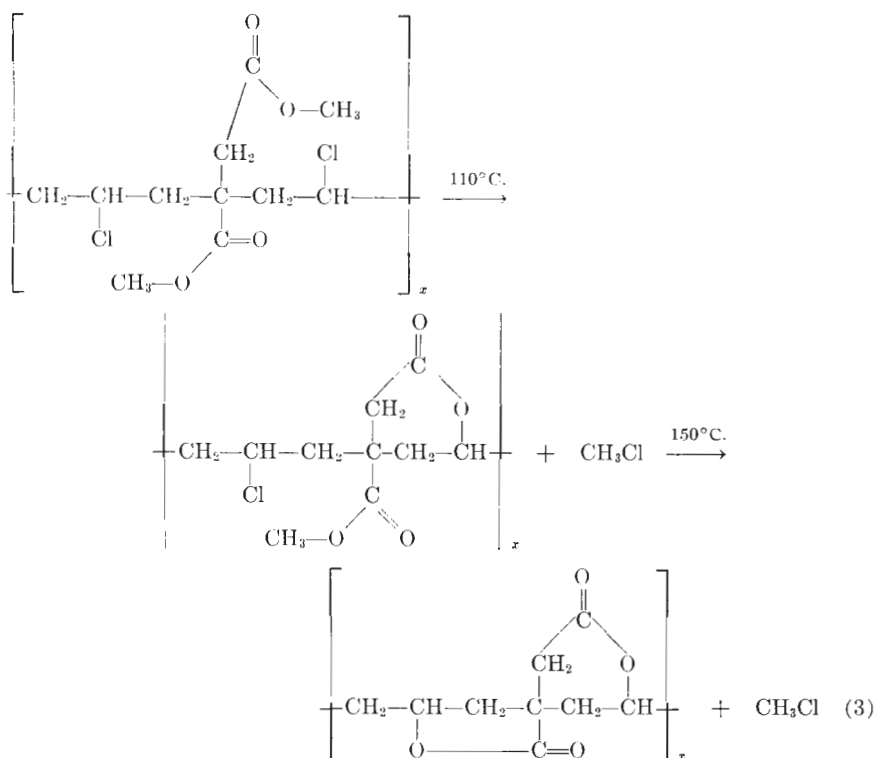
The pyrolysis of a uniform 20/80 wt.-% dimethylitaconate–vinyl chloride copolymer was followed by noting the disappearance of ester carbonyl and the appearance of lactone carbonyl by infrared techniques.[11] The six-membered δ-valerolactone was formed at 110-130°C. and the five-membered γ-butyrolactone at 150-170°C. No intermolecular reaction was found as determined by solubility measurements before and after pyrolysis. The reactions are given in eq. (3).

These experiments show, of course, that the six-membered ring is more easily formed than the five-membered ring. Presumably an alternating vinyl chloride–dialkylitaconate copolymer could yield only the six-membered lactone.

Lactonized Polymer Properties

When vinyl chloride–methyl methacrylate copolymers are heated to effect lactonization, the resulting linear chains may be considered to be terpolymers containing unreacted vinyl chloride units, unreacted methyl methacrylate units, and the resulting, newly formed, α-methyl-γ-butyrolactone units.

As might be expected, the formation of the lactone rings in the poly-

$$
\left[\begin{array}{c} \underset{\mid}{CH_2}-\underset{\underset{Cl}{\mid}}{CH}-CH_2-\underset{\underset{\underset{CH_3-O}{\nearrow}C=O}{\mid}}{\overset{\overset{O}{\parallel}}{\underset{CH_2}{\overset{C}{\overset{\nearrow}{\smallsetminus}}O-CH_3}}}\underset{\underset{\underset{}{}}{}}{CH_2}-\underset{Cl}{CH} \right]_x \xrightarrow{110^\circ C.}
$$

$$
\left[CH_2-\underset{\underset{Cl}{\mid}}{CH}-CH_2-\underset{\underset{\underset{CH_3-O}{\nearrow}\overset{C}{\underset{O}{\diagdown}}}{\mid}}{C}-CH_2-CH \right]_x + CH_3Cl \xrightarrow{150^\circ C.}
$$

$$
\left[CH_2-CH-CH_2-\underset{\underset{O}{\mid}}{C}-CH_2-\underset{\mid}{CH} \right]_x + CH_3Cl \quad (3)
$$

mer's backbone increases chain rigidity and thus raises the polymer's softening point. Table IV presents some data showing this phenomenon in two polymers, one of high and one of low methyl methacrylate content.

From the data in Table IV it can be seen that both copolymers lost chlorine (as methyl chloride) upon pyrolysis; that their molecular weights, measured by reduced viscosity, did not change appreciably during pyrolysis; and that in both polymers pyrolysis effected a large increase in heat distortion temperature.

Figures 1 and 2 show that the stiffness moduli versus temperature properties of these copolymers are only affected in the polymer's softening region by pyrolysis.

TABLE IV
Physical Properties of Vinyl Chloride–Methyl Methacrylate
Copolymers Before and After Pyrolysis

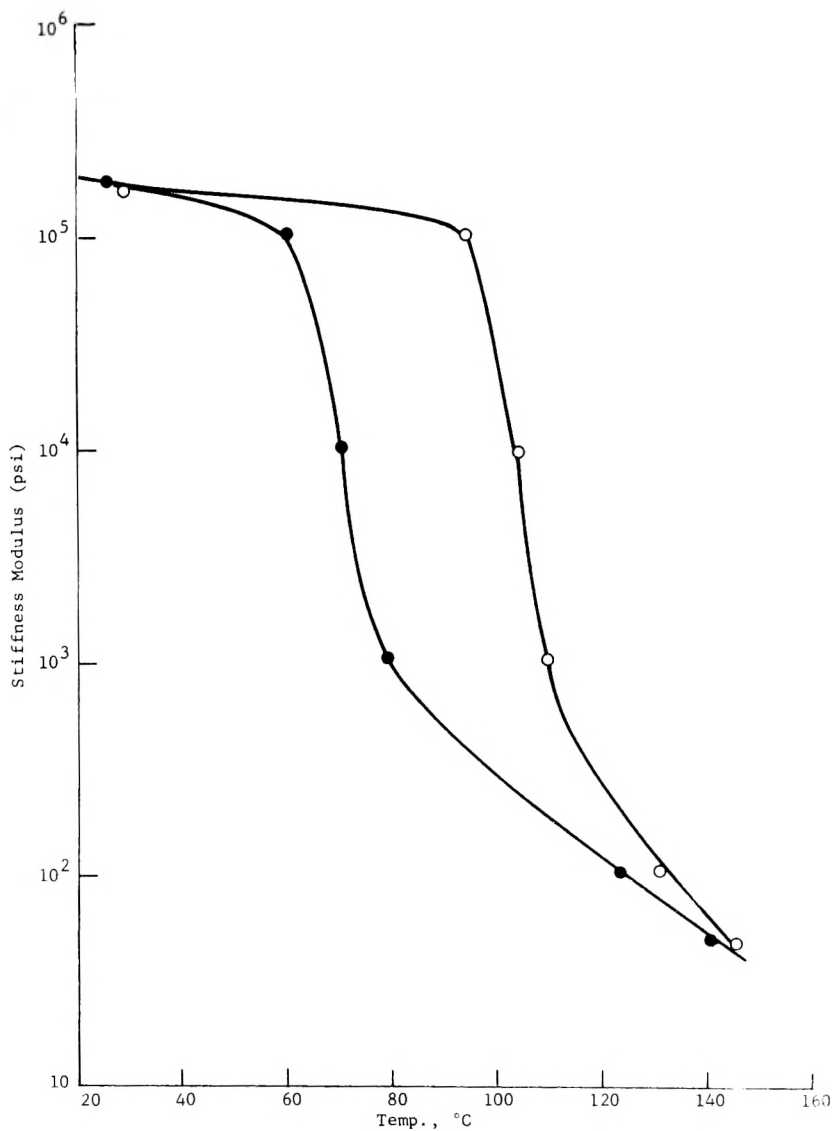|	Polymer A		Polymer B	
	Before	After	Before	After
Pyrolysis at 175°C., hr.	0	5	0	3
Vinyl chloride, wt.-%	29.6	12.5	72.0	69.0
Reduced viscosity, dl./g.	0.86	0.90	0.70	0.70
Heat distortion temp., °C.[a]	53	96	48	72

[a] ASTM Method D648–56 at 264 psi.

Fig. 1. Stiffness modulus vs. temperature for polymer A (Table IV): (●) before pyrolysis; (○) after pyrolysis.

When the lactone-containing polymers were tested for solubility and flammability it was found that the resins originally high in vinyl chloride behaved quite similarly to poly(vinyl chloride), being nonflammable and soluble in common solvents for poly(vinyl chloride), such as cyclohexanone and tetrahydrofuran. Those originally high in methyl methacrylate were, after pyrolysis, still soluble in ketones and aromatic hydrocarbons and burned readily.
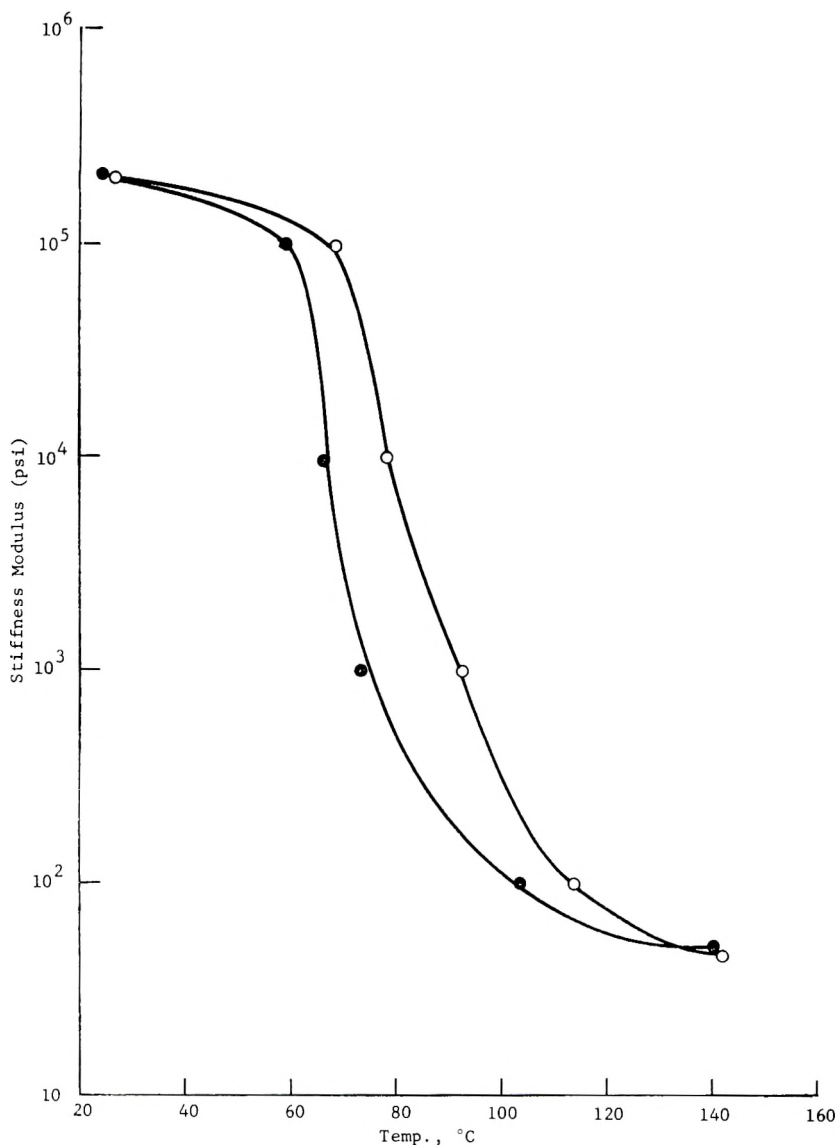
Fig. 2. Stiffness modulus vs. temperature for polymer B (Table IV): (●) before pyrolysis; (○) after pyrolysis.

Foaming of γ-Haloester Copolymers

It is quite simple to prepare foams from these γ-haloester containing copolymers. Table V describes some low density foams prepared by pyrolyzing several different copolymers in a mold sealed by O-rings under pressure at 180°C., then cooling the mold to 120°C., and releasing the pressure.

These foams generally had a rigid closed cell structure. Their room

TABLE V
Representative Foams Prepared by Pyrolysis of
Uniform γ-Haloester-Containing Copolymers

Resin[a]	Composition, wt.-%	Pyrolysis time at 180°C., min.	Foam density lb./ft.³
VCl/MMA	70/30	4	1.8
VCl/MMA	20/80	4	1.7
VCl/EMA	67/33	10	1.9
VCl/DMI	80/20	10	6.2
VCl/MMA/THFMA	18/50/32	10	4.6
VBr/MMA	63/37	2	5.9
VCl₂/MMA	67/33	2	2.6

[a] VCl = vinyl chloride; VCl$_2$ = vinylidene chloride; VBr = vinyl bromide; MMA = methyl methacrylate; EMA = ethyl methacrylate; THFMA = tetrahydrofurfuryl methacrylate; DMI = dimethyl itaconate.

temperature compressive strengths were equivalent to those of other foams, such as foamed rigid urethanes and foamed polystyrene of equivalent densities.

The low reactivity of nonuniform vinyl chloride–methyl methacrylate copolymers is vividly demonstrated in Figure 3. In Figure 3 the three samples are of equal weight, the smallest being a pyrolyzed but nonexpanded copolymer (obtained by the same pyrolysis conditions as the other samples but with cooling of the mold to room temperature before opening); the next larger shape is a completely expanded, nonuniform copolymer pre-

Fig. 3. Foamability of uniform and nonuniform vinyl chloride–methyl methacrylate copolymers.

pared by copolymerizing a mixture of vinyl chloride and methyl methacrylate to complete conversion; the largest shape is a foam prepared by pyrolyzing a uniform copolymer. Both the uniform and nonuniform copolymers in Figure 3 contained about 25 wt.-% methyl methacrylate before pyrolysis.

References

1. Blauer, G., and L. Goldstein, *J. Polymer Sci.*, **25**, 19 (1957).
2. Alfrey, T., Jr., H. Haas, and C. W. Lewis, *J. Am. Chem. Soc.*, **74**, 2025 (1952).
3. Marberg, R., *Ann.*, **294**, 104 (1897).
4. Wolff, L., and C. Schwabe, *Ann.*, **291**, 231, 234 (1896).
5. Wolff, L., and C. Ebstein, *Ann.*, **288**, 16 (1895).
6. Perkin, W. H., and J. F. Stone, *J. Chem. Soc.*, **1925**, 2275.
7. Marvel, C. S., E. D. Weil, L. B. Wakefield, and C. W. Fairbanks, *J. Am. Chem. Soc.*, **75**, 2326 (1953).
8. Smets, G., and P. Flore, *J. Polymer Sci.*, **35**, 519 (1959).
9. Crawford, J. W. C., and D. Plant, *J. Chem. Soc.*, **1952**, 4492.
10. Anspon, H. D., and F. E. Pschorr, U. S. Pat. 2,684,341 (1954).
11. Hendricks, E. G., private communication.

Résumé

Lorsqu'on pyrolyse à une température de 150°C. environ des copolymères de chlorure de vinyle et de méthacrylate de méthyle ayant une composition de chaîne uniforme, on obtient une lactonisation intramoléculaire formant des groupements α-méthyl-γ-butyrolactones dans la chaîne polymérique, concomittament à une élimination quantitative de chlorure de méthyle. On a montré que cette réaction est générale pour les copolymères contenant des groupements esters-α substitués et γ-halogénés dans leur chaîne. La formation de groupement lactonique dans ces polymères conduit à une augmentation de la rigidité de la chaîne et à des points de ramollissement plus élevés. On a utilisé le dégagement d'halogénure d'alcoyle gazeux pour produire des mousses vinyliques rigides ayant une bonne résistance à la compression.

Zusammenfassung

Bei der Pyrolyse von Vinylchlorid-Methylmethacrylatocopolymeren mit einheitlicher Kettenzusammensetzung bei Temperaturen um 150°C. tritt eine intramolekulare Lactonbildung auf, die zur Bildung von α-Methyl-γ-butyrolactongruppen in der Polymerkette mit gleichzeitiger quantitativer Eliminierung von Methylchlorid führt. Es wurde gezeigt, dass diese Reaktion allgemeine Bedeutung für Copolymere mit α-substituierten γ-Haloestergruppen in der Hauptkette hat. Die Bildung der Lactongruppen führt bei diesen Polymeren zu erhöhter Kettensteifigkeit und höherem Polymererweichungspunkt. Die Eliminierung des gasförmigen Alkylhalides konnte mit Vorteil zur Erzeugung starrer Vinylschaumstoffe mit guter Kompressionsfestigkeit benützt werden.

Carbonium Ion Rearrangement in the Cationic Polymerization of Branched Alpha Olefins

W. R. EDWARDS and N. F. CHAMBERLAIN, *Research and Development Humble Oil and Refining Company, Baytown, Texas*

Synopsis

The polymerization of olefins of the series (n-1)methyl-1-alkenes through carbonium ion intermediates appears to involve a rearrangement from a secondary to a tertiary carbonium ion. The structure of the final polymer, as determined by nuclear magnetic resonance, depends on the relative rates of rearrangement and polymerization. In the homogeneous aluminum chloride catalyzed systems investigated, the rate of rearrangement decreases with increasing length of the monomer and is comparable to the rate of polymerization for 4-methyl-1-pentene. The activation energy for rearrangement is lower than that for polymerization.

Introduction

The acid-catalyzed alkylation of benzene with 3-methyl-1-butene (I) produces different products with different catalysts and temperatures. Ipatieff et al.[1] showed that the homogeneous aluminum chloride system produced alkylation by the secondary carbonium ion giving 2-phenyl-3-methylbutane (II) while the two-phase sulfuric acid system produced alkylation by the tertiary carbonium ion giving *tert*-amylbenzene (III).
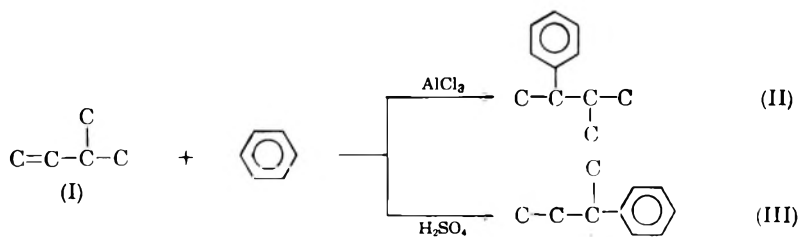
In a later study, Friedman and Morritz[2] found that at −40°C., with the aluminum chloride system, the alkylation produced pure *tert*-amylbenzene, whereas at 21°C., pure 2-phenyl-3-methylbutane was the product. These results can be explained by a mechanism in which isomerization precedes alkylation.

In a recent study by Ketley and Harvey[3] of the polymerization of propylene with aluminum halide catalysts, a mechanism was proposed which involved a rearrangement from the higher energy secondary to the lower energy

tertiary carbonium ion. The results obtained by Ipatieff et al.[1] and by Friedman and Morritz[2] may also be explained by this mechanism. In the high temperature alkylation of benzene with 3-methyl-1-butene, the rate of attack of the carbonium ion is sufficiently great that alkylation takes place before the carbonium ion shift can occur. At the lower temperature, however, the decreased rate of alkylation permits rearrangement to precede alkylation. It would be expected that in the sulfuric acid system, where a rate limiting step of passage through the interface is involved,[4] the shift occurs at a much faster rate than does the alkylation step. A nuclear magnetic resonance (NMR) study of the polymers of olefins of the series $(n-1)$-methyl-1-alkenes, where n is the number of carbons in the monomer chain, has provided strong evidence for the carbonium ion rearrangement and has indicated the relative rates and activation energies of rearrangement and polymerization.

Nuclear Magnetic Resonance Spectra

Although wide line NMR has been used for some time to characterize saturated polymers of this type[5−9] the application of high resolution NMR to the study of the structures of high molecular weight saturated hydrocarbons is relatively new.[10] The value of high resolution NMR in such cases stems partially from the fact that even though the chemical shifts are small, the spin-spin multiplets for the methyl groups are easily recognizable as distorted first-order multiplets. Methyl resonances from CH_3—CH_2 groups appear as triplets ($J = 4$–8 cycles/sec.), those from CH_3—CH groups appear as doublets ($J \sim 6$ cycles/sec.), and those from CH_3—C groups appear as singlets.[11] Mixtures of these groups produce complex but stable patterns which are recognizable by comparison with spectra of known compounds. The chemical shifts are large enough to produce usable band separations so that band positions and intensities can be used to estimate the relative numbers of CH_3, CH_2, and CH groups in the average repeating unit. It must be emphasized that satisfactory comparison of the spectra of saturates requires the use of a spectrometer of exceptionally high stability. Proton signal control of the magnetic field or of the field-frequency ratio is almost essential.

Nuclear magnetic resonance spectra representative of acid-catalyzed polymers of $(n-1)$methyl-1-alkenes produced at low temperature are presented in Figure 1. Although a number of acid catalysts would be expected to produce polymers of similar structural configuration, the molecular weights and physical properties would be unpredictable. The spectra shown in Figure 1 are all of high molecular weight elastomers produced with aluminum chloride catalyst at −73°C.

Polyisobutylene, which is known to have structure IV, produces the sharp singlet resonances characteristic of geminal methyls (CH_3—C groups) and isolated methylenes (Fig. 1A). This spectrum is offset toward low field from the spectra of the other polymers as a result of the extreme crowding and steric hindrance of the various sections of this molecule. A smaller
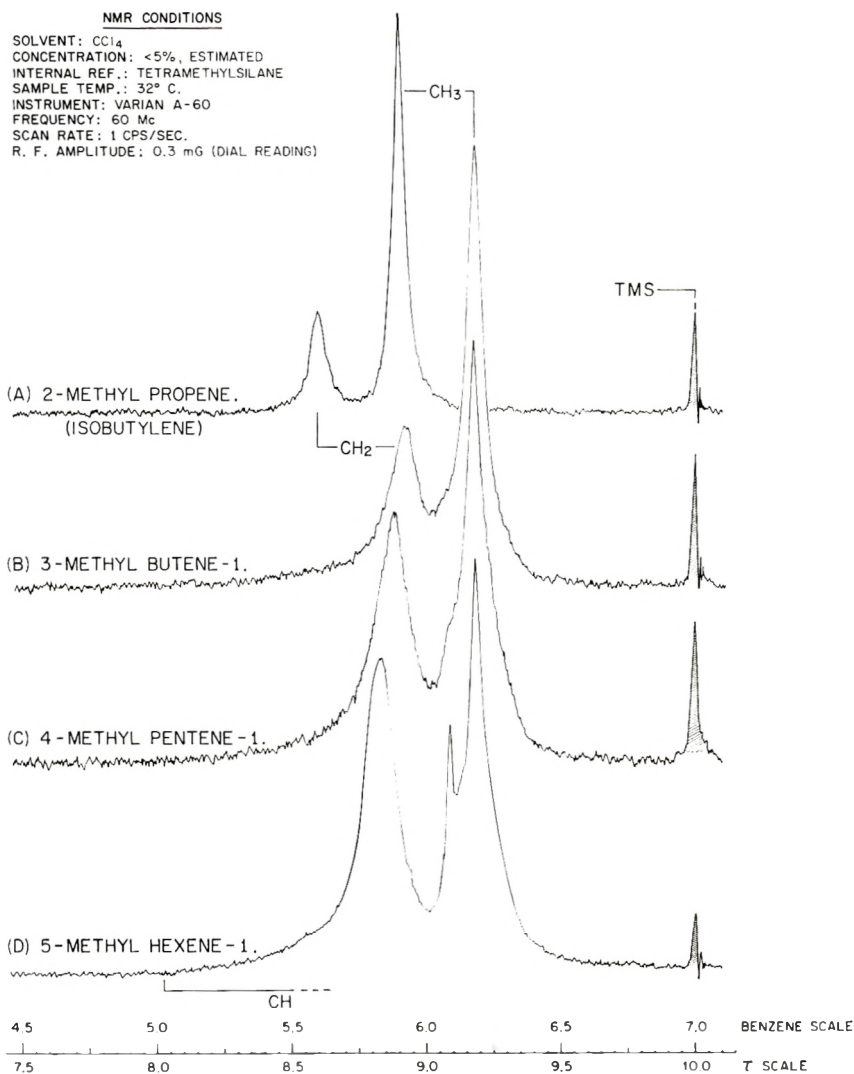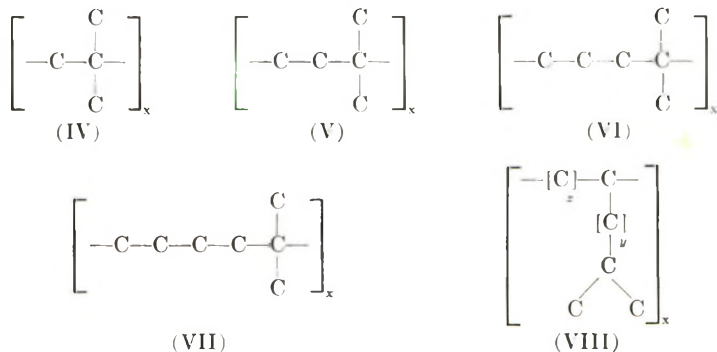
Fig. 1. Nuclear magnetic resonance spectra of acid-catalyzed polymers of the series (n-1)-methyl-1-alkene (AlCl₃ polymerized at −73°C.).

shift in the same direction is noted in the spectrum of 2,2,4,4-tetramethylpentane, in which the steric arrangement is similar to that of polyisobutylene. The downfield shift is less pronounced in the spectra of 2,2,3,3-tetramethylbutane and 2,2,5,5-tetramethylhexane, and is not present at all in the spectra of 3,3,4,4-tetramethylhexane and 2,2,7,7-tetramethyloctane. In the tetramethylbutane and the tetramethylhexane in which the quaternary carbons are adjacent, the geminal methyls are relatively free to rotate about the bond joining the quaternary carbons. The bending introduced by the methylene in the tetramethylpentane, however, produces much

greater crowding of the methyls and severe hindrance to all rotation (Stuart and Briegleb models), resulting in the downfield resonance shift. Introduction of two or more methylenes between the geminal methyls relieves the crowding and makes free rotation possible again, and the resonances resume their normal positions. Thus, the marked downfield shift of the hydrogen resonances, particularly of the methyl hydrogen resonances, indicates severe crowding of the methyl groups in the molecule.

$$\begin{bmatrix} & \text{C} & \\ & | & \\ -\text{C}- & \text{C}- \\ & | & \\ & \text{C} & \end{bmatrix}_x \qquad \begin{bmatrix} & & \text{C} & \\ & & | & \\ -\text{C}- & \text{C}- & \text{C}- \\ & & | & \\ & & \text{C} & \end{bmatrix}_x \qquad \begin{bmatrix} & & & \text{C} & \\ & & & | & \\ -\text{C}- & \text{C}- & \text{C}- & \text{C} \\ & & & | & \\ & & & \text{C} & \end{bmatrix}_x$$

(IV)   (V)   (VI)

$$\begin{bmatrix} & & & \text{C} & \\ & & & | & \\ -\text{C}- & \text{C}- & \text{C}- & \text{C}- & \text{C} \\ & & & | & \\ & & & \text{C} & \end{bmatrix}_x \qquad \begin{bmatrix} -[\text{C}]_z- & \text{C}- \\ | \\ [\text{C}]_y \\ | \\ \text{C} \\ / \quad \backslash \\ \text{C} \quad \text{C} \end{bmatrix}_x$$

(VII)   (VIII)

The spectrum of the polymer of 3-methyl-1-butene, Figure 1B, exhibits sharp resonances similar to those of Figure 1A, except that the resonances are in their normal positions. This indicates that this polymer has geminal methyls separated by more than one methylene, and is assigned the structure V. The polymer of 4-methyl-1-pentene, Figure 1C and structure VI, exhibits somewhat broader resonance bands, indicating that groups other than geminal methyls and isolated methylenes are beginning to show up in this polymer. The polymer of 5-methyl-1-hexene, Figure 1D, shows definite evidence of the doublet which is characteristic of CH_3CH (including isopropyl) groups. This resonance is attributed to the presence of structure VIII in the polymer. On the other hand, spectrum D still exhibits a reasonably sharp methyl peak which is superimposed on the aforementioned doublet, and a reasonably sharp methylene band, both of which are attributed to the presence of structure VII in this polymer. It is estimated from this spectrum that VII and VIII are present in about equimolar concentrations. For this series of polymers, the ratio of intensities of the methyl to methylene resonances decreases with increasing length of the monomer chain, as is required by the proposed polymer structures.

It is concluded that the structures produced by the cationic polymerization at −73°C. of this series of alpha olefins are characterized by geminal dimethyls and isolated methylene groups for the lower members of the series, with an increasing percentage of dangling isopropyl structures accompanying increasing chain length of the monomer.

The NMR spectra of the polymers produced from this series of olefins at 0°C. are presented in Figure 2. The spectrum of the polymer of 3-methyl-1-butene produced at 0°C., Figure 2A, is indistinguishable from that of the polymer produced at −73°C., Figure 1B. The spectra of the polymers of
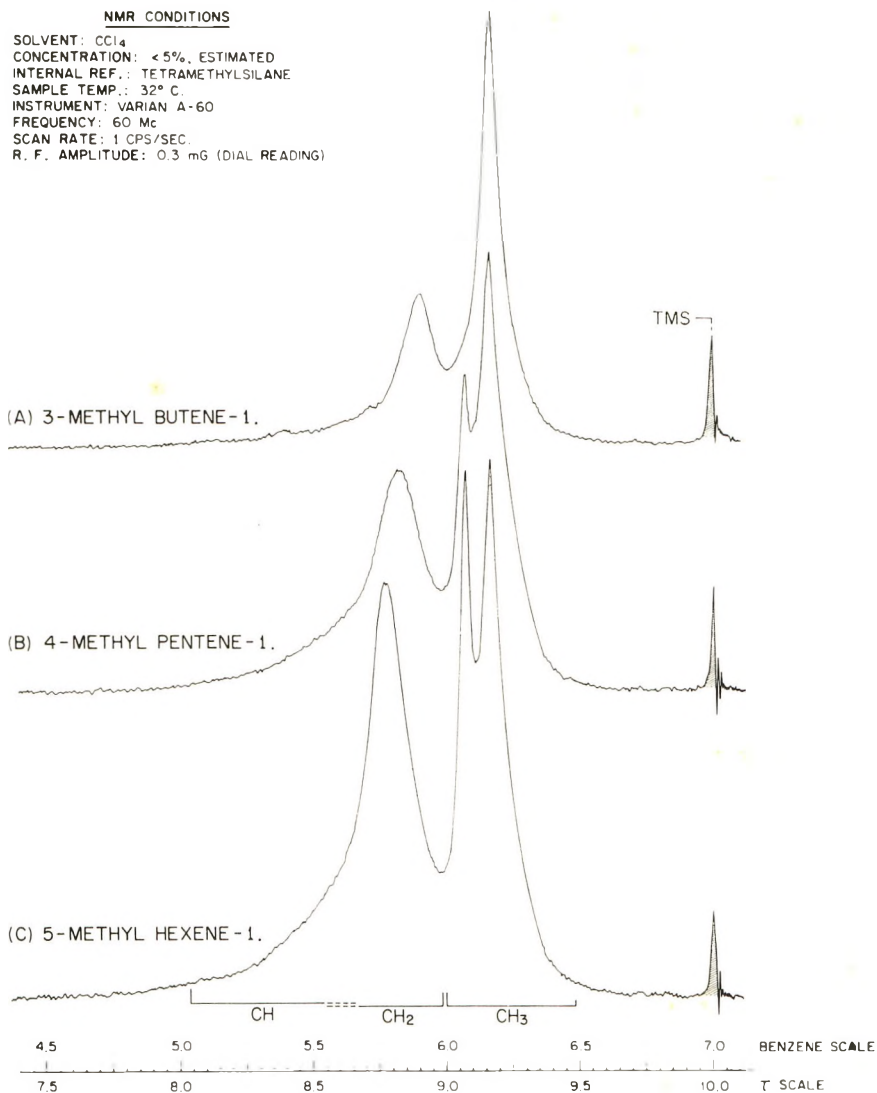
Fig. 2. Nuclear magnetic resonance spectra of acid-catalyzed polymers of the series (n-1)methyl-1-alkene (AlCl₃ polymerized at 0°C.).

4-methyl-1-pentene and 5-methyl-1-hexene, Figures 2B and 2C, on the other hand, exhibit significantly greater proportions of the doublet methyl resonance and of the broad low field resonance indicative of CH groups. It is therefore concluded that polymers produced from these two olefins at the higher temperature contain significantly higher proportions of dangling isopropyl groups than do those produced at the lower temperature. In fact, the 5-methyl-1-hexene polymer is almost entirely of structure VIII.

It is interesting to note that in both Figures 1 and 2 the center of the methylene resonance moves downfield slightly with an increase in the size
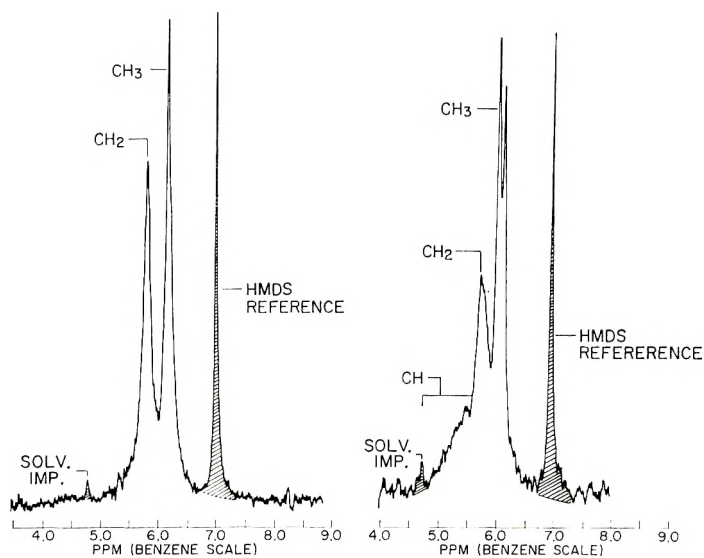
Fig. 3. Nuclear magnetic resonance spectra of polymers of 4-methyl-1-pentene. Solvent: 2-chlorothiophene; concentration: $<5\%$, estimated; internal ref.: hexamethyldisiloxane; sample temperature: 120°C.; instrument: modified Varian V-4300 with proton signal control of field; frequency: 60 Mc.; scan rate: 2 cycles/sec.; r.f. amplitude: 0.06 mg. (equivalent to 0.2 mg. dial reading on A-60). A (left): aluminum chloride catalyzed. B (right): alkyl metal catalyzed.

of the monomer, while the methyl resonance does not shift. The cause for this is not clear, but it may be tentatively attributed to the effects of increasing numbers of methylene groups between branches in the resulting polymers. If this is true, it means that the value of y in structure VIII is essentially zero. It is hoped that continued study of the spectra of pure paraffins will clear up this point.

The polymers produced from this same series of olefins by alkyl metal catalysis are generally considered to consist entirely of 1,2 enchainments, resulting in polymers which consist entirely of structure VIII with $z = 1$. Unfortunately, for study by NMR, these polymers are only very slightly soluble in acceptable solvents, even at elevated temperatures. It has not been possible to observe the NMR spectrum of the alkyl metal-catalyzed polymer of 3-methyl-1-butene, but it has been possible to observe the spectrum of the corresponding polymer of 4-methyl-1-pentene. The spectra of both the acid-catalyzed and alkyl metal-catalyzed polymers of 4-methyl-1-pentene monomer, obtained under identical conditions, are presented in Figure 3. The spectrum of the alkyl metal-catalyzed polymer, Figure 3B, is completely compatible with structure VIII ($z = 1$, $y = 1$), exhibiting the doublet methyl resonance, the broad resonance characteristic of the CH groups, and the CH$_2$ resonance. On the other hand, the sharp singlet methyl resonance, the sharp methylene resonance, and the absence of an observable resonance attributable to CH hydrogens makes the spectrum of

the acid-catalyzed polymer, Figure 3A, completely incompatible with structure VIII. This spectrum is completely compatible with structure VI. It is therefore concluded that the structures of the polymers produced by these two methods of catalysis are completely different, representing different methods of enchainment of the monomers.

The polymer structures described in the preceding paragraphs are not adequately explained as the result of isomerization of the olefins. For example, the structural units formed from 3-methyl-1-butene by isomerization followed by polymerization would be as follows:

$$\left(\begin{array}{c} \text{C} \\ | \\ -\text{C}-\text{C}- \\ | \\ \text{C} \\ | \\ \text{C} \end{array}\right)_x \quad \text{and} \quad \left(\begin{array}{c} \text{C}\ \ \text{C} \\ |\ \ | \\ -\text{C}-\text{C}- \\ | \\ \text{C} \end{array}\right)_x$$
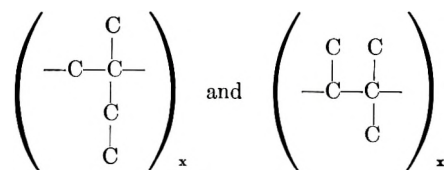
These structural units, which are readily detectible by NMR, are not observed.

Polymerization Mechanism

The structures found for the polymers produced by acid catalysis may be explained by a mechanism involving rearrangement of the carbonium ion through a hydride shift as follows:

1. Initiation:

$$\text{C}=\text{C}-(\text{C})_m-\underset{\underset{\text{C}}{|}}{\text{C}}-\text{C} + \text{H}^+ \rightarrow \text{C}-\overset{+}{\text{C}}-(\text{C})_m-\underset{\underset{\text{C}}{|}}{\text{C}}-\text{C}$$

2. Hydride shift:

$$\text{C}-\overset{+}{\text{C}}-(\text{C}_m)-\underset{\underset{\text{C}}{|}}{\overset{\overset{\text{H}}{|}}{\text{C}}}-\text{C} \rightarrow \text{C}-\text{C}-(\text{C}_m)-\underset{\underset{\text{C}}{|}}{\overset{\overset{\text{C}}{|}}{\text{C}}}{}^+$$

3. Propagation:

$$\text{C}-\text{C}-(\text{C})_m-\underset{\underset{\text{C}}{|}}{\overset{\overset{\text{C}}{|}}{\text{C}}}{}^+ + \text{C}=\text{C}-(\text{C})_m-\underset{\underset{\text{C}}{|}}{\text{C}}-\text{C} \rightarrow \text{C}-\text{C}-(\text{C})_m-\underset{\underset{\text{C}}{|}}{\overset{\overset{\text{C}}{|}}{\text{C}}}-\text{C}-\overset{+}{\text{C}}-(\text{C})_m-\underset{\underset{\text{C}}{|}}{\text{C}}-\text{C}$$
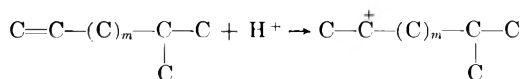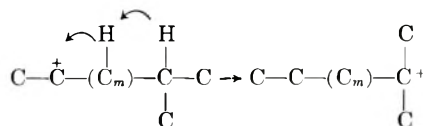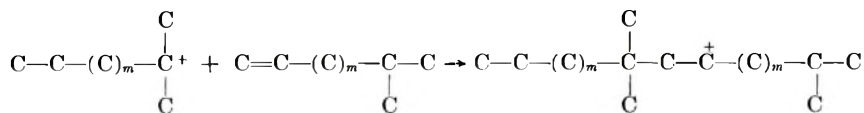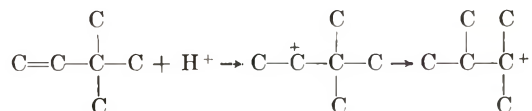
When $m = 0$, the rearrangement always occurs over the entire temperature range investigated. When $m = 1$, the increased length of the path over which the hydride shift must occur results in a substantial amount of non-1,4 polymerization at 0°C., although 1,4 polymerization is predominant at −73°C. For $m = 2$, non-1,5 polymerization occurs almost completely at 0°C., but is reduced to less than 50% at −73°C. These findings are consistent with a multiple step hydride transfer. Therefore, the 4-methyl-1-pentene polymer may contain 1,3 linkages and the 5-methyl-1-hexene

polymer may contain 1,3 and 1,4 linkages. These linkages are not distinguishable from 1,2 linkages by NMR.

It may be seen from the comparison of the polymers produced at $-73°C$. with those produced at $0°C$. that, at the lower temperature, the hydride shift is faster than the propagation step. As the temperature is increased, the rate of propagation increases faster than the rate of hydride shift, indicating that the activation energy for propagation is higher than that for the hydride shift.

If methyl groups as well as hydrogens can shift on a carbonium ion, it should be possible to produce 1,3 (or 1,4) polymerization in doubly branched alpha olefins:

$$C=C-\underset{\underset{C}{|}}{\overset{\overset{C}{|}}{C}}-C + H^+ \rightarrow C-\overset{+}{C}-\underset{\underset{C}{|}}{\overset{\overset{C}{|}}{C}}-C \rightarrow C-\underset{\underset{C}{|}}{\overset{\overset{C\ \ C}{|\ \ |}}{C}}-\overset{+}{C}$$

Attempts to polymerize 3,3-dimethyl-1-butene by procedure 3 were unsuccessful. This can be attributed to the severe steric hindrance associated with the polymer which would result from 1,2 polymerization. The NMR spectrum of the polymer of 4,4-dimethyl-1-pentene is indicative of a 1,2 polymerization mechanism. It is concluded that the carbonium ion rearrangement involving a methyl shift does not occur under the polymerization conditions of procedure 3.

Experimental

Materials

3-Methyl-1-butene and 4-methyl-1-pentene (99+ mole-% minimum) were purchased from the Phillips Petroleum Co. The 3-methyl-1-butene was passed over basic alumina; the 4-methyl-1-pentene was used as received. The 5-methyl-1-hexene, 3,3-dimethyl-1-butene, and 4,4-dimethyl-1-pentene were API standard samples purchased from the American Petroleum Institute and had a purity of 99.80–99.94 mole-%. The methyl chloride was purchased from Matheson Chemical Co., 99.5 mole-% minimum purity, and used as received. The aluminum chloride, reagent grade, was purchased from Mallinckrodt Chemical Corp. and used as received.

The polyisobutylene sample was commercial MM Vistanex. The alkyl metal-catalyzed polymers of 3-methyl-1-butene and 4-methyl-1-pentene were obtained from Dr. F. B. Marktscheffel of Esso Research and Engineering Co.

Procedure 1

Low temperature polymerization of 3-methyl-1-butene and 4-methyl-1-pentene. A mixture of 20 g. of methyl chloride and 0.25 g. of aluminum chloride was stirred for 30 min. in a Dry Ice-alcohol bath at $-73°C$. Five grams of olefin were added, and stirring was continued for 2–5 min. The

mixture was then poured into hot water to flash off the methyl chloride and quench the aluminum chloride. The solid, rubbery polymer was then dried under vacuum. Complete conversion was obtained.

Procedure 2

Low temperature polymerization of 5-methyl-1-hexene. Same as procedure *1* except stirring was continued for 30 min. after addition of the olefin.

Procedure 3

High temperature polymerization of all olefins. Aluminum chloride (0.02 g.) was added to 2 ml. of olefin in a test tube immersed in an ice bath at 0°C. The mixture was shaken at 5–10 min. intervals over a 3-hr. period. The mixture then was dissolved in benzene and the polymer was precipitated by the addition of acetone. The polymer, a heavy, viscous oil, was dried under vacuum.

References

1. Ipatieff, V. N., H. Pines, and L. Schmerling, *J. Org. Chem.*, **5**, 253 (1940).
2. Friedman, B. S., and F. L. Morritz, *J. Am. Chem. Soc.*, **78**, 2000 (1956).
3. Ketley, A. D., and M. C. Harvey, *J. Org. Chem.*, **26**, 4649 (1961).
4. Edwards, W. R., and R. D. Wesselhoft, unpublished data.
5. Slichter, W. P., *Fortschr. Hochpolymer.-Forsch.*, **1**, 35 (1958); *Bell Telephone System, Tech. Publ. Monographs*, **3049**.
6. Powles, J. G., *Polymer*, **1**, 219 (1960).
7. Herring, M. J., and J. A. S. Smith, *J. Chem. Soc.*, **1960**, 273.
8. Gupta, R. P., *Makromol. Chem.*, **42**, 248 (1961).
9. Woodward, A. E., A. Odajima, and J. A. Sauer, *J. Phys. Chem.*, **65**, 1384 (1961).
10. Stehling, F. C., "Stereochemical Configurations of Polypropenes by High Resolution Nuclear Magnetic Resonance," paper presented before the 141st National ACS Meeting, Washington, D.C., March 1962.
11. Mair, B. J., N. C. Krouskop, and T. J. Mayer, *J. Chem. Eng. Data*, **7**, 420 (1962).

Résumé

La polymérisation des oléfines de la série des (*n*-1)méthyl-1-alkènes, par un ion carbonium intermédiaire, cause apparemment un réarrangement de l'ion carbonium secondaire en un ion tertiaire. La structure du polymère final, déterminée par RMN, dépend des vitesses relatives de réarrangement et de polymérisation. Dans les systèmes homogènes étudiés, catalysés par le chlorure d'aluminium, les vitesses de réarranegment décroissent avec la longueur croissante du monomère. Pour le 4-méthyl-1-pentène, elle est comparable avec la vitesse de polymérisation. L'énergie d'activation du réarrangement est moins grande que celle de la polymérisation.

Zusammenfassung

Die Polymerisation von Olefinen der Reihe der (*n*-1)Methyl-1-alkene über einen Karboniumionmechanismus scheint mit einer Umlagerung vom sekundären zum tertiären Karboniumion verknüpft zu sein. Die Struktur des erhaltenen Polymeren, wie sie durch NMR bestimmt wird, hängt vom Verhältnis der Geschwindigkeit der Um-

lagerung und Polymerisation ab. In den untersuchten, homogenen, Aluminiumchlorid-katalysierten Systemen, nimmt die Umlagerungsgeschwindigkeit mit zunehmender Länge des Monomeren ab und ist beim 4-Methyl-1-penten der Polymerisationsgeschwindigkeit vergleichbar. Die Aktivierungsenergie der Umlagerung ist kleiner als die der Polymerisation.

Graft Copolymers of Polyacrylic Acid with Desoxyribonucleic Acid (DNA)

KWEI-PING SHEN KWEI, *Department of Chemistry, Newark College of Engineering, Newark, New Jersey*

Synopsis

Graft copolymers of polyacrylic acid with DNA were prepared and isolated. The grafted DNA copolymers had different solubility behaviors and ultraviolet absorption characteristics than those of the DNA.

INTRODUCTION

A theory has been developed by Scheraga[1] to account for the effect of side-chain hydrogen bonds on the elastic properties of protein fibers and on the configuration of proteins in solution.   The stabilization of the crystalline form of the protein by side-chain hydrogen bonding was proposed both in Scheraga's theory and in a previous theory from Schellman.[2]   However, no extensive experimental verifications of the theory were advanced, owing mainly to the difficulty in the synthesis of suitable model compounds.   In this paper, the preparation and the isolation of the graft copolymers of DNA with polyacrylic acid (PAA) side chains which are capable of hydrogen bonding will be discussed.   The DNA was noticed to be an effective chain transfer agent for a number of monomers.   It is hoped that this technique may be used to prepare suitable model compounds to test the proposed theories.

EXPERIMENTAL

The DNA from fish milt was obtained from the General Biochemicals Company in Chagrin Fall, Ohio.

1. Preparation of Graft Copolymers

Several graft copolymers were prepared by polymerizing acrylic acid (10% by weight) in a dilute NH_4OH solution of DNA (10% by weight) with the use of potassium persulfate (0.2%) as the initiator.   The pH values of the media before polymerization were varied between 9.6 and 7.0.   Several other graft copolymers were also prepared from a DNA (4%) solution in the sodium chloride–sodium citrate medium from pH 5.0 to 7.0.   The reaction mixtures were flushed with nitrogen and polymerized

in a water bath at 50°C. for 3 hr.   The polymer mixtures were then separated according to their different solubilities described as follows.

The DNA was insoluble in most of the organic solvents, but was sparingly soluble in pure water (about 10 mg./100 ml.), slightly soluble in $0.4M$ NaCl solution, and easily dissolved in the solution of sodium chloride and sodium citrate.   The polyacrylic acid was insoluble in $0.4M$ NaCl solution but was soluble in acetone, methanol, and water.   The graft copolymers were found to be insoluble in methanol but very soluble in water and $0.4M$ NaCl solution.   The following separative procedures were established according to the above solubility behaviors.

2. Isolation of the Graft Polymers

Copolymer A.   The polymerized mixtures of sample A (at pH 9.6) were precipitated dropwise into a large volume of acetone with vigorous stirring. The polyacrylic acid remained in acetone, while the graft copolymer and the unreacted DNA were precipitated out.   The precipitates were redissolved into water and the solution was adjusted to pH 7.0 by dilute HCl.   The pure DNA slowly settled down from the aqueous solution of the graft copolymer. After repeated times of filtration and centrifugation, the clear brownish solution of the graft copolymer was reprecipitated dropwise into a large volume of methanol.   The precipitate was freeze dried from its water solution which had a pH of 6.   The yield was 0.2 g. of yellowish powder.

Copolymer B.   The polymers from sample B (at pH 7.0) were similarly precipitated into acetone and redissolved in water.   A $0.4M$ NaCl solution was intended to be used as a precipitant to reprecipitate the polymer mixtures.   As the polyacrylic acid was insoluble in the $0.4M$ NaCl solution and the DNA was only slightly soluble in it, both of the two homopolymers and the graft copolymer might be precipitated out.   No precipitate, however, was obtained.   The brown $0.4M$ NaCl solution which contained only the graft copolymer was clear.   The solubility pattern of the graft copolymer did not fall between those of DNA and polyacrylic acid, but rather shifted to an increased solubility in the $0.4M$ NaCl solution.   After precipitating the graft copolymer into a large volume of methanol., the copolymer was freeze dried from its water solution to give 0.55 g. of yellowish powder.

Copolymer C.   The sample C was polymerized in a $0.4M$ NaCl–$0.04M$ $NaC_6H_5O_7$ medium at pH 5.0 without dilute ammonium hydroxide.   The separative procedure was similar to that of sample A.   The salts from the medium were partly carried down by the graft copolymers and partly remained in the acetone-water mixture.   The yield of graft copolymer was 0.75 g.

3. Ultraviolet Measurements

The ultraviolet absorption curves of the graft copolymers and the two homopolymers were measured separately by a Beckman DU spectrophotometer at room temperature.

4. Turbidimetry

The turbidimetric titrations of the 0.1% aqueous solutions of pure DNA and the isolated graft copolymer were carried out separately by using the Brice-Phoenix light-scattering spectrophotometer as in a previous paper.[3]   Acetone was used as the common precipitant.

5. Preparation of Graft Copolymers by High Energy Radiation

A mixture of 2 g. DNA and 10 ml. acrylic acid were irradiated in a frozen state at −60 C. by the Van der Graaff electron generator.   The total dosage was 1 m.e.v. after five continuous passages.   The mixture was noticed to have polymerized in the solid state, because the mixture did not melt when it was allowed to recover to room temperature.   The mixture was dissolved in water and separated according to the procedures for sample C.   All of the DNA were found to be reacted.   The yield of graft copolymers was 0.2 g.   The graft copolymers had the similar ultraviolet absorption characteristics as the other graft copolymers which were prepared through chain transfer reactions.

RESULTS AND DISCUSSION

A set of similar ultraviolet absorption curves (Fig. 2) were obtained from the aqueous solutions of the isolated graft copolymers of DNA with polyacrylic acid prepared from different media.   The absorption curves showed two separate peaks, namely, an intense one at 250 mμ and another at 265 mμ.   These characteristics were obviously different from those of DNA, which absorbed at 260 mμ and of polyacrylic acid which absorbed only below 230 mμ (Fig. 1).

The ultraviolet absorption curves of the mechanical mixtures of DNA and the graft copolymers showed the absorption characteristics of DNA between 220–320 mμ (Fig. 1).   The unreacted DNA from separative procedures did not change in the ultraviolet absorption characteristics.   It was therefore concluded that the graft copolymers were completely isolated from the unreacted DNA.   The presence of polyacrylic acid did not alter the absorption characteristics of DNA.

The separative procedures were also proved to be effective by the turbidimetric titrations.[3]   Owing to the different solubility behaviors of DNA and the graft copolymer, different amounts of acetone were required to precipitate the polymers.   The titrations of a pure 0.1% DNA aqueous solution and a 0.1% of the isolated graft copolymer aqueous solution by acetone were done separately.   The DNA solution required 2 ml. of acetone, and the graft copolymer required 4 ml. of acetone to give the maximum turbidities (Fig. 3).   The broad peak of the turbidity curve for the graft copolymer probably indicated a wide distribution of the molecular size, and molecular weight.   The DNA probably had a comparatively narrow distribution of macromolecular species.

The chemical analyses (Table I) for nitrogen and phosphorus in the graft copolymers of DNA were checked independently in two laboratories. The ratios of nitrogen to phosphorus in the graft copolymers B and C were about 1.8–2.3 times higher than that of DNA. Presumably some change in the DNA composition is indicated. Some of the phosphate groups in DNA probably have been displaced by hydrolytic cleavage[4] in acidic and neutral media. The presence of sodium chloride and sodium citrate salts
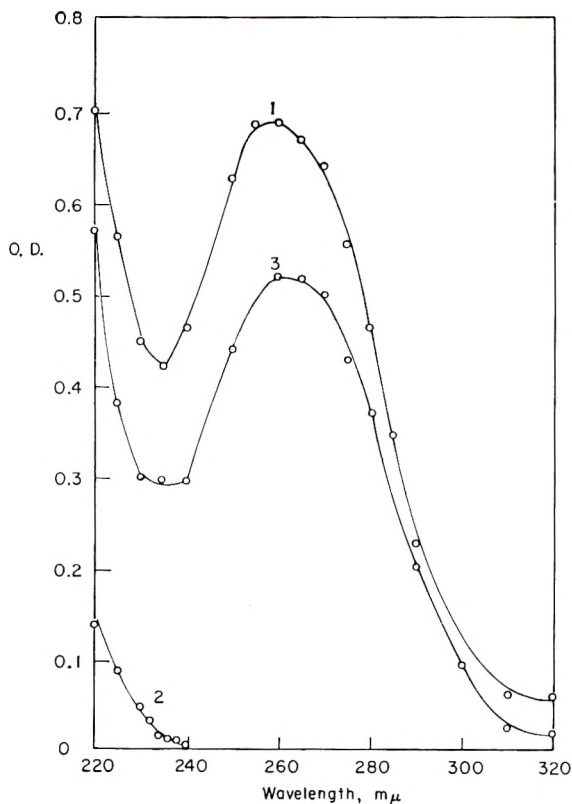

Fig. 1. Ultraviolet absorption curves of the homopolymers: (1) DNA separated after polymerization and before polymerization; (2) polyacrylic acid; (3) mixture of DNA and polyacrylic acid.

might also enhance the hydrolytic reactions.[4] The graft copolymer A, however, has the same nitrogen to phosphorus ratio as DNA. Apparently DNA is fairly stable in the slightly alkaline medium.

The proportions of DNA in the copolymers were calculated from nitrogen analysis to be approximately 66%, 46%, and 34% for the samples A, B, and C, respectively (Table I). These compositions agreed with the acidity of the aqueous solutions of the graft copolymers which increased with an increasing content of polyacrylic acid. The sample A had a higher ultra-violet absorbance than sample B, which contained only 40% DNA (Fig.
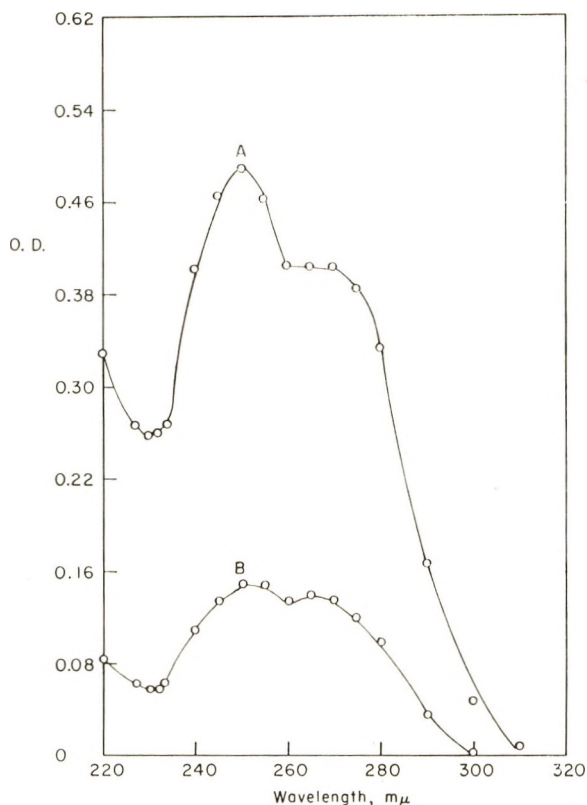
Fig. 2. Ultraviolet absorption curves of the graft copolymers of DNA and polyacrylic acid: (A) copolymer A; (B) copolymer B.

2).   The sample C which was not shown in Figure 2 had a similar type of ultraviolet absorption curve but a lower absorbance than sample B.

The yields of the graft copolymers seem to be dependent on the pH of the polymerization media.   The samples with their polymerization media at pH 7–8 gave the highest yields of the graft copolymers.   It seemed likely that the DNA molecules and the polyacrylic acid chain radicals were both highly charged in the solutions of high pH.   The repulsions between two similarly charged macromolecules in the expanded state may result in the

TABLE I
Chemical Analysis of Graft Copolymers

Sample	Copolymer type	C, %	H, %	N, %	P, %	DNA (cal'ed.), %	N/P	pH
A	DNA–PAA	36.08	4.67	9.32	6.13	66	1.5	6.0
B	DNA–PAA	—	—	6.47	2.21	46	2.9	5.5
C	DNA–PAA	—	—	4.74	1.24	34	3.8	2.5
D	DNA	35.30	4.44	14.13	8.80		1.6	6.0
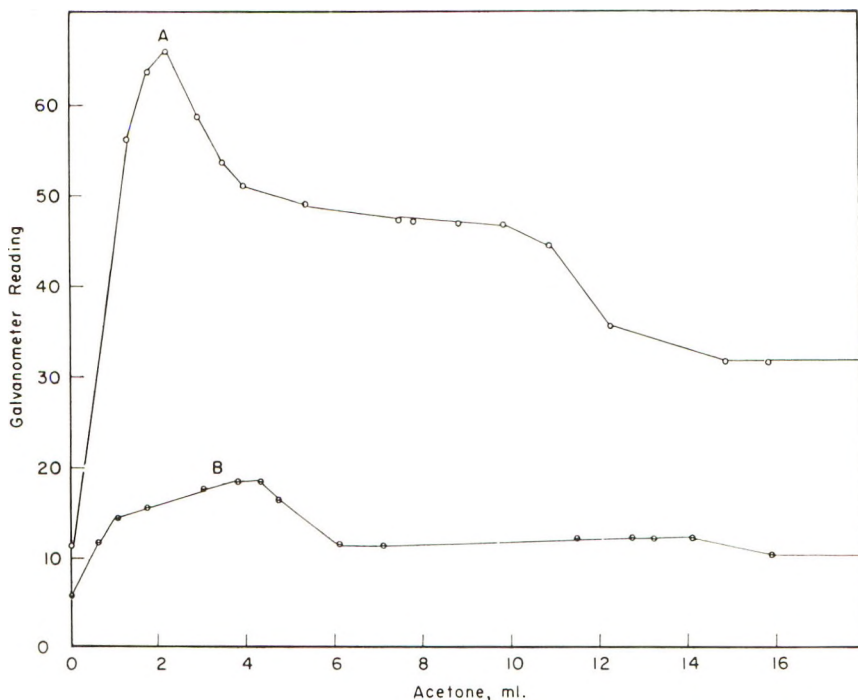
Fig. 3. Turbidimetric titration curves: (A) DNA, 0.1% solution; (B) DNA–PAA copolymer A, 0.1% solution.

physical inaccessibility of the chain transfer sites and consequently the marked reduction of the occurrence of the chain transfer reactions. On the other hand, the DNA molecules are highly hydrogen-bonded between the base pairs at pH 5.0, and the chain transfer sites on the DNA back-bone chains may again become sterically less accessible to the polyacrylic acid chain radicals.

In sample B, almost all of the DNA had reacted with the polyacrylic acid chain radicals in aqueous solution at pH 7.0. Therefore, the chain transfer constant of polyacrylic acid radical with DNA might be rather high at pH 7.0. It seems that the chain transfer sites on the DNA molecules became sterically most accessible at this more or less neutral state.

Comparing the much greater ease of the grafting reaction of polyacrylic acid with DNA to that of vinylpyrrolidone with dextran[5] which also con-tains sugar units, we may possibly explain as follows. Since the amine groups, amide groups, and the imide groups on the four bases in DNA, e.g., adenine, cytosine, guanine, and thymine, are chain stoppers,[6] they may be excluded as the chain transfer sites of DNA. The nitrogen group in DNA may possibly act as redox systems with the persulfate ions. Then, the available chain transfer sites would be from the sugar units in DNA which have three secondary hydrogen atoms, one methylene group adjacent to a phosphate group, and two primary hydrogen atoms

for each unit. The greatly increased chain transfer efficiency of the sugar units in DNA in comparison with those in dextran are probably due to the inductive effect of the nitrogen bases which enhances the chain transfer affinity of the hydrogen atoms in the sugar units. Other monomers such as styrene, acrylamide, dimethylaminoethyl methacrylate, *tert*-butyl-aminoethylmethyl methacrylate, and vinylpyrrolidone were also used in the grafting reactions with DNA.[7] All of the monomers were efficiently grafted onto DNA. This again demonstrated the efficiency of DNA as a macromolecular chain transfer agent.

References

1. Scheraga, H. A., *J. Phys. Chem.*, **64**, 1917 (1961); *ibid.*, **65**, 699 (1961).
2. Schellman, J. A., *Compt. Rend. Trav. Lab. Carlsberg*, **29**, 223, 230 (1955); *J. Phys. Chem.*, **62**, 1485 (1958).
3. Kwei, K.-P. Shen, and F. R. Eirich, *J. Polymer Sci.*, **53**, 81 (1961).
4. Vernon, C. A., *Chem. Soc. (London), Spec. Publ.*, **No. 8**, 17 (1959).
5. Kwei, K.-P. Shen, and F. R. Eirich, *J. Phys. Chem.*, **66**, 828 (1962).
6. Walling, C., *Free Radicals in Solution*, Wiley, New York, 1957, p. 432.
7. Kwei, K.-P. Shen, to be published.

Résumé

Des copolymères graffés d'acide polyacrylique avec le DNA ont été préparés et isolés. Les copolymères greffés de DNA ont des solubilités et des caracteristiques d'absorption dans l'UV différentes de celles du DNA.

Zusammenfassung

Pfropfcopolymere aus Polyacrylsäure und DNA wurden dargestellt und isoliert. Das aufgepfropfte DNA-Copolymere unterschied sich im Löslichkeitsverhalten und in der UV-Absorption von DNA.

Polypropylene Structure

PAUL G. SCHMIDT, *Film Research and Development Laboratory, E. I. du Pont de Nemours and Company, Experimental Station, Wilmington, Delaware*

Synopsis

The polarized infrared spectra of one-way and two-way oriented polypropylene films have been investigated and compared to nonoriented films. Evidence has been compiled to show that an amorphous helical isotactic structure is nonexistent, and that it is through the crystallization process that nonhelical isotactic polypropylene is converted to helical isotactic polypropylene.

Introduction

The structure of linear polypropylene, derived from the head-to-tail polymerization of propylene, is characterized by alternate asymmetric carbon atoms and methylene groups. In terms of this structure, three types of polypropylene chain segments may be defined: chain segments in which the optical forms of successive asymmetric carbon atoms alternate in steric configuration, chain segments in which the optical forms of successive asymmetric carbon atoms are in the same steric configuration, and chain segments in which the optical forms of the successive asymmetric carbon atoms are randomly distributed. The forms are termed syndiotactic, isotactic, and atactic, respectively.

Once propylene is polymerized via a given catalyst system, the amounts of syndiotactic, isotactic, and atactic structures are fixed. The relative amounts of each may only be changed by an SN2-type reaction, not by any heating or polymer drawing process. Most commercial polypropylene resins are of the isotactic-atactic species. Only recently has a syndiotactic species been made and isolated.[1]

The infrared spectra of atactic and molten isotactic polypropylene are essentially identical.[2] Upon cooling the isotactic species, however, some type of ordering or structural change comes about. This is indicative of the differences in the spectra of the atactic and the cooled isotactic species. This ordering or structural change cannot be attributed to any change in the amounts of atactic or isotactic structure, but only to some chain ordering of some or of all the isotactic species.

The x-ray pattern of polypropylene, among other types of vinyl polymers, has been investigated by Natta.[3] The unit cell of polypropylene is monoclinic and contains the molecular species in a helical arrangement.

This helical ordering is brought about by all the asymmetric carbon atoms having the same steric configuration; that is, being isotactic. Natta[1] points out, however, that a vinyl polymer segment in the isotactic form is the necessary but not the sufficient condition for crystallinity. An isotactic polymer does not necessarily have to be crystalline, likewise an isotactic polymer does not necessarily have to be helical.

Natta et al.[4] observed a second form in the x-ray spectrum of polypropylene which was obtained by a rapid cooling of the polymer melt. This form was attributed to a different crystalline packing of the helices. Miller[5] indicated that this form was intermediate between amorphous and crystalline. On the basis of x-ray analyses, however, it is believed to be a second crystalline modification. The problem is mainly that of semantics. The infrared spectra of these forms, however, were essentially identical. although their densities are quite different. From this it is concluded, that it is the molecular not the crystalline symmetry that is the main factor governing the appearance of the spectra and that the molecular symmetries of the two forms which give rise to the different x-ray patterns are essentially identical. The infrared bands that reflect chain ordering, then, are not crystalline sensitive bands in the sense that they arise from crystalline lattice interactions or vibrations. These infrared bands are characteristic of the amount of helical isotactic structure, which is some percentage of the total isotactic species and which may or may not also exist in the amorphous regions of the polymer.

Objectives

The primary objective of this investigation was to determine whether or not the helical isotactic molecules of polypropylene may exist outside of those regions which contribute to the x-ray Bragg reflections. If these molecular species do exist in the amorphous region of the polymer, then the amount of amorphous helical structure should be quite dependent upon external stresses such as drawing.[6]

A secondary objective of this investigation was to determine and to characterize the molecular orientation that polypropylene molecules undergo during the drawing process.

Experimental

Polypropylene films were made from Pro-Fax type of resins. Drawing was accomplished at 150°C. at the rate of 2000%/min. Samples were quenched by air or cold water.

The absorption band intensities were measured as the peak absorbance minus the absorbance at 770 cm.$^{-1}$. This was found to be the best way of obtaining consistent readings.

Theory

When an anisotropic solid such as an oriented polymer film is examined with polarized light two major consequences follow. The integrated

absorption over all sample configurations is dependent only on the number of absorbing species present and their absorption characteristics as long as the Beer-Lambert law is obeyed. This absorption is termed "structural dependent." Having measured the structure dependent absorption, one can calculate the absorbance of a hypothetical isotropic (random) configuration of the absorbing dipoles. It can be seen that this type of treatment is suited for the study of absorbing units which change concentration as a result of the physical treatment of the material. As an example, an absorption which is characteristic of the crystalline regions of a polymer will increase under conditions which increase the crystalline fraction of the specimen. This might not be seen experimentally using normal absorption measures if the increase were associated with an orientation process. The distribution of molecules between helical and nonhelical conformations should be amenable to the same sort of treatment.

The second consequence, once the hypothetical distribution of absorbance has been established, is that meaningful measures of anisotropicity can be made. This is termed an "orientation dependent absorption." The basic theory for this separation process was presented in a previous paper.[6] In essence, a set of orthogonal absorbances A_x, A_y, and A_z are measured from which the basic structurally dependent absorbance A_0 may be calculated. Various ratios such as A_y/A_x and A_y/A_0 then give the anisotropicity of the orientation dependent bands.

Results

The polarized infrared spectrum of polypropylene was investigated in the 1200- to 700-cm.$^{-1}$ region. Figures 1, 2, 3, 4, and 5 show how the
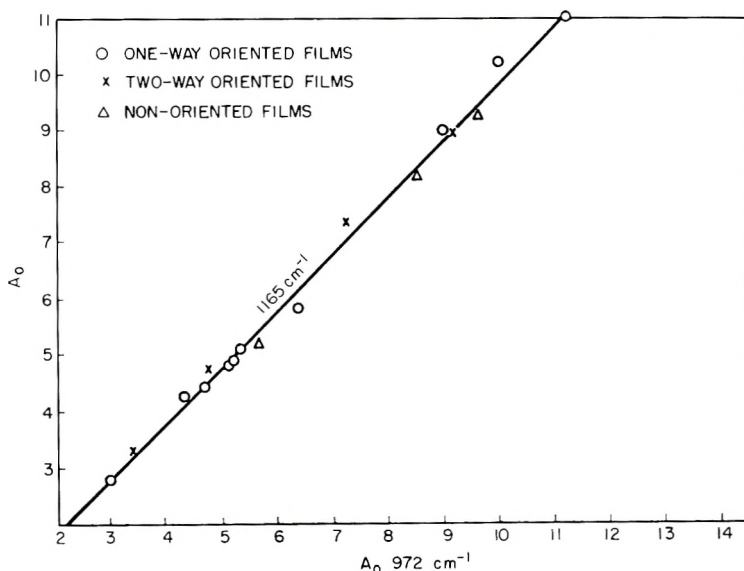
Fig. 1. Structural intensity of the 1165-cm.$^{-1}$ band vs. the structural intensity of the 972-cm.$^{-1}$ band (density = 0.9099 ± 0.0013 g./cc.).
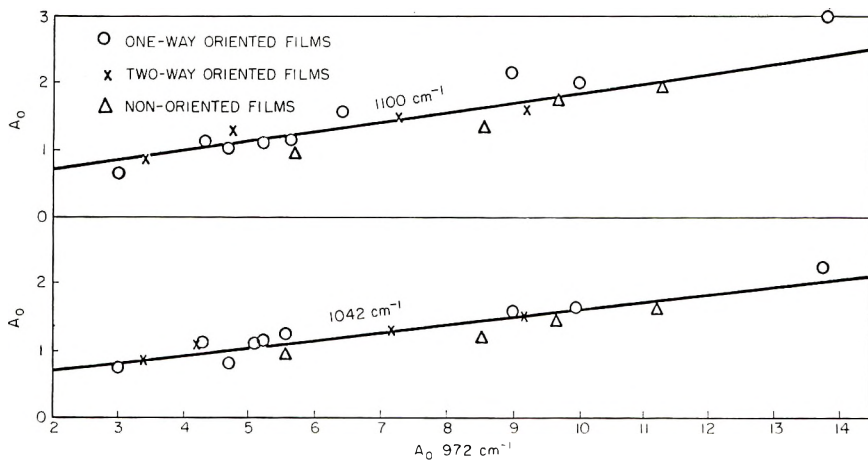
Fig. 2. Structural intensities of the 1100- and 1042-cm.$^{-1}$ band vs. the structural intensity of the 972-cm.$^{-1}$ band (density = 0.9099 ± 0.0013 g./cc.).
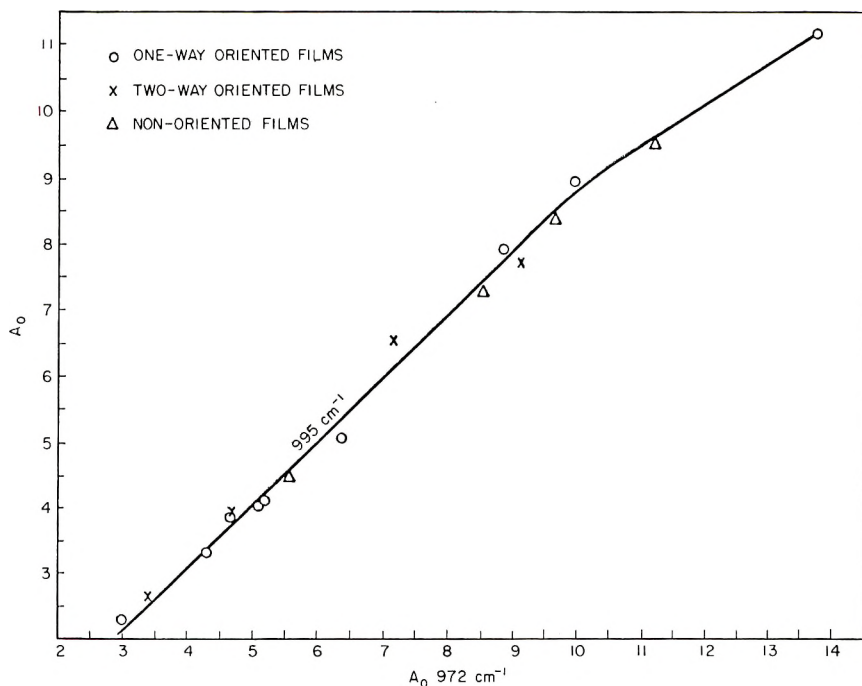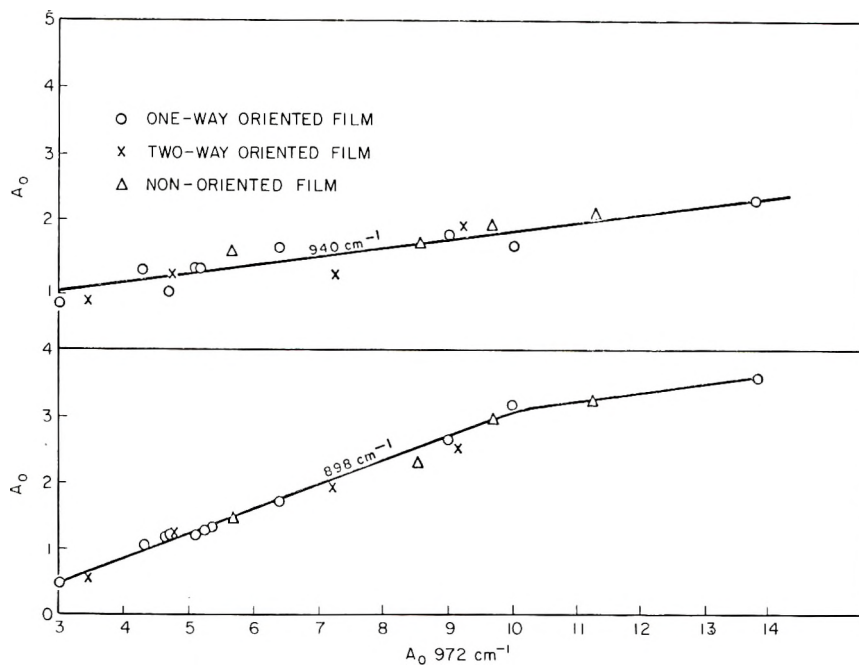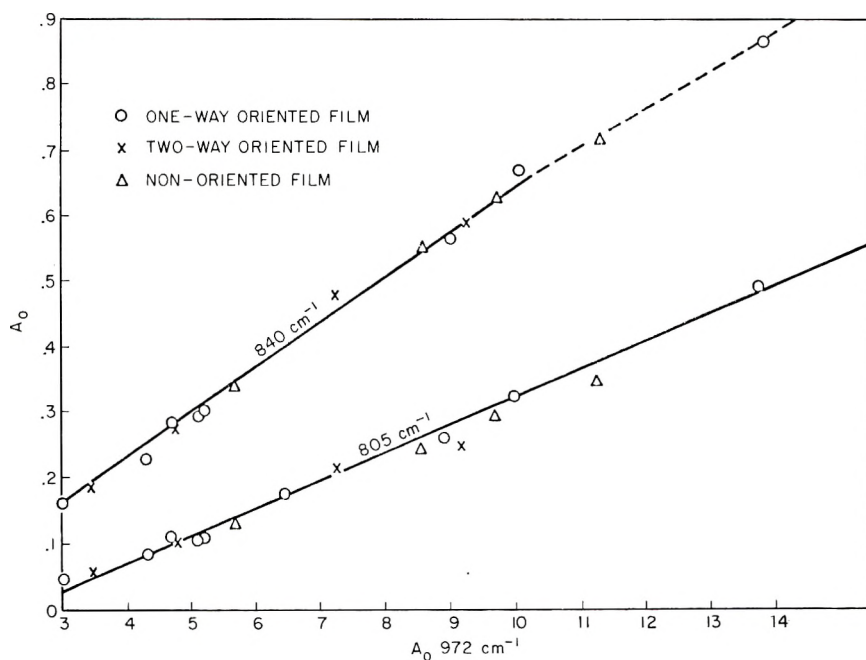

Fig. 3. Structural intensity of the 995-cm.$^{-1}$ band vs. the structural intensity of the 972-cm.$^{-1}$ band (density = 0.9099 ± 0.0013 g./cc.).

structural intensities of the 1165-, 1100-, 1042-, 995-, 940-, 898-, 840- and 805-cm.$^{-1}$ bands vary with the structural intensity of the 972-cm.$^{-1}$ band, for a series of one-way oriented, two-way oriented, and nonoriented films. The structural intensity of the 972-cm.$^{-1}$ band is an internal thickness band

Fig. 4. Structural intensities of the 940 and 898-cm.$^{-1}$ bands vs. the structural intensity of the 972-cm.$^{-1}$ band (density = 0.9099 ± 0.0013 g./cc.).

Fig. 5. Structural intensities of the 840- and 905-cm.$^{-1}$ bands vs. the structural intensity of the 972-cm.$^{-1}$ band (density = 0.9099 ± 0.0013 g.cc/.).
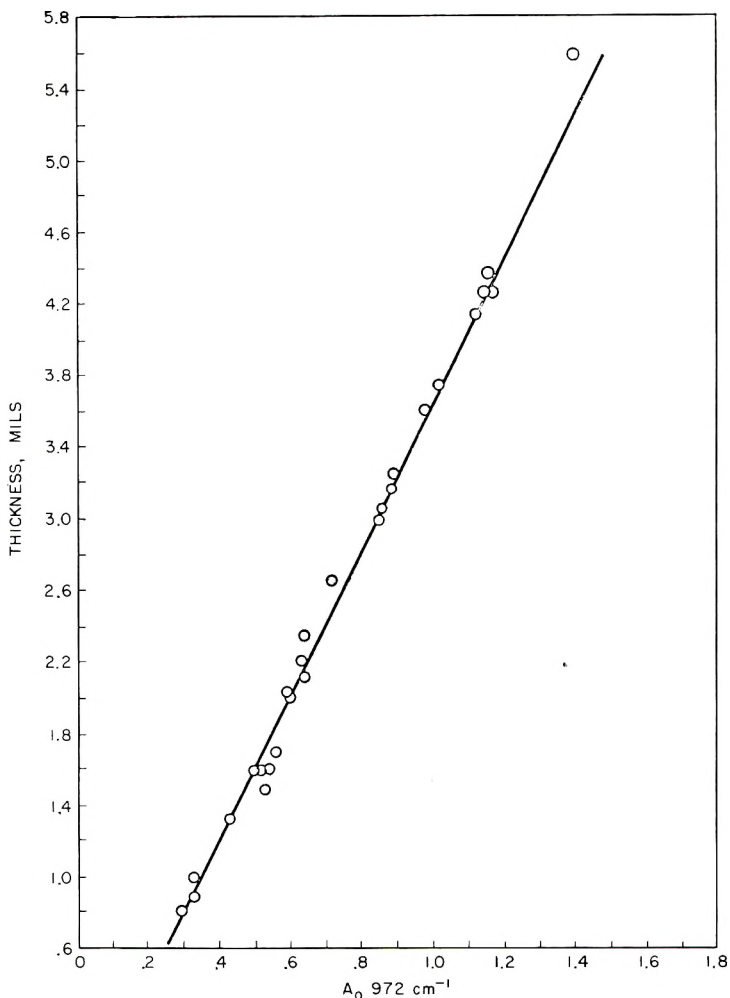
Fig. 6. A_0 972 cm.$^{-1}$ vs. film thickness.

(Fig. 6). These samples had been pretreated in order to eliminate the questionable second crystalline form. The significance of this is that at this density, in this case, at this percentage crystallinity,[7] there is one and only one value for the helical content of the film, regardless of the amount of drawing the polymer underwent. This, in addition to the fact[8] that the absorbances of the 995-, 840-, and 805-cm.$^{-1}$ bands have been correlated with the crystallinity of unoriented films, and that these absorbances tend toward zero intensity for the amorphous species indicated that an amorphous helical structure is nonexistent at any level of crystallinity. The crystallization process evidently transforms the nonhelical isotactic segment into the helical conformation.

Figure 7 shows how the dichroic ratio of the absorption bands investigated vary with draw ratio. The 840-, 995-, 1165-, 972-, and 1042-cm.$^{-1}$ bands
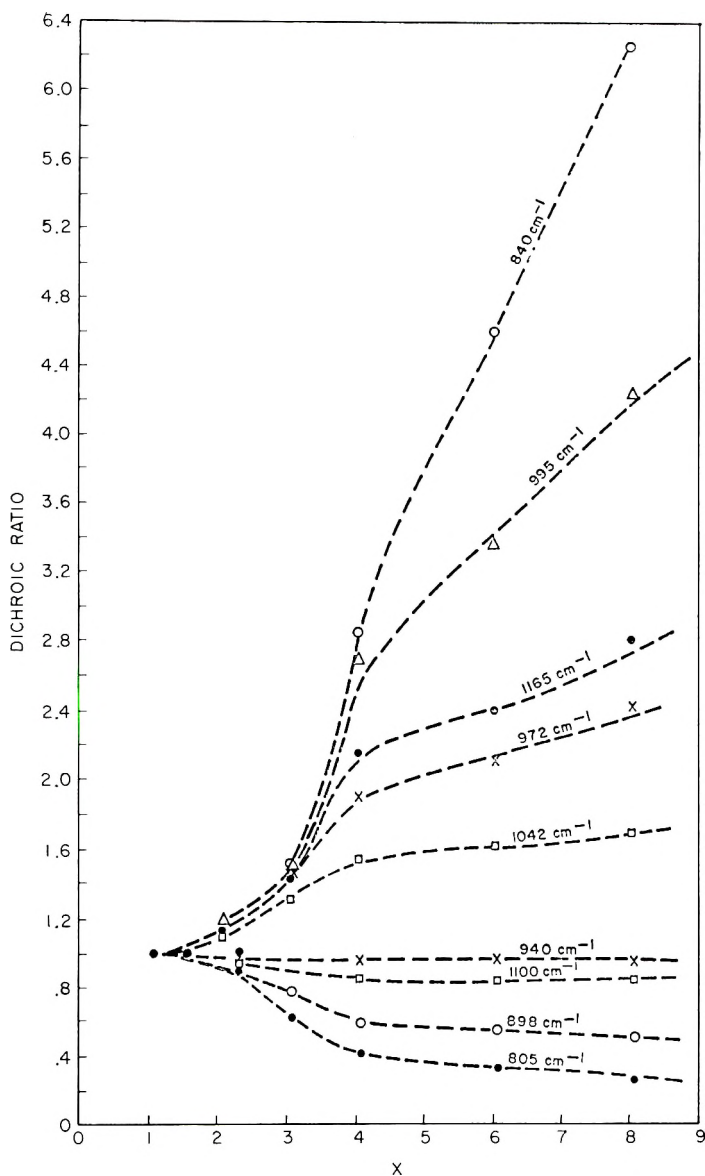
Fig. 7. Dichroic ratio vs. draw ratio.

exhibit parallel dichroism while the 940-, 1100-, 898-, and 805-cm.$^{-1}$ bands exhibit perpendicular dichroism. Table I shows how the $A_z - A_x$ values per mil thickness vary for each absorption band with draw ratio. The significance of this is that the transition moments and hence the molecules are axially distributed about the axis of stretching. There is no evidence of any planar or uniplanar structure.

From the above relationship between A_0 with A_x, A_y, and A_z, the structurally dependent and orientation dependent components of any absorp-

TABLE I

$A_z - A_x$/Mil vs. Draw Ratio

	1165 cm.$^{-1}$	1100 cm.$^{-1}$	1042 cm.$^{-1}$	995 cm.$^{-1}$	972 cm.$^{-1}$	940 cm.$^{-1}$	898 cm.$^{-1}$	840 cm.$^{-1}$	805 cm.$^{-1}$
2X	0.004	0.009	0.009	0.012	0.013	0.003	0.012	0.006	0.008
3X	0.002	0.001	0.001	0.010	−0.010	0.003	−0.003	0.009	−0.006
4X	0.004	0.011	0.019	0.021	0.013	0.016	0.014	0.011	0.026
6X	0.003	0.015	0.015	0.006	0.020	0.012	0.014	−0.016	0.041
8X	−0.008	0.012	0.015	0.023	0.008	0.009	0.006	0.011	0.005

tion band for a one-way drawn polypropylene film may be determined from the absorbances of that band in the A_y and A_z directions.

$$A_y + 2A_z = 3A_0$$

Summary

The polarized infrared spectra of one-way and two-way drawn polypropylene films have been examined. The infrared absorption bands which distinguish molten and solid isotactic polypropylene are not isotactic or crystalline sensitive bands. They are bands characteristic of the helical isotactic structure which may exist in different crystalline modifications. At a given level of crystallinity, there is one and only one value for the amount of helical structure. This indicates that an amorphous helical structure is nonexistent and that the measurements of the percentage crystallinity by infrared techniques are valid for oriented or nonoriented film of either crystalline modification.

The orientations of nine transition moments have been examined as a function of draw ratio. Each transition has been found to exhibit radial symmetry about the axis of drawing. A simplified method is brought forth which will measure the structural and orientational contributions for each transition moment for one-way drawn films.

References

1. Natta, G., *Makromol. Chem.*, **35**, 94 (1960).
2. Luongo, J. P., *J. Appl. Polymer Sci.*, **3**, 302 (1960).
3. Natta, G., *J. Polymer Sci.*, **16**, 143 (1955).
4. Natta, G., M. Peraldo, and P. Corradini, *Rend. Accad. Nazl. Lincei* [8], 26 (1959).
5. Miller, R. G., *Polymer J.*, **1**, 135 (1960).
6. Schmidt, P. G., to be published.
7. Sobue, H., and Y. Tabata, *J. Appl. Polymer Sci.*, **2**, 66 (1959).
8. Quynn, R., J. Riley, D. Young, and H. Notther, *J. Appl. Polymer Sci.*, **2**, 166 (1959).

Résumé

On a étudié les spectres infrarouges en lumière polarisée de films de polypropylène orienté dans une direction et dans deux directions, et on les a comparés avec des films non-orientés. On montre qu'une structure isotactique hélicoïdale amorphe n'existe pas

et que c'est grâce au processus de cristallisation que le polypropylène isotactique non-hélicoïdal est transformé en polypropylène isotactique hélicoïdal.

Zusammenfassung

Die polarisierten Infrarotspektren von einfach und doppelt orientierten Polypropylenfolien wurden untersucht und mit nichtorientierten Folien verglichen. Beweise für das Nichtvorhandensein einer amorphen, isotaktischen Helixstruktur und für die Umwandlung des nichthelixförmigen isotaktischen Polypropylens in das helixförmige isotaktische Polypropylen durch den Kristallisationsvorgang wurden zusammengetragen.

Interactions of Low Molecular Weight Compounds with Solid Polymers

MARIAN KRYSZEWSKI and MARTA SKORKO, *Institute of Physics, Polytechnic Institute of Łódź, Łódź, Poland*

Synopsis

In order to establish the kind of dispersion of low molecular weight compounds in solid polymers the absorption spectra of their solutions in liquid monomer and solid polymer were investigated. On this basis the oscillator strengths were calculated for solutions of the light stabilizers, 5-chloro-2-hydroxybenzophenone phenyl salicylate, and 1-naphthylamine in monomer and polymer. The change of oscillator strength is related to the change of dispersion character. Styrene and polystyrene were used as solvents. The hydroxybenzophenone and salicylate show molecular dispersion in the case of thermal polymerization, and are slightly incorporated into the chains during the initiated polymerization. Naphthylamine is incorporated into the chains in a higher degree. Besides it was stated that the oscillator strength is almost independent of conversion degree. If the incorporation of investigated substance into the chains takes place it occurs during the entire polymerization process.

I. Investigations on Dispersion of Low Molecular Weight Compounds in Solid Polymer

The interaction between low molecular weight compounds and solid polymers is of great interest both from a theoretical and a practical point of view. It can be investigated by different methods, e.g., diffusion of gases through polymer films, rate of dissolution, studies on compatibility of polymers with plasticizers and stabilizers, etc.

In all these investigations the basic question arises whether the low molecular weight substance forms a real molecular solution in the bulk of polymer or it is dissolved in the polymer in the form of aggregates or, when added to the monomer before polymerization, whether it is incorporated into the polymer chain.

It is possible to obtain information on the kind of dispersion of the low molecular weight compounds in solid polymer by comparison of their absorption spectra in monomer solution and in solid polymer. If the absorption spectrum of dissolved low molecular weight compound consists of regular bands it is possible to calculate the number of optical oscillators N_{osc} as well as the oscillator strength f. In the case where the low molecular weight compound is added to the monomer and the monomer is subsequently polymerized, if f stays constant during the polymerization, the

substance remains molecularly dispersed.   If f changes, the substance must either form aggregates or be incorporated into the chain.

The number of the optical oscillators and the oscillator strength can be evaluated from the absorption bands on the basis of the classical theory of Smakula[1] or quantum theory of Lax[2] and Dexter,[3] when the halfwidth of the band and the absorption constant $K_{max} = \epsilon c$ (where ϵ is the molar extinction coefficient and c is molar concentration) at the maximum absorption are known.   Using the generalized equations derived by Dexter we can relate the area under the absorption curve $K = f(\nu)$ to the number of optical oscillators

$$\int K(h\nu)d(h\nu) = (1/n)(2\pi^2c^2\hbar/mc)[(n^2 + 2)^2/3^2]N_0f \qquad (1)$$

where n is the refractive index of material which at low concentration of low molecular weight compound is equal to the refractive index of polymer or monomer at the wavelength corresponding to the maximum absorption, e is the electronic charge, m is the mass of the free electron, N_0 is the number of molecules of dissolved low molecular weight compound per cubic centimeter of polymer or monomer, and $\hbar = h/2\pi$, where h is Planck's constant.

When the absorption band is given with a good approximation by a Gaussian curve, then instead of measuring the area under the absorption curve we can simply use the approximation:

$$\int K(h\nu)d(h\nu) = {}^1\!/_2(\pi \ln 2)^{1/2}K_{max}H \qquad (2)$$

where H is the halfwidth of the band.   By inserting the numerical values of physical constants in eqs. (1) and (2) we obtain the value of $N_{osc} = N_0f$ in the form:

$$N_{osc} = 0.87 \times 10^{17}[n/(n^2 + 2)]^2K_{max}H \qquad (3)$$

If K_{max} and H are known, this relation permits calculation of the oscillator strength of the dissolved species.   In general, these calculations should be applied for simple organic molecules whose absorption spectra consist of separated bands of regular shape.   A similar method has been used by Rohleder and Olszowski[4] in the case of solid solutions of azobenzene in polystyrene and by Barker and Moulton for determination of color centers in polycarbonates.[5]   It seems, however, that these methods can also be used in the case where the investigated absorption band is symmetrical in that part of the curve where it is necessary to calculate the halfwidth.

The justification for the use of the approximate equation, eq. (2), can be proved by comparison of the experimental values of the absorption constant K plotted as a function of the frequency with values calculated from eq. (4):

$$K = K_{max} \exp\{-B(h\nu_0 - h\nu)^2\} \qquad (4)$$

where ν is the frequency at a given wavelength, ν_0 is frequency at the maximum absorption, and

$$B = 4 \ln 2H^{-2}$$

When the experimental curve $K = f(\nu)$ agrees with the curves calculated from the eq. (4) we can use the approximate eq. (2).

All these considerations can by applied only at concentrations of dissolved low molecular compound where Beer's law is fulfilled. We have used the above mentioned method to study the dispersion of some light stabilizers in polystyrene.

II. Experimental

Technical grade styrene monomer was washed with sodium hydroxide, dried, polymerized, purified, and degassed. The monomer was then distilled in all-glass apparatus into polymerization tubes which contained a known amount of the low molecular weight substance. The actual concentration of dissolved substance was calculated by weighing the sealed tubes.

The polymerization was carried out thermally at 140°C. or in the presence of benzoyl peroxide at 85°C. for the first hour, and then at 60°C. for 60 hrs. The concentration of benzoyl peroxide was 2.5×10^{-5} mole/l. and was kept constant in all experiments. Special care was taken in order to prevent overheating which might cause inhomogeneities in the polymer. Polymerization was stopped at a given degree of conversion which was established by dissolution in benzene and weighing of precipitated and dried polymer. To calculate the actual concentration of dissolved substance in the solid polymer we introduced the necessary corrections, taking into consideration the changes of density during the course of the polymerization. Absorption spectra of the polystyrene samples in the form of well polished plates were obtained with a Zeiss spectrophotometer. The detailed analysis of absorption spectra was done for the range of wavelengths where the absorption of styrene and polystyrene is small. The absorption spectra of dissolved substances in pure styrene and especially in polystyrene are influenced by the fluorescence of these solvents, since their fluorescence bands overlap to some extent the absorption bands of investigated substances. It was shown by Krenz[10] that in the case of γ-radiation-excited fluorescence of styrene the relative fluorescence intensity increases as the polymerization proceeds. The same is true for the ultraviolet-excited fluorescence. The effect of fluorescence of styrene on the absorption spectra of the investigated low molecular weight compounds is small. The observed absorption spectra may be influenced in a higher degree by the fluorescence of polystyrene (3000–3500 A.). With the knowledge of the spectral distribution of polystyrene fluorescence, each measurement could be corrected. As the intensity of the light source used (H lamp in the spectrophotometer) and the thickness of the investigated specimens are rather small, the intensity of that fluorescence could be considered as negligible, so any of these corrections were introduced. The investigated substances exhibit fluorescence at longer wavelength which does not interfere with the investigated phenomena.

Refractive indices for wavelengths corresponding to the absorption maxima were determined by the method of minimum deviation with

photographic modification[6] using monochromatic light of appropriate wavelength. The values of the refractive indices were checked by the use of the Cauchy formula[8] and constants A,B,C given by Boundy and Boyer.[7]

The low molecular weight substances used were purified by multiple crystallization and dried in vacuum. Known amounts were placed in polymerization tubes which were evacuated to 10^{-4} mm. Hg for several days before the monomer was distilled into the tubes.

Absorption spectra were taken for different concentrations of low molecular weight compound in monomer and polymer in order to check that the experiments were done in the range of concentrations where Beer's law is fulfilled.

The substances investigated were: 5-chloro-2-hydroxybenzophenone, phenyl salicylate, and 1- naphthylamine.

These compounds show maxima in monomer solution at 352, 312, and 322 mμ, respectively. The two first of the investigated substances are known to be good light stabilizers.

III. Results and Discussions

In order to illustrate the application of the method the case of 5-chloro-2-hydroxybenzophenone solutions is discussed in some details. Figure 1 shows the relation between log ϵ versus wavelength. For the investigated range of concentrations Beer's law is fulfilled. In our investigations the solvent effect, displacement of bands, as well as the effect of solvent polarity of styrene can be considered as very small so they can be neglected.

As seen in Figure 2, the experimental curves $K = f(\nu)$ for two concentrations $c = 5.11 \times 10^{-3}$ and $c = 2.56 \times 10^{-3}$ mole/l. correspond to the theoretical curves calculated by eq. (4). The discrepancies appear only for the shorter wavelengths owing to some overlapping of the next absorption band. This does not influence however the determination of H. From eq. (3) for known K_{max} and H, the values of N_{osc} and consequently f can be obtained.

For two other investigated substances the procedure is similar.

The results of our investigations are summarized in Table I. We reported f values for different concentrations only for 5-chloro-2-hydroxybenzophenone. For the two other compounds f values are given only for one concentration.

The values given in Table I show that for the investigated substances the oscillator strength changes very little when they are dissolved in monomer or in solid polymer. In the case where polymerization is carried out only by heating of monomer in the presence of these compounds, the oscillator strength is not dependent upon the concentration in the investigated range. This indicates that the investigated compounds exist as real molecular solutions in the polymer. In the case of polymerization initiated by benzoyl peroxide the changes in oscillator strength are more pronounced. It is not possible to explain in the present state of the investigation whether the observed changes in the oscillator strength are associated with local aggre-
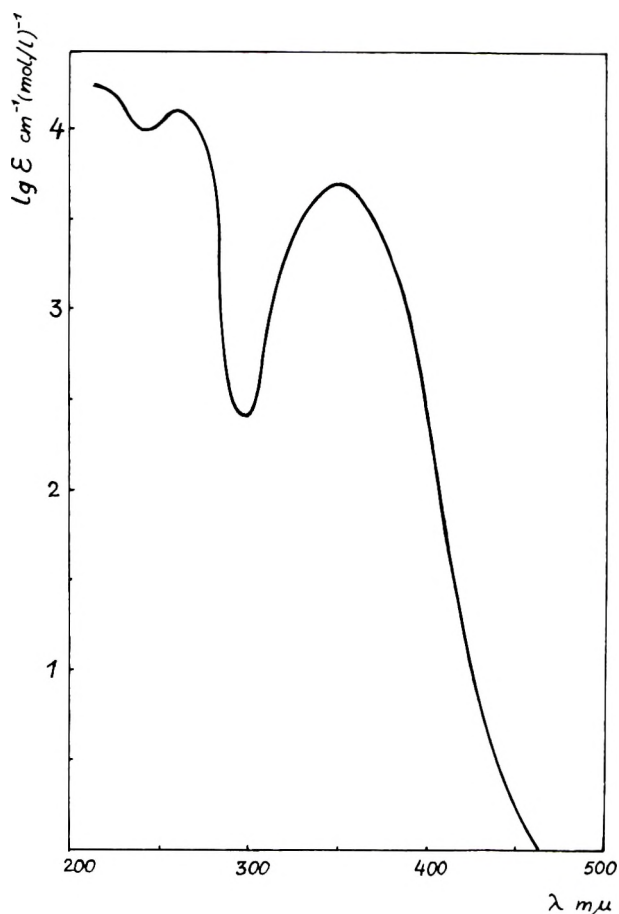
Fig. 1. Logarithm of molar extinction coefficient ϵ vs. wavelength for 5-chloro-2-hy-droxybenzophenone in styrene.

gations of dissolved molecules or if these substances are incorporated into the polymer chains as reported by Anufrieva, Vol'kensteïn, and Koton[9] for the case of polymerization of styrene in the presence of anthracene and its derivatives. In polymerization of styrene containing dissolved anthracene some molecules of the latter become attached to the ends of growing chains at the 9-position; this causes a spectral shift toward the longer wavelengths by 12 mμ from the spectrum of anthracene in isopropyl benzene.

Similar studies were made with substituted anthracenes. In the case of 9,10-substituted anthracenes the spectra remain identical regardless of whether these compounds are introduced before or after polymerization. In the case of 9-substituted anthracenes the spectrum changes and it is considered that the molecules become attached to polystyrene at the 10-position. It seems reasonable to assume that molecules of some of these compounds are bound to the polymer chains but insufficient data are
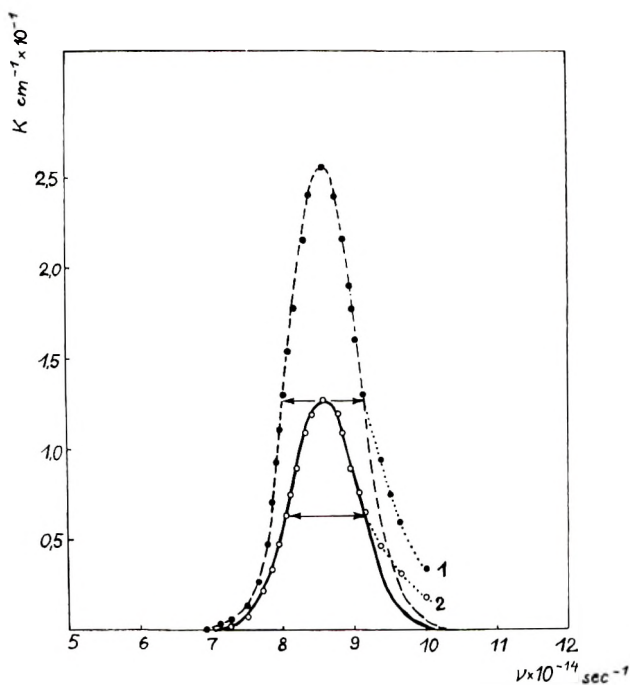
Fig. 2. Absorption constant K vs. frequency ν for 5-chloro-2-hydroxybenzophenone ($\bullet$) $c = 5.11 \times 10^{-3}$ mole/l.; (O) $c = 2.56 \times 10^{-3}$ mole/l.; (---) and (——) the theoretical curves for both concentrations. The halfwidth values are marked on the curves.

available on the oscillator strength to permit unequivocal conclusions to be drawn. Besides the products of decomposition of benzoyl peroxide can take part in the reaction with the dissolved low molecular substances.

In our investigations it was taken into consideration that changes of the dispersion occur during polymerization. In consequence polymers into which optical stabilizers were introduced as solutions in different solvents or plasticizers were not studied (e.g., films prepared by evaporation of solution of polymers with light stabilizers).

The oscillator strength does not depend markedly on the degree of conversion. This means that the small changes observed might be related to some interactions which occur in the solution but which are essentially independent of the concentration of unreacted monomer. These interactions take place during the entire polymerization and not only in the last stages when the concentration of monomer is small. The results for other light and heat stabilizers and other polymers will be published later.

The results of the present investigation show that the method used can not only indicate the state of dispersion of low molecular weight additives but that it is also useful for studying interactions between low molecular weight compounds and polymers. It is of special importance in the case of stabilizers (especially light stabilizers) and dyes. The necessary condition

TABLE I

Oscillator Strength of Low Molecular Weight Compounds Dissolved in Styrene and Polystyrene

Low molecular weight compound	Experimental conditions	Conver-sion, %	Concen-tration, mole/l. $\times 10^{-3}$	Calculated oscillator strength f $\times 10^{-2}$
5-Chloro-2-hydroxy-benzophenone	Dissolved in monomer	0.	5.11	3.31
		0.	2.56	3.26
		0.	0.512	3.29
	Thermal polymerization	98.7	5.12	3.15
		98.0	2.55	3.17
		98.3	0.510	3.14
		90.1	2.61	3.20
		80.2	2.63	3.18
	Initiated polymerization	98.6	5.18	2.81
		98.0	2.57	2.89
		98.3	0.520	2.79
		90.3	2.60	2.80
		80.4	2.64	2.92
Phenyl salicylate	In monomer	0.	2.66	3.20
	Thermal polymerization	98.9	2.61	3.06
		80.0	2.63	3.10
	Initiated polymerization	97.9	2.64	2.70
		80.3	2.73	2.64
1-Naphthylamine	In monomer	0.	2.65	1.97
	Thermal polymerization	98.6	2.49	1.87
		80.3	2.54	1.82
	Initiated polymerization	98.7	2.64	1.24
		80.4	2.73	1.49

is that one of the regular absorption bands of low molecular weight substance does not overlap the absorption band of the polymer and the absorption spectrum of the investigated compound dissolved in the solid polymer retains its regular character.

References

1. Smakula, A., *Z. Physik*, **59**, 603 (1930).
2. Lax, M., Paper presented at Photoconductivity Conference, Atlantic City, 1954.
3. Dexter, D. L., *Phys. Rev.*, **101**, 48 (1958).
4. Rohleder, J., and A. Olszowski, *Roczniki Chem.*, **34**, 1033 (1960).
5. Barker, R. E., and W. G. Moulton, *J. Polymer Sci.*, **47**, 175 (1960).
6. Polaroid Corporation, *Modern Plastics*, **23**, 116 (1946).
7. Boundy, H., and R. F. Boyer, *Styrene*, Reinhold, N. Y., 1952, pp. 524.
8. Jenkins, F. A., and H. E. White, *Fundamentals of Physical Optics*, McGraw-Hill, N. Y.
9. Anufrieva, E. W., M. W. Vol'kenstein, and M. M. Koton, *Zh. Fiz. Khim.*, **31**, 1532 (1956).
10. Krenz, F. H., *Trans. Faraday Soc.*, **51**, 172 (1955).

Résumé

Pour établir le genre de dispersion de composés de poids moléculaire faible dans des polymères solides, on a examiné les spectres d'absorption de leurs solution dans le monomère liquide et les polymères solides. Sur cette base on a calculé les forces d'oscillateur pour des solutions de substances examinées dans le monomère et le polymère. La variation de la force d'oscillateur est mise en relation avec le changement du charactère de la dispersion. On a utilisé les substances suivantes, connues comme stabilisateur à la lumière: (a) 5-chloro-2-hydroxybenzophénone, (b) phénylsalicylate, (c) 1-naphthylamine. Le styrène et le polystyrène ont été utilisés comme solvants. Les composés a et b manifestent une dispersion moléculaire dans le cas de la polymérisation thermique et ils sont faiblement incorporés dans les chaînes pendant la polymérisation initiée. Le composé c est incorporé dans les chaînes à un degré supérieur. En outre on a constaté que la force d'oscillateur est pratiquement indépendante du degré de conversion. Si l'incorporation de la substance examinée dans les chaînes a lieu, ceci se fait pendant le processus entièr de la polymérisation.

Zusammenfassung

Zur Ermittlung des Verteilungszustandes niedermolekularer Verbindungen in festen Polymeren wurde das Absorptionsspektrum der Lösungen in flüssigem Monomerem und festem Polymeren untersucht. Auf dieser Grundlage wurde die Oszillatorenstärke für die untersuchten Substanzen in Monomer- und Polymerlösung bestimmt. Die Oszillatorenstärke ist vom Dispersionscharakter abhängig. Folgende, als Lichtstabilisatoren bekannte Verbindungen, wurden verwendet: (a) 5-Chlor-2-hydroxybenzophenon, (B) Phenylsalicylat, (c) 1-Naphthylamin. Styrol und Polystyrol dienten als Lösungsmittel. Verbindungen a and b zeigen bei thermischer Polymerisation molekulare Dispersion und werden bei gestarteter Polymerisation etwas in die Ketten eingebaut. Verbindung c wird in stärkerem Ausmass in die Ketten eingebaut. Ausserdem erwies sich die Oszillatorenstärke als praktisch vom Umsatz unabhängig. Bei Stattfinden eines Einbaus der untersuchten Substanz in die Ketten erfolgt dieser während des gesamten Polymerisationsprozessss.

Determination of Number-Average Molecular Weights by Elastoosmometry*

S. YAMADA,† W. PRINS,‡ and J. J. HERMANS,§ *Cellulose Research Institute, State University College of Forestry, Syracuse, New York*

Synopsis

When a swollen elastomer is in equilibrium with a solution, the stress at constant length is a function of the chemical potential of the solvent, and thus of the concentration and number-average molecular weight of the solute in the solution. This is used to compare the molecular weights of some polystyrene samples among each other. The method is found to give satisfactory results. The theory of the method is given and is applied to ideal rubbery networks, for which explicit free energy expressions are available. The theoretical result obtained is used to reduce the experimental data to equal extension ratios.

Introduction

The swelling of an elastomer in a liquid or vapor is governed by the condition

$$\mu = \mu' \tag{1}$$

for any component that penetrates into the gel phase, μ being the chemical potential of this component inside the gel and μ' that on the outside. Changes in μ' will therefore be betrayed by changes in μ, and vice versa. One way of changing μ' is to add a solute to the outside phase. When this is done, the equilibrium degree of swelling of the elastomer will change in order to adjust μ. Since for low concentrations of solute the change in μ' is determined by the number-average molecular weight of the solute, the change in degree of swelling may be used to determine this molecular weight.[1] It is clear that other properties of the gel which are affected by the chemical potential of the solvent may likewise be used. In particular, μ will be changed when the gel is stretched.[2-4] It was pointed out by Prins and Hermans[4] that the force at constant elongation or the length at constant force can easily be measured with great accuracy and are therefore

admirably suited to study changes in μ.   The present paper deals with the effect on retractive force f at constant length.

Suppose a swollen elastomer is stretched reversibly to a certain length while in equilibrium with a solvent.   The retractive force is f_0.   The addition of a solute to the outside phase will cause a change in μ'.   The change in the degree of swelling which is needed to adjust μ will in general bring about a change in the retractive force from f_0 to f, say.   To a first approximation this change will be proportional to the change in chemical potential, which is

$$(1/\bar{v})\,\mu' = -RTc/\bar{M}_n + 0(c^2) \tag{2}$$

so that we may expect that

$$f - f_0 = Ac/\bar{M}_n + 0(c^2) \tag{3}$$

where c is the concentration of the solute and $\bar{M}_n$ its number-average molecular weight.   If the solute does not penetrate into the gel, the constant A will be independent of the nature of the solute and may be determined by calibration with a substance of known molecular weight.   In analogy with the method used in ordinary osmometry, it is convenient to plot $(f - f_0)/c$ versus c, and to derive $\bar{M}_n$ from the extrapolated value at $c = 0$.

Theory

If the length L of the sample is held constant when μ is changed, the measured change in the retractive force will be determined by the magnitude of $(\partial f/\partial \mu)_L$.

Now, quite generally, changes in temperature T, pressure P, length L, and solvent content n cause the Gibbs free energy of the gel to change by an amount

$$dG = -SdT + VdP + fdL + \mu dn$$

where S is the entropy and V the volume.   Or also,

$$d(G - \mu n) = -SdT + VdP + fdL - nd\mu$$

from which it follows that

$$(\partial f/\partial \mu)_L = -(\partial n/\partial L)_\mu = (\partial \mu/\partial L)_n\,(\partial \mu/\partial n)_L^{-1} \tag{4}$$

Temperature and pressure are supposed to be kept constant throughout. It is seen from eq. (4) that $(\partial f/\partial \mu)_L$ is known when the chemical potential of the solvent in the gel is known as a function of solvent content and sample length.   By way of illustration, the result will be applied to ideal rubbery networks, for which an explicit theoretical expression exists.

The equation that has been given for the Gibbs free energy of a stretched swollen network is as follows:[5,7]

$$G/kT = n \ln (1 - \phi) + \psi V \phi (1 - \phi) + \nu (q_1/q_0)^{2/3}(\alpha^2/2 + q/q_1\alpha - 3/2) - \nu \ln (q/q_0) \tag{5}$$

where k is Boltzmann's constant, T the Kelvin temperature, ν the total

number of polymer chains between crosslinks, q the degree of swelling of the stretched gel, q_1 that of the isotropic gel before stretching, α the length of the stretched gel divided by that of the isotropic gel before stretching, n the number of solvent molecules in the gel, ψ the Huggins interaction parameter and

$$\phi = 1/q$$

the volume fraction of polymer. The degree of swelling q_0 (isotropic "reference state") is that at which the mean-square end-to-end distance of the polymer chains between crosslinks is the same as in the solution of freely dispersed chains of the same contour length.

If p is the ratio between the volume occupied by a polymer chain and that occupied by a solvent molecule, one has

$$\phi = (p\nu + Q)(n + p\nu + Q)^{-1} \qquad (6)$$

where Q is the volume of the polymer that forms loose ends and wasted crosslinks[6] divided by the volume of a solvent molecule. It is convenient to introduce an effective chain length

$$p_e = p(1 + Q/p\nu) \qquad (7)$$

The chemical potential μ per mole of solvent is then given by

$$\mu/RT = \ln(1 - \phi) + \phi + \psi\phi^2 + L_0(Lp_eq_0)^{-1} - (p_eq)^{-1} \qquad (8)$$

where L_0 is the length in the reference state of volume V_0 (degree of swelling q_0). The application of eq. (4) gives, therefore,

$$\sigma_0^{-1}(\partial f/\partial\mu)_L = -\beta \qquad (9)$$

$$1/\beta = \bar{v}(L/L_0)^2(q_0/q)^2[1 + p_e(1 - 2\psi)\phi + p_e(\phi^2 + \phi^3 + \ldots)] \qquad (10)$$

Here $\sigma_0 = V_0/L_0$ is the cross section in the reference state and $\bar{v}$ is the molar volume of the solvent. Use has been made of the fact that $\partial/\partial n = (\bar{v}q_0/V_0)\partial/\partial q$.

The change in μ by the addition of the solute is equal to that in μ' which, at the limit of zero concentration, is equal to $-RTc/\bar{M}_n$. Therefore, eq. (9) becomes

$$\sigma_0^{-1}(\partial f/\partial c)_{c=0} = \bar{v}\beta RT/\bar{M}_n \qquad (11)$$

where β is given by eq. (10) in which for L and q one must substitute the length and degree of swelling at $c = 0$.

The foregoing calculation was given partly by way of illustration and partly because use will be made of eq. (10) to reduce all the experimental results to the same degree of elongation.

Description of the Elastoosmometer

A strip of polydimethylsiloxane (A) is held by the clamps G and immersed in toluene in a vessel that is thermostated by a water jacket (Fig. 1). The toluene may be replaced by a polymer solution by simultaneously operating the two stopcocks E and F. By means of a syringe the liquid
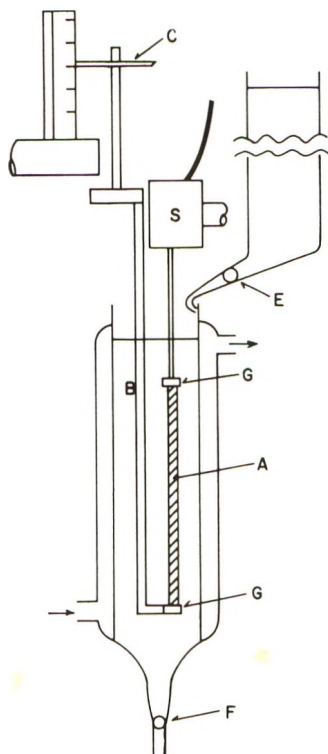
Fig. 1. Elastoosmometer. (A) silicone-strip, clamped at G; (B) Invar rod; (S) strain gage.

level is adjusted very precisely to a mark on the rod B. This rod consists of Invar metal with a linear thermal expansion coefficient of only 0.9×10^{-6} degree^{-1}. It serves to stretch the silicone strip to some known extent by operating the dial C. The stretching force is read on a Leeds-Northrup D.C. microvoltmeter connected with the strain gage S.

The measurements were done in a room of controlled humidity and temperature.

The dimethylsilicone, crosslinked by irradiation with electrons, was obtained through the courtesy of H. A. Dewhurst (General Electric Co., Schenectady, N. Y.). The swelling of this sample in toluene at 22°C. was isotropic within the experimental error of about 1% and the degree of swelling in toluene was about 5.5. The Young modulus at room temperature was about 3×10^6 dyne/cm.^{2} for the air-dry strip and 1.2×10^6 dyne/cm.^{2} when swollen in toluene.

Part of the metal rods are outside the temperature bath. However, a calculation of the effect of fluctuations in room temperature on the experimental results showed that it was negligible. The effect of fluctuations in room temperature on the sensitivity of the strain gage was not measured, but fortunately the changes in room temperature were sufficiently slow to eliminate their effect.

The possible error due to a deviation of the liquid level from its proper

height can be calculated from the buoyancy effect on the rod which con-
nects the silicone strip with the strain gage, and was found to be less than
7×10^{-4} g. Since the change in the retractive force due to changes in
solute concentration varied from about 15×10^{-3} to 90×10^{-3} g. in our
experiments, the relative error varied from less than 1% at high con-
centrations to less than 5% at low concentrations. The possible error in
the extrapolated value of $(f - f_0)/c$, that is, the possible error in $\bar{M}_n$, was
thus estimated at about 4% for $\bar{M}_n = 5000$ and about 16% for $\bar{M}_n =$
20,000. The change in buoyancy due to the density difference between
solvent and solution can be estimated easily from the solution densities and
is found to be less than 1% of the change in the retractive force.

Polystyrene Samples

All the five samples investigated had been prepared by anionic poly-
merization. They are listed in Table I.

TABLE I
Data Concerning the Polystyrene Samples Used

Sample no.	Source	$\bar{M}_n$	$\bar{M}_w/\bar{M}_n$
1	Syracuse	4470	—
2	Dow Chem. Co.	6400	1.64
3	Mellon Inst.	9160	1.03
4	Dow Chem. Co.	10,500	1.95
5	Syracuse	18,500 (16,000)[a]	—

[a] See text.

Samples 1 and 5 were prepared by C. Geacintov at Syracuse and S. Levy,
at Haifa, Israel respectively, and were subsequently purified by freeze-
drying. To determine the number-average molecular weight of these
samples, use was made of steady-state thermometry,[8] also called thermo-
electric osmometry,[9] based on the steady-state temperature difference
between a drop of solution and a drop of solvent when heat exchange is
allowed only through the vapor phase. The possible experimental error
is estimated at about 5% for sample 1 and about 20% for sample 5. The
number-average molecular weight of this sample is 16,000 on the basis of
the polymerization kinetics. Steady-state thermometry resulted in the
value 18,500.

Samples 2 and 4 were supplied by H. W. McCormick, Dow Chemical
Co., Midland, Michigan. The molecular weights were derived from
sedimentation.[10] At Dr. McCormick's suggestion, sample 4 was purified
by precipitation to remove some colored material resulting from catalyst
residues.

Sample 3 was provided by G. C. Berry, Mellon Institute, Pittsburgh,
Pennsylvania. It was one of five fractions removed from a polymer with
a (calculated) kinetic molecular weight of 9960 and an intrinsic viscosity
of 0.125 in benzene at 35°C. The $\bar{M}_w/\bar{M}_n$ ratio of the fraction was esti-

mated at less than 1.03; its intrinsic viscosity was 0.115, so that the estimated molecular weight of the fraction may be taken as $(115/125)9960 = 9160$.   The method of preparation for this polymer has been described by Wenger and Yen.[11]

Results and Conclusion

The curves of $(f - f_0)/c$ versus c are given in Figure 2, and the extrapolated values are plotted against $1/\bar{M}_n$ in Figure 3.   It is seen in Figure 2 that the results of the measurements done with sample 3 are somewhat out of line.   This is attributed to the fact that in these experiments a high strain of almost 7% was applied (as compared to about 3% in the other measurements).   This resulted in some stress relaxation, which affected the data.   Moreover, the results must be reduced to the same degree of stretch before a comparison with the other data can be made.   To this end, use was made of eq. (10), but this could be done only as far as the factor $(L/L_0)^2$ is concerned, which introduced a correction of about 8%.   It was assumed that this was the major correction.   The change in degree
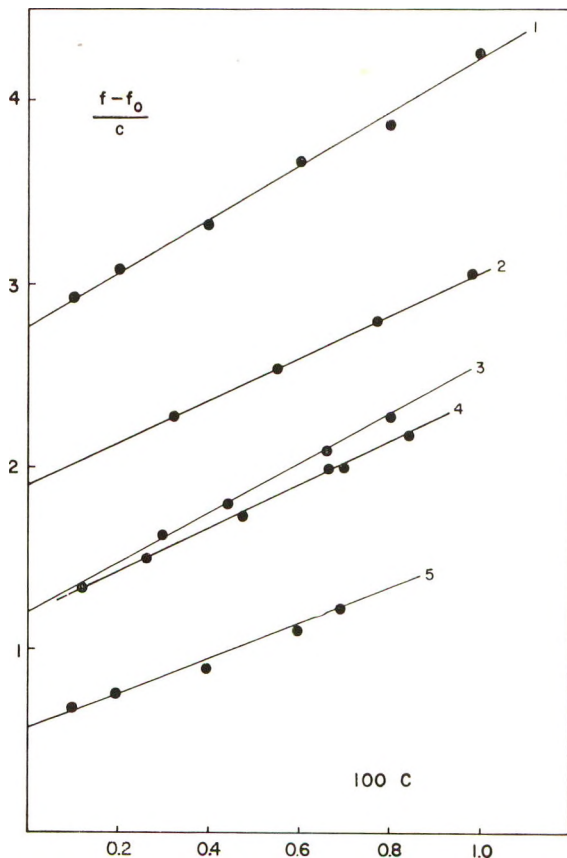
Fig. 2. Values of $(f - f_0)/c$ in arbitrary units as a function of polymer concentration c (g./ml.).
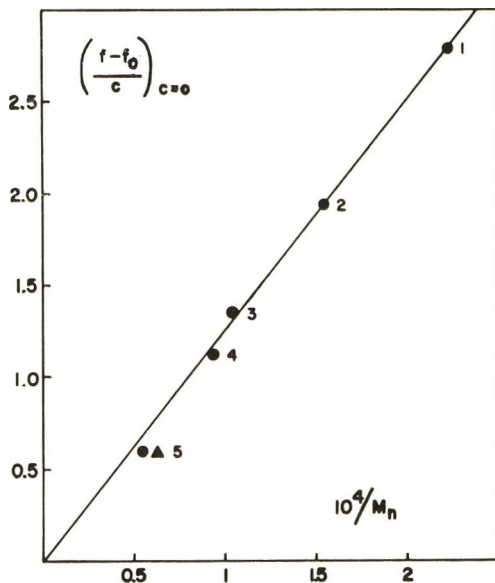
Fig. 3. Extrapolated values of $(f-f_0)/c$ in arbitrary units plotted against the reciprocal of the number-average molecular weight. For example 5: (●) for a molecular weight of 18,000; (▲) for a molecular weight of 16,000 (compare Table I).

of swelling with elongation was not measured. Unfortunately, there was no opportunity to repeat the measurements with sample 3 at a lower degree of stretch.

The data indicate that elastoosmometry gives satisfactory results. It is too early to make a definite statement concerning the general applicability of the method, but the following remarks may be useful.

The polymers studied had molecular weights ranging from 5,000 to 18,000. Like other techniques that exist for this range of molecular weights, the method became inaccurate in the neighborhood of 20,000, but it is important to realize that this does not by any means represent a natural upper limit to elastoosmometry. Depending on the elasticity modulus and on the response of the elastomer to the swelling agent, the effect of changes in solvent potential μ on the retractive force may be many times larger than that found in the present work. In fact, Gabrail and Prins[12] have found considerable changes in the retractive force in slightly stretched swollen cellulose when polymers were added to the swelling agent, even though the molecular weight of these polymers was of the order of 10^5. The effect could have been used to compare the molecular weights of these polymers among each other, if desired.

The experimental technique in elastoosmometry is quite simple and the method is rapid. Application at high temperatures is possible if an elastomer can be found that has the appropriate sensitivity to a solvent but is not affected by heat.

There is, admittedly, a practical limitation to the method due to the requirement that the polymer shall not diffuse into the swollen elastomer.

In this respect, elastoosmometry is similar to ordinary osmometry. It is to be expected, however, that in many cases in which diffusion occurs, the rate at which the osmotic equilibrium between gel and solution is established is much greater than the rate of diffusion, so that measurements may be possible before the solute has penetrated to any appreciable extent.

Some of these points are currently being investigated in more detail by one of the authors (W. P.) in Delft.

References

1. Boyer, R. F., *J. Chem. Phys.*, **13**, 363 (1945).

2. Katchalsky, A., S. Lifson, I. Michaelis, and H. Zwick, in *Size and Shape Changes of Contractile Polymers*, A. Wasserman, Ed., Pergamon Press, London, 1960.

3. Katchalsky, A., paper presented at Conference on Contractility, Mellon Institute, January 1960; J. J. Hermans, *Flow of Disperse Systems*, North Holland, Amsterdam, 1953, p. 72.

4. Prins, W., and J. J. Hermans, paper presented at Conference on Contractility, Mellon Institute, January 1960.

5. Hermans, J. J., *Trans. Faraday Soc.*, **43**, 591 (1947). In Flory's expression[6] for the free energy, the last term of eq. (5) is multiplied by $1/2$; see, however, reference 7.

6. Flory, P. J., *J. Chem. Phys.*, **18**, 108, 112 (1950); *Principles of Polymer Chemistry*, Cornell Univ. Press, Ithaca, N. Y., 1953; *Trans. Faraday Soc.*, **56**, 722 (1960).

7. Hermans, J. J., *J. Polymer Sci.*, **59**, 191 (1962).

8. Higuchi, W. I., M. A. Schwartz, E. G. Rippie, and T. Higuchi, *J. Phys. Chem.*, **63**, 996 (1959).

9. Brady, A. P., H. Huff, and J. W. McBain, *J. Phys. Colloid Chem.*, **55**, 304 (1951).

10. McCormick, H. W., *J. Polymer Sci.*, **36**, 341 (1959).

11. Wenger, F., and Shiao-Ping S. Yen, *Makromol. Chem.*, **43**, 1 (1961).

12. Gabrail, S., and W. Prins, *J. Polymer Sci.*, **51**, 279 (1961).

Résumé

Lorsqu'un élastomère gonflé est en équilibre avec une solution, la force à longueur constante est une fonction du potentiel chimique du solvant et dés lors, de la concentration et du poids moléculaire moyen en nombre du soluté dans la solution. Ceci a été utilisé pour comparer les poids moléculaires de quelques échantillons de polystyrène (lesuns par rapport aux autres). Cette méthode paraît donner des résultats satisfaisants. On a énoncée la théorie de la méthode et on a effectué une application à des réseaux idéaux en caoutchouc pour lesquels des expressions de l'énergie libre sont connues. Le résultat théorique obtenu est utilisé pour transformer les données expérimentales en rapports d'estension équivalents.

Zusammenfassung

Die Spannung bei konstanter Länge ist bei einem Elastomeren im Quellungsgleichgewicht mit einer Lösung eines Hochpolymeren eine Funktion des chemischen Potentials des Lösungsmittels und daher der Konzentration und des Zahlenmittelwertes des Molekulargewichts des Gelösten in der Lösung. Auf diese Weise werden die Molekulargewichte einiger Polystyrolproben untereinander verglichen. Die Methode liefert zufriedenstellende Ergebnisse. Die Theorie der Methode wird entwickelt und auf ideale Kautschuknetzwerke angewendet, für welche explizite Ausdrücke für die freie Energie vorhanden sind. Die theoretischen Ausdrücke werden zur Reduzierung der Versuchsdaten auf gleiches Dehnungsverhältnis benützt.

Generalized Approach to Adhesion Via the Interfacial Deposition of Amphipathic Molecules.
I. Adhesion of Polyethylene to Aluminum

HAROLD SCHONHORN, *Bell Telephone Laboratories, Inc., Murray Hill, New Jersey*

Synopsis

Oriented monolayers are employed as effective adhesives in the bonding of polyethylene to aluminum. Several monolayers are characterized and their physical properties elucidated. Measurement of the tensile shear and peel strength of polyethylene bonded to aluminum indicate that the bonds formed exceed the cohesive strength of the polymer. Contact angle and radioactive trace experiments helped to determine the conditions for maximum adhesion.

Introduction

Investigations[1] have demonstrated that decreasing the adhesive-film thickness between adherends increases the final bond strength of the system. The purpose of this communication is to demonstrate that the adsorption of condensed monolayers of amphipathic (i.e., polar-nonpolar) molecules between selected adherends, affords a bonding phase possessing a high degree of orientation, uniformity, and specificity. In principle, *oriented monolayer adhesives* can be adapted to any system and may be considered the ultimate bonding medium. The techniques and results embodied in the investigation of liquid–air interfaces enables one to predict the resultant character of a monolayer deposited onto an adherend surface. Knowledge of the interactions between amphipathic molecules and solid surfaces permits one to adjust the material parameters to bond properly selected adherend systems. Adopting these procedures, one can obtain, effectively, a uniform distribution of the *oriented monolayer adhesive* onto the available surface of the adherends. The degree of surface inhomogeneity then becomes a relatively minor consideration. The mechanism of adhesion can then be elucidated by investigating the interactions between polar and nonpolar surfaces which are separated by characterizable amphipathic molecules.

Previously, bonding of polyethylene to aluminum had been a challenging and frustrating problem.[2] Surface conditioning of the polyethylene was necessary to obtain reasonable bond strengths. It will be shown that, by employing a characterizable *oriented monolayer adhesive*, bond strengths exceeding the cohesive strength of polyethylene are realized.

Rideal and Tadayon[3] and Allen[4] have used the techniques of monolayer adsorption to demonstrate that there is orientation of the monolayer not only during the process of crystallization from the melt, when the molecules are relatively free to take up new positions, but also after solidification, when the molecules are normally regarded as completely fixed within relatively small limits. These investigators have shown that even in the solid state carboxylic acid groups buried in the substrate can come to the surface and there be anchored by water.

Lasoski and Kraus[5] have demonstrated a *decrease* in adhesion when decanoic acid was applied to steel before the bonding to the surface with polyvinyl acetate. The manner in which they applied their "monolayer" and the system chosen for investigation may account for the observed lack of adhesion.

Rideal and Tadayon[3] concluded that the irreversible adsorption of stearic acid onto copper and other metal species resulted, presumably, in the formation of the corresponding metal stearate.

Experimental

Materials

Stearic acid, labeled with ^{14}C in the carboxyl group, of specific activity 8.3 mc./mmole, was obtained from Tracerlab, Inc., Waltham, Massachusetts. A highly purified nonradioactive sample of stearic acid (m.p. $> 69.5°C.$) was obtained from Dr. James Kirn, formerly of Swift and Co., Chicago, Illinois. Octadecylamine was obtained from Armour Industrial Chemical Co., Chicago, Illinois, and recrystallized from benzene prior to use. The ethyl half-ester of octadecanedioic acid (ethyl hydrogen octadecanoate) in a highly purified state was furnished by Dr. E. Wasserman of the Bell Telephone Laboratories, Inc. Unless otherwise indicated, materials were not recrystallized further. The purity of these amphipathic materials was verified by Dr. Sharpe of the Bell Telephone Laboratories, Inc., by means of infrared spectroscopy involving total internal reflection.[6]

Solutions for surface balance studies were prepared by dissolving 50.0 mg. of the amphipathic molecule in 100 ml. of reagent-grade benzene (Merck and Co., Rahway, New Jersey).

Water, deionized by being passed through a mixed-bed resin, was used directly.

Ferric stearate was prepared by adding a suspension of 10 g. of sodium stearate in 100 g. of water to 200 ml. of a concentrated solution of ferric chloride ($\sim 1M$.) and shaking overnight; the ferric stearate was then filtered off. A pure product was obtained which was easily air-dried.

Polyethylene (Marlex 5003), obtained from Phillips Chemical Co., Bartlesville, Oklahoma, had a melt index of 0.3 and a density of 0.95. This was fabricated at about 1000 psi and 160°C. into sheets 0.010 and 0.063 in. thick, for use in the tensile shear and peel experiments.

The solid substrates used and the methods of preparing them are detailed

in Table I.   All were used as $5 \times 1 \times \frac{1}{16}$ in. rectangular aluminum plates. After cleaning and drying as noted, they were found to be completely wettable by water.   In all experiments the plates were freshly prepared before use.   When monolayer deposition from water surfaces was carried out, the plates were air-dried.

TABLE I
Solid Substrates

Substance	Type	Thickness, in.	Cleaning procedure
Aluminum	2024–T4	0.063	(1) Sulfochromate[a] (2) Alkali etch[b]
Aluminum	Alclad 2024–T3	0.063	Sulfochromate

[a] Sulfuric acid–sodium dichromate treatment; 65°C. for approximately 7 min.
[b] Exposure for 30 sec to hot alkali ($\sim$90°C.), then rinsing in diluted nitric acid.

Films spread on water were deposited from a Lucite tray $30 \times 30 \times 1$ cm. A rectangular well 10 cm. deep was built into the bottom of the trough near one end.   The trough was mounted on adjustable legs to allow for proper leveling.   The trough surfaces were made hydrophobic by being rubbed with ferric stearate to produce a monomolecular layer.

Plating of Monolayers onto Substrates

The constant film pressure device of Sher and Chanley[7] was employed. This procedure precludes surface contamination by leakage of ordinary piston oils[8] past the impregnated thread barriers.   Moreover, it enables one to plate out monomolecular layers at any desired surface pressure.

Monolayers of stearic acid and other long-chain amyhipathic molecules were formed by carefully layering onto the trough surface a sufficient quantity of a 0.05% solution of the surface-active materials in benzene, the proper quantity of acid being determined by adding the benzene solution until the first appearance of a "lens" on the surface.   At that point the barrier was moved back to just allow the lens to spread.   Prior to the addition of the spreading solution, the surface was swept several times with glass barriers, to remove any surface contamination that would cause faulty deposition of the monomolecular layer.   The trough substrate was deionized water except when various concentrations of aluminum chloride were employed.

The metal substrates were mounted on a dipping device.   The rate of dipping was controlled by a reversible motor and adjusted to approximately 3 cm.-min.$^{-1}$.   In all cases in which the Blodgett[8] technique was used, monolayer deposition occurred as the metal substrate was withdrawn from the trough.   Prior to plating, the film was allowed to stand 5 min. to allow for solvent evaporation.

Deposition of the monolayer was never of the "reactive" type,[9] i.e., one with rapid expulsion of the water film.   In our experiments, less interaction of monolayer and metal substrate occurred, so that a water film remained on

the plate after the deposition of the monolayer. Consequently, it was necessary to stand the plates vertically in air until the water was removed by drainage and evaporation, which usually occurred within 30 sec. after plate removal from the trough substrate.

Force–Area Isotherms

Force–area isotherms were measured with a commercial balance of the Langmuir-Adam type (Cenco Hydrophil Balance, Central Scientific Co., Chicago, Illinois) with a torsion wire exhibiting 0.61 dynes/cm. per degree of rotation.

Contact Angle

Contact angle measurements on sessile drops of molten polyethylene were determined with a device employed by Williams and Nielsen.[10] The metal substrates were prepared by depositing monolayers of stearic acid at various surface pressures. Polyethylene in the form of cylindrical sections 1.5 mm. in diameter and 1.0 mm. in thickness were placed on the substrate. This unit was transferred to a calibrated hot stage, set to the desired temperature. The sessile drop was observed through a telescope designed and built by the Gaertner Scientific Corporation, Chicago, Illinois. The telescope is equipped with an ocular protractor for measuring directly the angle of contact, and an ocular micrometer for measuring the linear dimensions of the sessile drop, these components having precisions of ±1.5 min. and ±0.00005 in., respectively. It is possible to see and photograph the drop simultaneously, the 35 mm. Ihagee Exakta camera being mounted on the telescope. The beam-splitting lens allows a duplicate of the image, as seen in the eyepiece, to occur at the focal plane of the camera. The telescope may be leveled by adjusting it in reference to a spirit level mounted parallel to its optic axis. It is capable of revolving 360° about its mounting post. The cross hairs of the eyepiece serve as a reference, in subsequent leveling of the test specimen.

Radioactive Tracer Studies

All counting measurements were made with a thin window flow counter. A conventional commercial scaling unit was used. The rectangular aluminum plates containing the adsorbed monolayers were mounted under the flow counter in a reproducible fashion.

Tensile Shear Experiments

For the measurement of tensile shear strengths, surface-treated aluminum plates having an adsorbed monolayer were bonded together with polyethylene in a special device designed to give a $1/2$ in. overlap. The interface is described schematically (not to scale) in Figure 1. A fine gold wire 0.003 in. in diameter was interposed between the two pieces of aluminum, to maintain a polyethylene glue line of constant thickness. The specimens
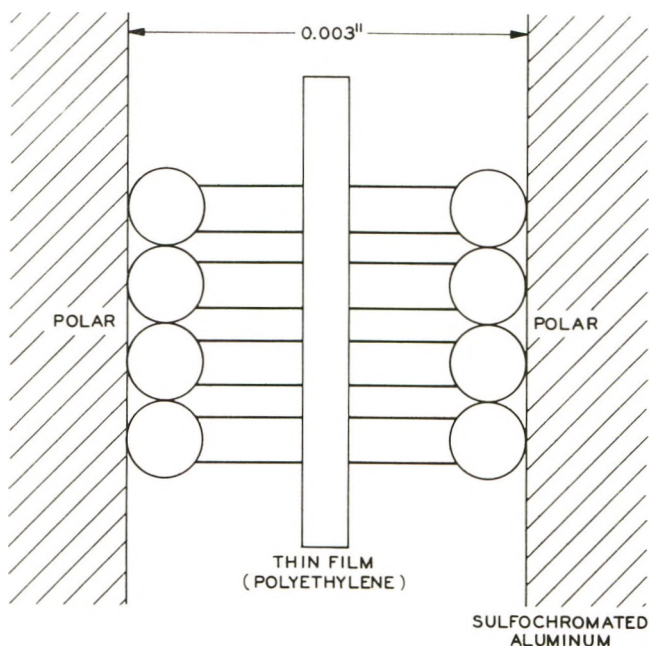
Fig. 1. Schematic diagram of interface of tensile shear specimens.

were fabricated into the final test units by elevating them to the desired temperature and pressure on a commercial, electrically heated press. It was found subsequently that a precoating of the aluminum surface was desirable for maximum bond strength.

This precoating procedure involved mild abrasion of the polyethylene surface, to expose the bulk phase, followed by washing in hot acetone. Polyethylene gloves and tweezers were used in all specimen preparations, to avoid possible contamination. Sections of abraded polyethylene 1×2 in. were placed over the metal substrate and bonded at $\sim 177°C$. for 5 min. Wetting of the metal surface was observed visually, and trapped air was removed. The two precoated sections were then joined together in the tensile shear bonding jig at 177°C. and 30 psi. for different lengths of time. The bonded specimens were tested in tensile shear in accordance with ASTM Designation D-1002, except that they were pulled apart at 0.1 in./min.

Peel Experiments

Sulfochromated Alclad aluminum test specimens ($5 \times 1 \times \frac{1}{16}$ in.) coated with a monolayer of stearic acid deposited at various surface pressures, were bonded with sections of abraded and acetone-washed polyethylene, $5 \times 1 \times \frac{1}{16}$ in., on a calibrated hot stage. They were cooled, aged for a minimum of 24 hr., and then peeled at 180° according to ASTM D-903-49: Test for Peel or Stripping Strengths of Adhesives, except that crosshead separation rates of 2 and 5 in./min. were employed.

All experiments reported here were carried out at room temperature (21–23°C.) unless otherwise noted.

Theory

The high degree of orientation of a condensed monomolecular film transferred to a solid matrix, as shown in Figure 2, coupled with intimate contact of essentially the entire surface of the substrate, leads to the formation of strong bonds.[11]

If an appropriate condensed monomolecular layer of an amphipathic material is interposed between carefully prepared hydrophilic and hydrophobic surfaces, adhesional failure should be minimized. We then approach as a limiting factor the cohesive strength of the adherends.

Some of the surface parameters involved in joint strength have been reviewed by Eley.[12] His main consideration was the nature of the molecular forces at the polar surface–amphipathic molecule interface. Vertical and lateral forces are treated, for a model consisting of a close-packed array of adsorbed molecules as shown in Figure 2, by means of the approach of Roberts.[13]

The principal forces holding molecules in place in a condensed monolayer at a liquid–vapor interface are threefold:[14] (a) van der Waals dispersion forces between adjacent chains, (b) interaction of the polar group with the substrate, and (c) external lateral pressure.

When the amphipathic monolayer is transferred to a solid substrate, a 1:1 correspondence in transfer being assumed, the third factor disappears and leaves cohesion of the film to the van der Waals forces and to the anchoring of the polar groups onto the metal surface.

A calculation of the adsorption energy for a condensed monolayer of stearic acid, made with Eley's[12] approach, yields, neglecting chemisorption, −700 ergs/cm.^{2}. By assuming a range of action of 2×10^{-8} cm., as
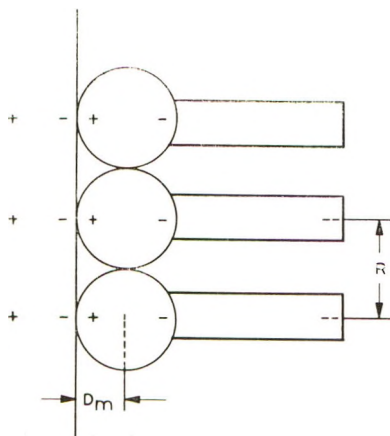

Fig. 2. Amphipathic molecules in the condensed monolayer on a polar substrate.

Harkins did, an interfacial force of approximately 1300 tons/in.[2] is obtained, orders of magnitude greater than experimental values.

The desorption of an adsorbed monolayer requires a considerable amount of energy. In adhesion experiments the force required to break real bonds never approaches the value calculated from theory.[15]

In principle, if a close-packed monolayer is adsorbed onto a polar substrate and then the hydrophobic adherend is properly applied, adhesional failure should be eliminated. Thus, the limiting consideration is the cohesive strength of the weaker adherend.

Results and Discussion

Force–Area Isotherms of Amphipathic Molecules

Force–area isotherms of the amphipathic molecules were determined on various solution substrates. The purpose of this experiment was to ascertain the optimum plating conditions and the molecular nature of the deposited films. Orientation and molecular packing are observed directly from consideration of these two-dimensional isotherms. The isotherm for stearic acid on deionized water agreed quite well with those recorded in the literature. For example, the area per molecule of stearic acid in a condensed monolayer is ~20.0 A.[2]. This is obtained by extrapolating the isotherm to zero compression of the monolayer. When aluminum chloride is added to the trough substrate, the stearic acid is partially converted to aluminum stearate, resulting in a greater area per molecule. The bulk of the experimental data is confined to the stearic acid system.

Adhesion of Polyethylene to Aluminum

Polyethylene was bonded to 2024-T4 aluminum with and without monolayers of various amphipathic molecules. Table II lists some of the tensile shear strengths of these joints. Interfacial deposition of octadecylamine from water and stearic acid from a trough substrate of $0.0005M$ aluminum chloride, both at 30 dynes/cm., increased the adhesive strength of tensile shear specimens by 15 and 24% respectively. The monolayer adhesive acted as a bridge between the polar and nonpolar adherends. Chemisorption of the polar functional group of the monolayer occurs when it comes into contact with the porous sulfochromated aluminum surface. The aliphatic portion of the monolayer is mechanically encapsulated in the molten hydrophobic polymer phase. When the ethyl half-ester of octadecanedioic acid was adsorbed there was no significant change in adhesion. The incompatibility of the ester group and the hydrophobic matrix of the polyethylene could account for the observed lack of increase in adhesive strength. The increase to 1607 psi in the case of the ethyl half-ester of octadecanedioic acid adsorbed from a $0.0005M$ aluminum chloride solution may be accounted for by considering the area per molecule at zero compression. The larger area per molecule enables the molten polyethylene to fill

TABLE II

Tensile Shear Strength of Polyethylene Bonded to 2024-T4 Aluminum at 177°C. for
10 min. with Various Monolayers Deposited at 30 dynes/cm.

Monolayer	Trough substrate	Aluminum treatment prior to deposition of monolayer	Adhesive strength, psi[a]	Range
—	—	Sulfochromate	1459	1000–1820
Octadecylamine	Deionized water	Sulfochromate	1683	1380–1900
Ethyl half-ester of octadecanedioic acid ($EtO_2C(CH_2)_{16}COOH$)	Deionized water	Sulfochromate	1408	1168–1952
Ethyl half-ester of octadecanedioic acid	$0.0005M$ $AlCl_3$	Sulfochromate	1607	1410–1840
Stearic acid	Deionized water	Sulfochromate	1561	1040–2040
Stearic acid	$0.0005M$ $AlCl_3$	Sulfochromate	1810	1488–2120
Stearic acid	Deionized water	(1) Alkali etch	463	433–510
		(2) Alkali etch	471	—

[a] Recorded value is average of twelve determinations.

the void space and interact with the hydrophobic chains of the amphipathic adsorbed species.

In the alkali etch process we evidently get no formation of a bond between the more polar functional group of the adsorbed molecules and the treated aluminum surface. It has been shown[6] that salt formation does indeed occur in the case of an interaction between stearic acid and a germanium crystal having an appreciable oxide layer. Probably, chemisorption occurs when the long-chain molecules are bonded to the sulfochromated substrate, while only mild physical adsorption occurs in the case of the alkali etch-treated specimens. Poorer monolayer coverage of the polar surface in the alkali etch process may also contribute to weaker bonds.

Previously one had to be content with adsorption of the adhesive onto only preferred sites of the substrate. Now, upon deposition of the appropriate monolayer, a close-packed array of sites that can participate in bonding is obtained. The surface microtopology of the substrate phase need no longer be a major deterrent to good adhesive joints. Capillary pressure should draw the polyethylene into the pores or channels that are coated with the adsorbed surface-active long-chain amphipathic molecules.

The nonstoichiometry of the metal surfaces (i.e., oxides, etc.) should have no bearing on the final adhesion strength. The polar portion of the surface-active material, when adsorbed onto the hydrophilic sites of the substrate surface, presents to the polyethylene a homogeneous hydrophobic phase for bonding. Increasing the chain length of the adsorbing species should increase the dispersion forces in the oriented phase. Ries and Kimball[16] have employed in their investigation an n-hexatri-
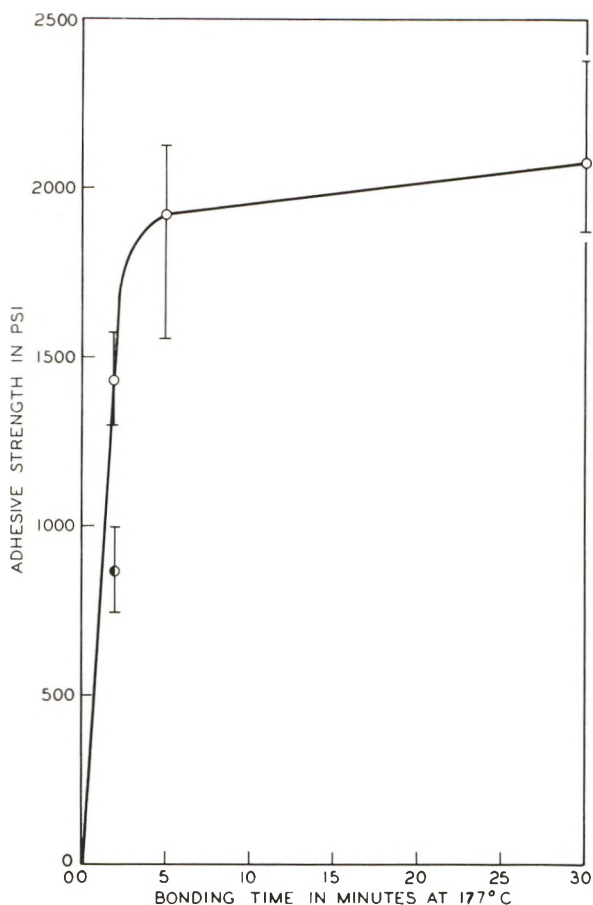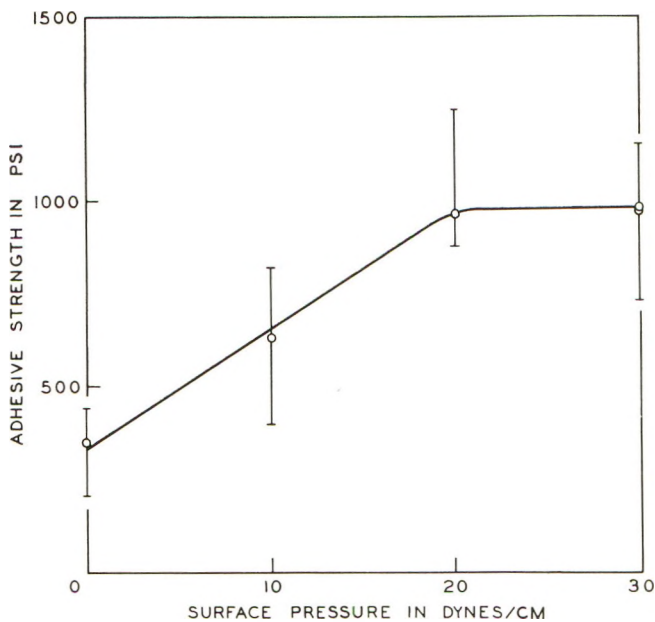
Fig. 3. Tensile shear strengths of polyethylene bonded to sulfochromated Alclad 2024-T3 aluminum having an adsorbed monolayer of stearic acid deposited at 30 dynes/cm. from deionized water: (O) stearic acid-coated specimens; (◐) no stearic acid, sulfochromated.

acontanoic acid containing 36 carbon atoms, whose monolayer had a high collapse pressure and a thickness of 50 Å. The strong cohesive forces in the hydrocarbon tails would account for their high collapse pressure. In general, the larger the van der Waals forces, the higher the collapse pressure. Moreover, the strong cohesive forces in the extended hydrocarbon portions of the adsorbed monolayer should preclude the overturning phenomenon demonstrated by Rideal and Tadayon[3] for the stearic acid system.

The extent of adhesion as a function of bonding time at a temperature of 177°C. was determined by employing a different substrate system consisting of an Alclad 2024-T3 aluminum. The high-purity aluminum surface of the Alclad material affords a better bonding medium than does the 2024-T4 aluminum. The adhesion of stearic acid to the sulfochro-

Fig. 4. Tensile shear strengths of polyethylene bonded for 2 min. at 177°C. to sulfochromated Alclad 2024-T3 aluminum having an adsorbed monolayer of stearic acid deposited at 10, 20, and 30 dynes/cm. from deionized water.
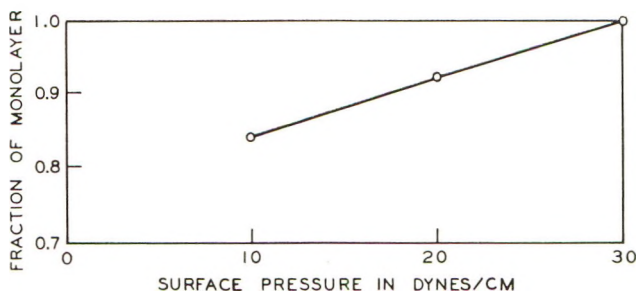

Fig. 5. Fraction of monolayer coverage of radioactive stearic acid deposited at 10, 20, and 30 dynes/cm. onto sulfochromated Alclad 2024-T3 aluminum.

mated Alclad surface is enhanced, as is apparent from the values of Figure 3. At the 10 min. interval a value of 1950 psi is obtained, considerably higher than the 1561 psi when the alloyed aluminum was used.

After an exposure period of 30 min. a maximum value of 2077 psi is reached. Prolonged exposure probably results in salt formation at the stearic acid–aluminum interface, increasing adhesion at these bonding sites. Figure 3 indicates that essentially 10 min. is sufficient for maximum bonding. It should be noted that in the group at $1/2$ hr. exposure there was 100% cohesive failure of the polyethylene. The strength of the bond exceeded the cohesive strength of the polyethylene. The ruptured surface
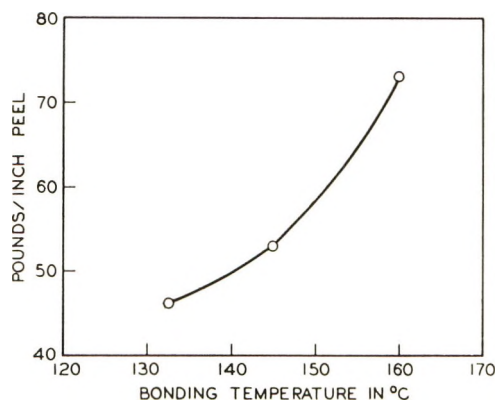
Fig. 6. 180° peel test corresponding to ASTM D-903-49. Polyethylene bonded for 10 min. to sulfochromated Alclad 2024-T3 aluminum having an adsorbed monolayer of stearic acid deposited at 30 dynes/cm. from deionized water.
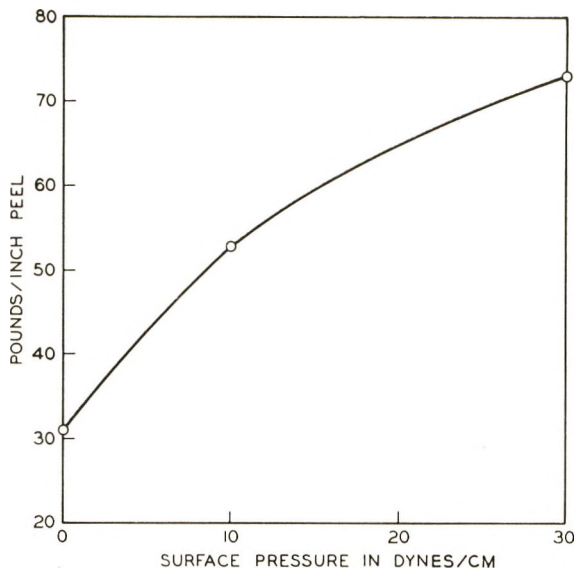

Fig. 7. 180° peel test corresponding to ASTM D-903-49. Polyethylene bonded for 10 min. at 160°C. to sulfochromated Alclad 2024-T3 aluminum having an adsorbed monolayer of stearic acid deposited at 10 and 30 dynes/cm. from deionized water.

was rough and dendritic, no aluminum being exposed. It is interesting to compare the sulfochromated surface with no adsorbed monolayer and with the stearic acid. A value of 1435 psi for 2 min. of bonding was obtained with the stearic acid, while only 867 psi was obtained without the monolayer. Unlike Lasoski and Kraus,[5] who used a *monolayer equivalent* of decanoic acid which definitely contains multilayers, we have constructed an *oriented monolayer*. It is known that multilayers will tend to lower adhesion, not because of the bonding of the amphipathic molecule to the
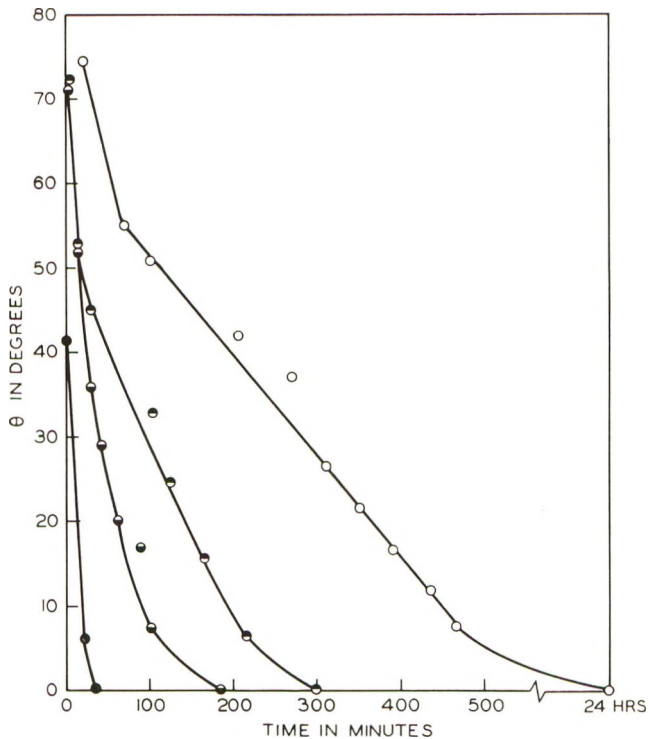
Fig. 8. Contact angle of polyethylene on sulfochromated Alclad 2024-T3 aluminum having an adsorbed monolayer of stearic acid deposited at 30 dynes/cm. from deionized water: (O) 125°C.; (◑) 137°C.; (◔) 155°C.; (●) 175°C.

substrate surface, but because of the adhesion of the monolayer to itself. The vertical lines in Figure 3 indicate the range over which failure occurred. The samples, Figure 3, were precoated; therefore, the time merely indicates the interval necessary to insure polyethylene-to-polyethylene bonding. For Figure 4, no precoating was permitted. Specimens were exposed to this temperature for a short period of time to get some idea of the effect of surface pressure on the adhesive strength. Low surface pressure indicates low coverage of the metal substrate by the monolayer. As shown in Figure 5, radioactive material being employed, the amount of coverage at a plating pressure of 10 dynes/cm. is only 84% of the exposed surface. At 20 dynes/cm., 92.5% of the available surface is covered with a monolayer of stearic acid. From the isotherm for stearic acid, one would expect to get for the 10 dynes/cm. surface pressure of a 86% monolayer. This agrees quite well with the value of 84% obtained by radioactive techniques in the present investigation. It can be concluded, therefore, that we have a 1:1 correspondence in transfer of the monolayer from the surface of the plating trough to the metal substrate.

The lower adhesive strengths obtained at 10 dynes/cm. are to be expected, since Ries and Walker[17] have demonstrated, by using electron
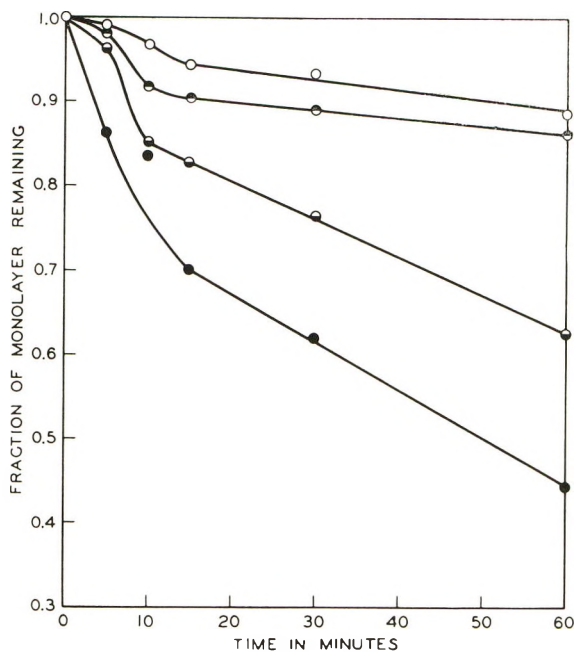
Fig. 9. Thermal desorption of radioactive stearic acid deposited at 30 dynes/cm. onto sulfochromated Alclad 2024-T3 aluminum: (O) 125°C.; (◐) 150°C.; (◖) 175°C.; (●) 205°C.

diffraction, the existence of islands of condensed and loosely packed regions. These inhomogeneities or surface defects are probably the sites where poor monolayer adhesion occurs, thereby weakening our final adhesive bond.

Perhaps a more conclusive type of test to ascertain the extent of bonding is the peel test. We have confined ourselves in this introductory work to a 180° peel test corresponding to ASTM test D-903-49. The variation of peel strength with bonding temperature results in some interesting effects, as indicated in Figure 6. At relatively low temperatures, such as 125°C. which is the melting point of polyethylene, a much lower value than the maximum of 73 lb./in. width peel was obtained. Low-temperature bonding evidently does not allow the hydrocarbon tails to enter fully the hydrophobic matrix of the polyethylene. Tests will be performed at higher temperatures in an attempt to obtain a maximum.

The effect of surface pressure on peel strength is shown in Figure 7. Low surface coverage results in lower peel strength. The condensed monolayer adsorbed onto the surface of the aluminum affords the best bonding surface. Relatively poor adhesion occurs when *no* monolayer is present on the metal substrate.

The contact angles of molten polyethylene on sulfochromated Alclad 2024-T3 specimens containing stearic acid deposited at a surface pressure of 30 dynes is depicted in Figure 8. As is observed, the equilibrium contact
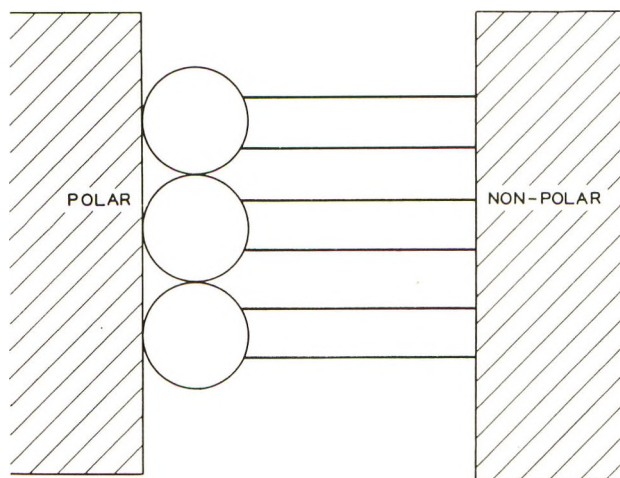
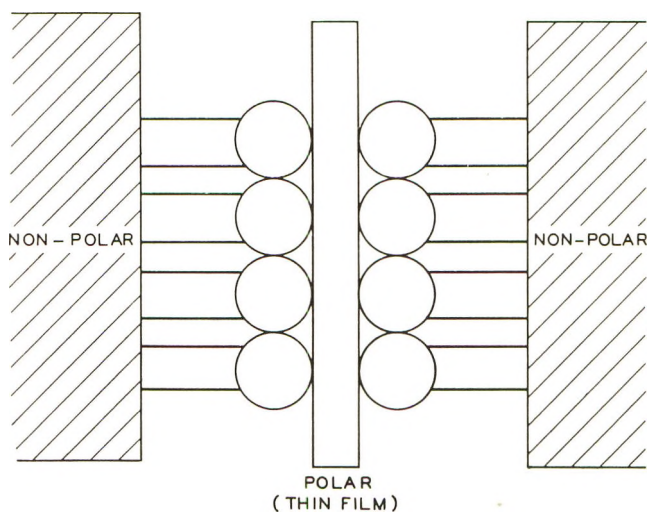Fig. 10. Nonpolar–polar adhesive system.

Fig. 11. Nonpolar–nonpolar adhesive system.

angle is zero in all cases. Contact angles do not appear to be affected by the fraction of monolayer adsorbed on the surface. Determinations made at 10 and 20 dynes/cm. as well as when no monolayer was present gave essentially the same contact angle as a function of time. Temperature appears to be the major factor in determining the length of time necessary to wet the surface. At 175°C. the entire surface is wet in a relatively short time. Heat desorption experiments at elevated temperatures (Fig. 9) indicated that only a small fraction of the monolayer was lost before wetting of the surface occurred. When the bonding surface was covered with polyethylene prior to heating, less material may have been lost because volatilization was avoided, although desorption of the ad-

sorbed monolayer into the hydrophobic polymer may proceed by a solubilization phenomenon. Evidently these are minor considerations since the extremely high tensile shear and peel strengths are not affected to any great extent.

In the tensile shear experiment, the bonding of aluminum to aluminum, polyethylene was employed as a matrix for the *oriented monolayer adhesive.* Polar and nonpolar adherends may be bonded in any combination, as is apparent from Figures 10 and 11.

The polyethylene–aluminum adhesive system has been considered first because previous investigators[1,2] have had difficulties in obtaining good bonds. Bikerman has argued in his "rheological theory" that poor adherence must be due to the presence of weak boundary layers.[2] The two alternatives posed by him are (*1*) to make polyethylenes more chemically

TABLE III
Effect of Van de Graaff Irradiation on 180°C. Peel Test Specimens

Bonding time, min.	Surface pressure, dynes/cm.	Bonding temp., °C.	Total dose, Mrads	Peel strength,[a] lbs. in width
6	30	200	10	>90
8	30	200	10	65
10	30	200	10	>85
4	30	220	10	>76
6	30	200	20	73
8	30	200	20	>102
10	30	200	20	>74
6	30	200	100	>46
8	30	200	100	>45
10	30	200	100	>44
4	30	200	100	>41
10	0[b]	200	13	>92
10	0[b]	200	27	>79
10	0[b]	200	94	25

[a] Symbol (>) indicates cohesive failure of polyethylene.

[b] Denotes no deposited monolayer.

active and (*2*) to remove from them substances giving rise to weak interfacial films. While a great deal of effort has been expended by Bikerman and his associates in expounding the virtues of their so-called rheological theory, the values of peel strengths reported by them for the system polyethylene–aluminum are remarkably low. The highest value of peel strength reported by Bikerman for "adhesionable" polyethylene bonded to a pure aluminum foil was 7.4×10^5 dynes/cm. of width. When one converts this figure to pounds per inch of width, the units employed here, the maximum of 7.4×10^5 dynes/cm. of width becomes the less respectable figure of 4.0 lb./in. of width. The values reported in Table III exceed this figure by more than one order of magnitude. It is obvious that the "exceptional" peel strengths reported by Bikerman are negligible. While

the highest value was 4.0 lb./in. of width, there are several that are less than 0.5 lb/in. of width.

It can be concluded that the peel strength has been increased considerably by employing the oriented monolayer adhesive. Most important is the fact that we have made *no* attempt in this study to alter the properties of the polyethylene as obtained from the manufacturer. If we had had a weak boundary layer in the system by virtue of not extracting substances that gave rise to weak interfacial films, poor adhesion should have resulted. It is not the impurities in the polyethylene that are contributing to poor adhesion but, rather, the lack of intermolecular forces between the adherends. Oriented monolayer adhesives act as a bridge between adherends. They are attached to both phases by virtue of chemisorption and mechanical encapsulation.

Conclusion

A generalized approach to adhesion has been presented and illustrated by considering the bonding of polyethylene to aluminum. It has been demonstrated that the adsorption of condensed monolayers of amphipathic molecules between selected adherends affords a bonding phase possessing a high degree of orientation, uniformity, and specificity. Employing the techniques of surface chemistry, a uniform distribution of the oriented monolayer adhesive is deposited onto our adherend surfaces.

The generalized approach to adhesion presented in this communication is adaptable, in principle, to the bonding of any pair of adherends, without regard to their surface polarities.

Future communications in this series will discuss the effect of Van de Graaff irradiation on our specimens and the bonding of polyethylene to other metal substrates with amphipathic molecules as oriented monolayer adhesives.

References

1. Bikerman, J. J., *Science of Adhesive Joints*, Academic Press, New York, 1961.
2. Bikerman, J. J., *J. Appl. Chem.*, **11**, 81 (1961).
3. Rideal, E., and J. Tadayon, *Proc. Roy. Soc.*, **A225**, 346 (1954).
4. Allen, A. J. G., *J. Colloid Sci.*, **14**, 206 (1959).
5. Lasoski, S. W., Jr., and G. Kraus, *J. Polymer Sci.*, **18**, 359 (1955).
6. Sharpe, L. H., *Proc. Chem. Soc.*, **1961**, 461.
7. Sher, I. H., and J. D. Chanley, *Rev. Sci. Instr.*, **26**, 266 (1955).
8. Blodgett, K. B., *J. Am. Chem. Soc.*, **57**, 1007 (1935).
9. Schulman, J. H., R. B. Waterhouse, and J. A. Spink, *Kolloid-Z.*, **146**, 77 (1956).
10. Williams, J. C., and J. W. Nielsen, *J. Am. Ceram. Soc.*, **42**, 229 (1959).
11. Patrick, R. L., C. M. Doede, and W. A. Vaugh, *J. Phys. Chem.*, **61**, 1036 (1957).
12. Eley, D. D., *Adhesion and Adhesives, Fundamentals and Practices*, Wiley, New York, 1954.
13. Roberts, J. K., *Trans. Faraday Soc.*, **34**, 1342 (1938).

14. Sobotka, H., *J. Colloid Sci.*, **11**, 435 (1956).

15. Czyak, J., *Am. J. Phys.*, **20**, 440 (1952).

16. Ries, H. E., and W. A. Kimball, *Proc. 2nd Intern. Congr. Surface Activity*, London, 1, 75 (1957); *Nature*, **181**, 901 (1958).

17. Ries, H. E., Jr., and D. C. Walker, *J. Colloid Sci.*, **16**, 361 (1961).

Résumé

On utilise des couches monomoléculaires orientées comme adhésifs effectifs pour lier le polyéthylène à l'aluminium. Diverses monocouches sont caractérisées et leurs propriétés physiques élucidées. La mesure de la tension de cisaillement et la force d'arrachement du polyéthylène de l'aluminium indiquent que les liaisons formées dépasse la force de cohésion du polymère. L'angle de contact et des essais aux traceurs radioactifs ont aidé à la détermination des conditions d'une adhésion maximum.

Zusammenfassung

Orientierte monomolekulare Schichten werden zur wirksamen Verklebung von Polyäthylenen mit Aluminium verwendet. Mehrere monomolekulare Schichten werden in bezug auf ihre physikalischen Eigenschaften näher untersucht. Messung der Schubspannung und der Abziehfestigkeit von Polyäthylen an Aluminium zeigt, dass die gebildete Verbindung fester ist als der Kohäsionsfestigkeit des Polymeren entspricht. Versuche über den Kontaktwinkel und mit radioaktiver Markierung waren bei der Bestimmung der Bedingungen für das Adhäsionsmaximum von Wert.

Elution Fractionation of Crystalline Polypropylene*

ROBERT A. MENDELSON, *Research Department, Plastics Division, Monsanto Chemical Company, Texas City, Texas*

Synopsis

A number of commercial and experimental samples of crystalline polypropylene were fractionated by sand column solvent gradient elution techniques. Two different solvent–nonsolvent systems were studied under several sets of experimental conditions. Deposition of polymer upon the sand from a thermodynamically poor solvent was found to be necessary to achieve selective fractionation according to molecular weights. Both selective and nonselective fractionation results are illustrated with the latter occurring whenever the polymer is deposited upon the substrate from a thermodynamically good solvent. Molecular weight distributions for ten samples are given as obtained from elution fractionation using o-dichlorobenzene–diethylene glycol monomethyl ether as solvent–nonsolvent system at 168°C. These molecular weight distributions could be adequately described by the logarithmic-normal probability distribution function found by Wesslau and others to be applicable for linear polyethylene and by Davis and Tobias for polypropylene. Many of the distributions observed in this work were found to be narrower than those previously reported in the literature.

Introduction

As in the case of other polymers, many of the important physical properties of crystalline polypropylene are determined either directly or indirectly by the average molecular weights and by the molecular weight distributions of the polymeric materials.[1] In addition, important kinetic information may be obtained from a knowledge of the molecular weight distribution. Hence, a rapid and reliable means for the determination of these molecular weight distributions is highly desirable.

The advantages of chromatographic[2,3] and elution[4-8] fractionation schemes for filling this need for polymers other than polypropylene have been fully discussed in the recent literature. In particular, elution techniques have been applied with considerable success by several investigators in the case of linear polyethylene.[5-8] Most recently, Davis and Tobias[9] have reported in detail a sand column elution fractionation scheme for polypropylene.

The present work summarizes the results of the fractionation of a number of commercial and experimental samples of crystalline polypropylene by gradient elution techniques. The necessity for selectivity according to

molecular weight in depositing the polymer on the substrate as indicated by Kenyon and Salyer[7] was confirmed and emphasized for highly crystalline polymers. The molecular weight distribution of most samples could be described by a logarithmic-normal probability distribution function, and many of the polymers were found to have relatively narrow distributions.

Experimental

All fractionations reported here were performed by column elution techniques using as substrate Ottawa silica sand between 40 and 80 mesh particle size. Figure 1 shows a diagram of the column and mixing reservoir similar in most respects to those previously reported. The lower section of the column is the fraction collector with a Soxhlet-type siphon drain designed to deliver the solution to an external flask automatically whenever a fixed volume is collected. Provision is made for a continuous nitrogen blanket in the chamber through the three-way stopcock shown. This serves the dual purposes of excluding oxygen and of providing a back-pressure to regulate the flow rate of liquid through the column. The pressure in the collector is equilibrated with pressure in the external collector flask by splitting the nitrogen feed line so that no pressure differential exists across the siphon.

The mixing reservoir shown at the top of Figure 1 is similar to that described by Davis and Tobias[9] and was used for most fractionations. Some few fractionations were performed using a continuous logarithmic

500 ML GRADUATE

THREE-WAY STOPCOCK

28/15 BALL JOINT TO BOILER

46/50 S

LEVEL OF SAND

OVERALL LENGTH OF COLUMN - 94 CM.

OUTSIDE DIAMETER - 9 CM.

INSIDE TUBE - 85 CM. LONG 5 CM. IN DIAMETER

SAND SUPPORT, GLASS-WOOL ON S.S WIRE SCREEN
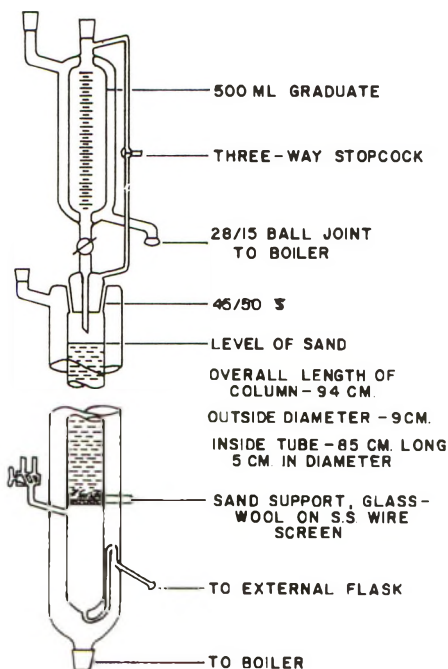
TO EXTERNAL FLASK

TO BOILER

Fig. 1. Diagram of elution fractionation column.

gradient addition of solvent-nonsolvent mixtures, and for these a separate solvent reservoir and a conical mixing vessel such as were described by Baker and Williams[3] were substituted.

Fractionations were performed with tetralin–o-dimethyl phthalate and with o-dichlorobenzene–diethylene glycol monomethyl ether (Methyl Carbitol) solvent–nonsolvent pairs. The tetralin–o-dimethyl phthalate (DMP) pair was used at 155°C. and at 178°C., and both logarithmic gradient addition of eluent and batch (fixed composition) addition of eluent mixtures of increasing solvent power were employed with this system. In all cases of fractionation with tetralin–DMP the polymer was deposited upon the substrate by slowly cooling overnight in the column the solution of ca. 0.7 wt.-% concentration of polymer in pure solvent (tetralin). All fractionations performed with the system o-dichloro-benzene–Methyl Carbitol were carried out at 168° C., a batch procedure being used for eluent addition. Several runs using this system were made wherein the polymer was deposited by slow cooling as described above from a solution of less than 0.5% polymer in pure solvent (o-dichloroben-zene). The majority of fractionations performed with this system in-volved, however, deposition of polymer on to the substrate by the same slow overnight cooling of the column as previously described, but from a solution of less than 0.5% polymer in a mixture of 60:40 (by volume) solvent to nonsolvent.

Eluent batches consisted of 270 ml. portions of the appropriate solvent-nonsolvent composition, and flow rates were adjusted by controlling the nitrogen back-pressure to give approximately 9 ml./min. (30 min./fraction). The same flow rate was maintained for the logarithmic gradient elution fractionations. The optimum compositions of the eluent mixtures were obtained by trial and error in the early fractionations, but as data were developed it became possible to predict these compositions from a knowl-edge only of the intrinsic viscosity of the whole polymer in question.

Careful purging and blanketing with nitrogen of all solvents and non-solvents used in the fractionation and characterization of the polymer and continuous blanketing of the column with high purity nitrogen were found to be essential to prevent degradation. Both solvent and nonsolvent were, in addition, inhibited by dissolving 0.3 wt.-% Ionol in them. These precautions were demonstrated to be adequate for the fractionation work reported here.

The polymer fractions were isolated from their respective solutions by precipitation with methanol, filtration, drying and weighing. The average molecular weight of each fraction was characterized by determining the specific viscosity of an approximately 0.1% solution of the polymer fraction in tetralin containing Ionol at 130°C. Intrinsic viscosities of whole polymers were determined by the usual double extrapolation of reduced specific viscosities and inherent viscosities to zero concentration from data obtained for four or more concentrations of polymer in tetralin (containing Ionol) at 130°C. Standard Cannon-Fenske number 50 viscometers,

chosen such that the flow times for solvent were all in excess of 200 sec., were used.

Calculations and Results

Calculations of fraction molecular weights from the single-point viscosity data and of the cumulative weight fraction distributions from fraction weights were performed in all cases using an IBM-650 computer. The intrinsic viscosities of the fractions were computed from η_{sp} at a single concentration C using the expression:

$$[\eta] = [(1 + 1.58\,\eta_{sp})^{1/2} - 1]/0.789C \tag{1}$$

derived from the usual Huggins equation with an average value of $k' = 0.395$. Molecular weights were obtained from the intrinsic viscosities according to Kinsinger's[10] equation for decalin at 135°C.:

$$[\eta] = 1.10 \times 10^{-4}\bar{M}_w^{0.80} \tag{2}$$

The cumulative weight fraction distributions, $I(M)$, were calculated according to the method of Schulz and Dinglinger[11]:

$$I(M) = {}^1\!/_2\,w_i + \sum_{i=1}^{n} w_{i-1} \tag{3}$$

where w_i is the weight fraction of the ith fraction.

Weight-average and number-average molecular weights of the whole polymers were calculated as part of the computer program according to the well-known equations

$$\bar{M}_w = \sum_{i=1}^{n} w_i M_i \tag{4}$$

and

$$\bar{M}_n = (\sum_{i=1}^{n} w_i/M_i)^{-1} \tag{5}$$

as well as the sum of the weighted intrinsic viscosities ($\Sigma w_i[\eta]_i$).
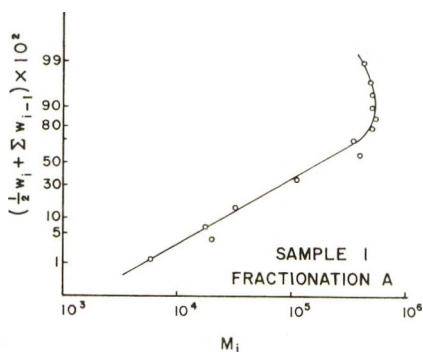

Fig. 2. Typical logarithmic-normal probability distribution curve resulting from deposition of polymer on substrate from a "good" solvent; sample 1, fractionation A.

Figure 2 shows a Wesslau[12] plot for sample 1 fractionated with the system tetralin–dimethyl phthalate with deposition of polymer onto the column occurring from a solution of polymer in tetralin only. This is a typical example of all fractionation results using a system of deposition from pure solvent.

In Tables I and II fractionation data are given for samples 2 and 6, respectively, which are typical of elution fractionation after deposition
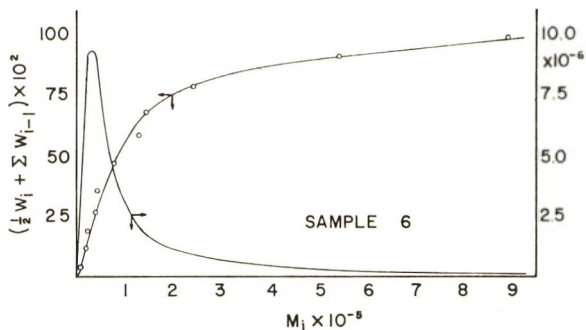

Fig. 3. Typical cumulative and differential distribution curves resulting from deposition of polymer on substrate from a relatively "poor" solvent; sample 6.
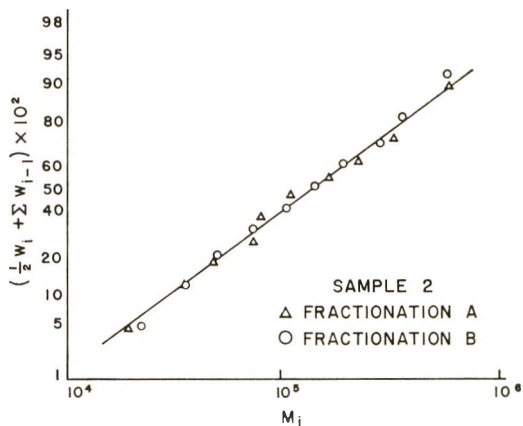

Fig. 4. Logarithmic-normal probability distribution curve for two fractionations of sample 2.

from a mixed solvent. Figure 3 shows a plot of the cumulative and differential distributions of sample 6. Figure 4 shows a comparison of two fractionations of sample 2 plotted on normal probability-logarithmic coordinates,[12] indicating the excellent reproducibility obtained, and demonstrating also the linearity usually observed for such plots. Table III summarizes the average molecular weights derived according to eq. (2) from the fractionations of ten commercial and experimental samples of

crystalline polypropylene. In all cases cited the fractionation procedure involved the use of the system o-dichlorobenzene–Methyl Carbitol with deposition of polymer onto the column occurring from a 60:40 solvent–nonsolvent mixture.

TABLE I
Fractionation Data, Sample 2A

Fraction i	$[\eta]_i$	Wt. fraction w_i	$(^{1}/_{2}\,w_i + \Sigma w_{i-1}) \times 10^2$	$M_i \times 10^{-4}$
1	0.304	0.0862	4.31	2.00
2	0.483	0.0731	12.28	3.57
3	0.630	0.0528	18.57	4.98
4	0.896	0.0931	25.87	7.73
5	0.950	0.1164	36.35	8.33
6	1.34	0.0945	46.89	12.8
7	1.69	0.0775	55.49	17.1
8	2.18	0.0851	63.62	23.5
9	2.93	0.1122	73.48	34.1
10	4.77	0.2091	89.54	62.5

TABLE II
Fractionation Data, Sample 6

Fraction i	$[\eta]_i$	Wt. fraction w_i	$(^{1}/_{2}\,w_i + \Sigma w_{i-1}) \times 10^2$	$M_i \times 10^{-4}$
1	0.150	0.0796	3.98	0.828
2	0.286	0.0724	11.58	1.86
3	0.338	0.0672	18.57	2.29
4	0.526	0.0896	26.40	3.98
5	0.555	0.0890	35.33	4.25
6	0.906	0.1337	46.47	7.84
7	1.34	0.0961	57.96	12.9
8	1.46	0.0999	67.76	14.3
9	2.22	0.1129	78.40	24.0
10	4.25	0.1352	90.80	54.2
11	6.33	0.0244	98.78	89.1

TABLE III
Fractionation Results According to Equation (2)

Sample	$\bar{M}_w \times 10^{-3}$	$\bar{M}_n \times 10^{-3}$	$\bar{M}_w/\bar{M}_n$	$[\eta]$	$\Sigma w_i [\eta]_i$
1	250	58.7	4.27	2.27	2.22
2	229	83.5	2.74	2.08	2.00
3	191	51.3	3.73	1.58	1.64
4	209	65.8	3.18	2.01	1.93
5	664	122	5.46	4.45	4.60
6	170	40.5	4.20	1.52	1.53
7	282	64.4	4.39	2.21	2.32
8	163	48.2	3.38	1.55	1.50
9	250	93.3	2.68	2.26	2.16
10	133	29.8	4.48	1.40	1.26

Discussion

A common characteristic of many of the early attempts at fractionation in this work was the tendency for the measured molecular weights of successive fractions in the higher molecular weight region not to continue rising, and indeed, to decrease or "backlash." This behavior is clearly illustrated in Figure 2 and has been observed in elution fractionation work by a number of experimenters.[4,6,13] It has been variously attributed to degradation of polymer during fractionation and to nonselective fractionation. In the case of the work done here several factors argued strongly against significant degradation as an explanation.

First, in one fractionation the high molecular weight fractions, which had exhibited the above-mentioned "backlash," were recombined and subjected to a second elution fractionation. The new fractions showed the same typical curvature of the distribution but with a displacement of the highest molecular weight values to still higher ones, thus indicating that polymer degradation had not been progressing. Second, in most cases where "backlash" occurred, the sum of the weighted intrinsic viscosities of the fractions $(\Sigma \; w_i[\eta]_i)$ was approximately equal to the intrinsic viscosity of the whole polymer, satisfying this necessary requirement. Thus, for sample 1 (Fig. 2) the value of $(\Sigma w_i[\eta]_i)$ was 2.22 whereas the whole polymer $[\eta]$ was 2.27. Finally, and perhaps most significantly, in no case where the polymer was precipitated onto a substrate from a single component solvent system (pure solvent rather than a mixture of solvent and nonsolvent) was it possible to obtain a satisfactory fractionation regardless of the solvent-nonsolvent or temperature used. On the other hand, the procedure utilizing precipitation of polymer onto the column substrate from a poor solvent (solvent-nonsolvent mixture) immediately yielded satisfactory fractionations with no "backlash," and the molecular weight distributions so obtained were, in the large majority of cases, linear when plotted on log-normal probability coordinates. This result rather clearly indicates that the backlash in the fractionation results obtained in the early experiments was due to nonselective elution of polymer rather than to actual degradation of the polymer.

The observation that selective fractionation according to molecular weight species could only be achieved with an elution procedure (at conveniently rapid rates of elution) by using a solvent-nonsolvent mixture for polymer deposition appears quite significant. The necessity for selective deposition of polymer from solution prior to elution has previously been noted,[7] and the procedure of allowing the column containing the polymer solution to cool slowly to room temperature to achieve partial selective precipitation according to molecular weight has generally been followed.[6,7,8] This procedure has proved adequate in the case of linear polyethylene to insure liquid–liquid phase separation rather than liquid–crystalline phase separation. However, the work conducted here on polypropylene indicates that isotactic polypropylene may be precipitated from

a thermodynamically good solvent, upon lowering of the temperature, at least partially by a liquid–crystalline phase separation leading to non-selective fractionation, particularly in the higher molecular weight region.

The precipitation step prior to elution is critical for any fractionation procedure utilizing reasonably rapid rates of elution (wherein diffusion plays a significant role in the elution step) and must be performed in such a way that the polymer leaves the solution and coats the substrate while in the amorphous, rather than crystalline, state. This was accomplished in the present work by employing as vehicle for the polymer when loading the column a mixture of a "good" solvent and a nonsolvent such that this resultant mixture constituted a thermodynamically "poor" solvent. The system used successfully was 60% o-dichlorobenzene (solvent) and 40% diethylene glycol monomethyl ether (nonsolvent). After filling the sand column with a solution of polypropylene in this poor solvent at the elevated temperature of 168°C., the entire system was allowed to cool slowly. Under these conditions the critical (or precipitation) temperature of each molecular weight species was apparently reached at temperatures above the crystalline melting point in solution and the desired precipitation selectivity according to molecular weight was achieved. On the other hand, when precipitation by cooling from a good solvent, e.g., 100% o-dichlorobenzene, was attempted, selectivity could not be achieved, and fractionations were invariably poor. This technique has broad applicability and in all probability will be a requirement for the successful elution fractionation of all highly crystalline stereoregular polymers. In this regard, the use of a mixed solvent seems to hold some practical advantage over a search for a single component theta-type solvent which additionally must demonstrate a suitably broad solubility range when mixed with nonsolvent to achieve molecular weight selectivity in the elution step.

The linearity of the data for sample 6 as depicted in Figure 4 is typical of results obtained in almost all cases summarized in Table III indicating that the normal probability-logarithmic distribution function proposed by Wesslau[12] for linear polyethylene applies also for isotactic polypropylene. This confirms the results of Davis and Tobias[9] in this regard. It should, however, be noted that the molecular weight distributions, as characterized by the ratio $\bar{M}_w/\bar{M}_n$, were determined in the present work to be considerably narrower than those reported by other authors.[9,13]

References

1. Wijga, P. W. O., in *The Physical Properties of Polymers*, Soc. Chem. Ind. Monograph No. 5, Macmillan, New York, 1959, p. 35.

2. Desreux, V., *Rec. trav. chim.*, **68**, 789 (1949); V. Desreux, M. C. Spiegels, *Bull. soc. chim. Belges*, **59**, 476 (1950).

3. Baker, C. A. and R. J. P. Williams, *J. Chem. Soc.*, **1956**, 2352.

4. Krigbaum, W. R., and J. E. Kurz, *J. Polymer Sci.*, **41**, 275 (1959).

5. Hawkins, S. W., and H. Smith, *J. Polymer Sci.*, **28**, 341 (1958).

6. Francis, P. S., R. C. Cooke, Jr., and J. H. Elliott, *J. Polymer Sci.*, **31**, 453 (1958).

7. Kenyon, A. S., and I. O. Salyer, *J. Polymer Sci.*, **43**, 427 (1960).

8. Henry, P. M., *J. Polymer Sci.*, **36**, 3 (1959).

9. Davis, T. E., and R. L. Tobias, *J. Polymer Sci.*, **50**, 227 (1961).

10. Kinsinger, J. B., and R. E. Hughes, *J. Phys. Chem.*, **63**, 2002 (1959).

11. Schulz, G. V., and A. Dinglinger, *Z. Physik. Chem.*, **B34**, 47 (1939).

12. Wesslau, H., *Makromol. Chem.*, **20**, 111 (1956).

13. Wijga, P. W. O., J. van Schooten, and J. Boerma, *Makromol. Chem.*, **36**, 115 (1960).

Résumé

Un certain nombre d'échantillons commerciaux et expérimentaux de polypropyléne cristallisé a été fractionné sur colonne de sable à l'aide de techniques d'élution de solvants progressivement différents. Deux différents systèmes solvant–non-solvant ont été étudiés dans plusieurs ensembles de conditions expérimentales. On a trouvé que la déposition du polymére sur le sable à partir d'un solvant thermodynamiquement pauvre est nécessaire pour exécuter un fractionnement sélectif en accord avec les poids moléculaires. Les résultats du fractionnement sélectif et du fractionnement non-sélectif sont illustrés dans le cas qui se présente lorsque le polymère est déposé sur le substrat à partir d'un solvant thermodynamiquement bon. Les distributions de poids moléculaire sont données pour 10 échantillons obtenus par fractionnement par élution utilisant l'*o*-dichloro-benzène monométhyl-éther du diéthylylène glycol comme système solvant–non-solvant à 168°C. Ces distributions de poids moléculaires seraient adéquatement décrites par la fonction de distribution probabilité logarithmique-probabilité normale trouvée par Wesslau et autres applicable au polyéthylène linéaire et par Davis et Tobias pour le polypropylène. De nombreuses distributions observées dans ce travail ont été trouvées proches de celles rapportées antérieurement dans la littérature.

Zusammenfassung

Eine Anzahl käuflicher und experimenteller Proben von kristallinem Polypropylen wurden nach dem Lösungsmittelgradient-Eluierungsverfahren an einer Sandsäule fraktioniert. Zwei verschiedene Lösungsmittel-Fällungsmittelsysteme wurden unter variierten Versuchsbedingungen untersucht. Zur Erreichung einer selektiven Molekulargewichtsfraktionierung war die Aufbringung des Polymeren auf den Sand aus einem thermodynamisch schlechten Lösungsmittel notwendig. Beispiele für selektive und nichtselektive Fraktionierungsergebnisse werden gegeben; letztere tritt bei Aufbringung des Polymeren auf das Substrat aus einem thermodynamisch guten Lösungsmittel auf. Molekulargewichtsverteilungen für zehn Proben werden angegeben; diese wurden durch Eluierungsfraktionierung mit *o*-Dichlorbenzol–Diäthylenglykolmonomethyläther als Lösungsmittel-Fällungsmittelsystem bei 168°C erhalten. Diese Molekulargewichtsverteilungen konnten durch die Log-normal-Wahrscheinlichkeitsverteilungsfunktion, die nach Wesslau und anderen für lineares Polyäthylen und nach Davis und Tobias für Polypropylen anwendbar ist, befriedigend dargestellt werden. Viele der hier gefundenen Verteilungen sind enger als früher in der Literatur angegebene Verteilungen.

Polymerization of Vinyl Ether with Magnesium Compounds.   II.   Catalytic Reactivity of Magnesium Compounds Other than Halides

K. IWASAKI, H. FUKUTANI, Y. TSUCHIDA, and S. NAKANO, *Central Research Laboratory, Mitsubishi Chemical Industries Limited, Kawasaki, Japan*

Synopsis

Magnesium compounds, especially Grignard reagents were studied as catalysts in the polymerization of vinyl ethers. The Grignard reagent and diethyl magnesium possessed no activity for polymerization of vinyl ether. However, if the Grignard reagent is combined with some sort of third substances, it shows good activity. For these substances, oxygen, aldehydes, some metal oxides, and halogenated hydrocarbons seemed to be effective. The molecular weight of the polyvinyl ether obtained from this combined catalyst system is markedly higher than those of polymers obtained with the Friedel-Crafts type of catalyst, but the polymer of vinyl ether obtained from this mixed catalyst possesses little crystalline structure. The possible mechanism of the polymerization with this mixed catalyst is thought to be a cationic initiation type, because the true active species are regarded to be intermediate compounds which are analogous to magnesium halides or alkoxymagnesium halides. In this connection, alkoxymagnesium halides and magnesium oxide were examined. They had a good activity for polymerization but did not yield a high polymer.

INTRODUCTION

In a previous paper,[1] we reported on the catalytic reactivity of magnesium halides in the polymerization of vinyl ethers. The present paper will be concerned mainly with the experiments of vinyl ether polymerization catalyzed by Grignard reagents.

Organometallic compounds are generally thought to be the initiators of anionic polymerization.   However, as we suggested in Part I of our report,[1] or as recently discovered by Kray,[2] Grignard reagents show catalytic action for vinyl ethers, which have been considered to be monomers polymerized by a cationic mechanism, and it has been never reported that vinyl ethers were polymerized by an anionic mechanism.   Therefore, we have been interested in the reason why Grignard reagents possess catalytic action for vinyl ether.   At first we considered that catalytic action might depend on the magnesium halides resulting from the disproportionation reaction:

$$2\ RMgX \rightleftharpoons R_2mg + MgX_2$$

but the results for Grignard reagents are different in some respects from those for magnesium halides described in part I; moreover, oxygen is found to play a very important role.

EXPERIMENTS WITH GRIGNARD REAGENTS

The Grignard reagents were prepared by usual method; the concentration was kept constant at 2 mole/1. in diethyl ether. Ethylmagnesium bromide, butylmagnesium bromide, phenylmagnesium bromide, ethylmagnesium iodide, benzylmagnesium bromide, benzylmagnesium chloride, and ethylmagnesium chloride were prepared and tested.

The polymerizations were carried out in an air-tight, ground-glass joint flask equipped with a stirrer; one neck of the flask was filled with a gasket device through which hypodermic injection of reagents could be made. After the reaction, the raw product was charged into an excess of methanol, and the polymer was precipitated and collected. It was washed with methanol and dried *in vacuo* at 50°C. The reduced viscosity η_{sp}/c was obtained for solutions of 0.50 g. polymer in 100 ml. benzene at 25°C. in an Ostwald viscometer.

1. Effect of Oxygen

Results of preliminary experiments with the effect of oxygen on reactions with 20 ml. of isobutyl vinyl ether and 20 ml. of cyclohexane as solvent at various catalyst concentrations [c] are given in Table I. The nitrogen was purified with pyrogallol solution.

It is clear that Grignard reagents display catalytic action in the presence of oxygen or aldehyde. Oxygen has an accelerating effect at higher temperature; on the other hand, aldehyde is an accelerator at lower temperature. In addition, complete exclusion of oxygen with nitrogen gas was not obtained in this experiment; thus, addition of a trace of tributylboron made the reaction virtually stop.

TABLE I
Effect of Oxygen at [C] = 4.5×10^{-2} mole/1.

Catalyst[a]	Temperature, °C.	Reaction time, hr.	Atmosphere	Yield, %	η_{sp}/c	Added
EtMgBr	50	2	Nitrogen	1.3	0.99	—
EtMgBr	50	2	Air	25.3	3.58	—
EtMgBr	50	2	Nitrogen	15.3	0.24	CH_3CHO[a]
BuMgBr	25–26	4	Nitrogen	1.1	1.71	—
BuMgBr	25–26	4	Air	trace	—	—
BuMgBr	30	1/2	Nitrogen	48.3	—	CH_3CHO[b]
BuMgBr	25–26	24	Nitrogen	0	—	Bu_3B[c]

[a] 0.1 mmole.

[b] 0.04 mmole.

[c] Trace.

Table II shows the results obtained by successive changes, in the amount of oxygen. This experiment was conducted as follows: 20 ml. of cyclohexane was charged into flask; then the reactor was evacuated, filled with purified nitrogen, and into it catalyst solution was injected. Successively,[2] defined volume of dry air was passed into the liquid phase with bubbling, and then 20 ml. of isobutyl vinyl ether was injected.

TABLE II
Effect of Oxygen at 50°C., [C] = 4.5 × 10⁻² mole/l.

TABLE II
Effect of Oxygen at 50°C., $[C] = 4.5 \times 10^{-2}$ mole/l.

Catalyst	Reaction time, hr.	Air volume, l.	Yield, %	η_{sp}/c
C_6H_5MgBr	2	0	2.0	3.19
C_6H_5MgBr	1	0.1	40.0	1.03
C_6H_5MgBr	1	10	51.9	1.87
C_6H_5MgBr	1	30	82.8	1.89

2. Effect of Aldehyde

Polymerizations were carried out by adding 1.36 mmole of BuMgBr to 20 ml. of dry benzene and reacting with a defined amount of acetaldehyde for several minutes; then 20 ml. of isobutyl vinyl ether was injected. Reactions were conducted for 1 hr. at 25°C.

From the results of Table III, it is evident that addition of an equimolar amount of acetaldehyde gives maximum velocity. In addition, an excess of aldehyde causes both retardation of the reaction and lowering of the

TABLE III
Effect of Acetaldehyde

CH_3CHO, mmole	$CH_3CHO/BuMgBr$, mole ratio	Yield, %	η_{sp}/c
0	0	0	—
0.30	0.22	0.8	—
0.61	0.45	5.9	1.84
0.91	0.67	19.9	2.32
1.22	0.90	24.6	2.40
2.13	1.57	19.8	0.19
3.04	2.24	10.0	0.26

molecular weight of the product. In this connection, we have also found the same accelerating effect for such carbonyl compounds as acetone and benzaldehyde.

3. Effect of Halogenated Hydrocarbons

The polymerization of vinyl ether with Grignard reagents was in some cases affected by various solvents. In Table IV, preliminary results on the effect of solvents are listed.
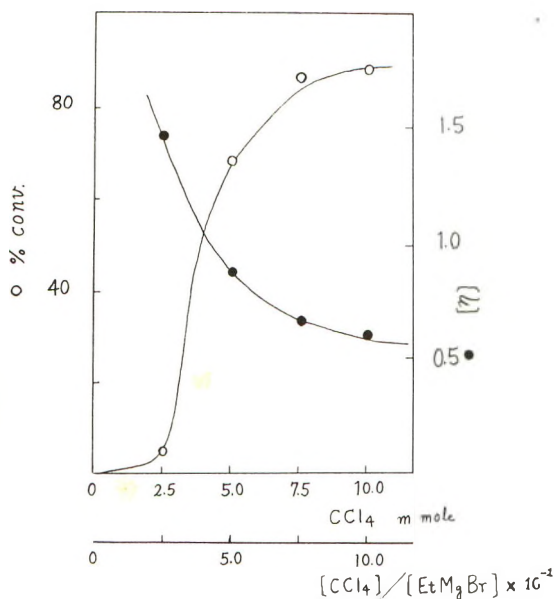
Fig. 1. Polymerization of isobutyl vinyl ether with EtMgBr and CCl₄ at 25°C. for 10 min.: (O) conversion; (●) η_{sp}/c.

From this result it is apparent that halogenated hydrocarbons accelerate the reaction very markedly; on the other hand, dioxane and diethyl ether stop the polymerization. In addition, the results of the polymerization of isobutyl vinyl ether with ethyl-magnesium bromide and carbon tetrachloride are given in Figures 1 and 2. The experiment in Figure 1 was conducted as follows. Successive amounts of carbon tetrachloride were added to each 10 ml. of monomer with 1 mmole of ethylmagnesium bromide in nitrogen atmosphere; the reaction mixture was then allowed to stand for 10 min. at 25°C. In the experiments for which results are given in Figure 2, carbon tetrachloride was added to each 20 ml. of monomer with 0.4 mmole of ethylmagnesium bromide catalyst; the mixture was then allowed to stand for 2 hr. at 40°C.

TABLE IV

Effect of Solvents in Polymerization with EtMgBr, [C] = 0.05 mole/l.; Isobutyl Vinyl Ether, 10 ml.; Solvent, 10 ml. at 0°C. for 24 hr.

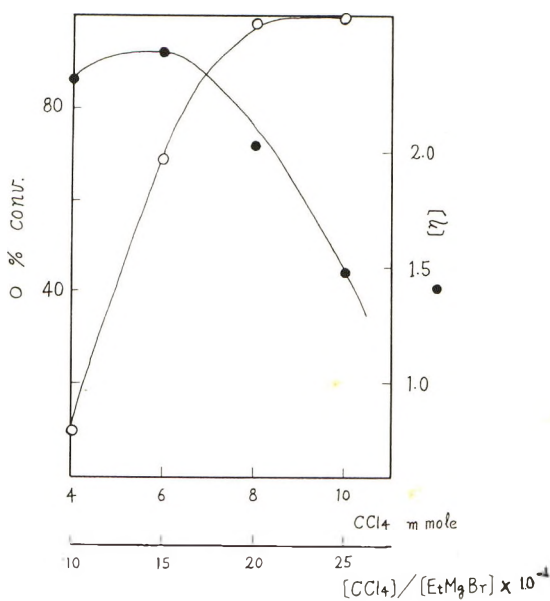| Solvent	Yield, %	η_{sp}/c
Petroleum ether	6.1	0.25
Dioxane	0	—
Carbon tetrachloride	100	0.35
Diethyl ether	0.1	—
Chloroform	54.6	0.28
Chlorobenzene	41.9	0.49

Fig. 2. Polymerization of isobutyl vinyl ether with EtMgBr and CCl₄ at 40°C. for 120 min.: (O) conversion; (●) η_{sp}/c.

These results show that increasing the amount of carbon tetrachloride with respect to ethylmagnesium bromide made the conversion of reaction higher and the molecular weight of polymer lower.

4. Effect of Metal Oxides

Finally we investigated the effect of metal oxides.   Polymerization was carried out as follows.   In test tubes, 2 mmole of metal oxide was added to 10 ml. of isobutyl vinyl ether with or without 2 mmole of ethylmagnesium bromide; the reaction mixture was allowed to stand for 24 hr. at 0°C.

The results obtained (Table V) indicate that metallic oxides possess some cocatalytic action.

TABLE V
Effect of Metal Oxides

Catalyst system	Conversion, %	η_{sp}/c
EtMgBr	6.7	0.15
EtMgBr + V₂O₅	47.1	0.36
EtMgBr + NiO	46.7	0.30
EtMgBr + HgO	53.6	0.35
V₂O₅	0.5	—
NiO	0	—
HgO	0	—

EXPERIMENTS WITH ROMgX

Ethoxymagnesium chloride was prepared by treating magnesium powder with HCl–ethanol solution.[3] The product seemed to be the dialcoholate, $C_2H_5OMgCl \cdot 2(C_2H_5OH)$, from analysis (Cl found, 18.1%, calc. 18.0%).

Benzoxymagnesium chloride was prepared by passing dry air into a benzylmagnesium chloride ether solution at room temperature for several hours, and the precipitate filtered. The white powder obtained was dried *in vacuo* at room temperature. Analysis of BzOMgCl indicated 20.6% (calc. 21.3%).

As described above, oxygen and oxygen compounds exhibit cocatalytic activity for the polymerization of vinyl ether catalyzed by Grignard reagents. On the other hand, it has been known that Grignard reagents react with oxygen or aldehyde and produce ROMgX. Therefore, we examined on the activity of ROMgX. The polymerization procedure was the same as in experiments with Grignard reagents.

The results are summarized in Tables VI and VII.

TABLE VI

Bulk Polymerization of Isobutyl vinyl Ether with BzOMgCl, $[C] = 5.2 \times 10^{-2}$ mole/l.

80°C.			70°C.			50°C.		
Time, min.	Conversion, %	η_{sp}/c	Time, min.	Conversion, %	η_{sp}/c	Time, min.	Conversion, %	η_{sp}/c
40	42.7	—	60	45.0	0.36	60	0.6	—
65	76.0	0.60	90	64.0	0.55	120	2.0	—
			180	90.0	0.55	250	7.1	0.15
						360	12.5	0.24

TABLE VII

Bulk Polymerization of Isobutyl Vinyl Ether with $C_2H_5OMgCl \cdot 2(C_2H_5OH)$

Temperature, °C.	$[C] \times 10^2$, mole/l.	Induction period, min.[a]	Reaction time, min.	Conversion, %	η_{sp}/c
50	2.61	120	30	77.5	0.76
65	1.74	30	6	60.7	0.77

[a] At the beginning of the polymerization some induction period was observed, after which there was relatively violent reaction.

From the result of Table VI, a value of 20.7 kcal./mole was obtained for the overall activation energy of polymerization.

These experiments thus established that alkoxymagnesium halides exhibit catalytic activity.

EXPERIMENTS WITH R_2Mg AND MgO

Diethylmagnesium was prepared by treating ethylmagnesium bromide with dioxane.

Reagent grade magnesium oxide was used in this experiment. Before polymerization, this fine powder was treated at 200°C. for 1 hr.

1. Polymerization with Diethylmagnesium

Polymerization with diethylmagnesium were carried out with isobutyl vinyl ether as a monomer, at 0, 25, and 80°C.; however, after 3 hr. no polymer was obtained.

2. Polymerization with Magnesium Oxide

In this experiment, pretreatment of the catalyst was found to be important to obtain reproducible results.

Polymerization was carried out with stirring at two different temperatures (Table VIII). The system of this reaction was quite heterogeneous and the catalyst concentration could not be defined.

TABLE VIII

Bulk Polymerization of Isobutyl Vinyl Ether with MgO, 18.7 mmole Catalyst in 100 ml. of Monomer

80°C.			50°C.		
Time, hr.	Conversion, %	η_{sp}/c	Time, hr.	Conversion, %	η_{sp}/c
2	63.4	0.22	2	30.7	0.36
4	81.4	0.20	4	54.1	0.37
6	88.8	0.19	6	66.4	0.35
8	90.1	0.18	8	68.8	0.36

TABLE IX

Comparison of Activity of Metal Oxides

Metal oxide	Amount catalyst, g.	Reaction time, hr.	Conversion, %	η_{sp}/c
BeO[a]	0.095	2	2.3	—
MgO[a]	0.152	2	28.3	0.22
CaO[a]	0.119	2	0.0	—
ZnO[a]	0.084	2	Trace	—
B$_2$O$_3$[a]	0.174	2	4.6	—
α-Al$_2$O$_3$[a,b]	0.206	2	0.4	—
γ-Al$_2$O$_3$[b,c]	0.253	4.5	7.2	0.97
SiO$_2$[d]	0.253	5	70.7	0.26
V$_2$O$_5$[e]	0.004	2.5	21.9	0.22
NiO	0.082	2	36.4	0.14
BF$_3$-etherate	0.004	2	90.0	0.22

[a] Before use commercial product was preheated at 100°C.

[b] Form determined by x-ray analysis.

[c] Prepared from aluminum nitrate and calcined at 500°C.

[d] Prepared from sodium silicate and calcined at 500°C.

[e] Prepared from ammonium vanadate,

Though magnesium oxide is an alkaline earth metal oxide, it possesses catalytic activity. The overall activation energy of polymerization with it, as obtained from reaction velocities at 50, 65, and 80°C., was 5.8 kcal./mole. This value is lower than those obtained with other magnesium compounds.

3. Polymerization with Metal Oxides

Since vinyl ether was polymerized with magnesium oxide, we observed the catalytic reactivities of other metal oxides. The results, including that for boron trifluoride–etherate, are summarized in Table IX. Experiments were carried out at boiling point of monomer.

DISCUSSION OF RESULTS

From these experiments described above, it appears that, first, Grignard reagents and diethylmagnesium alone are unable to initiate polymerization. These reagents show good activity when they are combined with third substances, such as oxygen, aldehyde, halogenated hydrocarbons, and some kinds of metal oxides, which readily reacts with the Grignard reagent and produces intermediate. This intermediate appears to be the true active species for initiating polymerization of vinyl ethers. As shown in eqs. (1)–(3) the active species can be regarded as alkoxymagnesium halide or magnesium halide, the activity of which has been examined independently.

$$RMgX + \tfrac{1}{2}O_2 \rightarrow ROMgX \tag{1}$$

$$RMgX + R'CHO \rightarrow \underset{\underset{R}{|}}{R-CHOMgX} \tag{2}$$

$$RMgX + R'-X' \rightarrow MgXX' + R-R' \tag{3}$$

It must be noted however, that the results obtained with the binary catalyst system comprising Grignard reagent and a third substance are markedly different from those obtained with magnesium halide or alkoxymagnesium halide. The molecular weight of the polyvinyl ethers in (Figs. 1 and 2) are considerably higher than the values reported in our previous paper (Part I).[1] An analogous relation is also found between the results of Table II and Tables VI and VII. In both cases, molecular weights obtained with the binary catalyst system are higher than with single catalyst system. In this connection, further results are given in Tables X–XII.

These results, do not show clearly the relative reactivities of Grignard reagents, and the optimum conditions for obtaining high molecular weight polymer may vary, depending on the nature of Grignard reagent and particularly the procedure used to prepare the catalyst system.

In Table XII it is clear that a high polymer of $\eta_{sp}/c = 7.3$ was obtained easily at 80°C. In cationic polymerization, it has been difficult to obtain high polymer at elevated temperature, and also such a high polymer of a vinyl ether has never been obtained at such a high temperature, except for

TABLE X

Polymerization of Isobutyl Vinyl Ether with Grignard Reagents and Air with Monomer: 20 ml.; Cyclohexane: 20 ml.; Catalyst 2 mmole, Dry Air 10 l., at 50°C.

Grignard reagent	Reaction time, hr.	Conversion, %	η_{sp}/c
EtMgBr	1.5	57.1	4.98
n-BuMgBr	1.5	50.0	1.78
C_6H_5MgBr	1.5	75.3	4.69
$C_6H_5\text{-}CH_2MgBr$	1.5	15.3	1.18

TABLE XI

Polymerization of Isobutyl Vinyl Ether with $C_6H_5CH_2MgCl$ and Air; Monomer: 20 ml., at 50°C. for 1 hr.

Catalyst, mmole	Air volume, l.	Conversion, %	η_{sp}/c
2	10	57.0	1.02
1	5	46.6	1.68
0.4	2	47.3	3.50
0.2	1	45.4	4.52
0.1	0.5	48.3	4.81
0.04	0.2	12.0	1.16

TABLE XII

Polymerization of Isobutyl Vinyl Ether with EtMgBr and CCl_4 at 80°C. with Monomer: 20 ml., EtMgBr: 0.4 mmole; CCl_4: 5 mmole

Time, hr.	Conversion, %	η_{sp}/c
1.5	7.8	6.52
2.0	26.9	6.75
3.0	69.0	7.31

the polymerization of vinyl ethers with aluminum hexahydrosulfate at 10–120°C.[5] Consequently, polymerization with this binary catalyst system constitutes a novel method for obtaining high molecular weight polymers of vinyl ethers at elevated temperatures. However, it must be mentioned that the high molecular polymers of isobutyl, isopropyl, and ethyl vinyl ether obtained by this method are amorphous, as determined by x-ray analysis and the solubility in methyl ethyl ketone.

The activity of alkoxymagnesium halide is apparently as high as that of magnesium halide discussed in the previous paper.[1] The molecular weight of polyvinyl isobutyl ether obtained with ROMgCl lies between those of the polymers obtained with MgF_2–HF and $MgCl_2$. The activity of magnesiumethyl alcoholate,[3] was also examined; polymerization with this compound was not successful.

The activity of magnesium oxide was not predicted. This result may be explained by the role of active protons on magnesium oxide in the poly-

merization of vinyl ether, although magnesium oxide is regarded as basic oxide. This consideration is supported by the low value of the overall activation energy and the dependence of activity on pretreatment. To clarify the possible mechanism of the binary catalyst system and the possibility for obtaining high polymers, it must be noted that complete decomposition of the R-Mg bond by such a substance as CCl_4 or oxygen causes a decrease in the molecular weight of the resultant polymer. The effective structure[6] of the catalyst leading to formation of high polymer is as follows:
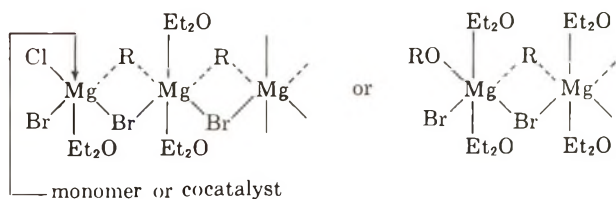
The active site for initiating polymerization may be a Mg atom which has been positively charged, for example, by replacement of a Mg-R bond by the Mg-Cl bond. However, we cannot explain the reason why such a structure remaining as a R-Mg bonding retards the termination of chain propagation during polymerization and as a consequence produces high molecular weight polyvinyl ethers. Relative to this problem we are now in the process of studying vinyl ether polymerization with catalyst systems including organometallic compounds.

References

1. Iwasaki, K., H. Fukutani, and S. Nakano, *J. Polymer Sci.*, **1**, 1937 (1963).
2. Kray, R. J., *J. Polymer Sci.*, **44**, 264 (1960).
3. Meerwein, H., and R. Schmidt, *Ann.*, **444**, 236 (1925).
4. Meisenheimer, J., *Ber.*, **61**, 709 (1928).
5. U. S. Pat. 2,549,921 (1951).
6. Rochow, E. G., D. T. Hurd, and R. N. Lewis, *The Chemistry of Organometallic Compounds*, Wiley, New York, 1957, p. 92.

Résumé

Dans la polymérisation d'éthers vinyliques avec des composés du magnésium, le réactif de Grignard a été étudié en particulier. Il ne possède pas autantd' activité à polymériser l'éther vinylique que le diéthyl magnésium. Cependant s'il est combiné avec une troisième substance particulière, il montre alors une bonne activité. Pour ces substances, l'oxygène, les aldéhydes, certaines sortes d'oxydes métalliques et les hydrocarbures halogénés semblent étre efficaces. Le poids moléculaire de l'éther polyvinylique obtenu à partir de ce système de catalyseur combiné est nettement plus élevé que celui obtenu avec le catalyseur du type Friedel–Crafts. Toutefois le polymère à haut poids moléculaire de l'éther vinylique obtenu à partir de ce mélange catalytique possède une structure de moindre cristallinité. On est porté à croire que le mécanisme probable de la polymérisation par ce mélange catalytique est du type cationique parce que les

espèces actives vraies sont regardées comme les composés intermédiaires lesquels sont semblables aux halogénures de magnésium ou aux alcoxy-halogénures de magnésium. C'est dans ce sens que les alcoxy-halogénures de magnésium et l'oxyde de magnésium ont été examinés. Ils ont une bonne tendance à faire polymériser mais ils ne donnent pas un haut polymère.

Zusammenfassung

Bei der Polymerisation von Vinyläthern mit Magnesiumverbindungen wurde besonders die Wirkung der Grignard-Verbindung untersucht. Die Grignard-Verbindung besass ebenso wie Diäthylmagnesium keine Fähigkeit Vinyläther zu polymerisieren. Wenn sie jedoch mit gewissen dritten Substanzen kombiniert wird, zeigt sie gute Aktivität. Als solche Substanzen waren Sauerstoff, Aldehyde, gewisse Metalloxyde und halogenierte Kohlenwasserstoffe geeignet. Das Molekulargewicht des mit diesen kombinierten Katalysatorsystemen erhaltenen Polyvinyläthers ist merklich höher als das mit Friedel–Crafts-Katalysatoren erhaltene. Das mit den Mischkatalysatoren gewonnene hochmolekulare Polymere besitzt aber nur einen geringen Anteil an kristalliner Struktur. Der Polymerisationsmechanismus mit diesem Mischkatalysator wird als kationisch betrachtet und als wirklich aktive Stoffe werden intermediär gebildete Verbindungen angenommen, die den Magnesiumhalogeniden oder Alkoxymagnesiumhalogeniden analog sind. In diesem Zusammenhang wurden Alkoxymagnesiumhalogenide und Magnesiumoxyde auf ihre Wirkung untersucht. Sie besassen eine gute Polymerisationsaktivität, führten aber nicht zur Bildung eines Hochpolymeren.

Phthalocyanine-Crosslinked Polyvinylphthalic Acid

EUGENE C. WINSLOW and NANCY E. GERSHMAN,*
University of Rhode Island, Kingston, Rhode Island

Synopsis

Copper phthalocyanine-crosslinked poly-4-vinylphthalic acid was prepared with the expectation that some increased thermal stability could be achieved with these thermally stable linkages. Thermal decomposition in air occurs at about 310°C. The crosslinked polymer proved to be less stable than the starting material, poly(4-vinylphthalic acid). Analysis shows that an average of one copper phthalocyanine crosslink is formed for every twelve 4-vinylphthalic acid segmers in the poly(4-vinylphthalic acid) chain. A new compound, 4-vinylphthalic anhydride, was produced in this investigation.

INTRODUCTION

An earlier paper in this journal[1] discussed the preparation and properties of polyvinylphthalic acid. The possibility of phthalocyanine crosslinks between the vinyl chains was also mentioned. This investigation discusses the preparation of polyvinylphthalic acid with copper phthalocyanine crosslinks. There was some expectation that thermal stability could be imparted to the polymer by introducing thermally stable crosslinks of copper phthalocyanine. It was hoped in this investigation that a conventional polymer chain could be made thermally stable by introduction of thermally stable crosslinks during the molding process. The thermal stability of the polymers formed in this investigation was disappointing.

DISCUSSION

Before attempting to synthesize a polymer containing phthalocyanine crosslinks, it was necessary to consider the steric feasibility of forming such a cumbersome, crosslinked system. The dimensions of the metal-free phthalocyanine molecule have been elucidated completely by x-ray diffraction studies.[2] The distance between the 4-positions on adjacent benzene rings of the phthalocyanine unit is 8.37 A. This distance is too large to allow phthalocyanine crosslinks to form at every possible position between adjacent polyvinylphthalic acid chains. By construction of a model it can be shown that it is possible sterically for phthalocyanine crosslinks to form at every third position on the polyvinyl backbone. The resulting crosslinked polymer would have many unreacted acidic functional groups.

* Present address: Rutgers University, New Brunswick, N. J.

These probably contribute to the lack of thermal stability which was observed for the polymer.

Several attempts were made to prepare 4-vinylphthalonitrile as the monomer for preparation of the desired polymer. It would have been desirable to prepare the phthalocyanine crosslinks by use of copper powder and polyvinylphthalonitrile rather than by use of copper salts, boric acid, urea, and polyvinylphthalic acid. The latter procedure, which was used, involves a greater possibility of contamination in the resulting polymer. During the attempts to prepare 4-vinylphthalonitrile, a new compound, 4-vinylphthalic anhydride was prepared.
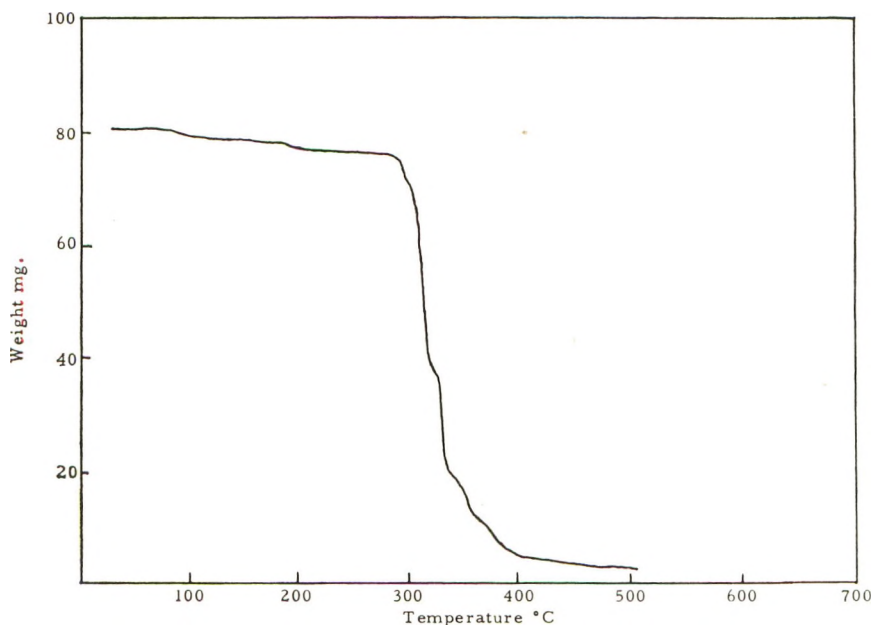
Fig. 1. TGA thermogram for phthalocyanine-crosslinked poly(4-vinylphthalic acid). Air atmosphere, heating rate 2°C./min.

A thermogravimetric analysis curve for copper phthalocyanine cross-linked polyvinylphthalic acid is shown in Figure 1. The determination was conducted in an air atmosphere. The thermal decomposition of phthalocyanine-crosslinked polyvinylphthalic acid in air occurs at a temperature which is fifty degrees lower than the decomposition temperature of polyvinylphthalic acid itself.

The phthalocyanine-crosslinked polymer is green in color and flaky in texture. It is insoluble in all of the common solvents tested. It dissolved in hot concentrated sulfuric acid but was insoluble in boiling concentrated nitric acid. It does not melt or fuse when heated in a flame on the end of a spatula.

Determination of Phthalocyanine Crosslinks

Polyvinylphthalic acid was polymerized as described in an earlier paper.[1] The molecular weight of the polymer resulting from such polymerization has been found to be in the range of 10^4–10^5. After copper phthalocyanine crosslinks were formed, the weighed sample was decomposed at a temperature of 500°C. in an air atmosphere to leave a residue of cupric oxide. The weight of the residue when compared with the weight of the material before decomposition indicates that one copper phthalocyanine crosslink on the average is formed for every twelve vinylphthalic acid segmers in the polyvinyl chain. The steric effects of the bulky phthalocyanine groups obviously prevented the formation of more crosslinks. In view of the large number of unreacted acidic functional groups it is not surprising that additional thermal stability was not derived by the formation of some phthalocyanine crosslinks.

The temperature at which the copper phthalocyanine crosslinks were formed was 200°C. Polyvinylphthalic acid has proved to be stable at that temperature, and it is reasonable to assume that the vinyl chains were not broken during the crosslinking process.

EXPERIMENTAL

Preparation of 4-Vinylphthalic Anhydride

A 1-g. portion of 4-vinylphthalic acid[1] was placed in a sublimation apparatus. Under a vacuum of approximately 1 mm. the sublimation tube was heated to 85°C. in an oil bath. After 2 hr. of reaction time clear white crystals were scraped off the cold finger of the sublimation apparatus. The process could be continued for several hours to give a yield in excess of 90%. The melting point of the white crystals was 95–96°C. Calc. for $C_{10}H_6O_3$: C, 68.9%; H, 3.45%. Found: C, 68.9%; H, 3.55%.

Preparation of Phthalocyanine-Crosslinked Poly-4-vinylphthalic Acid

In a 50-ml. beaker were placed 1 g. (0.0052 equivalents) of poly-4-vinylphthalic acid, 5.0 g. (0.084 moles) of urea, 0.4 g. (0.0029 moles) of cupric chloride, a trace of boric acid, and 10 ml. of distilled water. The solution was heated to dryness on a steam bath. The residue was transferred to a glass stoppered bottle and heated to 200°C. for 3 hr. The green-black residue was digested in 100 ml. of water in a steam bath and then filtered. The washing procedure with water was repeated and the residue was washed successively with hot dilute sodium hydroxide solution and with hot dilute hydrochloric acid until the filtrate was clear. It was then washed several times with hot water.

References

1. Winslow, E. C., and A. Laferriere, *J. Polymer Sci.*, **60**, 65 (1962).
2. Robertson, J. M., *J. Chem. Soc.*, **1936**, 1195.

Résumé

On a préparé de l'acide poly-4-vinylphtalique ponté avec de la phtalocyamine cuivrique dans l'espoir de pouvoir réaliser une stabilité thermique accrue grâce à ces liens thermiquement stables. La décomposition thermique a lieu aux environs de 310°C à l'air. Le polymère ponté s'est montré moins stable que le matériel de départ, l'acide poly-4-vinylphtalique. Par analyse, on montre qu'il se forme en moyenne un pont de phtalocyamine pour douze segments d'acide 4-vinylphtalique de la chaîne d'acide poly-4-vinylphtalique. Dans ce travail on a produit un composé nouveau: l'anhydride 4-vinylphtalique.

Zusammenfassung

Mit Kupferphthalocyanin vernetzte Poly-4-vinylphthalsäure wurde in der Erwartung hergestellt, mit dieser thermisch stabilen Verknüpfung eine gewisse Erhöhung der thermischen Stabilität erreichen zu können. Thermische Zersetzung findet unter Luft bei etwa 310°C statt. Das vernetzte Polymere erwies sich als weniger stabil als das Ausgangsmaterial, Poly-4-vinylphthalsäure. Die Analyse zeigte, dass sich im Mittel auf je zwölf 4-Vinylphthalsäurebausteine in der Poly-4-vinylphthalsäurekette eine Kupferphthalocyaninvernetzung bildet. Eine neue Verbindung, 4-Vinylphthalsäureanhydrid, wurde im Verlauf dieser Untersuchung dargestellt.

Molecular Configuration of Polystyrene in Benzene

P. DEBYE, B. CHU,* and H. KAUFMANN, *Chemistry Department, Cornell University, Ithaca, New York*

Synopsis

The particle scattering factor $P(\theta)$ with Gaussian statistics for polydispersed systems has been treated. For a polystyrene sample with a sharp molecular weight distribution ($M_w/M_n < 1.02$, $M_w = 1.5 \times 10^6$), the measured angular dependence of scattered intensity indicates that the polymer coil does obey Gaussian statistics. This holds for a range of concentrations provided the variation of the constant representing the radius of gyration with concentration is adjusted.

In dilute solutions, the extension of a polymer coil of high molecular weight can be calculated from the observed angular dependence of the scattered intensity of visible light, since the scattering from the dipoles in different parts of the molecule has considerable phase differences. From a plot of scattered intensity versus angle of observation, it is possible to obtain either higher moments of the density distribution of a monodispersed polymer coil in solution or some guide to the effects of polydispersity and branching of the polymer through the shape of the curve.[1–3] In this paper, the particle scattering factor $P(\theta)$ with Gaussian statistics for polydispersed systems has been treated. For a polystyrene sample with a sharp molecular weight distribution ($M_w/M_n < 1.02$, $M_w = 1.5 \times 10^6$), the measured angular dependence of scattered intensity indicates that the polymer coil does obey Gaussian statistics. This holds for a range of concentrations provided the variation of the constant representing the radius of gyration with concentration is taken into consideration.

PARTICLE SCATTERING FACTOR WITH GAUSSIAN STATISTICS

1. Monodispersed Systems

If we visualize the polymer chain as a series of emitters, each located at the intersection of two bonds and all of the same strength, the average intensity of scattering observed in any direction is proportional to the particle scattering factor $P(\theta)$:

$$P(\theta) = \sum_i \sum_j \sin ksr_{ij}/ksr_{ij} \tag{1}$$

* Present address: Chemistry Department, University of Kansas, Lawrence, Kansas.

where s stands for $2\sin(\theta/2)$ in which θ is the angle between the secondary and the primary beam, $k = 2\pi/\lambda$ in which λ is the wavelength as measured in the liquid surrounding the particle, and r_{ij} is the distance between the emitter i and another emitter j. The summation goes twice over all emitters. The effect of polarization has been omitted. Equation (1) holds for a molecule of definite and unvariable shape in the average over-all orientations in space which it occupies without discrimination.

If the shape is variable and the Gaussian statistics are applied to the distances r_{ij}, the scattering factor is obtained by taking the average of eq. (1). In this way it follows that for a coiling molecule, the scattering function $P(\theta)$ is:[4]

$$P(\theta) = (2/x^2)[e^{-x} - (1 - x)] \tag{2}$$

where $x = k^2 s^2 r_g^2$, and r_g^2 is the square of the radius of gyration. By the experiment reported in this paper we try to investigate how well eq. (2) represents the measured intensity distribution.

If the dissymmetry measurements have been made with a rigid polymer, it will be possible to represent the (normalized) intensity as a function of s in the form

$$I = 1 - \alpha_1 s^2 + \alpha_2 s^4 - \ldots \tag{3}$$

where

$$\alpha_1 = (k^2/3)\,(1/V)\int r^2 d\tau = (k^2/3)r_g^2$$

V is the volume of the particle, and r is the distance of any point in the interior of the particle from its center of gravity. The integration extends over all the elements of volume $d\tau$ in the interior of the particle. Debye pointed out that irrespective of the shape, the radius of gyration can always be determined from the first coefficient α_1 in eq. (3). When the change of scattering with the angle is sufficiently large more detailed information about the size and shape can be obtained from higher coefficients.

2. Polydispersed Systems

In this section we investigate the effect of polydispersity on $P(\theta)$. A distribution with a variable number of monomers ν is used. For this distribution we accept the distribution function

$$dZ/Z = [p^{p+1}/\Gamma(p+1)](\nu/N)^p\, e^{-p(\nu/N)}\, d(\nu/N) \tag{4}$$

in which Z is the total number of molecules; the fraction dZ/Z lies in the interval ν and $\nu + d\nu$, p is a number, and N is the number of monomers per coil at the maximum of the distribution curve. From eq. (4), it follows that the maximum of the plot dZ/Z versus ν/N happens at $\nu/N = 1$. The relative half-width of the distribution ϵ (at $\nu/N = 1 \pm \epsilon$) is

$$(1/2)\, e^{-p} = (1 \pm \epsilon)^p\, e^{-p(1 \pm \epsilon)}$$

or

$$\epsilon^2 \cong 2\ln2/p \tag{5}$$

Since the integral

$$\int_0^\infty [p^{p+1}/\Gamma(p+1)](\nu/N)^p e^{-p(\nu/N)} \, d(\nu/N) = 1$$

the number-average molecular weight is

$$M_n = Nm \int_0^\infty [p^{p+1}/\Gamma(p+1)](\nu/N)^{p+1} e^{-p(\nu/N)} \, d(\nu/N)$$

$$= Nm\,(p+1)/p$$

where m is the molecular weight of the monomer, and the weight-average molecular weight is

$$M_w = Nm \int_0^\infty [p^{p+1}/\Gamma(p+1)](\nu/N)^{p+2} e^{-p(\nu/N)} \, d(\nu/N)$$

$$= Nm(p+1)(p+2)/p^2$$

Thus,

$$M_w/M_n = (p+2)/p \tag{6}$$

This number p is very large for a sharp distribution as shown in Table I. A molecule with $\nu/N = 1$ will have an x_0-value

$$x_0 = k^2 s^2 r_N{}^2$$

in which r_N is the radius of gyration for a molecule with $\nu = N$. This definition of x_0 will be used throughout, and the subscript zero will hence be omitted.

TABLE I[a]

M_w/M_n	p	$\epsilon \times 10^2$
1.001	2000	2.62
1.01	200	8.27
1.02	100	11.6
1.04	50	16.5
1.08	25	23.5
1.10	20	26.4

[a] Values calculated from eqs. (5) and (6).

After these preliminaries, it follows immediately that the total intensity scattered by Z molecules is

$$I_p = Z[p^{p+1}/\Gamma(p+1)]N^2\,[2/x^2] \int_0^\infty (e^{-\mu x} - 1 + \mu x)\mu^p\, e^{-p\mu} \, d\mu \tag{7}$$

with $\mu = \nu/N$. Calculated this gives the exact formula:

$$I_p = ZN^2\,(2/x^2)\{[1 + (x/p)]^{-(p+1)} - 1 + x\,[1 + 1/p]\} \tag{7a}$$

Now if eq. (7a) is developed in powers of $1/p$ and the first power of $1/p$ applied, since p is large for polymers with sharp distributions, instead of eq. (7a), the following is obtained:

$$I_p = ZN^2\{(2/x^2)(e^{-x} - 1 + x) + (1/p)(2/x^2)[1 - (1 - x/2)e^{-x}]\} \tag{7b}$$

Development of eq. (7b) in powers of x, can be written

$$I_p = ZN^2 \{ [1 + (3/p)] - [(1/3) + (2/p)]x +$$
$$[(1/12) + (5/6)(1/p)]x^2 - [(1/60) + (1/4)(1/p)]x^3 + \ldots \} \quad (7c)$$

Also, it may be added that the general formula according to eq. (7c) is

$$I_p = ZN^2 \sum_{n=0}^{\infty} (-1)^n \frac{2}{(n+2)!} \left[1 + \frac{(n+2)(n+3)}{2} \frac{1}{p} \right] x^n$$

EXPERIMENTAL

Materials

The polystyrene sample was prepared, fractionated, and characterized by Wenger and Yen.[5] It was fractionated into eight fractions (Table II) from a 0.2% solution in methyl ethyl ketone by addition of methanol. The fractions were freeze-dried from benzene solution. From the fractionation data, assuming Newtonian behavior in viscosity measurements, $M_w = 1.42 \times 10^6$, $M_n = 1.40 \times 10^6$, with $M_w/M_n = 1.02$. The integral weight distribution curve is plotted in Figure 1 according to Schultz.[6]

TABLE II
Fractionation of Original Polymer. Polystyrene 2.3721 g., 0.2% In Methyl Ethyl Ketone. Precipitant: Methanol 30°C.

Fraction No.	g	W_i	$[\eta]^a$	$M_v \times 10^{-6b}$
I	0.0252	0.0106	3.918	1.55
II	0.5016	0.2117	3.829	1.50
III	0.4107	0.1734	3.822	1.49
IV	0.2561	0.1081	3.798	1.48
V	0.2375	0.1003	3.789	1.47
VI[c]	0.8384	—	3.618	1.39
VI$_1$	0.5475	0.2311	3.683	1.42
VI$_2$	0.2909	0.1228	3.349	1.25
VII	0.0994	0.0420	2.353	0.777

[a] In benzene, 25°C., from $[\eta] = (1/c) [\ln r_r + (1/4)(\eta_{sp}) - \ln n_r]$ with c in g./100 ml.
[b] $[\eta] = 1.03 \times 10^{-4} M^{0.74}$ as given by Flory.[9]
[c] Aliquot fractionated in subfractions VI$_1$ and VI$_2$.

Fractions III and IV of the original polymer (Table II) were combined by dissolving in benzene, followed by freeze-drying. Viscosity data are shown in Figure 2. Based on the graphical extrapolation of the viscosity data, Yen arrived at a value of 3.80 for the intrinsic viscosity $[\eta]$, with a corresponding molecular weight of approximately 1.5×10^6. This was the sample used in light-scattering measurements. The benzene used as solvent was ACS reagent grade. It was dried with calcium chloride and distilled before use.
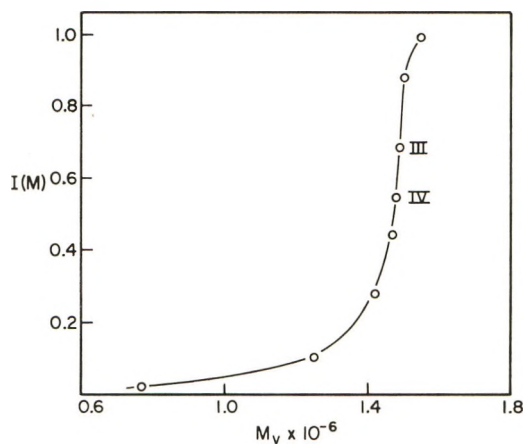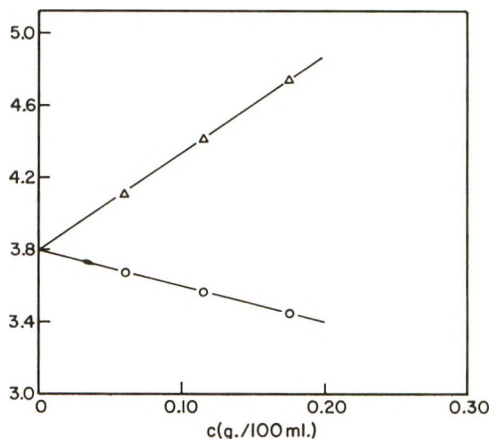
Fig. 1. Integral weight distribution.

Fig. 2. Plot of η_{sp}/c ($\triangle$) and ln η_r/c (O) vs. concentration.

Light-Scattering Measurements

The basic design of the apparatus has been described elsewhere.[7] The cross section of the primary beam (approx. 3 × 10 mm.) was defined by two slits in front of the scattering cell. The scattered light passed through a set of seven parallel slits of 0.5 mm. width (as roller slit), each with an angular acceptance of approximately 2°. The primary beam was polarized by means of a Nicol prism. The wavelength of 4360 A. (vacuum) was selected by a set of Corning filters. The light-scattering cell consisted of a Pyrex glass stoppered tube of 4.5 cm. diameter with a light trap to eliminate back reflections of the incident light. The close match of the refractive indices of Pyrex glass and the polystyrene solutions effectively reduced stray reflections from the scattering cell. Angular deviations, based on the symmetrical scattering of benzene and Ludox, are less than 3%. Solutions

of known concentrations were filtered through a "fine pores" (F) glass frit directly into the cleaned cells for light-scattering measurements.

RESULTS AND DISCUSSIONS

Equation (3) permits the investigation of whether it is possible to represent the (normalized) scattered intensity within the range of the experiment as a function of s by the expression

$$I = A - Bs^2 + Cs^4 \tag{3a}$$

with three constants A, B, and C. I is the scattered intensity in relative units. The coefficients A, B, and C may be obtained by the method of least squares. A plot of scattered intensity versus $\sin^2(\theta/2)$ is shown in Figure 3. The solid lines represent values calculated according to eq. (3a) and show that the representation is adequate.
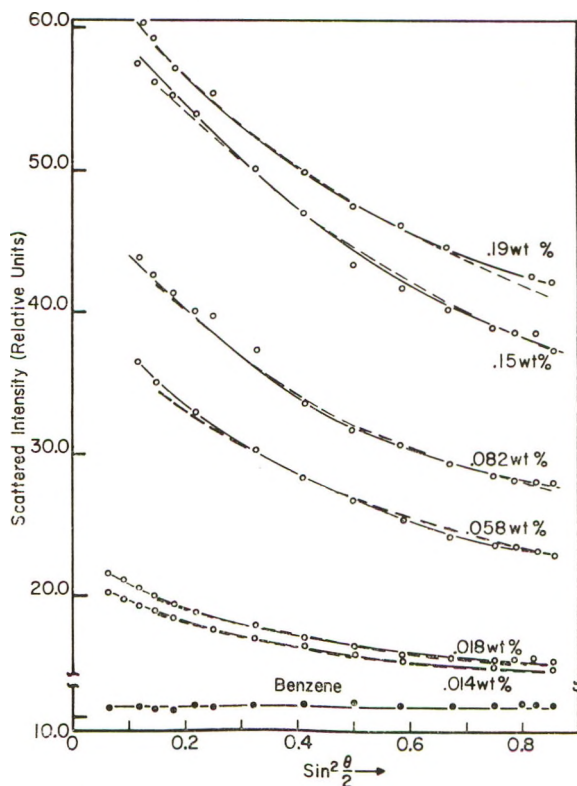
Fig. 3. Plot of relative intensity vs. $\sin^2 \theta/2$. Polystyrene-benzene; $\bar{M}_w = 1.5 \times 10^6$, $\bar{M}_w/\bar{M}_n < 1.02$.

The particle scattering factor $P(\theta)$ from eq. (2) can be approximated by the first three terms of a series expansion:

$$P^*(\theta) = 1 - (x/3) + (x^2/12)$$

if x is small (less than 1). When $x (= k^2s^2r_g^2)$ is greater than one, $P^*(\theta)$ no longer represents $P(\theta)$.

From a Zimm plot, $M_w = 1.48 \times 10^6$, which agrees well with the value of 1.5×10^6 calculated from viscosity data. The radius of gyration compares favorably with the results of Kunst.[8] A wavelength of 4360 A. was used, and the scattered intensity measured up to an angle of $135°$. The value of x which belongs to this angle is approximately two which is considerably greater than one. However, the radius of gyration calculated from $P(\theta)$ is approximately correct. Since

$$I = A\left\{(2/x^2)[e^{-x} - (1 - x)]\right\} \tag{2a}$$

in which $x = k^2r_g^2s^2 = \rho s^2$, the best values of A and r_g^2 can then be obtained simultaneously, according to eq. (2), by a variational method of least squares combined with a power development. The effect of polydispersity can be neglected because the sample was a polymer with a very sharp distribution. $M_w/M_n < 1.02$ (p is greater than 100). The dotted lines in Figure 3 are plotted according to eq. (2) and constants A and ρ are shown in Table III. Since the calculated values and experimental data agree within the error of the measurements (estimated at approx. 5%), it may be concluded that the mass distribution of polystyrene in benzene can be represented by using the Gaussian approximation.

TABLE III

Concn., wt.-%	A	ρ	$r_g^2 \times 10^{-5}$
0.19	54.32	0.61	1.3
0.15	52.59	0.72	1.5
0.082	37.14	0.91	1.9
0.058	28.08	0.90	1.9
0.018	10.92	1.08	2.3
0.014	9.79	1.06	2.3

References

1. Zimm, B. H., *J. Chem. Phys.*, **16**, 1093, 1099 (1948).

2. Benoit, H., *J. Polymer Sci.*, **11**, 507 (1953).

3. Benoit, H., A. M. Holtzer, and P. Doty, *J. Phys. Chem*, **59**, 635 (1954).

4. Debye, P., *J. Chem. Phys.*, **51**, 18 (1947).

5. Courtesy of Dr. F. Wenger, Mellon Institute, Pittsburgh, Pa.; polymerization technique according to F. Wenger and Shiao-Ping S. Yen, *Makromol. Chem.*, **43**, 1 (1961).

6. Schultz, G. V., and A. Dinglinger, *Z. Physik Chem.*, **43B**, 47 (1939).

7. Debye, P., and A. M. Bueche, Tech. Rept., 2242 (1942), Reconstruction Finance Corp., Office of Rubber Reserve, Polymer Research Branch.

8. Kunst, E. D., *Rec. Trav. Chim.*, **69**, 125 (1950).

9. Flory, P. J., *Principles of Polymer Chemistry*, Cornell Univ. Press, Ithaca, N. Y., 1953, p. 312.

Résumé

On discute de la relation entre le facteur de diffusion particulaire $P(\theta)$ et la statistique Gaussienne pour des systèmes polydispersés.   Pour un échantillon de polystyrène ayant une distribution étroite du poids moléculaire, $(M_w/M_n < 1.02, M_w = 1.5 \times 10^6)$, la dépendance de l'intensité diffusée avec l'angle montre que la pelote polymérique obéit à la statistique Gaussienne.   Cela est valable pour un domaine de concentrations pourvu que l'on tienne compte de la variation de la constante représentant le rayon de gyration en fonction de la concentration.

Zusammenfassung

Der Streufaktor $P(\theta)$ für polydisperse Gauss'sche Knäuel wurde behandelt.   Die an einer Polystyrolprobe mit enger Molekulargewichtsverteilung $(M_w/M_n < 1,02, M_w = 1.5 \times 10^4)$ gemessene Winkelabhängigkeit der Streuintensität zeigt, dass der Polymerknäuel einer Gauss'schen Verteilung gehorcht.   Das gilt bei Berücksichtigung der Konzentrationsabhängigkeit des Trägheitsradius über einen weiten Konzentrationsbereich.

On the Polymer–Solvent Interaction in Polymer Solutions

NOBUHIRO KUWAHARA, *Department of Polymer Science, Faculty of Science, Hokkaido University, Sapporo, Japan*

Synopsis

Osmotic pressure and viscosity measurements afford mutually supplementary data for the thermodynamic parameters governing the interaction between polymer segments and solvent molecules. With the object of studying the effects of the structural characteristics of polymer and solvent on the interaction between polymer segments and solvent molecules, we have performed osmotic pressure and viscosity measurements at different temperatures. It appears that the Θ temperature deduced from the intrinsic viscosity agrees with that obtained from the second virial coefficient. The entropy of dilution for the polyisobutylene–benzene system appears to be comparable to that found for polydimethylsiloxane in benzene. However, the entropy of dilution has been found to differ widely for a given polymer in different solvents. It appears that the entropy of dilution varies not only with the geometrical character of the solvent molecule in relation to the polymer segment, but also with the preferential ordering induced by the difference in the binding forces between the molecules solvent–solvent, solvent–solute, and solute–solute. A brief discussion is also given on the influence of hindrance to free rotation on the polymer configuration.

INTRODUCTION

The interaction between polymer segments and solvent molecules is of great importance in polymer solutions, since the extension of a high polymer molecule in solution is markedly influenced by the existence of this interaction. The interaction between polymer and solvent has been investigated by many authors in the past several years. It is gradually becoming clear that the entropy of dilution is comparable in importance to the enthalpy of dilution in its influence on the extension of a polymer molecule, and that the entropy of dilution differs widely for a given polymer in different solvents.[1-3] Several attempts have been made by taking the geometrical character of the polymer segment and the solvent molecule into account.[4] None of them seems to give a unique explanation of the experimental results mentioned above.

Studies have been made mainly of polyisobutylene and polystyrene, in several solvents.[1-3] Thermodynamic investigations in which the enthalpy and entropy of dilution are determined seem to be still necessary to obtain the detailed information concerning the interaction in polymer solutions. The work reported here was done with the object of studying

the effects of the structural characteristics of polymer and solvent on the interaction between polymer segments and solvent molecules. To compare the results polydimethylsiloxane and polyisobutylene were chosen as the solute, because the structure of the polydimethylsiloxane chain is relatively simple and is analogous to that of the polyisobutylene chain. The viscosities and the osmotic pressures have been measured in several solvents at different temperatures, since they afford mutually supplementary data for the thermodynamic parameters governing the interaction between polymer and solvent.

EXPERIMENTAL

Materials

Four polydimethylsiloxanes (PDS) and two polyisobutylenes (PIB) were fractionated by standard procedures. Characteristics of polymer fractions used here are given in Table I. All solvents were purified by the usual method.[5]

TABLE I
Characteristics of Polymer Fractions

Polymer fraction	$\bar{M}_n$	$\bar{M}_v$	Solvents employed in $\bar{M}_v$ detn.
PDS 3-1	107,000	120,000	$C_6H_5CH_3$ (25°C.)[a]
PIB 2-1	63,000	71,000	C_6H_6 (25°C.)[b]

[a] Data of Kolorlov et al.[6]
[b] Data of Fox and Flory.[7]

Osmotic Pressure

Osmotic pressure measurements were carried out with the use of modified Fuoss-Mead type osmometers. The membranes employed were collodion. These membranes gave the specific permeability as $2.5-3.5 \times 10^{-12}$ cm. poise sec.$^{-1}$. A water bath was controlled within ± 0.003°C. at the desired temperature. The osmotic pressures were determined by the static method. The concentrations of all solutions were determined by dry weights.

Viscosity

Viscosity measurements were made in an Ubbelohde-type viscometer calibrated for kinetic energy corrections with the aid of a water bath controlled within ± 0.01°C. All solutions were filtered into the viscometer through a medium glass filter. Since the effect of the rate of shear on the observed specific viscosity η_{sp} should be small for polymers having intrinsic viscosities in the range of those used here, a correction to zero rate of shear was not applied.

RESULTS

The osmotic pressure data were fitted to the equation

$$(\pi/C)^{1/2} = (\pi/C)_0^{1/2}[(1 + \Gamma_2/2)C]$$

according to the procedure applied by Krigbaum and Flory.[8] These data are shown in Figures 1 and 2. The second virial coefficient A_2 has been calculated from the values evaluated for $(\pi/C)_0$ and Γ_2. In Figure 3 the values of A_2 are plotted against the absolute temperature.

The solution viscosities were measured over the range of concentrations most suitable for an extrapolation to zero concentrations. Values of η_{sp}/C and $(\ln \eta_r)/C$ were plotted against concentration as is shown in Figure 4. The intrinsic viscosity $[\eta]$ has been taken as the ordinate inter-
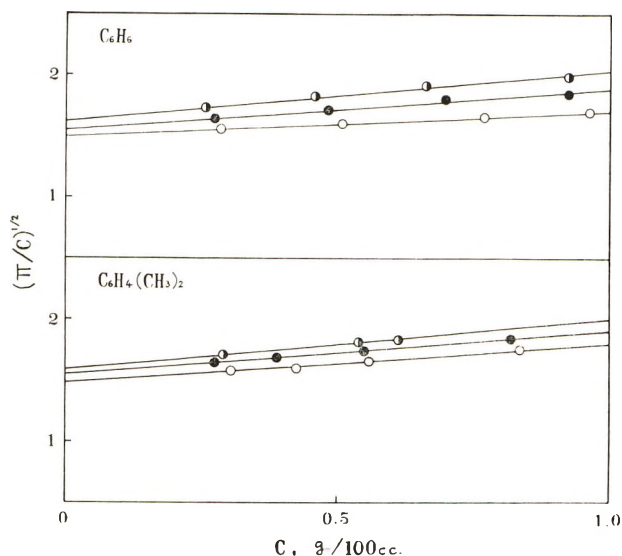
Fig. 1. $(\pi/C)^{1/2}$ plotted against polymer concentration for a polydimethylsiloxane fraction in benzene and xylene: (O) 15°C.; (●) 35°C.; (◑) 50°C.
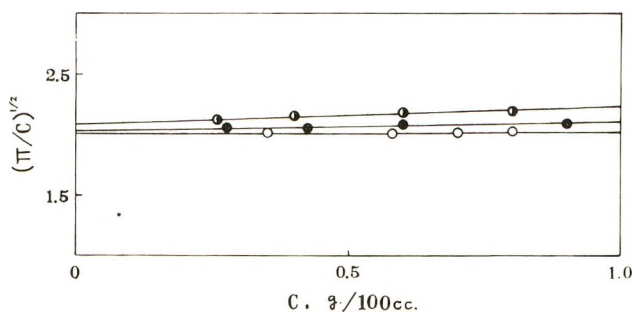
Fig. 2. $(\pi/C)^{1/2}$ plotted against polymer concentration for a polyisobutylene fraction in benzene: (O) 25°C.; (●) 35°C.; (◑) 50°C.
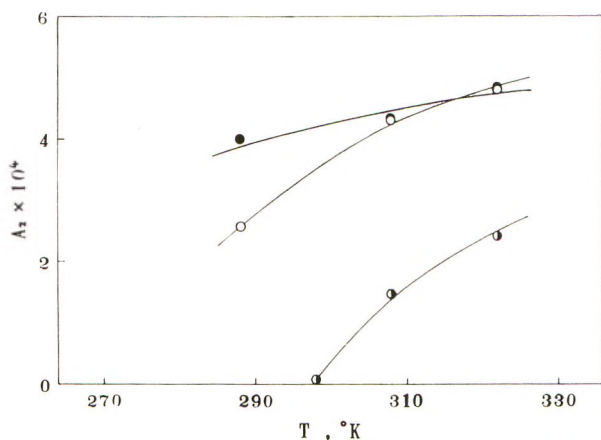
Fig. 3. Values of $A_2 \times 10^4$ plotted against the absolute temperature: (O) polydimethylsiloxane fraction in benzene; (●) polydimethylsiloxane fraction in xylene; (◑) polyisobutylene fraction in benzene.
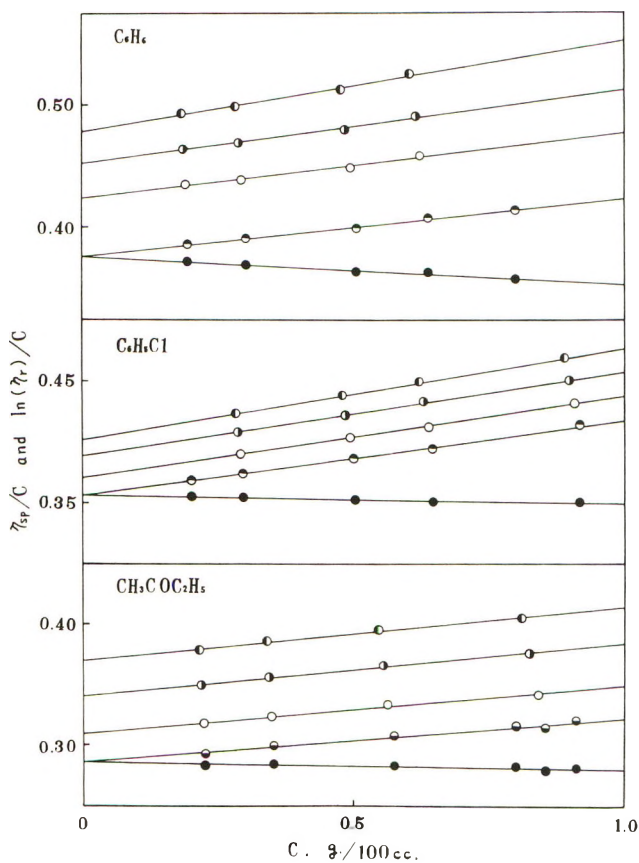

Fig. 4. η_{sp}/C and $(\ln \eta_r)/C$–C relationships for a polydimethylsiloxane fraction of $M = 107{,}000$ in benzene, chlorobenzene, and methyl ethyl ketone: η_{sp}/C at (◓) 15°C., (◒) 20°C., (O) 30°C., (◑) 45°C., and (●) 60°C.; (◐) $\ln(\eta_0/C)$.
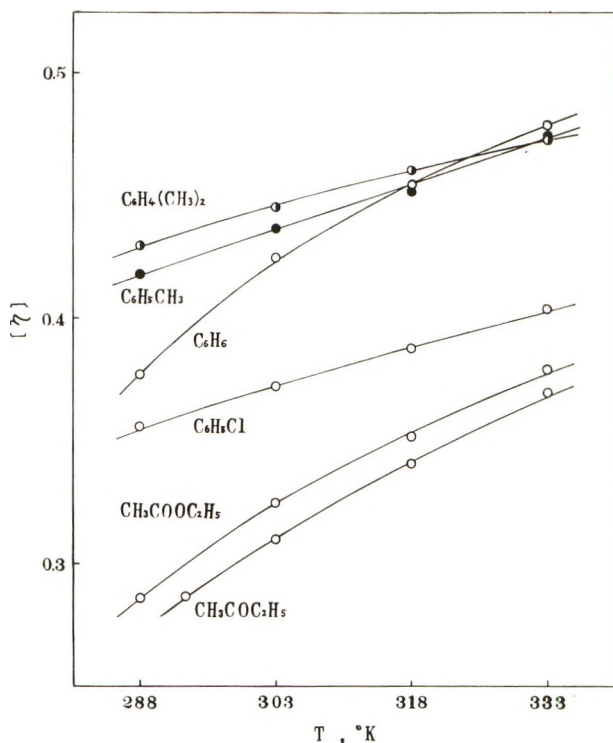
Fig. 5. $[\eta]$–T relationships for a polydimethylsiloxane fraction of $M = 107{,}000$ in various solvents.
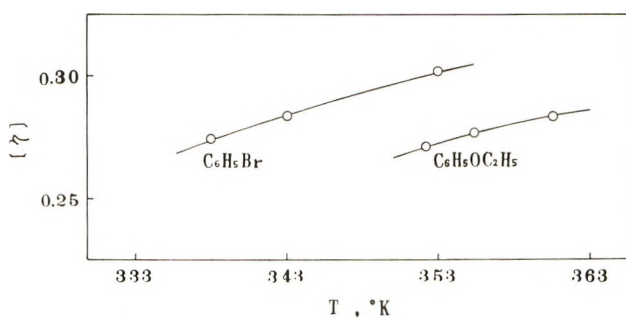
Fig. 6. $[\eta]$–T relationships for a polydimethylsiloxane fraction of $M = 107{,}000$ in various solvents.

cept for the straight lines drawn through the two sets of points, η_{sp}/C and $(\ln \eta_r/C)$. The intrinsic viscosities are plotted against temperature in Figures 5–7.

According to the statistical treatment of dilute polymer solutions, the second virial coefficient may be expressed in the form[9–13]

$$A_2 = (\bar{v}^2/V_1)\psi_1(1 - \Theta/T)F(X) \qquad (1)$$
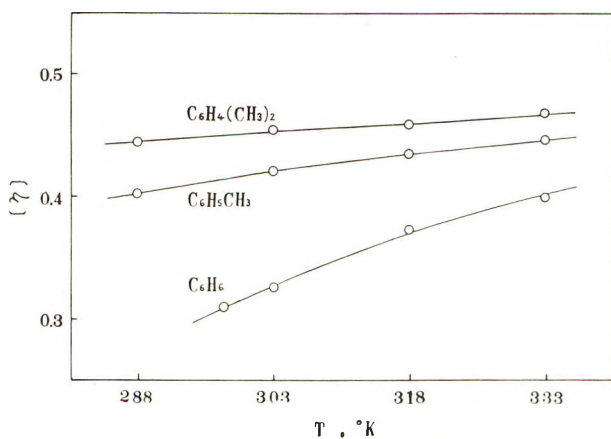
Fig. 7. $[\eta]-T$ relationships for a polyisobutylene fraction of $M = 63,000$ in various solvents.
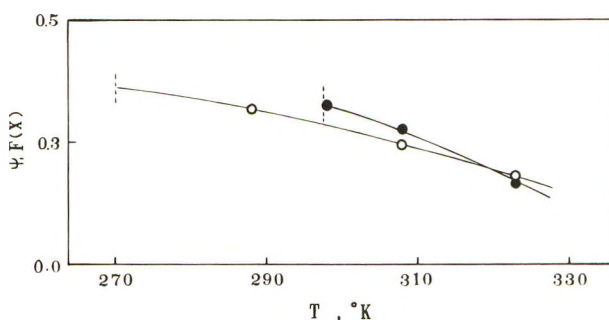

Fig. 8. Experimental values for $\psi_1 F(X)$ products plotted against absolute temperature: (O) a polydimethylsiloxane fraction in benzene; (●) a polyisobutylene fraction in benzene.

where v and V_1 are the partial specific volume of polymer and the molar volume of solvent, respectively, Θ is the temperature at which the second virial coefficient vanishes, and ψ_1 is the pair interaction entropy parameter. The function $F(X)$ depends upon the molecular weight, temperature, and thermodynamic parameters characterizing the polymer–solvent interaction. At the Θ temperature, the function $F(X)$ is equal to unity. The thermodynamic parameters may be evaluated from measurements performed in the vicinity of the Θ temperature without relying on the form of the function $F(X)$. From Figure 2, the Θ temperature for polydimethylsiloxane in benzene is found to lie between 268 and 272°K. The Θ temperature is 297.5°K. for polyisobutylene in the same solvent. The $\psi_1 F(X)$ products calculated from the A's are plotted against the absolute temperature in Figure 8. Since $F(X) = 1$ at $T = \Theta$, these plots lead to the conclusion that $\psi_1 = 0.39$ and 0.36 for polydimethylsiloxane and polyisobutylene in benzene, respectively.

As is well known, the results of the application of the theory of intramolecular interaction in a dissolved polymer molecule to the interpretation of intrinsic viscosity are summarized in eqs. (2) and (3):[13, 14]

$$[\eta] = \Phi(\langle r_0^2 \rangle / M)^{3/2} M^{1/2} \alpha^\gamma \tag{2}$$

$$\alpha^5 - \alpha^3 = C_M \psi_1 (1 - \Theta/T) M^{1/2} \tag{3}$$

where α is the expansion factor arising from intramolecular interaction, $\langle r_0^2 \rangle$ is the mean-square end-to-end length for the unperturbed chain, and C_M is a numerical constant modified by Stockmayer for a given polymer–solvent system.[14] The exponent γ was given as three in the original theory.[14] Recent attempts at refinement have recommended a somewhat lower value in the neighborhood of $\gamma = 2.4$.[13] Therefore, the exponent γ is assigned a value of 2.4.

The intrinsic viscosities in solvents at the Θ temperatures are given in Table II.[2, 16] The values of K are derived from the Θ viscosities by means of Flory's equation $K = [\eta]_\Theta / M^{1/2}$. The values of K for the two polymers slightly decrease with an increase in temperature. Then, the dependence of the value of K on temperature has been assumed to be linear. The values of α have been calculated from the intrinsic viscosities by means of eq. (2). The values of $(K_T/K_{25})(\alpha^5 - \alpha^3)/M^{1/2}$ have been plotted against $1/T$, where K_T and K_{25} are the values of K at T and at 25°C., respectively. As shown in Figure 9, these plots are observed to be accurately linear. The values of Θ and ψ_1 have been deduced from the intercepts and slopes of these lines. The thermodynamic parameters are sum-
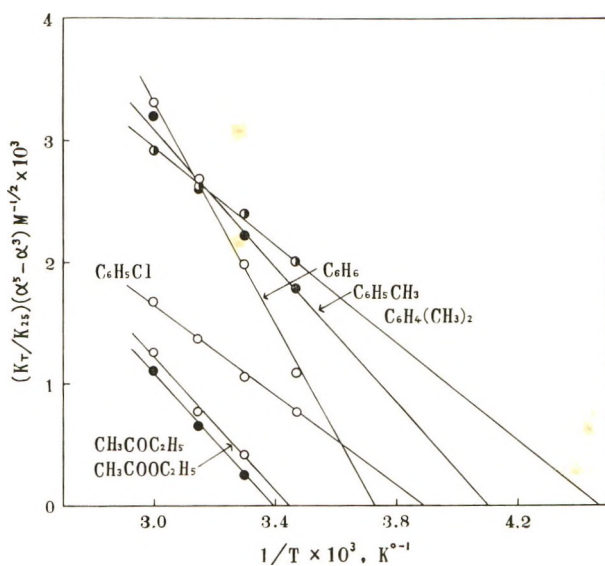

Fig. 9. Plots of $(K_T/K_{25})(\alpha^5 - \alpha^3)M^{-1/2}$ vs. $1/T$ for a polydimethylsiloxane fraction in various solvents.

TABLE II
Values of K Determined in Various Solvents

Polymer Fraction	Solvent	Θ, °K.	$[\eta]_\Theta$ at $T = \Theta$	$K \times 10^4$
PDS 3-1	Methyl ethyl ketone	293[a]	0.287	8.78
	Phenetole	356[a]	0.277	8.47
PIB 2-1	Benzene	297.5	0.310	12.4
	Phenetole	359[b]	0.271	10.8

[a] Data of Flory et al.[16]
[b] Data of Fox and Flory.[2]

TABLE III
The Thermodynamic Interaction Parameters

Polymer	Solvent	Θ, °K.	ψ_1	κ_1 at 25°C.	V_1 at 25°C., cc.
Second Virial Coefficient					
PDS	Benzene	270	0.39	0.34	89.4
Intrinsic Viscosity					
PDS	Benzene	268	0.35	0.31	89.4
	Toluene	245	0.29	0.24	106.9
	Xylene	217	0.24	0.17	123.5
	Chlorobenzene	258	0.18	0.16	128.8
	Bromobenzene	341	0.15	0.18	105.5
	Phenetole	356	0.10	0.12	127.2
	Methyl ethyl ketone	293	0.18	0.18	90.2
	Ethyl acetate	289	0.21	0.20	98.5
Second Virial Coefficient					
PIB	Benzene	297.5	0.36	0.36	89.4
Intrinsic Viscosity					
PIB	Benzene	297.5	0.40	0.40	89.4
	Toluene	259	0.38	0.37	106.9
	Xylene	228	0.37	0.28	123.5

marized in Table III. The values of the pair interaction enthalpy parameter κ_1 which is defined by $\kappa_1 = \psi_1\Theta/T$ are given in the last column.

DISCUSSION

The ψ_1 value for the system polyisobutylene–benzene obtained from the osmotic measurements, 0.36, agrees with the value reported by Krigbaum and Flory, 0.34.[17] This is, also, comparable to the value for polydimethylsiloxane in the same solvent obtained from the osmotic measurements, 0.39. It is now well known that the entropy parameter depends on the coordination number of the lattice, the molecular weight, and the number of intramolecular segmental contacts in excess of the chemical

bonds.[18] The effect of the molecular weight on the entropy parameter should be small for a given polymer having high molecular weight. The number of intramolecular segmental contacts is expected to have a very close relation to the average statistical dimension of the polymer chain and vary with expansion of the chain. It is also expected that the number of intramolecular contacts never tends to zero, even at infinite dilution, but reaches a finite value, depending on the nature of a given chain, such as flexibility. In the existing theories the number of intramolecular segmental contacts cannot be evaluated explicitly. For this reason the correct coordination number cannot be estimated from the ψ_1 value. It is sure that the effect of the coordination number on the entropy parameter is more dominant than any other effect. With a crude approximation, it will be assumed that the number of intramolecular contacts is insensitive to the characteristics of the given chain molecule. Upon considering the two ψ_1 values, 0.39 and 0.36, the coordination number for polydimethylsiloxane seems to be comparable to that for polyisobutylene.

The mean-square end-to-end lengths for the unperturbed chain, $\langle r_0^2 \rangle$, calculated from K for a value of $\Phi = 2.5 \times 10^{21}$, are given in Table IV. The corresponding values, $\langle r_{0_f}^2 \rangle$, calculated from bond lengths and angles assuming free rotation about each single bond of the chain also are included in Table IV. The sizes of the statistical segment at different temperatures are given in the last column of Table IV.[2]

TABLE IV
Dimensions of Randomly Coiled Polymer Chains Unperturbed by
Thermodynamic Interactions

Polymer	T, °K.	$(\langle r_0^2 \rangle / M)^{1/2} \times 10^{11}$		$(\langle r_0^2 \rangle / \langle r_{0_f}^2 \rangle)^{1/2}$	Number of chain atom per equivalent segment
		Calcd. from K	Calcd. for free rotation		
PDS	293	705	456	1.55	6.78
	356	697	456	1.53	6.61
PIB	297.5	791	412	1.92	7.38
	359	756	412	1.83	6.70

The values of $(\langle r_0^2 \rangle / \langle r_{0_f}^2 \rangle)$ for the polydimethylsiloxane chain are considerably smaller than those for the polyisobutylene chain. This discrepancy seems to arise from the difference of the effect of steric interactions between methyl groups. The values of $\langle r_0^2 \rangle$ for polydimethylsiloxane is nearly independent of the temperature, while those for polyisobutylene show a tendency to decrease with an increase in temperature. The variation of $\langle r_0^2 \rangle$ with temperature seems to be due to the effect of preferentially overcoming the barrier to free rotation. The size of the statistical segment for these polymers at room temperature is considered to be about 11 A.

Kurata and his co-workers have recently calculated intrinsic viscosity by taking the non-Gaussian character of the chain configuration into account, and indicated that the hydrodynamic radius of the polymer chain increases less rapidly than the statistical radius as the excluded volume between segments increases.[13] Their conclusion has been confirmed by the recent measurements carried out by Krigbaum and Carpenter.[19] Therefore, it seems to be rather preferable to calculate the α value by $\alpha^{2.4} = [\eta]/[\eta]_\Theta$.

As shown in Table III, the Θ temperature for polydimethylsiloxane in benzene deduced from the intrinsic viscosity agrees with that obtained from the second virial coefficient within the experimental error. The Θ values obtained from the present measurements stand in good agreement with corresponding values appearing in the literature.[2,17] It has been established in the past several years that the Θ values for two systems—polyisobutylene in benzene and polystyrene in cyclohexane—deduced from viscosity are in good agreement with those obtained by either of the other two measurements, osmotic pressure and precipitation temperature.[17,19,20] Then, one would expect both osmotic pressure and viscosity to yield the same value of Θ.

The ψ_1 values deduced from viscosity agree to some extent with those obtained from the osmotic measurements. However, the ψ_1 values for polyisobutylene in benzene and toluene do not agree with corresponding values reported by Fox and Flory from viscosity.[2] We have obtained the α value by $\alpha^{2.4} = [\eta]/[\eta]_\Theta$ from the viscosity data, while Fox and Flory have used $\alpha^3 = [\eta]/[\eta]_\Theta$.[2] Use of $\alpha^3 = [\eta]/[\eta]_\Theta$ instead of $\alpha^{2.4} = [\eta]/[\eta]_\Theta$ results in the ψ_1 value which is lower by about 30%. Therefore, the disagreement mentioned above may be attributed to the method of analysis of the intrinsic viscosity.

The ψ_1 values for polyisobutylene in nonpolar solvents seem to agree with one another within experimental error, although a small difference between those values is observed. However, it appears that the ψ_1 values differ distinctly for polydimethylsiloxane in nonpolar solvents. This is also shown by comparisons of the observed temperature dependences of the second virial coefficients in Figure 2 and the intrinsic viscosities in Figure 5. The conclusion drawn from these results that the entropy of dilution varies with the geometrical character of the solvent molecule in relation to the polymer segment is supported by the works of Flory and Fox on viscosity, and Schick, Doty, and Zimm on osmotic pressure.[1-3]

Moreover, the ψ_1 values for polydimethylsiloxane in polar solvents are consistently lower than those in nonpolar solvents. In view of the fact that the entropy of dilution varies with the geometrical character of the solvent molecule, it seems to be rather preferable to compare the ψ_1 values for polar solvents with the values for nonpolar solvents having the analogous size and shape. From Table III, it is possible to show that the ψ_1 values for polar solvents differ distinctly from the values for nonpolar solvents having the analogous molar volume. These discrepancies between

the values for the entropy parameter may be considered to arise from the preferential ordering induced by the difference in the binding forces between the molecules solvent–solvent, solvent–solute, and solute–solute.

From the present results, it is obvious that the entropy of dilution differs widely for a given polymer in different solvents. In order to explain the observed thermodynamic data in terms of molecular concepts, one would have to take into account the binding forces of the two components and also the size and shape of the solvent molecule in relation to the polymer segment.

References

1. Schick, M. J., P. Doty, and B. H. Zimm, *J. Am. Chem. Soc.*, **72**, 530 (1950).

2. Fox, T. G, and P. J. Flory, *J. Am. Chem. Soc.*, **73**, 1909 (1951).

3. Fox, T. G, and P. J. Flory, *J. Am. Chem. Soc.*, **73**, 1915 (1951).

4. Kawai, T., *Bull. Chem. Soc. Japan*, **29**, 560 (1956).

5. Weissberger, A., E. S. Proskauer, T. A. Riddick, and E. E. Toops, *Organic Solvents*, Interscience, New York–London, 1955.

6. Kolorlov, A., K. Andrianov, L. Uchecheva, and T. Vuegenskaya, *Dokl. Akad. Nauk. S S S R*, **89**, 65 (1953).

7. Fox, T. G, and P. J. Flory, *J. Phys. Colloid Chem.*, **53**, 197 (1949).

8. Krigbaum, W. R., and P. J. Flory, *J. Am. Chem. Soc.*, **75**, 1775 (1953).

9. Flory, P. J., and W. R. Krigbaum, *J. Chem. Phys.*, **18**, 1086 (1950).

10. Ishihara, A., and R. Koyama, *J. Chem. Phys.*, **25**, 712 (1956).

11. Krigbaum, W. R., D. K. Carpenter, M. Kaneko, and A. Roig, *J. Chem. Phys.*, **33**, 921 (1960).

12. Zimm, B. H., *J. Chem. Phys.*, **14**, 164 (1946).

13. Kurata, M., and H. Yamakawa, *J. Chem. Phys.*, **29**, 311 (1958).

14. Flory, P. J., and T. G Fox, *J. Am. Chem. Soc.*, **73**, 1904 (1951).

15. Stockmayer, W. H., *J. Polymer Sci.*, **15**, 595 (1955).

16. Flory, P. J., L. Mandelkern, J. B. Kinsinger, and W. B. Shultz, *J. Am. Chem. Soc.*, **74**, 3364 (1952).

17. Krigbaum, W. R., and P. J. Flory, *J. Am. Chem. Soc.*, **75**, 5254 (1953).

18. Kurata, M., *Ann. N. Y. Acad. Sci.*, **89**, 635 (1961).

19. Krigbaum, W. R., and D. K. Carpenter, *J. Phys. Chem.*, **59**, 1166 (1955).

20. Krigbaum, W. R., *J. Am. Chem. Soc.*, **76**, 3758 (1954).

Résumé

Les mesures de pression et de viscosité fournissent mutuellement des renseignements supplémentaires sur les paramètres thermodynamiques qui gouvernent l'interaction entre les segments de polymères et les molécules de solvant. En vue d'étudier l'influence des caractéristiques structurelles du polymère et du solvant sur l'interaction entre les segments de polymère et les molécules de solvant, nous avons effectué des mesures de pression osmotique et de viscosité à différentes températures. La température Θ obtenue à partir de la viscosité intrinsèque est en accord avec celle obtenue à partir du second coefficient du viriel. L'entropie de dilution pour le système polyisobutylène–benzène est comparable à celle trouvée pour le polydiméthylsiloxane dans le benzène. Cependant, on a trouvé que l'entropie de dilution différait fortement pour un polymère

donné dans différents solvants.   Il semble que l'entropie de dilution varie non seule-
ment avec la géométrie de la molécule de solvant en relation avec le segment de
polymère, mais également avec une organisation préférentielle induite par la différence
dans les forces de liaison entre les molécules de solvant–solvant, solvant–soluté et
soluté–soluté.   On discute également brièvement de l'influence de l'empêchement à la
rotation libre sur la configuration du polymère.

Zusammenfassung

Messung des osmotischen Druckes und der Viskosität liefern sich gegenseitig ergän-
zende Daten für die thermodynamischen Parameter der Wechselwirkung zwischen
Polymersegmenten und Lösungsmittelmolekülen.   Solche Messungen wurden bei
verschiedenen Temperaturen mit der Absicht ausgeführt, die Einflüsse der Struktur-
charakteristik von Polymerem und Lösungsmittel auf die Wechselwirkung zwischen
Polymersegmenten und Lösungsmittelmolekülen kennen zu lernen.   Die aus der Visko-
sitätszahl abgeleitete Θ-Temperatur stimmt offensichtlich mit der aus dem zweiten
Virialkoeffizienten erhaltenen überein.   Die Verdünnungsentropie für das System Poly-
isobutylen–Benzol ist mit der für Polydimethylsiloxan in Benzol gefundenen vergleich-
bar.   Für ein gegebenes Polymeres weist jedoch die Verdünnungsentropie in verschied-
enen Lösungsmitteln grosse Unterschiede auf.   Es scheint, dass die Verdünnungsentropie
nicht nur vom geometrischen Charakter des Lösungsmittelmoleküls in bezug auf das
Polymersegment abhängt, sondern auch von der durch die Unterschiede in den moleku-
laren Bindungskräften Lösungsmittel–Lösungsmittel, Lösungsmittel–Gelöstes und
Gelöstes–Gelöstes bedingten, bevorzugten Ordnung.   Eine kurze Diskussion des Ein-
flusses der Hinderung der freien Rotation auf die Polymerkonfiguration wird gegeben.

Polymerization of α-Methylstyrene with Al(C₂H₅)₃–TiCl₄ Catalyst

YUTAKA SAKURADA,* *Research Laboratory, Kurashiki Rayon Company, Ltd., Kurashiki, Okayama, Japan*

Synopsis

Polymerization of α-methylstyrene was carried out in the presence of AlEt₃–TiCl₄ at −78°C. The activity of the catalyst and the degree of polymerization were affected by the AlR₃/TiCl₄ molar ratio, the mixing and the aging conditions of catalyst, and the kinds of solvent. The advantageous AlR₃/TiCl₄ molar ratio was found to be between 1.0 and 1.2; at ratios higher than 2.0 the polymerization did not proceed. For this catalyst to have enough activity, the mixing and the aging of catalyst must be carried out below room temperature, and the valence state of titanium must be kept between IV and III after the reaction between AlEt₃ and TiCl₄. From comparison of the present results with other catalyst systems it is speculated that the polymerization reaction by this catalyst system is cationic, and that its active species are the intermediate complex [(TiCl₃)⁺-(AlEt₃Cl)⁻] and the reaction product AlEt₂Cl. This speculation is confirmed by the molecular weight distribution curves of the poly-α-methylstyrene obtained, measured by a column fractionation method. The distribution curves have two maxima, at molecular weights of about 5 × 10⁴ and 65 × 10⁴. This suggests that two kinds of active species are present, in agreement with the above hypothesis. The resultant poly-α-methylstyrene shows superior stereoregularity, compared with that prepared with other catalyst systems.

INTRODUCTION

Natta and his co-workers[1] have carried out the polymerization and copolymerization of various vinyl aromatic compounds, such as those of α-olefins, dienes, and polar vinyl compounds, in the presence of Ziegler-type catalysts, obtaining stereospecific polymers. In their publications they reported that α-substituted monomers like α-methylstyrene are completely inactive or show very low reactivities with this catalyst system. In Natta's review[2] of stereospecific polymerization and catalysis, polymerization reactions of various monomers with Ziegler-type catalysts are classified systematically according to the monomer structure and the polymerization mechanism. In the classification, however, CH₂=CRR′, vinylidene hydrocarbon monomers, are left uncertain. With regard to these, a considerable amount of information has been published on the polymerization of isobutene,[3] but no report on the polymerization of α-methylstyrene has yet appeared.

* International Fellow, Stanford Research Institute Menlo Park, California, 1962–1963.

We have tried the polymerization of α-methylstyrene with $AlEt_3$–$TiCl_4$ and other Ziegler-type catalyst systems and have successfully found that the coordinated catalysts prepared under certain conditions are active, particularly at low temperature, and that the resultant poly-α-methylstyrene shows superior stereoregularity. The results reported herein include studies of the following factors which are known to affect the usual Ziegler polymerizations: the molar ratio of $AlR_3/TiCl_4$, the mixing and aging conditions of the catalyst, and the type of solvent. This report will be limited to the case of $AlEt_3$–$TiCl_4$. From the results of our experiments, it is suggested that the polymerization proceeds cationically, as does the polymerization of vinyl ether[4] with the same catalyst system. The discussion deals with the polymerization mechanism, especially the kinds of active species. A relationship is observed between the mixing and aging conditions of the catalyst and the molecular weight distributions of the polymer.[5] This relationship supports the conclusions reached in the discussion of the active species.

EXPERIMENTAL

Materials

α-Methylstyrene (Allied Chemical) was washed successively by dilute sodium hydroxide solution (5%) and water, dried over potassium carbonate, and fractionally distilled under vacuum. n-Hexane was purified by successive washings with concentrated sulfuric acid, water, dilute sodium hydroxide solution (5%), alkaline potassium permanganate solution (5%), and water. Toluene was purified with concentrated sulfuric acid and water. After drying over phosphorus pentoxide, these solvents were fractionally distilled over metallic sodium and stored over calcium hydride.

Catalyst

Titanium tetrachloride was purified by fractional distillation over copper powder. Commercial triethyl aluminum, diethyl aluminum chloride, and ethyl aluminum dichloride (Ethyl Corporation) were used.

Polymerization Procedures

Preliminary tests were made on the order and the method of addition of each component, since they were considered to have a great influence on the polymerization. As a result, the following procedure was preferred and employed throughout the experiments.

The required amount of n-hexane (5 ml.) was poured into a glass tube having a self-sealing rubber stopper. After the atmosphere inside the tube was replaced by purified nitrogen, $TiCl_4$ was added through the sealing stopper by means of a hypodermic syringe. $AlEt_3$ was then added to the solution through a hypodermic syringe at the temperature designated for the catalyst aging. The tube was shaken continuously during the injection

of these components. After the mixing of TiCl$_4$ and AlEt$_3$, the catalyst solution was aged for the designated time. The tube was then placed in a constant temperature bath and left standing for 5 min. ($-78°$C.) to adjust the temperature of the catalyst solution to the polymerization temperature. In a separate tube, the mixed solution of the required amounts of solvent (35 ml.) and α-methylstyrene (10 ml.) was cooled and kept at the polymerization temperature. This mixed solution was rapidly added to the catalyst solution under a nitrogen atmosphere. Polymerization took place instantaneously. The polymer solution was poured into methanol. The polymer coagulated, forming a large mass under rigorous shaking. The polymer was powdered mechanically, soaked in alcohol overnight, and then dried under vacuum at 45°C. for 2 days.

Molecular Weight Measurements

The molecular weights of all the products were determined by viscometry in toluene solution at 30°C. employing the relationship proposed by Sirianni and his co-workers:[6]

$$[\eta] = 1.08 \times 10^{-4} M^{0.71}$$

RESULTS

Effect of Solvent

As polymerization solvents, n-hexane and toluene were used. These hydrocarbon solvents are commonly used for the polymerization of α-olefins
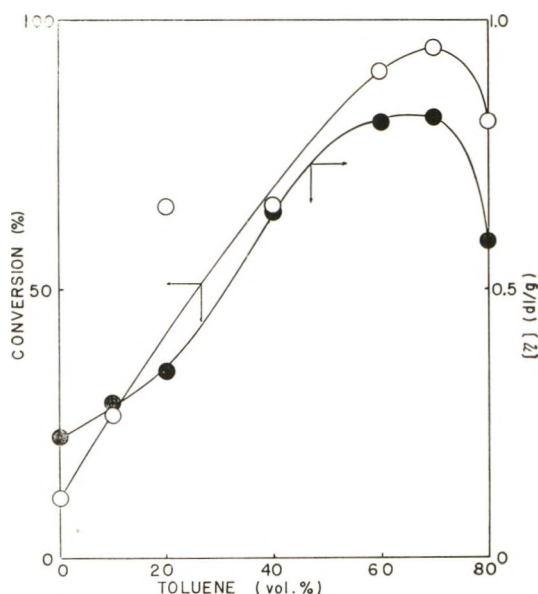

Fig. 1. Effects of solvent composition on (O) conversion: (●) [η]. Polymerization conditions: α-methylstyrene 10 ml., solvent 40 ml., AlEt$_3$ 0.0279 mole/l., Al/Ti 1.2, $-78°$C., 20 hr.; aging conditions: 0°C., 15 sec.

with Ziegler-type catalysts; they do not solidify at the polymerization temperature ($-78°$C.). Polymerization was carried out with the mixed solvent system of toluene and n-hexane at an Al/Ti ratio of 1.2 for 20 hr. The results are shown in Figure 1, where conversion and intrinsic viscosity are plotted against solvent composition for constant polymerization temperature and time.

Conversion and intrinsic viscosity are dependent on the solvent composition and have a maximum at a toluene concentration of 70 vol.-%. This is remarkably similar to the results obtained in the polymerization of α-methylstyrene with the typical cationic catalyst $BF_3 \cdot OEt_2$ in the same mixed solvent at $-78°$C.[7]

Effect of Al/Ti Ratio

The molar ratio of AlR_3 to $TiCl_4$ is an important factor in Ziegler polymerization. Although the polymerization of α-methylstyrene does not occur with $AlEt_3$ alone, it is well known that cationic polymerization proceeds easily with $TiCl_4$ catalyst. The effect of the $AlR_3/TiCl_4$ mole ratio was examined for four solvent compositions (80, 70, 50, and 30 vol.-% toluene), at $-78°$C. for 20 hr. The results are shown in Figures 2 and 3. In Figure 2, conversion is plotted against $AlR_3/TiCl_4$ ratio. Each curve has a maximum at molar ratio 1.2 for 80 vol.-% toluene and 1.0 for 50 and 30 vol.-%. The shape of the curve near the maximum for 70 vol.-% is not
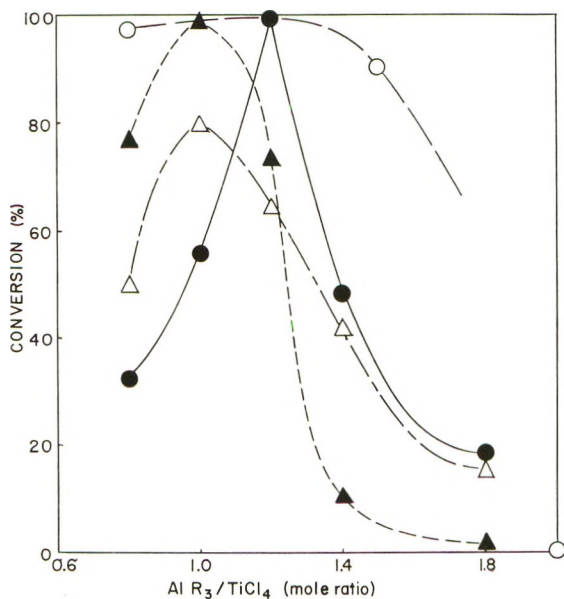

Fig. 2. Effect of $AlR_3/TiCl_4$ molar ratio on conversion at various toluene concentrations: (●) 80 vol.-%; (○) 70 vol.-%; (▲) 50 vol.-%; (△) 30 vol.-%. Polymerization conditions: α-methylstyrene 10 ml., solvent 40 ml., $AlEt_3$ 0.0279 mole/l., Al/Ti 1.2, $-78°$C., 20 hr.; aging conditions; 0°C., 15 sec.
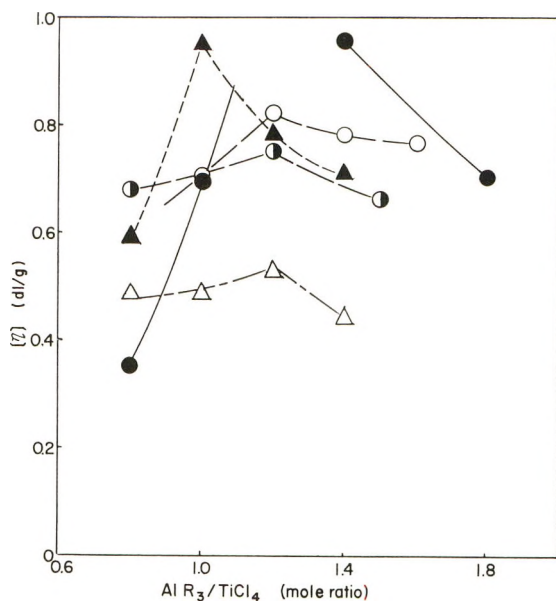
Fig. 3. Effect of $AlR_3/TiCl_4$ molar ratio on intrinsic viscosity at various toluene concentrations: (●) 80 vol.-%; (○, ◑) 70 vol.-%; (▲) 50 vol.-%; (△) 30 vol.-%.

as sharp as the others, probably due to the excess of catalyst. In Figure 3, the intrinsic viscosities of these polymers are plotted against $AlR_3/TiCl_4$ ratio. The intrinsic viscosity–molar ratio relationship also has a maximum at the molar ratio 1.2 for 70 and 30 vol.-%, and 1.0 for 50 vol.-%. Good reproducibility with regard to the relationship between the degree of conversion and the $AlR_3/TiCl_4$ molar ratio and with regard to the relationship between [η] and the $AlR_3/TiCl_4$ molar ratio was shown by the smoothness of the curves representing each series of experiments at constant solvent composition. The reproducibility between the experiments at different solvent compositions seems to be poor. This is probably due to slight differences in quality between the different lots of material, because each series of experiment was made with materials prepared separately. Taking these conversion and intrinsic viscosity results into account, we may conclude that the catalyst activity is most effective in the molar ratio range of 1.0–1.2.

Effect of Catalyst Aging Condition

In the Ziegler polymerization of ethylene,[8] butene,[9] styrene,[10] isoprene,[11] and other monomers, it has been reported that the catalyst activity depends strongly on the conditions of preparation of the coordinated catalyst in the absence of monomer. In order to examine this effect on the present system, the catalyst aging was carried out in n-hexane at three different temperatures, 0, −30, and −78°C. for various times, the catalysts being supplied to the polymerization system under uniform conditions (i.e., $AlR_3/TiCl_4$

ratio of 1.2 and toluene concentration of 70 vol.-%). Figure 4 shows the relationships between aging time and conversion. At the aging temperature of 0°C., conversions at a constant polymerization time decrease markedly
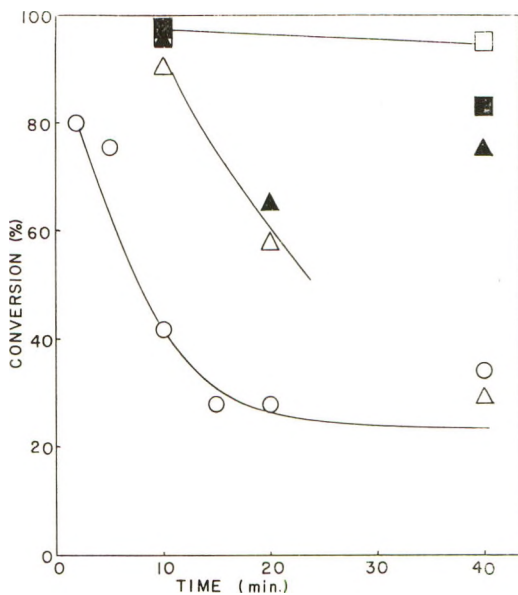

Fig. 4. Relationship between aging time and conversion at various aging temperatures: (O) 0°C.; (△, ▲) −30°C.; (□, ■) −78°C. Polymerization conditions: α-methylstyrene 10 ml., toluene 35 ml., n-hexane 5 ml., AlEt₃ 0.0047 mole/l., Al/Ti 1.2, −78°C., 20 hr.
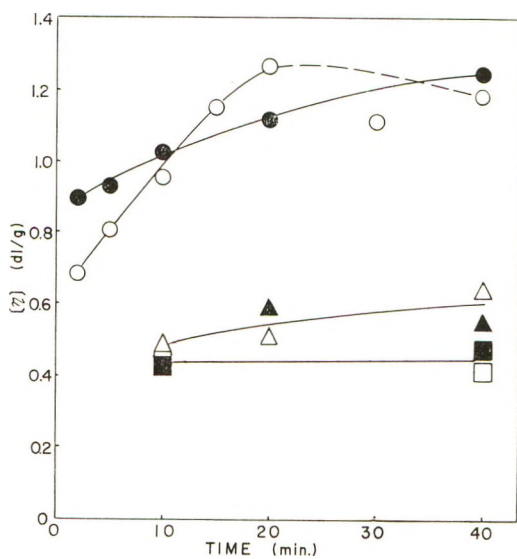

Fig. 5. Relationship between aging time and intrinsic viscosity at various aging temperatures: (O, ●) 0°C.; (△, ▲) −30°C.; (□, ■) −78°C.

with increase of aging time. The lower aging temperature gives the higher conversion, being less affected by aging time. At an aging temperature of $-78°C$., conversion reaches a value of ca. 95%, independent of the aging time. The intrinsic viscosities of the polymers are related to aging time in Figure 5. The curve for $0°C$. shows an increase of $[\eta]$ with increase of aging time. The molecular weights corresponding to aging times of 2 and 40 min. are 2000 and 4000, respectively. The effects of aging time upon $[\eta]$ become less as the aging temperature is lowered and eventually the effects are not observable, as shown by the curve for $-78°C$.

Comparison with Other Catalyst Systems

Polymerization by Ziegler-type catalysts was compared with polymerizations using other catalyst systems, such as alkylaluminum halides, titanium chlorides, or $BF_3 \cdot OEt_2$. The results of polymerizations with those catalyst systems are given in Table I.

TABLE I
Comparison with Other Catalyst Systems
Polymerization conditions: α-Methylstyrene 10 ml., Toluene 35 ml., n-Hexane 5 ml., $-78°C$., 20 hr.

| System | Catalyst | | Catalyst concn., mole/l. | Conversion, % | $[\eta]$, dl./g. | Degree of polymerization |
	$AlR_3/$ $TiCl_n$	Aging condition				
$AlEt_3$–$TiCl_4$	1.2	$0°C$., 10 min.	$TiCl_4$ 0.0039	41.4	0.954	3030
$AlEt_3$–$TiCl_4$	1.2	$0°C$., 20 min.	"	27.5	1.263	4510
$AlEt_3$–$TiCl_4$	1.2	$-78°C$., 10 min.	"	98.0	0.428	990
$AlEt_3$–$TiCl_4$	1.2	$-78°C$., 40 min.	"	83.5	0.471	1140
$AlEt_3$–$TiCl_3$	20		$TiCl_3$ 0.0583	Trace	—	—
$AlEt_3$–$TiCl_3$	10		"	"	—	—
$AlEt_3$–$TiCl_3$	1.0		"	None	—	—
$AlEt_3$			0.0039	None	—	—
$AlEt_2Cl$			"	14.5	1.258	4480
$AlEtCl_2$			"	44.6	0.582	1520
$TiCl_4$			"	89.8	0.575	1500
$TiCl_3$			0.0583	Trace	—	—
$BF_3 \cdot OEt_2$			0.0039	3.6	—	—
$BF_3 \cdot OEt_2$			0.0480	70.7	1.460	5590

These results may be summarized as follows. Polymerization does not proceed by means of $TiCl_3$ alone or $AlEt_3$–$TiCl_3$ systems. The catalyst activity of $AlEt_3$–$TiCl_4$ is so high that the comparable value in conversion was obtained with a catalyst concentration less than $1/10$ that of $BF_3 \cdot OEt_2$. The results of polymerization with an alkyl aluminum halide ($AlEt_nCl_{3-n}$, $n = 1, 2, 3$) catalyst alone without $TiCl_4$ reveals that the orders of catalyst

to give high conversion and intrinsic viscosity are: $TiCl_4 \simeq (AlCl_3) >$ $AlEtCl_2 > AlEt_2Cl > AlEt_3 = 0$ (for conversion) and $AlEt_2Cl > AlEtCl_2 >$ $(AlCl_3) \simeq TiCl_4$ (for intrinsic viscosity). It is interesting to note that the order for conversion is completely opposite to that for intrinsic viscosity.
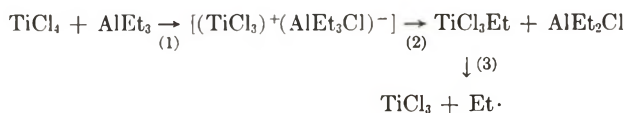
Properties and Stereoregularity of Polymers Obtained

The physical properties of poly-α-methylstyrene polymerized with $AlEt_3$–$TiCl_4$ at $-78°C$. were compared with those of poly-α-methylstyrene polymerized with $BF_3·OEt_2$ and $TiCl_4$ at $-78°C$., and with metallic Na and K at room temperature. No x-ray fiber diagram has been observed for poly-α-methylstyrene polymerized by any other catalyst systems. Poly-α-methylstyrene prepared with $AlEt_3$–$TiCl_4$, like that prepared with other catalyst systems by ordinary methods, was not crystallizable. However, after heat stretching under certain conditions the polymer became crystallizable, giving a clear fiber diagram with a fiber identity period of 6.5 A.; this may be due to its isotactic structure. The glass-transition temperature,[12] solubility in methyl ethyl ketone,[12] infrared absorption spectrum,[12] x-ray scattering curve,[13] nuclear magnetic resonance spectrum,[14] density,[12] and Huggins parameter k' in toluene solution[12] were measured on the (substantially amorphous) polymers prepared with varying polymerization conditions. Some differences, depending on the polymerization conditions, were observed in the glass-transition temperature, the infrared spectrum, nuclear magnetic resonance spectrum, and x-ray scattering curves. These differences may result from differences in the tacticity of polymer. According to these methods the order of tacticity for polymers prepared with different catalysts is: $AlEt_3$–$TiCl_4 > BF_3·OEt_2 >$ $TiCl_4 > Na \geq K$. Detailed results and discussions will be published later.[12-16]

DISCUSSION

The mechanism of the Ziegler polymerization of α-methylstyrene will be discussed especially with regard to the active species indicated by the present experimental results. The molar ratio of $AlR_3/TiCl_4$ is an important variable in polymerization catalyzed with $AlEt_3$–$TiCl_4$. The most suitable molar ratio depends on the type of monomer: it is, for instance, 2.5–2.8 for styrene,[15] 2.0 for propylene,[16] 1.5–1.7 for butene,[9] and 1.2 for isoprene. The value for α-methylstyrene is in the range 1.0–1.2 similar to that for cis-1,4 polymerization of isoprene. From the results of copolymerization experiments,[18] it has been suggested that the Ziegler polymerization of α-olefins, such as ethylene, propylene, and styrene, proceeds by an anionic mechanism and that in the case of isoprene the polymerization is anionic at an $AlR_3/TiCl_4$ molar ratio higher than 1.0, with a cationic mechanism probably superposed at an $AlR_3/TiCl_4$ molar ratio lower than 1.0. In spite of an $AlR_3/TiCl_4$ molar ratio ranging from 1.0 to 1.2 in our experiments, polymerization of α-methylstyrene seems to be cationic as in

the case of vinyl isobutyl ether.[4]   This conclusion is based on the following evidence.   (1) The effect of the mixed solvent composition on conversion and intrinsic viscosity is similar to that for typical cationic polymerization. (2) The intrinsic viscosity of the polymer obtained decreases with the increase of polymerization temperature.   (The intrinsic viscosities of polymer prepared at room temperature are 0.01–0.02 dl./g.)   (3) The valence of titanium must be kept between IV and III for the reaction of AlEt₃ and TiCl₄ for this catalyst system to exhibit enough activity.   If the valence state of titanium becomes lower than III, this catalyst system completely loses its activity.   (4) The polymerization of styrene under the same conditions as the polymerization of α-methylstyrene at −78°C. gives a polymer having an intrinsic viscosity of 0.05–0.10 dl./g., like the polymers prepared with cationic catalysts.

From the relationship between the aging conditions of the catalyst and the conversion or degree of polymerization, one can speculate about the active species of this catalyst system as follows.   The reaction between AlEt₃ and TiCl₄ is one in which the TiCl₄ is reduced by the AlEt₃.   Referring to other studies[13] using various methods, the reaction scheme may be as follows:

$$TiCl_4 + AlEt_3 \underset{(1)}{\rightarrow} [(TiCl_3)^+(AlEt_3Cl)^-] \underset{(2)}{\rightarrow} TiCl_3Et + AlEt_2Cl$$

$$\downarrow (3)$$

$$TiCl_3 + Et\cdot$$

The secondary reduction with the reaction product AlEt₂Cl does not occur under present experimental conditions because the reducing power of AlEt₂Cl is considerably lower than that of AlEt₃.   In explaining the dependence of the degree of conversion and the degree of polymerization upon the aging conditions (time and temperature), one must consider the reaction state of the AlEt₃–TiCl₄ system.   The facts that conversion and degree of polymerization are completely independent of catalyst aging time at −78°C. indicate that the reaction between AlEt₃ and TiCl₄ does not occur during the polymerization period at −78°C.   According to this reasoning, the effects of the aging conditions shown in Figures 4 and 5 are direct results of changes of the active species formed in the aging period. Since TiCl₃Et is reported to be extremely unstable and TiCl₃ is found to be inactive for the present polymerization, TiCl₃Et can also be assumed to be inactive.

The intermediate complex [(TiCl₃)⁺(AlEt₃Cl)⁻] and the reaction product AlEt₂Cl may therefore be considered to be the two kinds of active species existing in the present system.   The effects of the aging condition may be explained satisfactorily by this assumption.   Since reaction (1) proceeds instantaneously, and reaction (2) does not proceed with the aging at −78°C., only the soluble intermediate complex prepared by reaction (1) acts as an active species at this temperature.   With the aging at the higher temperatures of 0°C. and −30°C. the reactions (2) and (3) also proceed, with the formation of a brownish black precipitate, and the active species
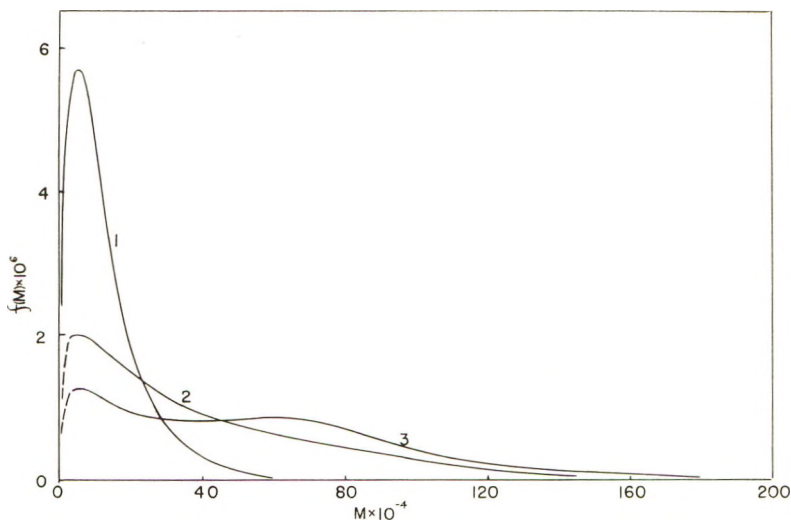
Fig. 6. Change of molecular weight distribution of poly-α-methylstyrene with the aging of catalyst (AlEt₃-TiCl₄): (*1*) −78°C., 40 min., (*2*) 0°C., 5 min.; (*3*) 0°C., 40 min. Polymerization conditions: α-methylstyrene 10 ml., toluene 35 ml., n-hexane 5 ml., AlEt₃ 0.0047 mole/l., Al/Ti 1.2, −78°C., 20 hr.

AlEt₂Cl increases with decrease of the intermediate complex. This indicates that two kinds of active species act competitively during polymerizations with the catalysts prepared at 0 and −30°C. This is consistent with the results of the reduction curve of TiCl₄ with AlEt₃ studied by Yamazaki.[21] To confirm this conclusion, the molecular weight distributions of polymers prepared under various aging conditions were measured, using a fractionation column with a benzene–n-hexane system. Although detailed results and discussions will be published later,[5] differential distribution curves are shown in Figure 6. The low molecular weight portions of the curves are represented by dotted lines, because of the lack of experimental measurements in this region. The fractionation was performed with sufficient accuracy to enable the following conclusions to be drawn. The distribution curve for the polymer obtained with the catalyst prepared at −78°C. has a sharp maximum at molecular weight of ca. 5×10^4, but the curve for the polymer obtained with catalyst prepared at 0°C. for 40 min. has two maxima at molecular weights of ca. 5×10^4 and 65×10^4. The aging lowers the height of the low molecular weight maximum at 5×10^4 and raises that of the high molecular weight maximum at 65×10^4. The active species of the complex gives the maximum at a molecular weight of 5×10^4, and the AlEt₂Cl active species gives the maximum at a molecular weight of 65×10^4. The polymerization induced by the former seems to be homogeneous polymerization, and that induced by the latter seems to be heterogeneous polymerization. From these results, it is hard to draw a definite conclusion at present as to whether the polymerization induced by AlEt₂Cl is coordinated polymerization involving the absorption of

AlEt$_2$Cl onto the surface of TiCl$_3$ or simple cationic polymerization by AlEt$_2$Cl in a substantially homogeneous system.

It is very interesting to note that the conditions for the preparation of Ziegler catalysts have a great influence upon the shape of the molecular weight distribution curve, because of the dependence of this shape on the relative proportions of two active species. Carrick and his co-workers[21] have reported that polyethylene produced by the AlR$_3$–TiCl$_4$ catalyst has a very broad distribution with $\bar{M}_w/\bar{M}_n$ of the order of 15–30, whereas another soluble catalyst AlX$_n$–Sn(C$_6$H$_5$)$_4$–VX$_m$ gives a narrow distribution product. This observation is interesting in view of the results reported here.

For the preparation conditions of catalyst and the polymerization conditions employed here, the present results with α-methylstyrene can be considered as indicative of the general character of the polymerization of more complex binary catalyst systems of the Ziegler type.

Additional studies will be made of the relationships between the two kinds of active species confirmed above, the stereoregularity of the polymers obtained, and the heterogeneity of the catalysts.

References

1. Natta, G., F. Danusso, and D. Sianesi, *Makromol. Chem.*, **28**, 253 (1958); G. Natta, F. Danusso, and D. Sianesi, *ibid.*, **30**, 238 (1959).

2. Natta, G., *Gazz. Chim. Ital.*, **89**, 89 (1959).

3. Topchiev, A. V., and B. A. Krentsel, paper presented at International Symposium on Macromolecular Chemistry, Prague, Czechoslovakia, September 1957; A. V. Topchiev, et al., *Dokl. Akad. Nauk SSSR*, **111**, 121 (1956).

4. Lal, J., *J. Polymer Sci.*, **31**, 179 (1958); E. J. Vandenberg, Ital. Pat. 571741 (Jan. 14, 1958); E. J. Vandenberg, R. F. Heck, and D. S. Breslow, *J. Polymer Sci.*, **41**, 519 (1959); G. Natta et al., *Angew. Chem.*, **71**, 205 (1959).

5. Sakurada, Y., and M. Ueda, paper presented at the Meeting on Macromolecular Chemistry Osaka, Japan, November 1961; *Kobunshi Kagaku*, in press.

6. Sirianni, A. F., D. J. Worsford, and S. Bywater, *Trans. Faraday Soc.*, **55**, 2124 (1959).

7. Okamura, S., T. Higashimura, and Y. Imanishi, *Kobunshi Kagaku*, **16**, 69 (1959).

8. Orzechowski, A., *J. Polymer Sci.*, **34**, 65 (1959).

9. Medalia, A. I., et al., *J. Polymer Sci.*, **41**, 241 (1959).

10. Kern, B. J., H. G. Hurst, and W. R. Richard, *J. Polymer Sci.*, **45**, 195 (1960); N. Yamazaki, *Kobunshi Kagaku*, **15**, 49 (1958).

11. Adams, H. E., et al., *Ind. Eng. Chem.*, **50**, 1507 (1958); S. Kanbara, N. Yamazaki, and N. Suzuki, *Kogyo Kagaku Zasshi*, **61**, 1640 (1958).

12. Sakurada, Y., M. Matsumoto, and K. Imai, paper presented at ACS meeting in Miniature, Berkeley, Calif., December 1962; *Kobunshi Kagaku*, in press.

13. Sakurada, Y., M. Matsumoto, and T. Mochizuki, *Kobunshi Kagaku*, in press.

14. Sakurada, Y., et al., paper presented at the meeting on Macromolecular Chemistry, Nagoya, Japan, May 1962.

15. Danusso, F., and D. Sianesi, *Chim. Ind. (Milan)*, **40**, 450 (1958).

16. Natta, G., et al., *Gazz. Chim. Ital.*, **87**, 549 (1957).

17. Saltman, W. M., W. E. Gibbs, and J. Lal, *J. Am. Chem. Soc.*, **80**, 5615 (1958); H. E. Adams et al., *Ind. Eng. Chem.*, **50**, 1507 (1958).

18. Natta, G., *J. Polymer Sci.*, **34**, 24 (1959); Y. Sakurada, *Kobunshi Kagaku*, **18**, 496 (1961).

19. Groenewege, M. P., *Z. Physik. Chem. (Frankfurt)*, **18**, 147 (1958); M. L. Cooper and J. B. Rose, *J. Chem. Soc.*, **1959**, 795 (1959); M. Roha, et al., *J. Polymer Sci.*, **38**, 51 (1959); C. Beermann and H. Bestian, *Angew. Chem.*, **71**, 618 (1958); M. N. Berger and T. H. Boultbee, *J. Appl. Chem. (London)*, **9**, 490 (1959); H. Uelzmann, *J. Polymer Sci.*, **32**, 457 (1958); H. Uelzmann, *ibid.*, **37**, 561 (1959).

20. Yamazaki, N., *Kogyo Kagaku Zasshi*, **63**, 1085 (1960).

21. Carrick, W. L., et al., *J. Am. Chem. Soc.*, **82**, 3883 (1960).

Résumé

On fait la polymérisation de l'α-méthylstyrène en présence de AlE t₃–TiCl₄ à −78°C. L'activité du catalyseur et le degré de polymérisation sont influencés par le rapport molaire $AlR_3/TiCl_4$, par le mélange, par les conditions d'action du catalyseur et par la nature des solvants. On trouve que le rapport molaire $AlR_3/TiCl_4$ le plus avantageux est situé entre 1,0 et 1,2; à des rapports plus élevés que 2,0 la polymérisation n'a pas lieu. Pour avoir une activité suffisante avec de tels catalyseurs, on doit effectu er le mélange et le vieillissement du catalyseur en dessous de la température de chambre, et l'on doit garder l'état de valence du titane entre IV et III après la réaction entre $AlEt_3$ et $TiCl_4$. Par comparaison de ces résultats avec d'autres systèmes catalytiques on a établi que la réaction de polymérisation par ce système catalytique est cation ique et que les espèces actives sont les complexes intermédiaires $[(TiCl_3)^+, (AlEt_4Cl)^-]$ et le produit le réactions $AlEt_2Cl$. Ceci est confirmé par les courbes de distribution des poids moléculaires du poly-α-méthylstyrène obtenu, qui est obtenu par la méthode de fractionnement sur colonne. Les courbes de distribution ont deux maxima de poids moléculaire d'environ 5×10^4 et 65×10^4. Ceci suppose que deux sortes d'espèces actives sont présentes en accord avec l'hypothèse ci-dessus. Le poly-α-méthylstyrène obtenu possède une stéréorégularité très grande par rapport à celui préparé par les autres systèmes catalytiques.

Zusammenfassung

Die Polymerisation von α-Methylstyrol wurde in Gegenwart von $AlEt_3$–$TiCl_4$ bei −78°C. ausgeführt. Die Aktivität des Katalysators und der Polymerisationsgrad waren vom Molverhältnis $AlR_3/TiCl_4$, von den Mischungs- und Alterungsbedingungen des Katalysators und von der Art des Lösungsmittels abhängig. Als vorteilhaft erwies sich ein Molverhältnis $AlR_3/TiCl_4$ von 1,0 bis 1,2; bei einem höheren Verhältnis als 2,0 trat keine Polymerisation ein. Um eine genügende Atktivität dieses Katalysators zu erreichen, muss das Mischen und die Alterung des Katalysators unterhalb Raumtemperatur ausgeführt werden und der Valenzzustand des Titans muss nach der Reaktion zwischen $AlEt_3$ und $TiCl_4$ zwischen IV und III gehalten werden. Aus einem Vergleich der vorliegenden Ergebnisse mit denen an anderen Katalysatorsystemen kann man zu der Ansicht kommen, dass dieses Katalysatorsystem eine kationische Polymerisation hervorruft und dass die aktive Spezies der intermediäre Komplex $[(TiCl_3)^+(AlEt_2Cl)^-]$ und das Reaktionsprodukt $AlEt_2Cl$ sind. Diese Vermutung wird durch die durch Säulenfraktionierung erhaltenen Molekulargewichtsverteilungskurven des Poly-α-methylstyrols bestätigt. Die Verteilungskurven besitzen zwei Maxima, bei Molekulargewichten von etwa 5×10^4 und 65×10^4. Das spricht, in Übereinstimmung mit der aufgestellten Hypothese, dafür, dass zwei Arten von aktiver Spezies vorhanden sind. Das gebildete Poly-α-methylstyrol zeigt im Vergleich mit dem mit anderen Katalysatorsystemen erhaltenen eine überlegene Stereoregularität.

Synthesis of Styrene–Methyl Methacrylate Nonrandom Copolymers in Emulsion Systems with Cobalt-60 Gamma Radiation

G. J. K. ACRES* and F. L. DALTON, *Radiation Branch, Isotope Research Division, Wantage Research Laboratory (A.E.R.E.), Wantage, Berks, England*

Synopsis

Graft copolymers have been prepared by the irradiation of polymer latices swollen with monomer.   The latices used were prepared by radiation polymerization of emulsions to avoid the presence of initiator molecules in the second stage.   Latices of polystyrene swollen with methyl methacrylate and polymethyl methacrylate swollen with styrene have been used.   Polymerizations were followed dilatometrically and the dependence of polymerization rate on monomer concentration and radiation intensity obtained for both systems studied. Separation of copolymer from homopolymers has been attempted by thermal gradient elution chromatography; the method proved satisfactory when the solvent–nonsolvent system benzene–petroleum ether was used, but failed to give separations when benzene–methanol was used.   This failure is thought to be due to cosolution phenomena.

INTRODUCTION

Numerous techniques have been devised for the synthesis of block and graft copolymers,[1] the most common method involving the polymerization of a monomer in the presence of a preformed polymer.   Many initiating systems have been used, including high energy radiation.   Polymerization of a monomer present in the particles of a preformed latex has several advantages, notably the high speed of reaction characteristic of emulsion polymerizations and the possibility of using polymer–monomer combinations which are not completely miscible in bulk.   The present work is an attempt to obtain some quantitative data on two systems: a polystyrene latex swollen with methyl methacrylate and a polymethyl methacrylate latex swollen with styrene.   Since in the latter case, particularly, it is uncertain whether a block or a graft polymer, or a mixture of both, is formed, we have preferred the term "nonrandom copolymer" to describe our products.   The uncertainty of structure arises because of the range of possible reactions leading to nonrandom copolymer: direct radiation attack, attack of $H\cdot$ and $\cdot OH$ radicals on polymer chains, and various chain transfer reactions must all be considered.

* Present address: Chemistry Department, University of Nottingham, Nottingham, England.

The preparation of a nonrandom copolymer in an emulsion system involves two stages. Firstly, it is necessary to prepare a polymer latex which is free from soap micelles and unpolymerized monomer. This is achieved by using Co^{60} γ-rays to initiate polymerization in an emulsion where composition was such that all the soap was absorbed by the latex particles at 100% conversion. Secondly, a different monomer must be added to the latex to give a system of polymer particles swollen with monomer, together with droplets of monomer. It is the irradiation of this system, and the separation of the polymeric products formed, which is the subject of this communication.

EXPERIMENTAL

Radiation Facility

One of the standard 2K irradiation cells now in use at Wantage Research Laboratory was used for all the irradiations described in this work. The design and operation of the facility have been described previously.[2] Dosimetry measurements were made by means of the Fricke dosimeter $(G_{Fe^{3+}} = 15.6)$.

Materials

Methyl methacrylate and styrene (British Drug Houses Ltd.) were purified by several washings with a 5% aqueous solution of caustic soda, followed by washing with distilled water until all alkali had been removed. The monomers were then dried over anhydrous sodium sulfate, fractionated in an atmosphere of nitrogen under reduced pressure, and transferred to a vacuum line. After outgassing they were prepolymerized to about 10% conversion by means of a 125-w. Osira ultraviolet lamp and finally distilled *in vacuo*.

Preparation of Samples and Determination of Polymerization Rate

A monomer emulsion of known composition was prepared *in vacuo* in a breakseal tube by our usual method, which has been described previously,[3] and then placed in a thermostat bath at a fixed distance from the radiation source and irradiated until all the monomer had polymerized. To obtain reproducible results it was found necessary to outgas the initial soap solution thoroughly, and six cycles of freezing and thawing were used. It was also necessary after distilling monomer into the sample to thaw it at the temperature at which it was to be irradiated (21.5°C.).

The reaction vessel shown in Figure 1 enabled the second monomer to be mixed with this polymer latex *in vacuo* without freezing the latex. This vessel was connected to the vacuum line by means of a B14 cone and evacuated until a pressure of 10^{-4} mm. of mercury was obtained. A small bulb B, containing a nickel breaker was cooled in liquid nitrogen, and a known volume of the previously purified second monomer distilled into it from a
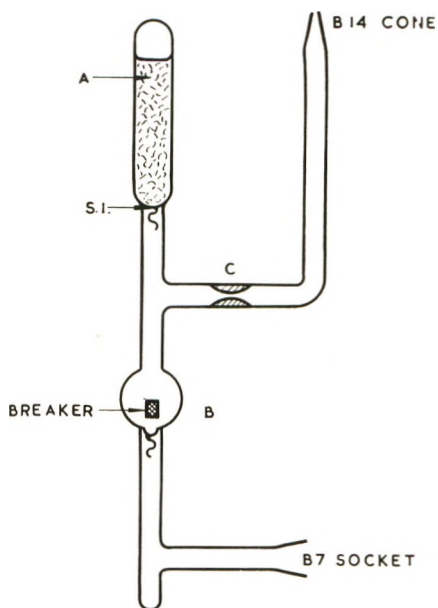
Fig. 1. Reaction vessel.

graduated buret.   Great care was necessary during this operation to avoid freezing the polymer latex in bulb A since, if frozen, the latex coagulated and could not be re-emulsified on thawing.   After distilling in the monomer the vessel was exposed to the pumps, sealed at the constriction C, and placed in a thermostat bath at 21.5°C.   When the contents of the vessel had reached 21.5°C. the breakseal S1 was opened and the contents of bulbs A and B mixed by shaking until a stable polymer–monomer latex was obtained.   The reaction vessel was then connected to a mercury recording dilatometer, details of which have been published previously.[4]   The dilatometer was placed in position in a thermostat bath surrounding the source tube, connected to the recording apparatus, and irradiated.   Immediately after irradiation the polymer was isolated by precipitating the reaction products into a twentyfold excess of methanol.   The polymer was filtered and dried at 60°C. *in vacuo.*

Some experiments, involving latices in which styrene had been added to polymethyl methacrylate, were carried out in the presence of air, and in this case the technique was slightly changed.   The polymethyl methacrylate latex was prepared *in vacuo* as described above, then opened to the atmosphere, and a known volume of styrene added.   The mixture was shaken until a stable latex formed.   This latex was introduced into the modified dilatometer shown in Figure 2.   With reservoir R2 filled with mercury, tap T2 was opened and the mercury allowed to flow into the dilatometer (which is not evacuated) until it reached the level B.   A known volume of latex was then introduced into the dilatometer bulb through tap T2 by means of a hypodermic syringe.   Mercury was run into the dilatometer from R2 until
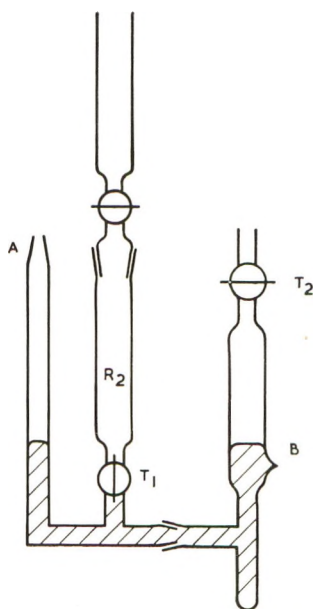
Fig. 2. Modified dilatometer.

the latex was forced into the bore of tap T2, which was then closed. A capillary tube was connected to A, and by applying pressure above R2 and opening T1 mercury was forced through A into the capillary. Tap T1 was closed and the dilatometer immersed in a water thermostat bath and irradiated as before.

Separation of Reaction Products

Early attempts to separate the copolymers produced from homopolymer with which they might be mixed were made by means of the fractional precipitation technique described by Ceresa.[5] These authors used the method to separate polystyrene–polymethyl methacrylate copolymers prepared by cold mastication. Results obtained with this technique were not entirely satisfactory, however, as the method is a nonequilibrium one and results varied with the time allowed between addition of nonsolvent and separation of the phases. Considerable tailing, due to solution held on the precipitate, was also experienced. More reproducible separations were obtained by use of the gradient elution technique described by Williams,[6] and the separations to be described were obtained using this technique. Our column was basically that described by Williams, though several modifications were made to improve the performance. A diagram of our apparatus is shown in Figure 3. The glass column C, 35 mm. long and 24 mm. in outside diameter, was packed with glass beads in the form of a slurry in nonsolvent. The glass beads, Ballotini, average diameter 0.1 mm. were supplied by the English Glass Company. The beads were supported in the
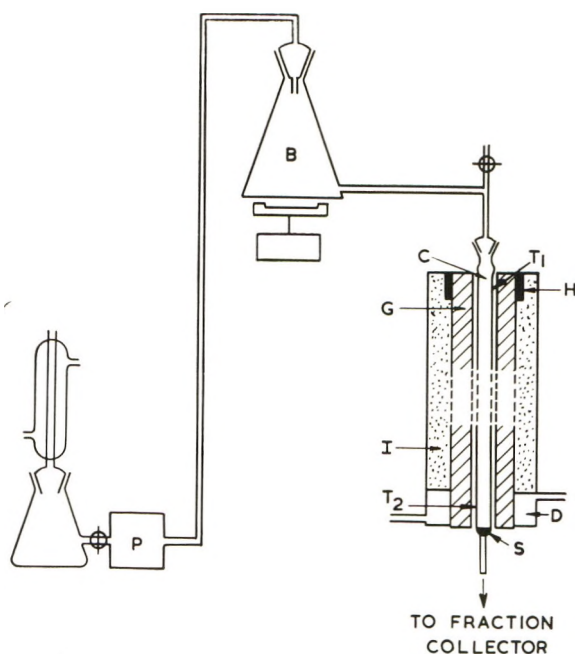
Fig. 3. Gradient elution apparatus.

column by a wad of silica wool S.   The polymer mixture was dissolved in benzene (ca. 0.5%), 20 g. of ballotini added, and the solution evaporated to dryness in a hot air stream with constant stirring.   The beads, now coated with a thin film of polymer, were poured on to the top of the column as a slurry in the nonsolvent and filled a distance of 4.5 cm. along its length, the approximate length of the heating element H at the top of the column. The column was jacketed with an aluminum block G, 37 cm. long and 5 cm. in diameter with a $2^{1}/_{2}$-cm. diameter hole drilled through its center.   The top of the jacket was heated by a 60-w. circular heating element H; the bottom was cooled by means of a reservoir D, through which water was pumped.   The aluminum jacket was well insulated so that a linear temperature gradient was obtained down the column.   The temperature at the top and bottom of the column was measured by means of thermocouples T1 and T2.   The temperature at the top of the column was controlled by means of a variable transformer fed from a constant voltage supply, and the temperature at the bottom of the column by a thermostatically controlled refrigerated tank from which water was circulated through the reservoir D.   The solvent gradient was supplied by means of the pump P and the mixing vessel B.   This pump (Distillers Co. Ltd.) could be set to deliver any required volume of liquid from 0 to 60 ml./hr. and was used to force solvent into the mixing vessel and to control the rate of flow of liquid through the apparatus.   All connections were made by glass cones containing neoprene gaskets and spring-loaded.   To avoid any dislocation of

the packing in the column by air being expelled from the solvent on heating, all nonsolvents were thoroughly boiled immediately prior to use, and pump P was supplied from a refluxing reservoir of solvent.   In each experiment thirty fractions, each weighing 20 g., were collected in a fraction collector. The weight of polymer in each fraction was determined by transferring the solution from each tube into a small, flat-bottomed sample tube of known weight.   The solution was then evaporated to dryness, the tube and its contents dried *in vacuo* at 60°C., and the tube reweighed to find the weight of polymer.   This technique was found to give satisfactory results, although the use of redistilled solvents and precipitants was essential.   Slight pressurization of the column caused by the micro pump was a few centimeters only and varied with the viscosity of the liquid emerging from the bottom of the column.   However, the throughput from the column was constant, whereas using the gravity feed of Williams with our extremely high molecular weight polymers, flow tended to stop when a polymer peak was reached.

RESULTS

Rate of Polymerization Measurements

The following recipes were taken as standard in the first stage of the preparation of nonrandom copolymers.

(*1*)   Methyl methacrylate recipe for the polymethyl methacrylate–styrene nonrandom copolymer was methyl methacrylate, 1.25 g.; water. 4.5 g.; Manoxal OT, 0.0625 g.; temperature, 21.5°C.; radiation intensity, 4.2 × 10⁴ rads/hr.; time for 100% conversion, 90 min.

(*2*)   Styrene recipe for the polystyrene–methyl methacrylate nonrandom copolymer was styrene 0.715 g.; water, 4.5 g.; Manoxal OT, 0.125 g.; temperature, 21.5°C.; radiation intensity, 4.2 × 10⁴ rads/hr.; time for 100% conversion, 145 min.

(By a polymethyl methacrylate–styrene nonrandom copolymer is meant a nonrandom copolymer prepared from a polymethyl methacrylate latex with styrene as the added second monomer, while a polystyrene–methyl methacrylate nonrandom copolymer is a nonrandom copolymer prepared from a polystyrene latex with methyl methacrylate as the added second monomer.   This terminology will be used throughout this paper.)

Various rates of polymerization may be calculated from conversion verus time curves.   In this work, the rate at about 20–60% conversion is of most interest, since over this range the rate of polymerization is proportional to the number of particles *N* and it is this rate which is measured in all the subsequent experiments.

Polystyrene–Methyl Methacrylate Latex System

a. Influence of Initial Methyl Methacrylate Concentration on the Rate of Polymerization.   The standard polystyrene latex was used as the basis of these experiments, and the effect on the rate of polymerization of vary-
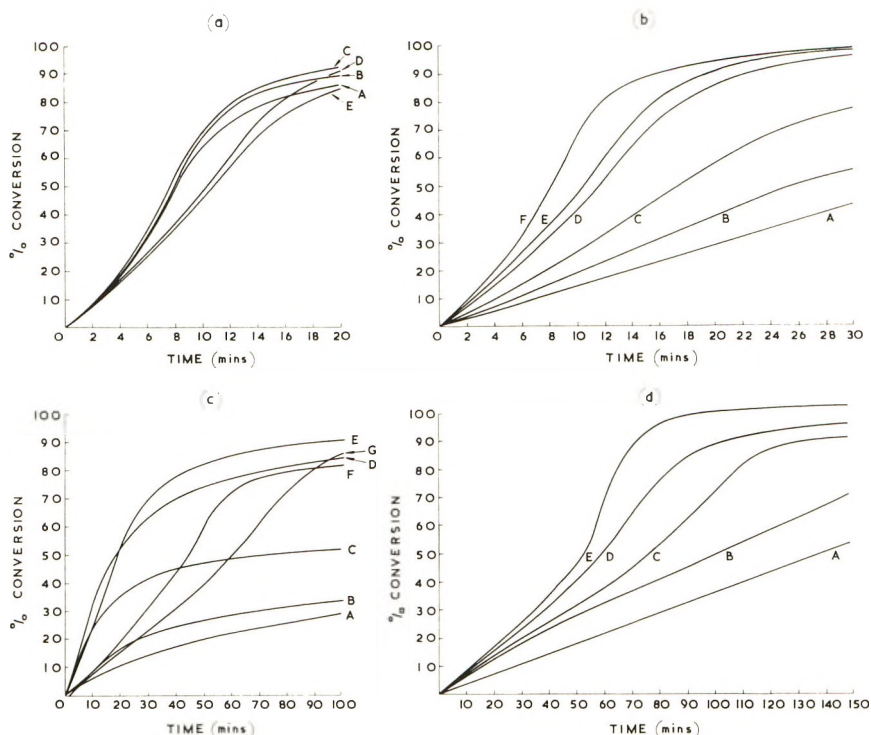
Fig. 4. (a) Conversion vs. time curves for polystyrene–methyl methacrylate latices with varying initial monomer concentration: (A) 1.20 moles/l.; (B) 1.62 moles/l.; (C) 2.40 moles/l.; (D) 3.24 moles/l.; (E) 4.85 moles/l. Intensity 4.2 × 10⁴ rads/hr. (b) Conversion vs. time curves for polystyrene–methyl methacrylate latices irradiated at various intensities: (A) 10³ rads/hr.; (B) 1.7 × 10³ rads/hr.; (C) 4.0 × 10³ rads/hr.; (D) 1.6 × 10⁴ rads/hr.; (E) 4.2 × 10⁴ rads/hr.; (F) 9.0 × 10⁴ rads/hr. (c) Conversion vs. time curves for polymethyl methacrylate–styrene latices with varying initial monomer concentration: (A) 0.63 moles/l.; (B) 0.75 moles/l.; (C) 1.01 moles/l.; (D) 1.26 moles/l.; (E) 1.89 moles/l.; (F) 2.52 moles/l.; (G) 3.24 moles/l. Intensity 4.2 × 10⁴ rads/hr. (d) Conversion vs. time curves for polymethyl methacrylate–styrene latices irradiated at various intensities: (A) 10³ rads/hr.; (B) 3.5 × 10³ rad/hr.; (C) 1.8 × 10⁴ rads/hr.; (D) 4.2 × 10⁴ rads/hr.; (E) 2 × 10⁵ rads/hr.

ing the methyl methacrylate concentration between 1.2 and 4.85 mole/l. was studied at a radiation intensity of 4.2 × 10⁴ rads/hr. The conversion versus time curves obtained are shown in Figure 4a, and a log/log plot of the rate versus initial methyl methacrylate concentration is given in Figure 5a. Over the range 1.2–2.4 mole/l., the rate of polymerization is proportional to the initial monomer concentration. Above 2.4 mole/l., the polymerization rate approaches independence of initial monomer concentration with increasing concentration.

b. Influence of Radiation Intensity on the Rate of Polymerization. The effect was studied on a 1:2 polystyrene–methyl methacrylate latex at 21.5°C. The conversion versus time curves obtained are shown in Figure 4b, and a log/log plot of the rate of polymerization versus the radiation intensity is
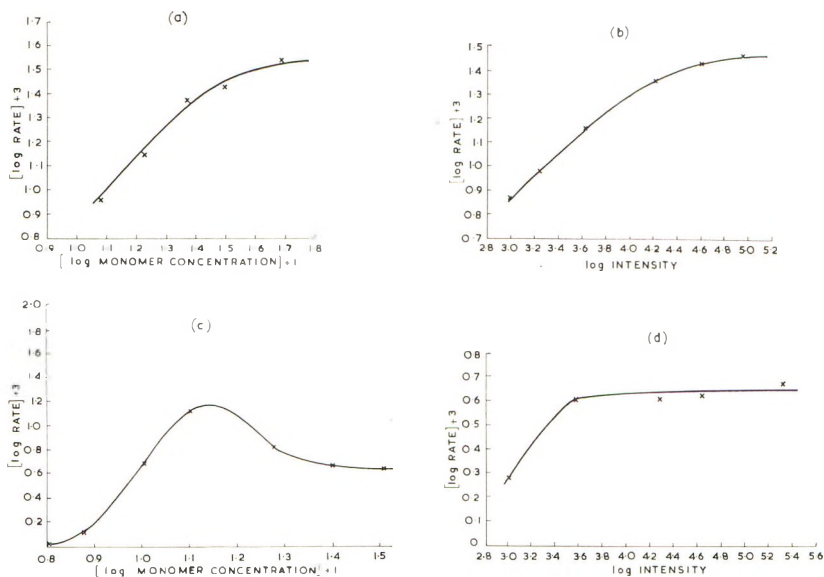
Fig. 5. (a) Influence of monomer concentration on rate of polymerization: polystyrene–methyl methacrylate latex; (b) influence of radiation intensity on rate of polymerization: polystyrene–methyl methacrylate latex; (c) influence of monomer concentration on rate of polymerization: polymethyl methacrylate–styrene latex; (d) influence of radiation intensity on rate of polymerization: polymethyl methacrylate–styrene latex.

given in Figure 5b.   Between 10^3 and 4×10^3 rads/hr., the polymerization rate is proportional the square root of radiation intensity.   Above 4×10^3 rads/hr., the rate approaches independence of intensity as intensity increases.

Polymethyl Methacrylate–Styrene Latex System

In preliminary experiments the second stage of this reaction was carried out *in vacuo*.   However, the results were not reproducible due to polymerization of the added styrene prior to irradiation.   To overcome this problem, the styrene was added to the polymethyl methacrylate latex in the presence of air, though the initial methyl methacrylate latex was prepared and polymerized in the usual way.

a. Influence of the Initial Styrene Concentration of the Rate of Polymerization.   The standard polymethyl methacrylate latex was used in these experiments, and the effects of the initial styrene concentration on the rate of polymerization was studied between 0.63 and 3.24 moles/l. at an intensity of 4.2×10^4 rads/hr., the temperature being 21.5°C.   The conversion versus time curves are shown in Figure 4c and a log/log plot of the rate versus initial styrene concentration is given in Figure 5c.   This latter curve exhibits a maximum at a styrene concentration of 1.4 moles/l.

Below this concentration the rate falls rapidly with decreasing styrene concentration, while above 1.4 moles/l. the rate decreases with increasing styrene concentration.

b. Influence of Intensity on the Rate of Polymerization.   The effect was studied on a polymethyl methacrylate styrene latex containing 2.52 moles/l. of styrene at 21.5°C.   The conversion versus time curves are shown in Figure 4d, and a log/log plot of rate versus radiation intensity is shown in Figure 5d.   Above an intensity of 4×10^3 rads/hr. the rate is virtually independent of intensity, increasing only slightly over a fifty-fold rise in intensity.   Below 4×10^3 rads/hr. the rate decreases with decreasing intensity.

Fractionation Experiments

Separation of reaction products was carried out by gradient elution chromatography.   Optimum separation conditions were found by use of equal weight mixtures of polystyrene and polymethyl methacrylate. Benzene–methanol and benzene–petroleum ether (boiling point 100–120°C.) were used as solvent–nonsolvent systems.   The effect on the efficiency of separation of the volume of the mixing vessel, the amount of polymer loaded on to the column and the flow rate through the column were investigated.   A temperature gradient of 40 to 15°C. was used throughout the experiments; the lower limit was imposed by the viscosity of the solution leaving the column being extremely high due to the high molecular weight of the polymers used.   The effect of the volume of the mixing vessel can be readily calculated by use of the equation $X = V (1 - \exp \{ - v/V \})$, where V is the initial volume of nonsolvent in the mixing vessel and X the fraction by volume of solvent in the mixing vessel after v milliliters of mixture have been run off from this vessel.   Since, under ideal conditions, a particular polymer is eluted from the column over a specific range of solvent/nonsolvent ratios, calculated composition versus fraction number curves may be used to give some idea of the separation obtained with a particular mixture of polymers, using different mixing vessel volumes V, when the range of solvent/nonsolvent ratios over which the polymer is eluted is known.   Conversely, from such curves this range may be determined.   It was confirmed by experiment that a 500-ml. mixing vessel charged with 400 ml. of nonsolvent and 100 ml. of solvent gave good separations.   The optimum loading of the column was found to be 0.1 g. of polymer, since the use of smaller amounts gave little improvement in separation, while if larger amounts were used the quality of the separation deteriorated rapidly.   This amount of polymer is considerably less than that used by Williams and by other workers, but again the extremely high molecular weight of our polymers must be borne in mind.   Using these conditions on the column, it was found possible to use a flow rate of liquid through the column of 30 ml./hr.   Although this rate appears rather high, use of lower flow rates did not improve the separation.

Polymethyl Methacrylate–Styrene Latex System

The composition of the latex used to study the influence of radiation intensity on the composition of the reaction mixture produced was polymethyl methacrylate, 0.982 g.; styrene, 1.25 g.; 1.39% Manoxal OT solution, 3.5 ml.; temperature, 21.5°C.

The polymer monomer latex was irradiated to maximum conversion, irradiation intensities of 2×10^5, 4.2×10^4, and 10^3 rads/hr. being used.
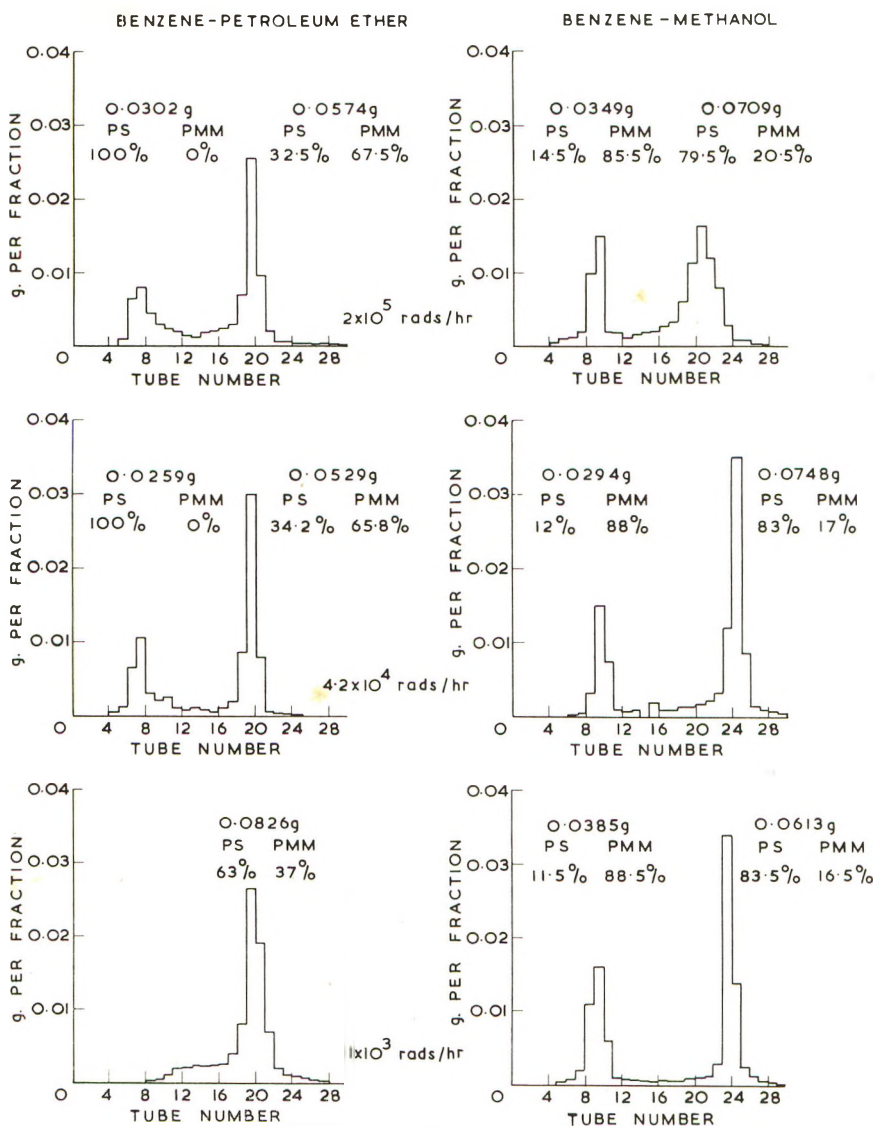

Fig. 6. Elution chromatograms showing the effect of varying radiation intensity on the composition of the reaction product: polymethyl methacrylate–styrene system.
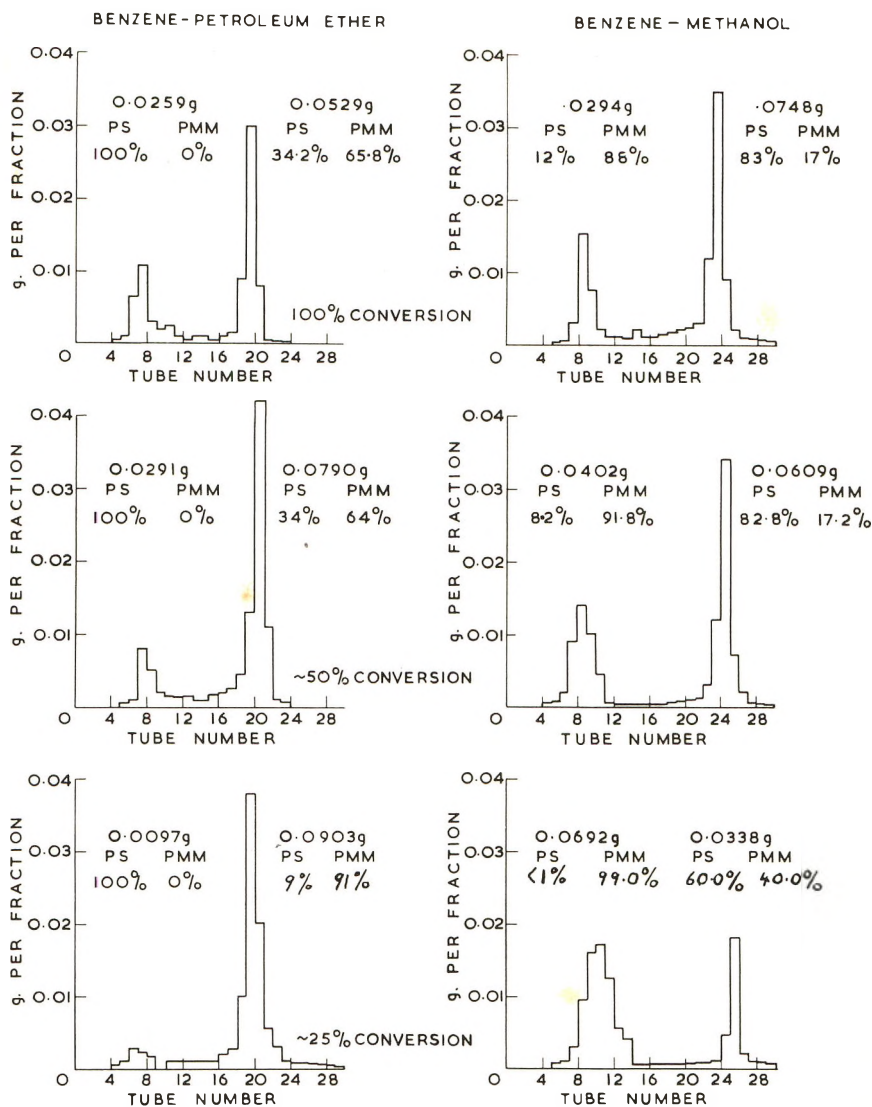
Fig. 7. Elution chromatograms showing the variation of product composition with monomer conversion: polymethyl methacrylate–styrene system.

The gradient elution chromatograms of the mixture produced at these intensities are shown in Figure 6.

The same latex composition was used to investigate the variation of the composition of the polymeric products with conversion, and the chromatograms are shown in Figure 7.

The effect of initial styrene concentration was studied with the same recipe and two other recipes in which the amount of styrene was 0.45 g. and 0.225 g., all other conditions being identical. The chromatograms obtained are shown in Figure 8.

Fig. 8. Elution chromatograms showing the variation of product composition with initial monomer concentration: polymethyl methacrylate–styrene system.

Polystyrene–Methyl Methacrylate Latex System

The composition of the latex used to study effect of radiation intensity on the composition of the reaction mixture was polystyrene, 0.715 g.; methyl methacrylate, 1.430 g.; 2.87% Manoxal OT solution, 4.5 ml.; temperature, 21.5°C.
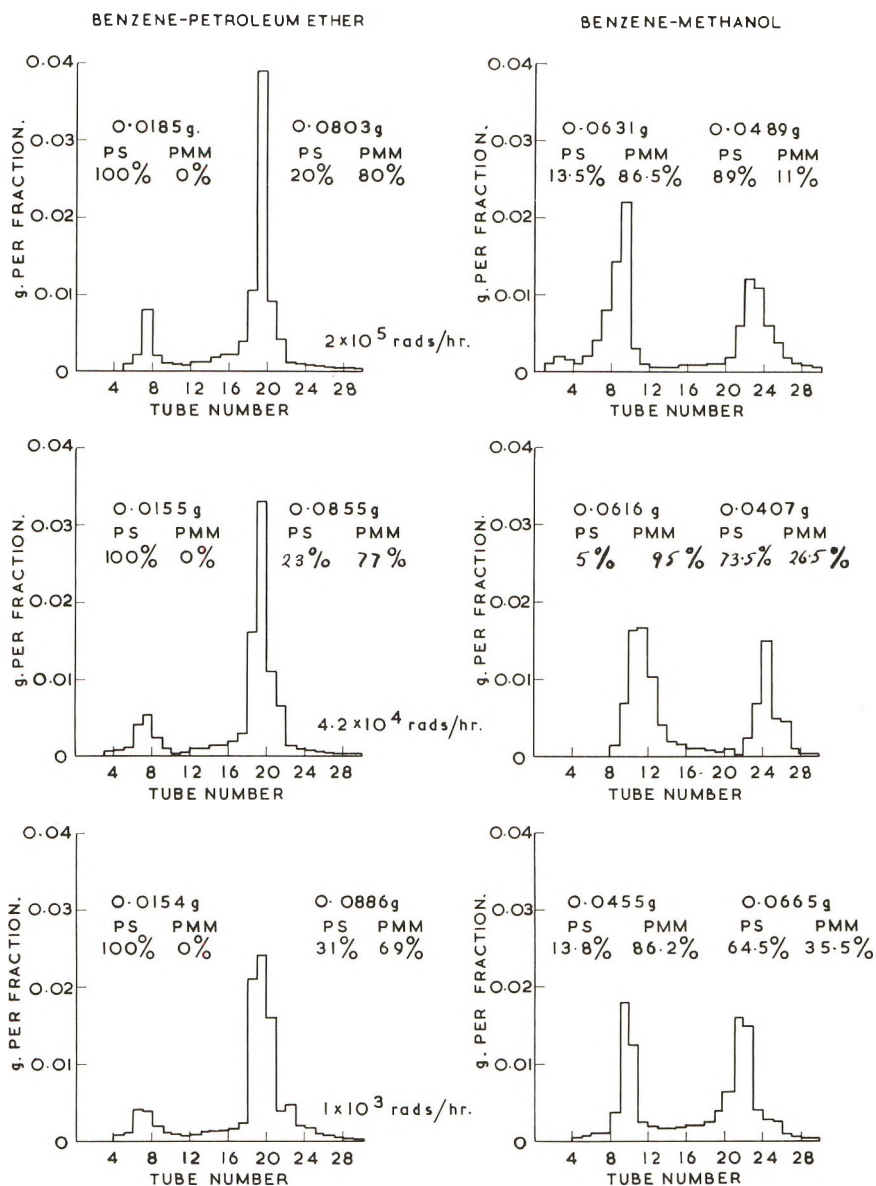
Fig. 9. Elution chromatograms showing the effect of varying radiation intensity on the composition of the reaction product:polystyrene–methyl methacrylate system.

The latices were irradiated to maximum conversion at intensities of 2×10^5, 4.2×10^4, and 10^3 rads/hr. The elution chromatograms of the products are shown in Figure 9.

The effect of initial methyl methacrylate concentration was studied at an intensity of 4.2×10^4 rads/hr. with the use of the above recipe and two others in which the amount of methyl methacrylate was 1.07 and 0.36 g.,
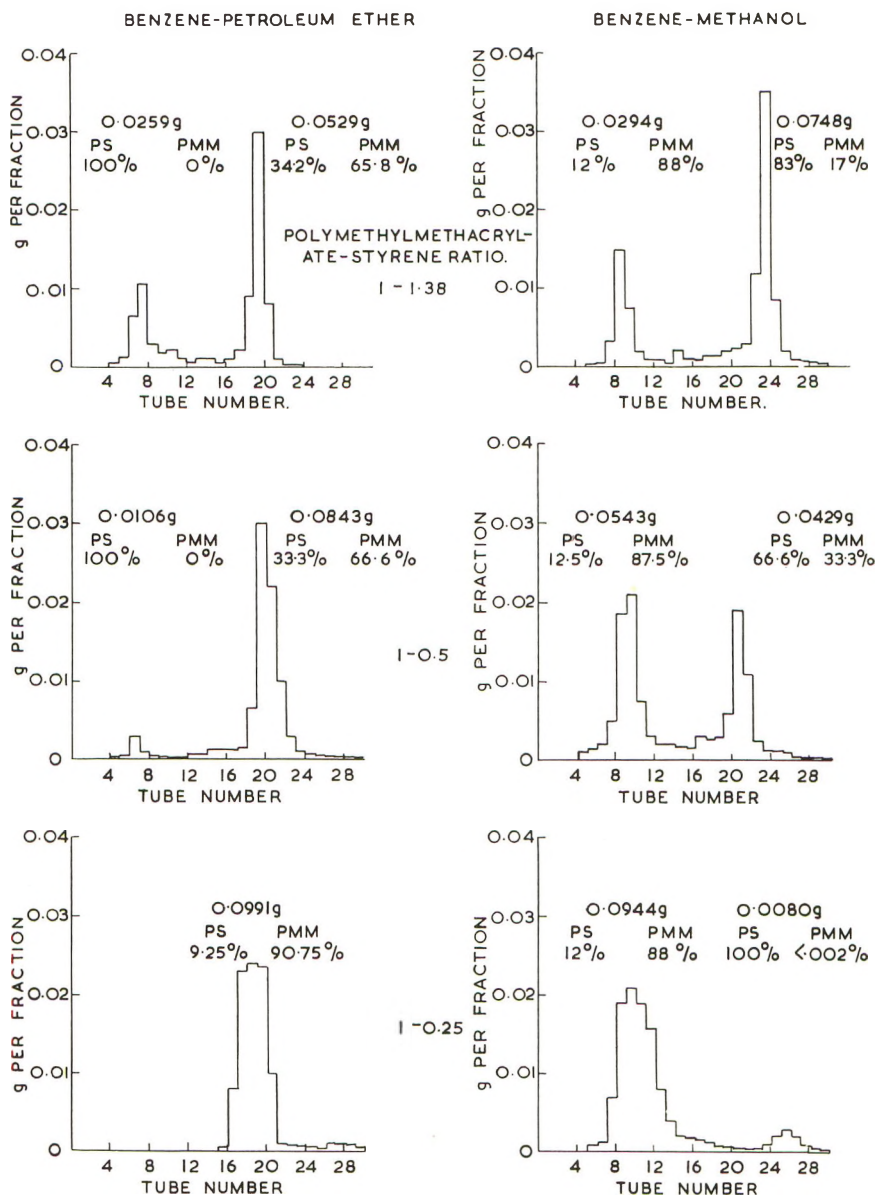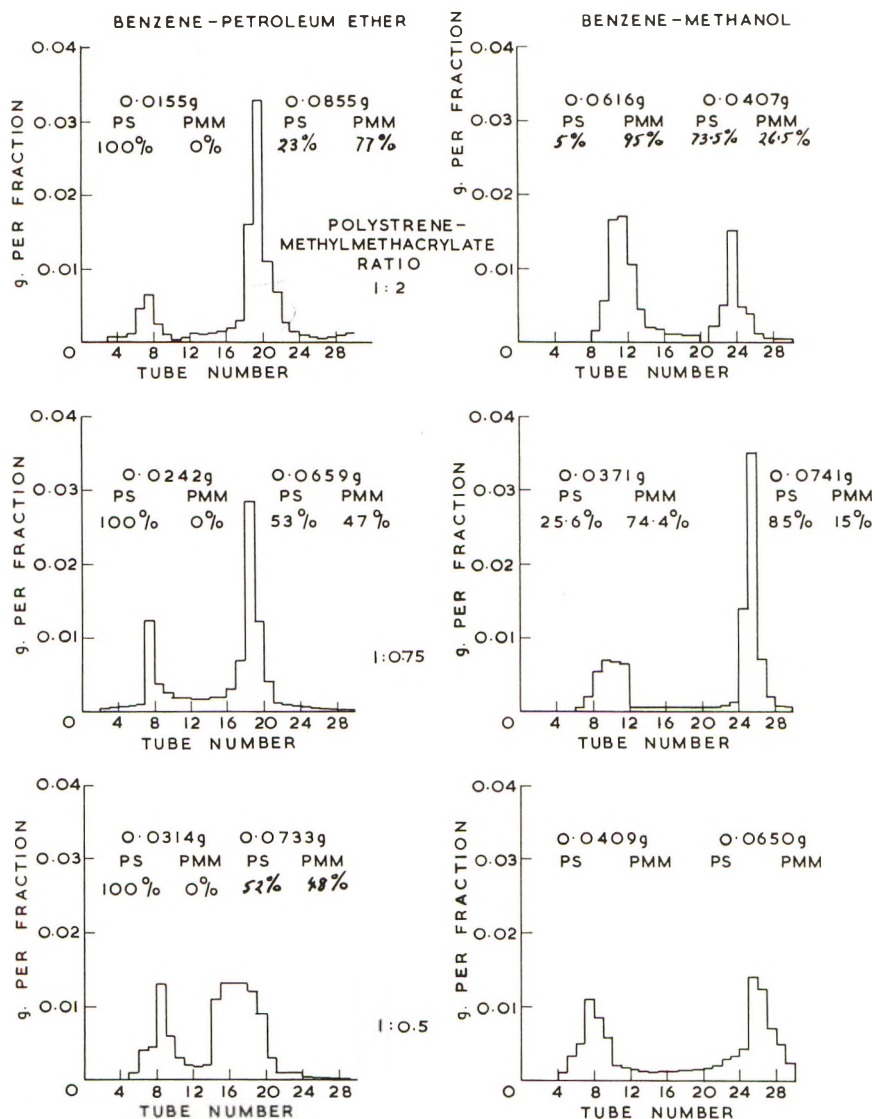
Fig. 10. Elution chromatograms showing the variation of product composition with initial monomer concentration: polystyrene–methyl methacrylate system.

all other factors being identical.   The chromatograms obtained are shown in Figure 10.

DISCUSSION

In the polystyrene–methyl methacrylate latex system, the added methyl methacrylate did not polymerize until irradiated if the necessary precautions were taken, whereas in the polymethyl methacrylate–styrene latex prepared *in vacuo* the added styrene polymerized slowly prior to irradiation.

This prepolymerization was stopped by adding the styrene to the polymethyl methacrylate latex in air. The reason for this prepolymerization is not known, but it is probably due to some initiating species produced in the polymethyl methacrylate latex during the first irradiation, and it is relevant to notice that a much larger concentration of trapped radicals is produced in polymethyl methacrylate by gamma radiation than is produced in polystyrene. No induction period was observed in either monomer–polymer system. This is somewhat surprising in the case of the polymethyl methacrylate–styrene system, the second stage of which was not carried out *in vacuo*. A polystyrene–methyl methacrylate latex was therefore prepared in the same way, that is, the second stage was carried out in the presence of oxygen. At a radiation intensity of 4.2×10^4 rads/hr., a 45-min. induction period was observed, and it is interesting to notice that after this induction period the conversion versus time curve was identical to the curve obtained when the polymerization was carried out *in vacuo*.

Some of the conversion versus time curves shown in Figure 4 show a Trommsdorff effect similar to that observed in the gamma ray-initiated emulsion polymerization of methyl methacrylate.[3] The effect is found only at high monomer concentrations and high radiation intensities and increases with increasing monomer concentration and radiation intensity. We have previously discussed the occurrence of the Trommsdorff effect in emulsion polymerization and the influence of the monomer concentration and radiation intensity on it,[3] and our present results are in accord with our earlier conclusions.

If a monomer is added to a polymer latex in which there are no free micelles, the monomer is absorbed by the polymer particle, and if excess is added a separate monomer phase will be formed. On irradiation, polymerization proceeds in the polymer–monomer particles which may be supplied with monomer from the monomer phase by diffusion through the water. Since no micelles are present, no new particles are formed. Thus, the polymerization rate should not increase with increasing initial monomer concentration, since it has been shown by Smith and Ewart[7] that when the average number of radicals per particle $\bar{n}$ equals $^1/_2$, the rate of polymerization depends only on the number of particles, which is constant. Thus, as in the case of a simple emulsion polymerization, the rate would be expected to increase with increasing monomer concentration until a critical concentration is reached, at which point the rate would become independent of monomer concentration. It may be seen from the results that this simple scheme does not apply to either polymer–monomer latex system. It is also apparent that the influence of the initial monomer concentration on the rate of polymerization is markedly different in the two systems.

Radiation intensity also affects the rate in a different manner in each of the two systems. The Smith-Ewart theory predicts that if $\bar{n}$ equals $^1/_2$ and the monomer concentration in the particles remains constant, the rate of polymerization depends only on the total number of particles N; since N remains constant in the polymer monomer latices used, the rate of poly-

merization should be independent of the radiation intensity. In the poly-methyl methacrylate–styrene latex system this relationship is found to apply over the range 4×10^3–2×10^5 rads/hr., but the rate is not inde-pendent of intensity in the polystyrene–methyl methacrylate latex system. It is thought that the divergence from Smith-Ewart kinetics may be ac-counted for by considering the composition of the latex and the particle size. The Smith-Ewart theory assumes that $\bar{n} = \frac{1}{2}$, and that the time for which two radicals coexist in a particle, δt, is negligible compared with the time t_1 for which a single radical exists in a particle. In our case, reac-tion takes place in two stages, and considerably larger particles appear than in a simple emulsion polymerization. With increasing particle size the time for which two growing radicals can exist in a particle increases, and this rise in δt is effectively a retardation of the termination reaction occurring independently of the Trommsdorff effect. If δt is no longer negligible compared with t_1, $\bar{n}$ is no longer equal to $\frac{1}{2}$. The effect of an increase in the number of radicals per particle with increasing particle size has been reported in the literature,[8,9] and is found to be especially important in experiments with seed latices and in the competitive growth method. The effect may be explained qualitatively by the simple equation deduced by Gerrens:[10] $\bar{n} = \frac{1}{2} + (\delta t/t_1)$. It will be seen that $\bar{n}$ increases with increas-ing δt and decreasing t_1. In our case, increasing monomer concentration will lead to larger particles and hence an increase in δt, while an increase in the radiation intensity will lead to a decrease in t_1. If δt can increase until it is greater than or equal to t_1, this simple equation becomes inade-quate and it is necessary to use Stockmeyer's[11] deriviation which is appli-cable for all values of $\bar{n}$, or the less complex Roe and Brass[12] approximation which may be used if $\bar{n}$ is less than six. From the results in the polymethyl methacrylate–styrene system irradiated at an intensity greater than 4×10^3 rads/hr. (Fig. 5d), it will be seen that the rate is independent of in-tensity and therefore $\bar{n} = \frac{1}{2}$. One would, therefore, expect the rate of polymerization to be independent of the initial monomer concentration, but it may be seen from Figure 5c that this is not the case. As the initial concentration of styrene in the polymethyl methacrylate–styrene latex increases from zero, it would be expected that the rate of polymerization would increase until the activity of the styrene in the polymer–monomer particles was constant, after which the rate of polymerization would remain constant. The observed falling off of rate with increasing styrene con-centration above the maximum value is probably due to energy transfer processes. Turner,[13] who irradiated rubber–styrene mixtures, has re-ported a decrease in polymerization rate with increasing styrene concentra-tion, and this effect was considered due to energy transfer, since if energy transfer can take place between the polymethyl methacrylate and the styrene in the polymer–monomer particles and/or between the aqueous phase and the styrene, then the radical concentration and hence the rate of polymerization will decrease with increasing styrene concentration.

In the case of the polystyrene–methyl methacrylate latex, the poly-

merization rate increases with increasing radiation intensity, and hence $\bar{n}$ is not equal to $1/2$, and one would not expect the rate of polymerization to be independent of the initial monomer concentration. Although energy transfer to the polystyrene may occur in this system, no maximum is obtained in the log rate versus log monomer concentration curve, since the amount of polystyrene and water in the latex is constant, and the rate will increase steadily with increasing monomer concentration.

Gradient elution chromatography was used in an attempt to determine the composition of the homopolymer copolymer mixtures produced at various radiation intensities and initial monomer concentrations. The results were shown in Figures 6–10, and the principal features are as follows. In no case were three separate fractions corresponding to polymethyl methacrylate, a nonrandom copolymer and polystyrene, obtained. With one exception (Fig. 7; ca. 25% conversion) no free polymethyl methacrylate was recovered from either solvent–nonsolvent system from any of the mixtures studied. Although the benzene–petroleum ether system will separate a pure polystyrene fraction, no pure fraction is eluted from the same mixture with benzene–methanol. When some of the mixtures are eluted by benzene–petroleum ether, only one fraction is obtained at a point midway between pure polystyrene and pure polymethyl methacrylate, and one might deduce that 100% nonrandom copolymer had been formed. However, if the same mixture is eluted with the benzene–methanol system, two fractions are obtained, both containing polystyrene and polymethyl methacrylate, one containing a greater percentage of polymethyl than polystyrene and the other a greater percentage of polystyrene than polymethyl methacrylate (see Figs. 6 and 8). The failure of the benzene–methanol system to elute a pure polystyrene fraction from a reaction mixture which is known to contain one is surprising, since the system will quite clearly separate a mixture of the two homopolymers. It may be that the effect is due to the occurrence of cosolution phenomena, and if this is indeed the case, then the benzene–methanol system is not a suitable one for the separation of our copolymers. Similar behavior has been noticed in the separation of cellulose acetate–methyl methacrylate copolymers with the use of an acetone–water system.[14] It may be noted, however, that in the synthesis of rubber–methyl methacrylate nonrandom copolymers by gamma radiation in emulsion, it was found impossible to separate homopolymer copolymer mixtures by fractional precipitation,[15] and molecular weight studies on polymethyl methacrylate chains which were removed from rubber by ozonolysis showed two distinct fractions, one of high molecular weight and the other of low molecular weight.[16] If a similar phenomenon occurs in our system, it could be that copolymer having low molecular weight chains of one component is not separated from the homopolymer by this system.

In considering the influence of reaction conditions on the composition of the homopolymer–copolymer reaction mixtures, we shall ignore the results obtained with the benzene–methanol system and concentrate our attention

on the results obtained with the benzene–petroleum ether system. As the amount of free polymethyl methacrylate, and hence, the amount of non-random copolymer in the reaction mixture, has not been determined by our technique, a complete analysis of either polymer–monomer system is not possible unless the complete absence of free polymethyl methacrylate is assumed. In both polymer–monomer latex systems the amount of free polystyrene in the reaction product is found to decrease with a decrease in the radiation intensity, and it is clear that a low radiation intensity favors the formation of graft polymer. Variation of the concentration of monomer in the latex shows that if styrene is added to a polymethyl methacrylate latex the ratio copolymeric styrene:polystyrene homopolymer decreases with increasing styrene concentration, while if methyl methacrylate is added to a polystyrene latex the ratio copolymeric styrene:polystyrene homopolymer remains constant from a polymer:monomer ratio of 1:2 to one of 1:0.75, while the ratio is somewhat lower if the monomer:polymer ratio is 1:0.5. In reaction mixtures from polymethyl methacrylate–styrene latices with a high initial styrene concentration 100% polymer recovery was not obtained when the reaction mixture was eluted with benzene in the benzene–petroleum ether system. By passing pure benzene through the column after the elution, a small third fraction was obtained containing both polystyrene and polymethyl methacrylate. It is thought that this effect is due to a small amount of crosslinking which will be favored by high concentrations of styrene. Such crosslinked material would be less soluble than the rest of the reaction mixture and, hence, is eluted only by pure benzene. Figure 7 shows chromatograms obtained with the poly-methyl methacrylate–styrene system when the reaction is continued to various conversions. It can be seen that the ratio of copolymerized styrene:styrene homopolymer falls only slightly with conversion between 25 and 50% conversion, while it is markedly lower at 100% conversion.

Although considerably more information could be obtained if a more successful separation procedure could be found, our results show that in both polymer–monomer systems studied it is necessary to use a low radiation intensity to ensure a high yield of nonrandom copolymer. The information obtained on the effect of variation of added monomer is incomplete due to the partial failure of the separation technique, and it is difficult to offer general conclusions. Grafting efficiency appears to fall off at higher conversions in the polymethyl methacrylate–styrene system, probably due to the relative inactivity of the polystyrene chains formed earlier in the reaction.

Exact calculation of the amount of copolymer formed under various experimental conditions has been carried out by Voeks[17] for homogeneous systems of polymer dissolved in monomer. Such calculations appear impractical in our case, since conversions are carried to 100% and also initiation occurs not only from the water phase but by direct action in the particles, if the latter are large enough to allow more than one radical to exist

within them for a significant time: it is, however, interesting to note that the trends found in this work are similar to those found by Voeks.

Our experience with the benzene–methanol system suggests that considerable care is necessary selecting a solvent precipitant system for elution chromatography, and it seems not unlikely that similar considerations would apply if separation by fractional precipitation methods were attempted. The whole question of methods of separating nonrandom copolymers from their constituent homopolymers would seem to merit a more critical study than has yet been reported.

References

1. See, for example, Burlant, W. J., and Hoffman, A. S., *Block and Graft Polymers*, Reinhold, New York, 1960.

2. Dove, D., G. S. Murray, and R. Roberts, U.N.E.S.C.O. Int. Conf. on Radiation in Scientific Research Unesco/NS/RIC/19.

3. Acres, G. J. K., and F. L. Dalton, A.E.R.E./R3420.

4. Acres, G. J. K., and F. L. Dalton, Nature, **184**, 335 (1959).

5. Ceresa, R. J., in *Techniques of Polymer Characterization*, P. Allen, Ed., Butterworths, London, 1959.

6. Baker, C. A., and R. J. P. Williams, *J. Chem. Soc.*, **456**, 2353 (1956).

7. Smith. W. V., and R. P. Ewart, *J. Chem. Phys.*, **16**, 592 (1948).

8. Smith, W. V., *J. Am. Chem. Soc.*, **70**, 3695 (1948).

9. Bradford, E. B., and J. W. Vanderhoff, *J. Colloid Sci.*, **11**, 135 (1956).

10. Gerrens, H., *Z. Elektrochem.*, **60**, 400 (1956).

11. Stockmeyer, W. H., *J. Polymer Sci.*, **24**, 314 (1957).

12. Roe, C. P., and P. D. Brass, *J. Polymer Sci.*, **24**, 401 (1957).

13. Turner, D. T., *J. Polymer Sci.*, **35**, 17 (1959).

14. Dalton, F. L., unpublished results.

15. Merrett, F. M., *Trans. Faraday Soc.*, **50**, 759 (1954).

16. Kobryner, W., and A. Bandaret, *J. Polymer Sci.*, **35**, 381 (1959).

17. Voeks, J. F., *J. Polymer Sci.*, **18**, 123 (1955).

Résumé

On a préparé des copolymères greffés par irradiation de réseaux de polymére gonflés dans le monomère. Les réseaux utilisés ont été préparés au moyen d'une polymérisation par radiation afin d'éviter la présence de molécules d'initiateur lors du second processus. On s'est servi de réseaux de polystyrène gonflé dans le méthacrylate de méthyle et de réseaux de polyméthyacrylate de méthyle gonflés dans le styrène. On a suivi la polymérisation par dilatométrie et on a étudié la dépendance de la vitesse, de polymérisation vis-à-vis de la concentration en monomère et de l'intensité de radiation pour les deux systèmes. On a essayé de séparer les copolymères et homopolymères au moyen de chromatographie d'élution en créant un gradient thermique. La méthode s'est revélée satisfaisante quand on utilise comme système solvant'nonsolvant le benzène et l'éther de pétrole, mais le système benzène–méthanol ne convient pas à la séparation. Ce fait est attribué à des phénomènes de cosolution.

Zusammenfassung

Pfropfcopolymere wurden durch Bestrahlung von mit Monomerem gequollenen Polymerlatices dargestellt. Die verwendeten Latices wurden, zur Vermeidung der Gegenwart von Startermolekülen in der zweiten Phase, durch Strahlungsemulsionspolymerisation hergestellt. Mit Methylmethacrylat gequollene Polystyrollatices und mit Styrol gequollene Polymethylmethacrylatlatices wurden verwendet. Die Polymerisation

wurde dilatometrisch verfolgt und die Abhängigkeit der Polymerisationsgeschwindigkeit von Monomerkonzentration und Strahlungsintensität für beide Systeme bestimmt. Versuche zur Trennung des Copolymeren vom Homopolymeren wurden durch Eluierungs-chromatographie mit Temperaturgradienten unternommen: die Methode erwies sich bei Verwendung des Lösungsmittel-Fällungsmittelsystems Benzol-Petroläther als befriedigend, lieferte aber mit Benzol-Methanol keine Trennung. Dieses Versagen wird vermutlich durch Cosolvenserscheinungen verursacht.

A Comparison of Dynamic Methods for Osmotic Pressure Measurements

D. B. BRUSS and F. H. STROSS, *Shell Development Company, Emeryville, California*

Synopsis

A comparison of dynamic methods for osmotic pressure molecular weight determinations has been made between the authors' method, the recently published method of Elias, and two other commonly used procedures. Samples containing various amounts of membrane-permeating solute were studied while using the same osmometer and gel-cellophane membrane. Good agreement is shown between the authors' method and that of Elias for all of the samples. The Fuoss-Mead technique and Philipp's method do not measure as much of the permeating solute when present in large amounts. The method of Elias is subject to continual calibration because of pore blockage and was found to be considerably more time-consuming than the authors' method.

For a given membrane/solvent/solute system, in which the solute is either partially or completely capable of permeating the membrane, there exists a pressure, π_s, which is the maximum pressure the membrane is capable of measuring. A static measurement can not indicate the value of π_s since the measurement is made at equilibrium and only the pressure caused by those molecules which are retained completely by the membrane is obtained. Only a dynamic method, based on a fast measurement or on a suitable extrapolation procedure, affords a chance of obtaining the π_s pressure under these conditions. Since many different polymer samples produced by a variety of catalytic systems have shown the presence of low molecular weight material, it is questionable whether static determinations should ever be used for the determination of number-average molecular weight. Even supposedly well-fractionated samples have sometimes shown solute capable of permeation. The argument for the dynamic approach rests on its ability to measure at least a portion of those molecules which would otherwise be lost. The degree of the error which can occur from this source has been demonstrated by the results on polybutadiene samples for which the dynamic number-average molecular weights were sometimes two to three times lower than those obtained by the static method with the use of the same membrane. To what level the dynamic method can be used reliably is a subject of continuing investigation.

That the π_s pressure will always be less than π, the theoretical osmotic pressure, is due to the Staverman effect[1,2] which has been investigated

experimentally by several authors.[3-7] Staverman has shown that molecules capable of permeating the membrane do not contribute to their full extent to the osmotic pressure, even if they have not permeated the membrane at the instant of measurement. The consequence of this statement is that no dynamic method or extrapolation procedure can give the theoretical osmotic pressure if there is solute present which can permeate the membrane. It remains, therefore, to be determined which dynamic method offers the easiest and closest approach to π_s. The magnitude of the difference between π_s and π will depend on the pore size distribution of the membrane. The magnitude of the difference between ΔH, the experimentally measured dynamic pressure, and π_s will depend on the method used for the measurement. The relationship between these pressures may be summarized as:

$$\Delta H \leq \pi_s < \pi$$

Highly retentive membranes, such as the ultrafine filters[8] and glass membranes,[9] may be used for static measurements down to very low molecular weight levels, but the equilibration times are usually quite long. The selection of membranes exhibiting a high degree of retentivity is a lengthy process since only a few membranes from a large batch may prove suitable. However, dynamic methods can be applied to slow and highly retentive membranes to extend their range and speed.[10]

Of the dynamic methods described in the literature, four appear to be the most attractive from the standpoint of simplicity of equipment and the ease of manipulation. Each method was examined using the same membrane/solvent/solute systems for the case where the solute was either partially or completely capable of permeating the membrane. The methods selected for comparison were the method of Philipp,[11] the half-sum method of Fuoss and Mead,[12] the recently described method of Elias,[10] and the method described previously by the authors of this paper.[13]

Each of the methods has the advantage that it can be done by using a simple osmometer of the type commonly employed for static methods. All are dependent on the fact that the rate of solvent flow through the membrane is proportional to the driving head h, which is related to the hydrostatic head H and the osmotic pressure by

$\pi = H - h$ for H greater than π; $\pi = H + h$ for H less than π.

The methods differ in the manner in which H is measured as a function of the time and in the manner in which the data are interpreted. Discussion of each method in detail is presented in the following sections of the paper.

APPARATUS AND REAGENTS

A small volume osmometer,[14] equipped with capillaries of 0.36 mm. diameter, was used for all of the determinations. The osmometer was immersed in a solvent jar which was controlled at $30 \pm 0.003°C$. by means of a circulating water bath.

Gel-cellophane membranes of grade No. 600 (J. V. Stabin Company, Brooklyn, New York) and ultrafine filter membranes of type allerfeinst (Membranfiltergesellschaft, Göttingen, Germany) were gradually conditioned to toluene by successive immersion in solvent baths of alcohol, alcohol–toluene, and finally pure toluene.

A Gaertner cathetometer (Gaertner Scientific Company, Chicago, Ill.) reading to 0.005 cm. over a 100-cm. scale was used to measure the hydrostatic heads.

The samples of poly-α-methylstyrene (PAMS) were prepared by a process of anionic polymerization.[15] PAMS-2 had a $\bar{M}_w$ of 4900 and a $\bar{M}_n$ of 3700 (ebullioscopic). PAMS-3 had a $\bar{M}_w$ of 23,000 and a $\bar{M}_n$ of 21,000 (osmotic). E-2 was a polystyrene sample of $\bar{M}_w = 49,000$ and $\bar{M}_n = 25,000$ (osmotic).

DISCUSSION AND RESULTS

The Elias Method

In a recent publication,[10] Elias describes several methods by which dynamic determinations of samples containing permeating solute can be made. The method most suitable for rapid dynamic measurement is based on the equation:

$$\Delta H_o = \Delta H_t + V_t K'_e \qquad (1)$$

where ΔH_o is the dynamically obtained pressure in centimeters, ΔH_t is the hydrostatic head in centimeters at time t in minutes, V_t is the velocity of solvent through the membrane at ΔH_t, and K'_e is a constant dependent on the osmometer geometry, the solvent, and the permeation constant of the membrane.

From the adjusting curve of the hydrostatic head with time, starting at any initial head, ΔH_0, values of ΔH_t and V_t may be obtained. V_t is calculated from the slope of the tangent to the curve at ΔH_t.

K_e' is obtained by measuring the permeability of the membrane to solvent. The permeability of a membrane, according to Kuhn,[16] is given by:

$$G = df/FgD \cdot 2.303(\log H_0 - \log H_t)/t \qquad (2)$$

where d is the membrane thickness in centimeters, f is the capillary area in square centimeters, D is the solvent density, g is the acceleration due to gravity in centimeters squared per second, and F is the effective membrane area in square centimeters.

This relation is derived from the fact that the rate of change of head is a function of the head, i.e., $dH/dt = -KH$ and $2.303 \log (H_0/H_t)/t = K$, the permeation constant.

Since the permeation constant is directly proportional to the membrane area and the density of the solvent, and is inversely proportional to the capillary area and the membrane thickness, we may write:

$$2.303 \log (H_0/H_t)/t = K = GFgD/fd$$

which is equivalent to eq. (2). The value of K may be obtained by measuring the decrease of the hydrostatic head with time with pure solvent on each side of the membrane. We may write, for convenience:

$$K'_e = 1/K$$

which gives the proportionality constant relating the velocity, V_t, to hydrostatic head. Elias considers that the following conditions must be met for satisfactory dynamic measurements: (a) absence of any balloon effect of the membrane (if K is constant with time, there should be no balloon effect); (b) absence of capillary drainage and temperature differences between solvent and solution; (c) stability of the membrane (the K value should be constant before and after the measurement); (d) tightness of the measuring system.

For his examination of eq. (1), Elias used a two-chambered osmometer equipped with capillaries of 1.2 and 2 mm. diameter, and cellophane 600 membranes. Measurements were made on polyethylene glycols in methanol, dimethylformamide, formamide, and water. These solvents were shown to give "stable gel systems" with cellophane 600.[7] Equilibration times for nonpermeating samples were quite long, on the order of 60 to over 100 hr. for samples in methanol. From the data presented in his paper for the times required to reach maximum pressures, we conclude that his measuring system is some 50 to 100 times slower than ours. This is due partially to the smaller capillary diameter and larger membrane area of our osmometer and partially to the smaller pore size of his cellophane membranes.

The suitability of our system for making dynamic measurements by this method was tested using the criteria of the preceding section.

To test for possible balloon effect, the value of the permeation constant was determined at various hydrostatic heads and as a function of time. For the gel cellophane 600 membranes, the permeation constant did not vary more than 1% over the length of the capillary as shown in Table I. Further proof of the rigidity of the membrane support is furnished by flow rate studies of pressures above and below the equilibrium pressure for solutions of non-permeating polymers and of pure solvent.[17] If the membrane does not exhibit viscoelastic behavior, graphs of the flow rate versus applied pressure for the approach to equilibrium from above and below should show perfectly symmetrical behavior. The argument is based on the fact that the force applied to the membrane by movement of the pressure adjusting rod is opposite in these two cases and any balloon effect should be reflected by differences in the slope of the extrapolations made from above and below the equilibrium position. For the test cases mentioned above, perfectly symmetrical behavior was obtained.

The permeation constant for the ultrafine filter membranes does not exhibit this uniformity with hydrostatic head, but varies as much as 4% over the length of the capillary as shown in Table II. The decrease in the permeation constant with the decrease in hydrostatic head indicates an

TABLE I
Determination of the Permeation Constant for Cellophane 600 Membranes
Avg. $= 5.10 \times 10^{-2}$ min.$^{-1}$ ($= K/2.303$); $K'_e = 8.51$ min.

t, min.	ΔH_t, cm.	H_0/H_t	$\log (H_0/H_t)/t$ $\times 10^2$, min.$^{-1}$
0	8.81		
1	7.83	1.125	5.12
2	6.95	1.268	5.16
3	6.21	1.419	5.07
4	5.51	1.599	5.10
5	4.90	1.798	5.10
6	4.36	2.021	5.09
7	3.87	2.276	5.10
8	3.44	2.561	5.11
9	3.06	2.879	5.10
10	2.72	3.239	5.10
11	2.42	3.640	5.10
12	2.15	4.098	5.10
13	1.91	4.613	5.11
14	1.70	5.182	5.10
15	1.51	5.834	5.11
16	1.35	6.526	5.09
17	1.20	7.342	5.09

increased resistance of the membrane to solvent flow as the head is lowered. Since the membrane support is the same as for the cellophane 600 membranes, we can assume that this effect is not due to a ballooning of the membrane.

Elias suggests that swelling and shrinkage of the membrane can cause a change in the permeation constant and states that a membrane should only

TABLE II
Determination of the Permeation Constant for Ultrafine Filter Membranes
Avg. $= 0.702 \times 10^{-2}$ min.$^{-1}$; $K'_e = 61.9$ min.

t, min.	ΔH_t, cm.	H_0/H_t	$\log (H_0/H_t)/t$ $\times 10^2$, min.$^{-1}$
0	8.65		
5	7.97	1.085	0.709
10	7.35	1.177	0.708
15	6.76	1.280	0.715
25	5.73	1.510	0.716
40	4.51	1.918	0.707
50	3.85	2.247	0.703
60	3.29	2.629	0.700
75	2.60	3.327	0.696
85	2.21	3.914	0.697
102	1.70	5.088	0.693
120	1.29	6.705	0.689
135	1.02	8.480	0.688

be used in solvents in which it forms a stable gel system. Examples of such solvents for gel cellophane 600 membranes are given, namely water, formamide, dimethylformamide, methanol, and benzyl alcohol.[7,10] From many measurements of the permeation constant in toluene, our data indicate that the short range stability of the cellophane 600 membranes is excellent. Variations of about 4 or 5% in the permeation constant have been noted over a period of weeks, but we have concluded that this variation is a function of the type of polymer sample to which the membrane has been exposed, rather than a swelling or shrinking effect of the membrane. The data of Table III show the effect of exposing the membrane to a polydisperse polymer sample. Determinations A through G were made either after the osmometer had been exposed to very low molecular weight material or had been standing in solvent for several days. Runs H and I were made immediately after the osmometer had been used for the determination of polydisperse samples of higher molecular weight. Run J was then made after the osmometer had been standing in pure solvent for several days.

TABLE III
Stability of the Permeation Constant for Cellophane 600 Membranes

Run	Date	K'_o, min.
A	9/20	8.13
B	9/22	8.28
C	9/25	8.20
D	9/28	8.40
E	10/2	8.31
F	10/9	8.19
G	10/17	8.23
H	10/19	9.26
I	10/20	9.46
J	10/23	8.50

We conclude from these data that the most serious effect on the permeation constant is caused by a blocking of the pores of the membrane by polymer molecules of size sufficient to enter but not pass through the pore. This effect is reversible on long standing in pure solvent. The change in the permeation constant of the membrane will then depend on the molecular weight distribution of the polymer sample and its relation to the pore size distribution of the membrane. Some samples would show little or no effect on the permeation constant while others would change it greatly. More important, one can never be sure that the permeation constant does not change during the course of the measurement by an increasing amount of blockage unless a measure of the permeation constant before and after each run yields the same value.

For fresh ultrafine filter membranes, the permeation constant was found to change as much as 10% after the initial exposure to polymer.

That capillary drainage and temperature equilibration of the filling solution are not problems can be demonstrated by measuring the pressure–
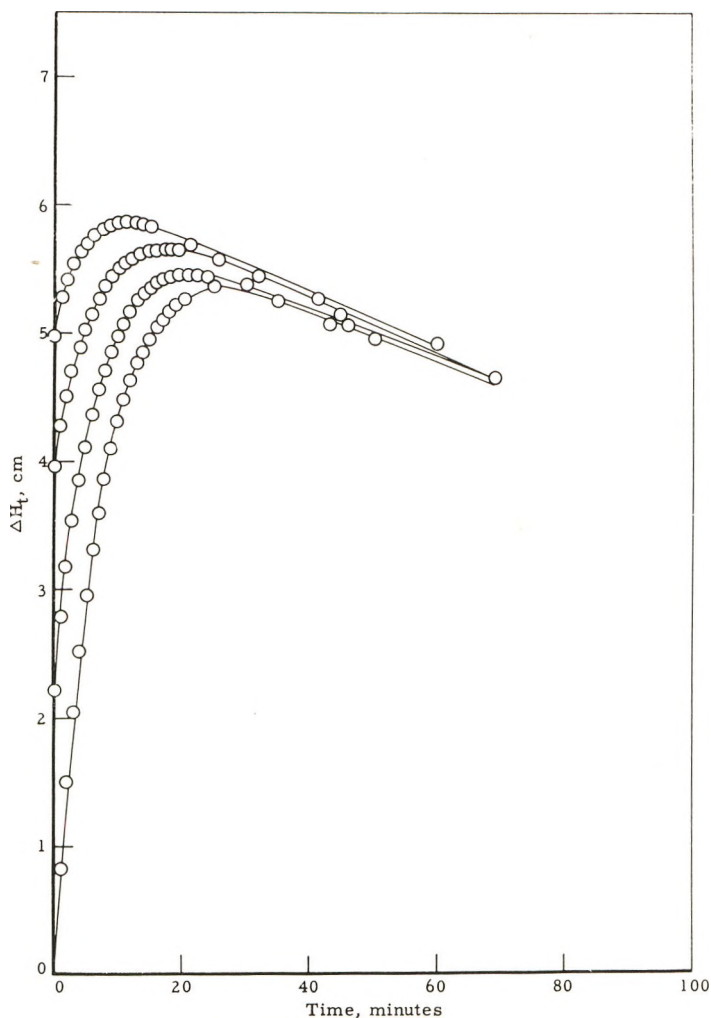
Fig. 1. Equilibration curves starting at different initial heads, GC-600 membranes, 0.2% PAMS-2.

time curve with solvent on each side of the membrane after the 5-min. period allowed for temperature equilibration. There was no movement of the meniscus after adjusting the hydrostatic head to the asymmetry pressure.

That the measuring system is "tight" is indicated by the constancy of the permeation constant at different hydrostatic heads and by the ability of the osmometer to hold a constant pressure for a nonpermeating polymer sample.

A test of the Elias eq. (1) was made with the use of a 0.2% solution of PAMS-2 (MW = 4000). At this molecular weight level, membrane blockage should not be a problem. This was substantiated by the fact that the

permeation constant did not vary more than two percent between determinations made before and after the experiment.

The pressure–time curves for several initial heads, ΔH_0, are shown in Figure 1. According to Elias, the ΔH_r value extrapolated to time zero should be independent of the initial head. The analysis of a set of data from the curve having $\Delta H_0 = 3.99$ cm. is given in Table IV.

The values of V_t were calculated from the adjusting curve by drawing tangents to the curve at the various ΔH_t values and obtaining the slope of the tangent. Extrapolation of the ΔH_v data to zero time is shown in Figure 2. The extrapolation gives a value of 6.45 cm. for $(\Delta H_v)_{t=0}$. The pressure–time curve shows a maximum of 5.67 cm. at 15 min. (Fig. 1). Data for all of the pressure adjusting curves were analyzed in the same manner. The ΔH_v–time extrapolations for the curves of Figure 1 are shown in Figure 3. Only the data at $\Delta H_0 = 3.99$ and 5.01 gave suitable extrapolations. Table V summarizes the information obtained from this experiment.

Elias also suggested the extrapolation of ΔH_{max} to zero time as another method for obtaining π_s. Using the data of Table V, we obtain a value of approximately 6.30 cm. for ΔH_{max} at time zero, where $\Delta T'_{max}$ is the time to

TABLE IV

Analysis of the Adjusting Curve for a 0.2% Solution of PAMS-2
GC-600 Membranes, $K'_e = 8.20$ min.

t, min.	ΔH_t, cm.	$V_t \times 10^2$, cm./min.	$V_t K'_e$, cm.	ΔH_v, cm.
0	3.99			
1	4.28	25.8	2.12	6.40
2	4.52	22.0	1.80	6.32
3	4.73	18.6	1.53	6.26
4	4.91	16.3	1.34	6.25
5	5.06	13.9	1.14	6.20
6	5.18	11.4	0.94	6.12
7	5.28	9.7	0.79	6.07
8	5.37	8.2	0.67	6.04
9	5.45	6.4	0.52	5.97
10	5.51	5.0	0.41	5.92
11	5.56	4.3	0.35	5.91

TABLE V

Summary of the Data Obtained from the Pressure–Time Curves of PAMS-2 at Different Initial Heads

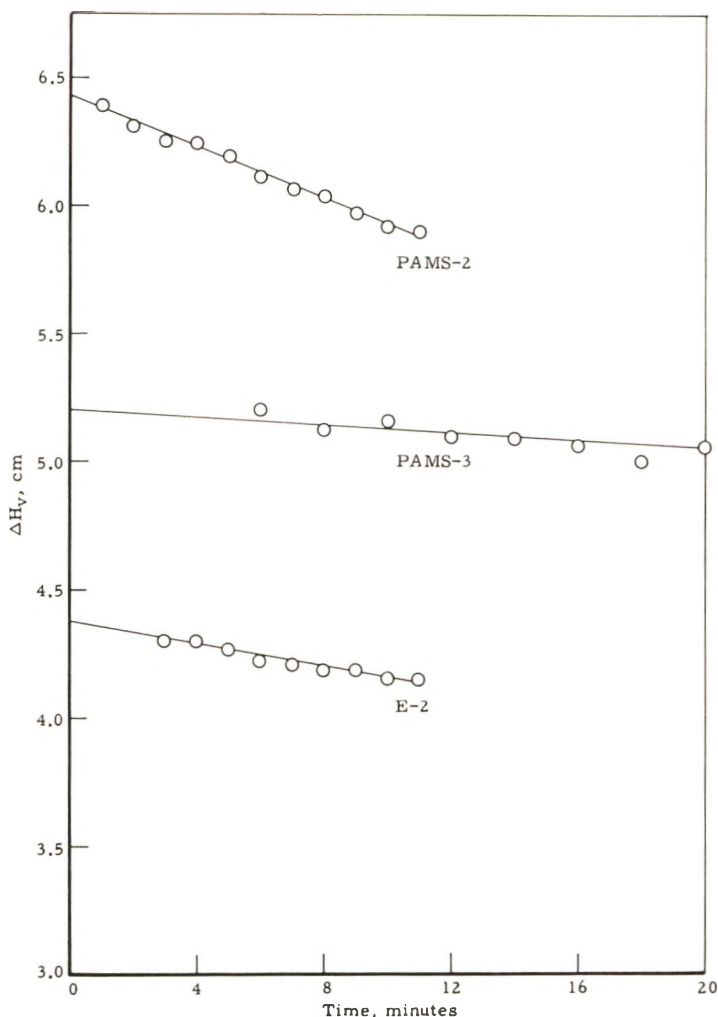| ΔH_0, cm.	$(\Delta H_v)_{t=0}$, cm.	ΔT_{max}, min.	ΔH_{max}, cm.	ΔH_{ext}, cm.
0	. . .	24	5.38	5.80
2.22	. . .	19	5.46	5.95
3.99	6.45	15	5.67	6.06
5.01	6.48	10	5.87	6.25

Fig. 2. Extrapolation of ΔH_v to zero time by the method of Elias.

reach ΔH_{max}.   The last column of Table V gives the intercept obtained by extrapolating the adjusting curve to zero time.

From the data obtained by using the Elias method, it appears that a value of about 6.50 cm. represents a good approximation of the π_s value for this membrane–solute system.   Application of our dynamic method (extrapolation to zero flow rate), using the same system, gives values of 6.50 and 6.45 cm. for $(\Delta H)_{v=0}$, in which the subscript denotes extrapolation to zero flow rate.   The flow rate versus applied pressure extrapolation is shown in Figure 4.   The agreement between the values of $(\Delta H_e)_{t=0}$ and $(\Delta H)_{v=0}$ is excellent.   The Elias method is more time consuming and requires considerably more calculation.   Moreover, an accurate value for the permeation constant is needed.   Finally, the data obtained by the
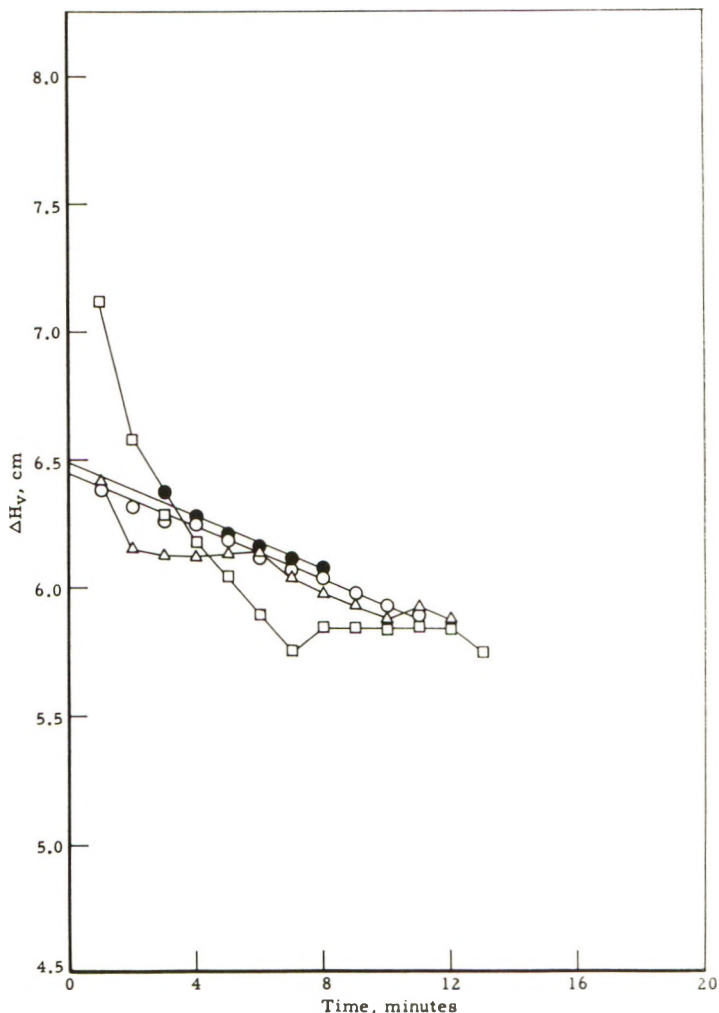
Fig. 3. Extrapolation of ΔH_v from data at various initial heads: ($\bullet$) $\Delta H_a = 5.01$ cm.; (O) $\Delta H_a = 3.99$ cm.; ($\triangle$) $\Delta H_a = 2.22$ cm.; ($\square$) $\Delta H_a = 0$.

Elias method may not always be capable of interpretation as shown by the curves of Figure 3. The reason for the poor results at the lower ΔH_0 is not understood. The use of higher V_t values in eq. (1) leads to more erratic results. Elias, using much slower equipment, does not report data at the early portion of the pressure adjusting curve.

A determination of the dynamic pressure of a 0.4% solution of PAMS-3 (MW = 21,000) by the Elias method gave a value of 5.18 cm. for $(\Delta H_v)_{t=0}$ (see Fig. 3) compared with 5.07 cm. determined by the flow rate method (Fig. 4). PAMS-3 contains a small portion of low molecular weight material as indicated by the static pressure reading of 4.38 cm. after some 1000 min. The pressure–time curves, at different ΔH_0 values, are shown in
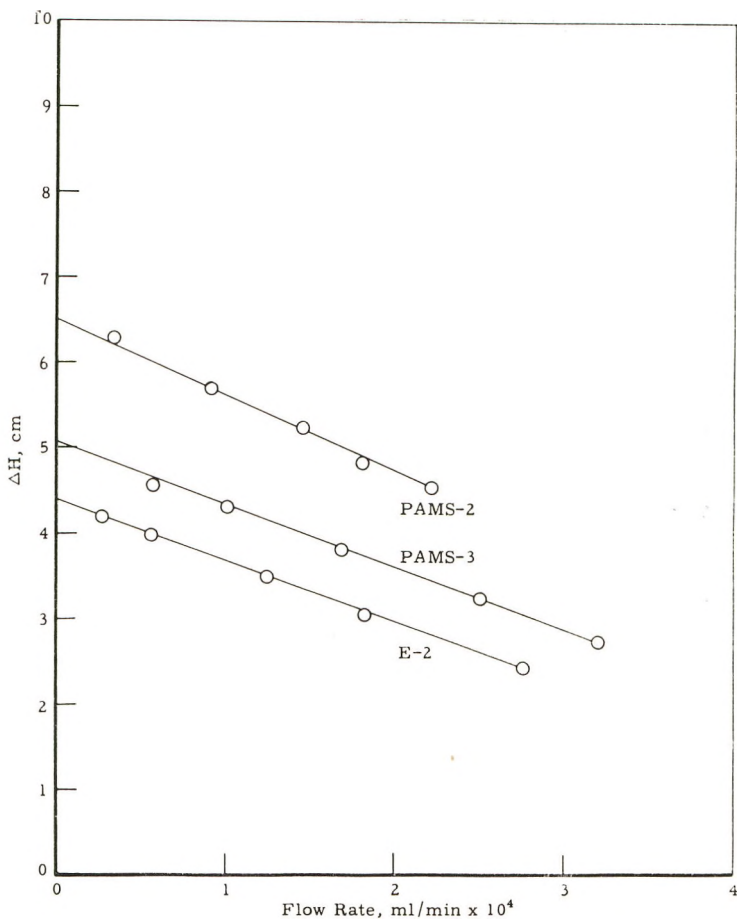
Fig. 4. Flow rate–applied pressure extrapolations by the Bruss-Stross method.

Figure 5. It is impossible to estimate ΔT_{max} values from curves of this type, since a well-defined maximum, such as is present with excessive permeation, does not occur. Again, only one of the three adjusting curves gave data which were suitable for the determination of $(\Delta H_v)_{t=0}$.

Fraction E-2 contains a relatively larger amount of solute capable of permeating the membrane. Application of the Elias method gave a value of 4.41 cm. $(\Delta H_v)_{t=0}$ which is in excellent agreement with the value of 4.40 cm. obtained by the flow rate method (see Figs. 3 and 4). A static equilibrium pressure of 2.82 was read after 63 hr.

The Fuoss-Mead Method

The Fuoss-Mead technique involves measuring a portion of the pressure adjusting curve, starting with an initial head above or below the estimated equilibrium position. From this curve, an asymptote is estimated and the process is repeated with a fresh solution, but approaching the equilibrium

position from the opposite direction. The descending and ascending branches of these adjusting curves are averaged and the points obtained are extrapolated back to zero time.

The chief difficulty with this technique lies in the estimation of the asymptote to the initial adjusting curve, particularly when there is permeating solute present in the solution. Application of the Fuoss-Mead
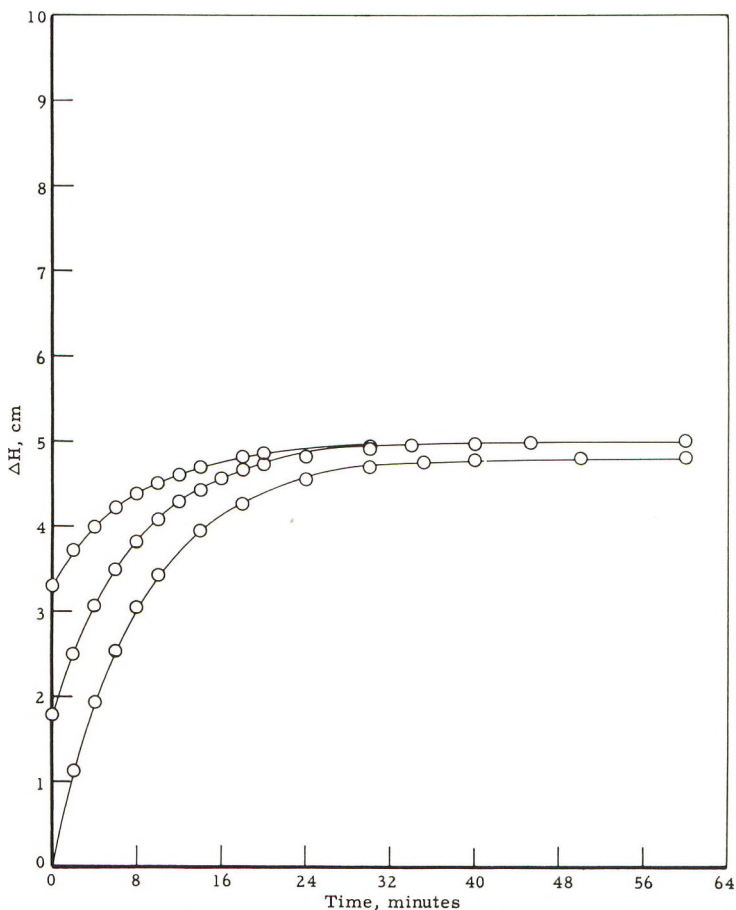

Fig. 5. Equilibration curves starting at different initial heads. GC-600 membranes; 0.4% PAMS-3.

method to the PAMS-2 sample resulted in the curves of Figure 6. It is evident that permeation has caused considerable asymmetry in the ascending and descending branches of the adjusting curves. If one uses curve b to estimate the asymptote, a value of about 5.6 cm. might well be taken from the adjusting curve. The descending branch e is then determined starting at an initial head which is equidistant above the asymptote from the initial head used for the ascending branch. Averaging curves b and e yields curve

d, which can be extrapolated to zero time, giving a value of 6.03 cm. However, if one chooses to run the descending branch (e) initially, a different result would be obtained. Because of the effect of solute diffusion, one would be inclined to estimate a lower asymptote than in the previous case. A reasonable estimate would appear to be approximately 5 cm., leading to a

Fig. 6. Fuoss-Mead plot for PAMS-2.
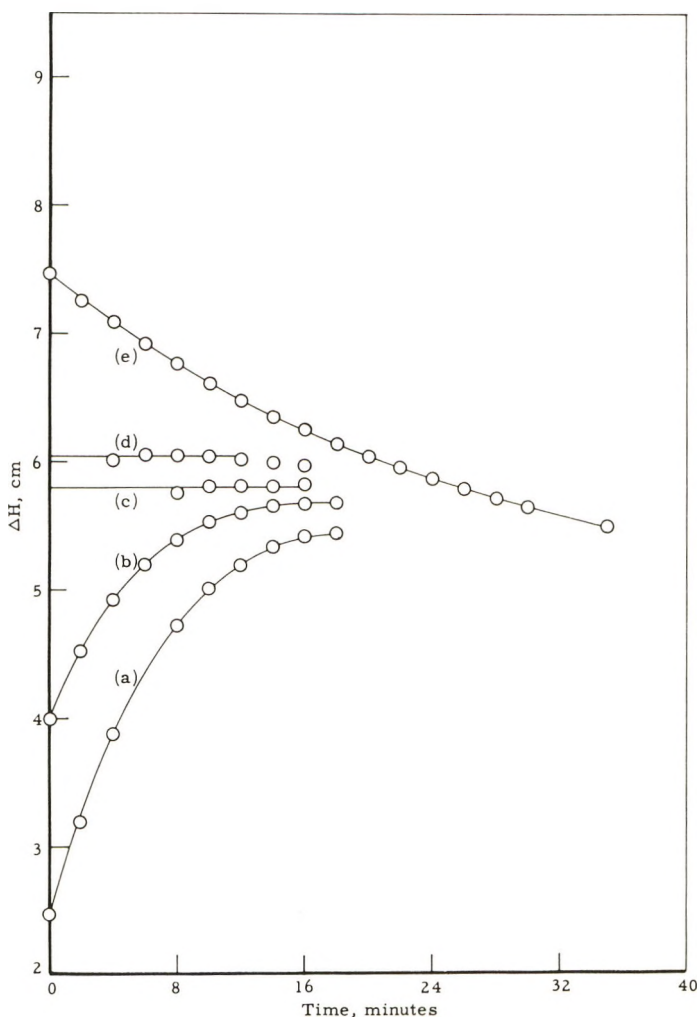
much smaller initial head for the ascending branch of the curve a than was used in the first curve (b). Averaging curves a and e produces curve c with an intercept value of 5.65 cm. For the case of excessive solute permeation, it is evident that the Fuoss-Mead method is dependent on which branch of the plot is determined first and on the choice of a rather arbitrary asymptote.

The experiment in which the permeation is not excessive is shown in Figure 7. The ascending branch of the plot for a solution of PAMS-3 was determined first. The descending branches (d) and (e) were determined after estimating the asymptote to be 5.0 and 5.3 cm., respectively. This represents only a 6% difference in the choice of the asymptote, but results in the two extrapolations (b) and (c) having intercept values of 5.11 and 5.25 cm., respectively. These values are in fair agreement with the values of
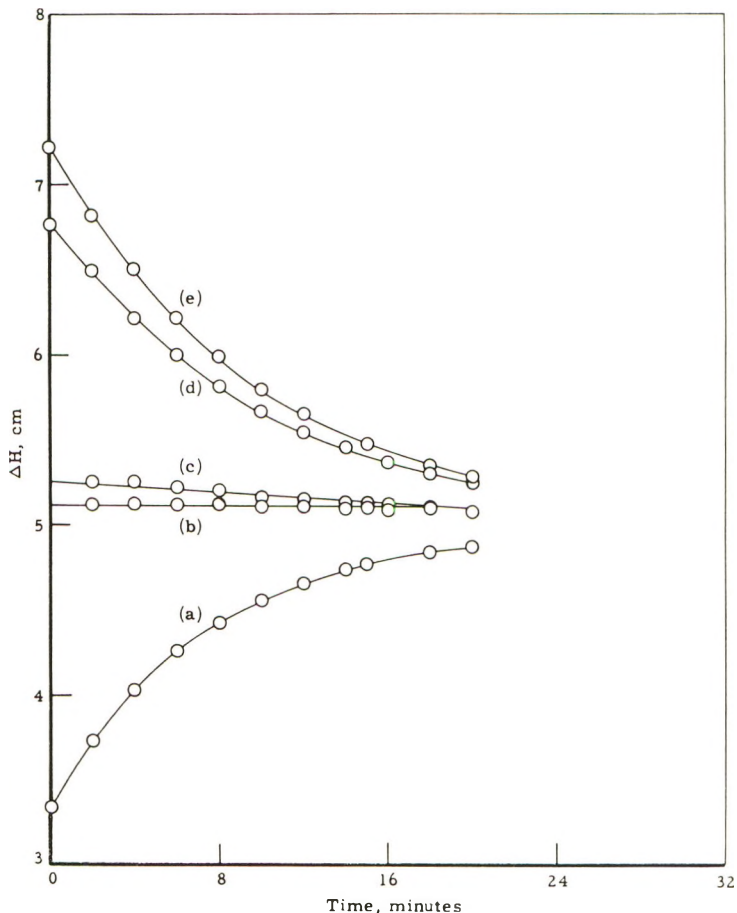
Fig. 7. Fuoss-Mead plot for PAMS-3.

5.18 cm. determined by the Elias method and 5.07 cm. determined by the flow rate method; but, nevertheless, the method relies upon the proper choice of the asymptote for reproducible results. Unfortunately, this appears to be a procedure of trial and error. Since the Fuoss-Mead technique requires two fillings of the osmometer for each concentration, the experimental time required is more than twice that needed for the Bruss-Stross method.

Philipp's Method

Philipp's method is based on the fact that the rate of flow of solvent through the membrane is proportional to the driving head h, which is related to the osmotic pressure π and the hydrostatic head H by:

$$h = H - \pi$$

and on the assumption that the driving head is an exponential function of the time. In this case, the ratio of the driving heads at fixed time intervals is constant, and we have:

$$h_2/h_1 = h_3/h_2$$

for three consecutive driving heads. Substitution of $H - \pi$ for the driving head yields:

$$(H_2 - \pi)/(H_1 - \pi) = (H_3 - \pi)/(H_2 - \pi)$$

and

$$\pi = (H_1 H_3 - H_2^2)/(H_1 + H_3 - 2H_2)$$

The equation, as expressed above, is valid for samples which do not contain permeating solute. For samples which do contain solute capable of membrane permeation, the true osmotic pressure π is not obtained by the measurement, but rather an experimental pressure, ΔH_p, which is calculated by the same method:

$$\Delta H_p = (H_1 H_3 - H_2^2)/(H_1 + H_3 - 2H_2)$$

When permeating solute is present in the sample, the driving head is no longer an exponential function but is also dependent on the increasing effect of solute diffusion. For this reason, the results obtained by using the Philipp's equation will depend on the time interval selected between the consecutive heads measured and on the position of these heads on the

TABLE VI

Calculation of the Osmotic Pressure ΔH_p from PAMS-2 Data Using Philipps' Method

ΔH_0, cm.	Time intervals, min.	ΔH_p, cm.[a]
0	2,4,6	5.48
	4,8,12	5.62
	5,10,15	5.59
2.22	2,4,6	5.93
	3,6,9	5.77
	4,8,12	5.71
3.99	2,4,6	5.78
	3,6,9	5.85
	4,8,12	5.79
5.01	1,2,3	5.93
	2,4,6	5.93

[a] Pressures are normally repeatable to 1 or 2 units in second decimal place.

pressure adjusting curve.   It will also depend on the initial head at time
zero.   The data of Table VI illustrate this point.

One is caught by a conflict of interests when attempting to use Philipp's
method for samples containing permeating solute.   If one chooses an early
portion of the adjusting curve with short time intervals, solute permeation
will be minimized, but the data are less reliable, since the calculation must
extrapolate from a short time base.

If one chooses longer time intervals, then permeation can become exces-
sive before the final reading is taken.

For the solution of PAMS-3, in which permeation is not excessive, con-
sistent results are only obtained for the longer time intervals.   Data calcu-
lated from the descending and ascending curves of Figure 7 are shown in
Table VII.

TABLE VII

Calculation of the Osmotic Pressure ΔH_p from PAMS-3 Data Using Philipp's Method

ΔH_0, cm.	Time intervals, min.	ΔH_p, cm.
6.77	2,4,6	4.80
	0,5,10	4.82
	4,12,20	5.00
3.32	2,4,6	5.11
	5,10,15	4.97
	4,12,20	4.95

Summary of Results with Cellophane 600 Membranes

When using the relatively fast cellophane 600 membranes, it is obvious
that some sort of dynamic method is required if a reasonable estimate of the
Staverman pressure is to be attained.   In spite of the rapidity of the
osmometer/membrane system, permeation of solute is so rapid that the use
of the maximum in the pressure–time curve or extrapolation to zero time
from this curve will not yield satisfactory results even at relatively high
ΔH_0 values.   This fact is amply demonstrated by the data of Table V.   Of
course, as the initial hydrostatic head chosen approached the "equilibrium"
pressure, both the maximum and the extrapolation made from the pressure–
time curve will approach the π_s pressure, but such procedures are based on
trial and error and defeat the purpose of dynamic measurements.

The results obtained by the various dynamic methods considered in this
report are summarized in Table VIII.   The data obtained by the Philipp's
method are given as a range of values and serve to indicate the variation of
the values with the time interval selected. ΔH_{eq}, the equilibrium pressure,
represents the static value attained after about 1000 min.

It is evident that the best approximation of the π_s pressure is obtained by
using either the Elias method or the method of Bruss-Stross.   Both the
Fuoss-Mead technique and the method of Philipp are dependent on the
initial conditions selected for the experiment.   The Fuoss-Mead technique

TABLE VIII

Comparison of Results for the Cellophane 600 Membranes

Sample	$(\Delta H_r)_{t=0}$[a]	$(\Delta H)_{r=0}$[b]	$(\Delta H_{max})_0$[c]	ΔH_p[d]	ΔH_{fm}[e]	ΔH_{eq}[f]
PAMS-2	6.48	6.50	6.30	5.56–5.93	5.65–6.00	0
E-2	4.41	4.40	—	3.97–4.43	4.48	2.82[g]
PAMS-3	5.18	5.07	—	4.78–5.11	5.11	4.38

[a] $(\Delta H_r)_{t=0}$, Elias method. $\Delta H = \Delta H_t - V_t K'_t$.

[b] $(\Delta H)_{r=0}$, Bruss-Stross method.

[c] $(\Delta H_{max})_0$, Elias extrapolation of ΔH_{max}.

[d] ΔH_p, Philipp's method.

[e] ΔH_{fm}, Fuoss-Mead method.

[f] ΔH_{eq}, Equilibrium value (static).

[g] After 63 hr.

requires two fillings of the osmometer. In addition, the choice of the asymptote to the adjusting curve, when permeation is excessive, can introduce a large measure of uncertainty into the final result. Philipp's method gives a rather wide range of results depending on the values selected for the calculation. Both methods give results which are substantially lower than those obtained by the Elias and Bruss-Stross techniques when membrane permeation is large.

The Elias method requires a calibration of the membrane after each determination in the toluene and considerably more calculation than the Bruss-Stross technique. Poor data were frequently obtained, in spite of apparently reliable membrane behavior. When the data were satisfactory, the agreement with our results was very good, indicating that the final result was probably a good approximation of the π_s value for these cellophane membranes.

Summary of Results with the Ultrafine Filter Membranes

Vaughan[8] reported that the most selective ultrafine filter membranes retain molecules at about 1500 molecular weight. Our earlier experience with these membranes had indicated that, in general, they were much less retentive than the cellophane 600 membranes. However, the membranes used in this investigation, which were randomly selected from a large batch, exhibit an amazing degree of retentivity. The equilibration curves for a 0.1% solution of PAMS-2 (one-half the concentration used in the previous sections of this paper) for the ultrafine filter membranes and the best of the cellophane 600 membranes are shown in Figure 8. The cellophane 600 membranes show the expected behavior: a sharp inflection in the curve followed by a gradual decrease to zero pressure as the sample permeates the membrane. On the other hand, the ultrafine filter membranes show a more gradual rise to almost the theoretical pressure with very little permeation occurring even after extended time. Though the ultrafine filters are about six times slower than the cellophane 600 membranes, they may be used quite satisfactorily for flow rate measurements with little increase in the time

required for analysis.   Application of our dynamic method to the PAMS-2 sample, using these membranes, gave a molecular weight of 3700, which is in excellent agreement with the ebullioscopic results of 3800 and the Mechrolab vapor pressure osmometer result of 3700.   This result is more encouraging, in view of the fact that the PAMS-2 sample is not extremely narrow but has material of molecular weight below the value reported. Since membranes last indefinitely at low temperature, the search for membranes of this caliber is certainly justified, since the apparatus is capable of rapid dynamic analysis with considerable overlap in the ebullioscopic region.
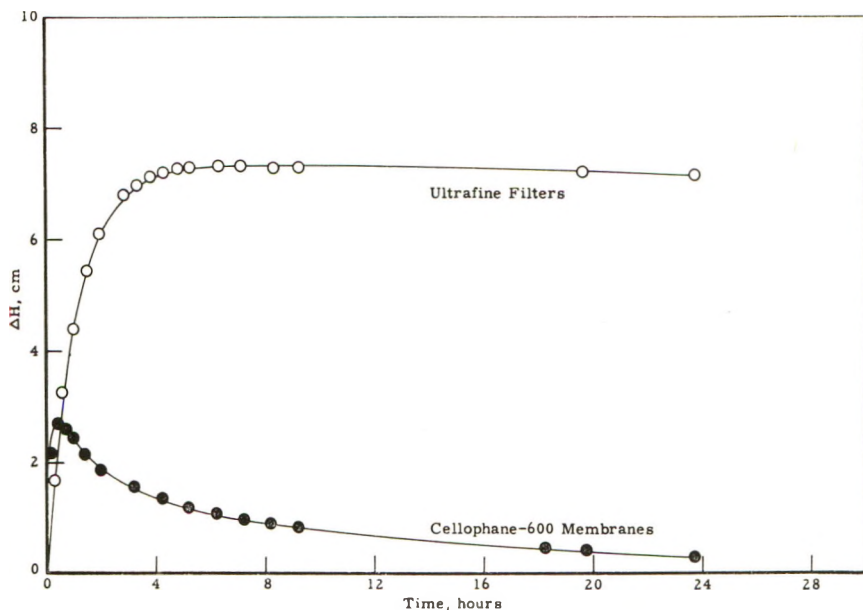

Fig. 8. Equilibration curves for 0.1% PAMS-2.

Use of the Elias technique with the ultrafine filter membranes gave generally poorer data than those obtained with the cellophane 600 membranes, particularly in the region of the adjusting time below 20 min. Since the permeation constant of the ultrafine filters was found to be less stable and the membranes were found to be more susceptible to pore blocking than the cellophane 600 membranes, a calculation of the type proposed by Elias becomes less attractive from the standpoint of the continual calibration required.

The Fuoss-Mead technique and the Philipp's method will perform better at low molecular weight levels with the ultrafine filters simply because permeation is much less of a problem.   However, the disadvantages which were described for the cellophane 600 membranes are just shifted to a lower molecular weight range and as the permeation again becomes excessive, these methods will become increasingly less reliable.

References

1. Staverman, A. J., *Rec. Trav. Chim.*, **70**, 344 (1951); *ibid.*, **71**, 623 (1952).

2. Staverman, A. J., D. T. F. Pals, and Ch. A. Krussink, *J. Polymer Sci.*, **23**, 57 (1957).

3. Allen, P. W., and M. A. Place, *J. Polymer Sci.*, **26**, 386 (1957).

4. Alvang, F., and O. Samuelson, *J. Polymer Sci.*, **24**, 353 (1957).

5. Elias, H. G., *Z. Physik. Chem. (Frankfurt)*, **28**, 303 (1961).

6. Elias, H. G., and E. Manner, *Makromol. Chem.*, **40**, 207 (1960).

7. Ritscher, Th. A., and H. G. Elias, *Makromol. Chem.*, **30**, 48 (1959).

8. Vaughan, M. F., *J. Polymer Sci.*, **33**, 417 (1958).

9. Elias, H. G., and Th. A. Ritscher, *J. Polymer Sci.*, **28**, 648 (1958).

10. Elias, H. G., *Chem. Ing. Tech.*, **33**, 359 (1961).

11. Philipp, H. J., *J. Polymer Sci.*, **6**, 371 (1951).

12. Fuoss, R. M., and D. J. Mead, *J. Phys. Chem.*, **47**, 59 (1943).

13. Bruss, D. B., and F. H. Stross, *J. Polymer Sci.*, **55**, 381 (1961).

14. Bruss, D. B., and F. H. Stross, *Anal. Chem.*, **32**, 1456 (1960).

15. Burge, D. E., and D. B. Bruss, *J. Polymer Sci.*, in press.

16. Kuhn, W., *Z. Electrochem.*, **55**, 207 (1951).

17. Bruss, D. B., unpublished work.

Résumé

On a effectué une comparaison des méthodes dynamiques de détermination de poids moléculaire par osmométrie entre la méthode des auteurs, la méthode d'Elias récemment publiée et deux autres méthodes utilisées couramment. On a étudié des échantillons contenant des quantités différentes de soluté perméable à travers la membrane; on a utilisé le même osmomètre et une même membrane de gel de cellophane. On observe pour tous les échantillons une bonne concordance entre la méthode des auteurs et celle d'Elias. La technique de Fuoss-Mead et la méthode de Philipp ne mesurent pas assez de soluté perméable lorsque ce dernier est présent en grande quantité. La méthode d'Elias est sujette à un calibrage et nécessite un laps de temps plus long que la méthode des auteurs.

Zusammenfassung

Ein Vergleich von dynamischen Methoden zur Molekulargewichtsbestimmung durch Messung des osmotischen Drucks wurde zwischen der von den Autoren angegebenen Methode, der kürzlich von Elias publizierten und zwei andern, viel benützten Methoden durchgeführt. Proben mit verschiedenem Gehalt an permeationsfähigen Anteilen wurden im gleichen Osmometer und mit der gleichen Gelcellophanmembran untersucht. Bei allen Proben besteht zwischen der von den Autoren angegebenen Methode und der von Elias gute Übereinstimmung. Die Methode von Fuoss–Mead und die von Philipp finden nicht so viel von dem permeationsfähigen Anteil, sobald dieser in grosser Menge vorhanden ist. Die Methode von Elias erfordert wegen der Blockierung der Poren eine kontinuierliche Kalibrierung und erwies sich als viel zeitraubender als die von den Autoren angegebene Methode.

Unrestricted Rotation in Polymers with Discrete Rotational States

JACK B. CARMICHAEL and JACK B. KINSINGER, *Department of Chemistry, Michigan State University, East Lansing, Michigan*

Synopsis

The authors propose that a polymer chain with equally probable but discrete rotational states be called a chain with "unrestricted" rotation. This model is equivalent to the "freely rotating" model only under specific circumstances. At the present time, it is customary to compare unperturbed mean-square end-to-end dimensions of polymers $(\bar{r}_0^2/nl^2)$ with the corresponding values calculated from the freely rotating model of a polymer chain. However, comparison of $(\bar{r}_0^2/nl^2)$ to the equivalent unrestricted rotation model dimensions $(\bar{r}_u^2/nl^2)$ is an improved measure of chain stiffness or conformational order. Calculations are performed for polydimethylsiloxane, polyethylene, isotactic polypropylene, and polyisobutylene. The significance of $\bar{r}_0^2/\bar{r}_u^2$ for these polymers is discussed.

In recent years, mathematical models for the mean-square end-to-end dimensions of polymers with restricted but discrete rotational states have been developed.[1] These models have meaning for a real polymer molecule only when the chain is in an unperturbed state. From the unperturbed dimensions and the stress-temperature coefficient of the vulcanized elastomers,[2,3] it is possible to determine one or two parameters which can be related to the potential difference between preferred and nonpreferred rotational states. It is customary to compare unperturbed mean-square end-to-end dimensions of polymers $(\bar{r}_0^2)$ with the value for the corresponding freely rotating model $(\bar{r}_{0f}^2)$. For a chain with one bond angle and one bond length (i.e., polyethylene), the freely rotating dimensions are given by the following well-known equation (for long chains):[4]

$$\bar{r}_{0f}^2 = nl_2\,\frac{(1 + \cos\theta)}{(1 - \cos\theta)} \tag{1}$$

where n is the number of links in the polymer chain, l is the bond length in the chain backbone, and θ is the supplement of the valence angle.

Benoit[5] developed a chain model with restricted rotation with the following mathematical form:

$$\bar{r}_r^2 = nl^2\,\frac{(1 + \cos\theta)(1 - \langle\cos\phi\rangle)}{(1 - \cos\theta)(1 + \langle\cos\phi\rangle)} \tag{2}$$

where ϕ is the rotational angle. The reference point chosen for this equation is *trans* $= 180°$.*

An early model with restricted and discrete rotation was proposed by Taylor[6] and was based on the rotational states in the ethane molecule. Three statistically independent states are defined as *gauche* left (g_l), *trans* (t), and *gauche* right (g_r). These states occur as minima in the potential energy versus rotational angle curve at $60°$, $180°$, and $300°$, respectively. If the three rotational states of this model are equally probable, the mean-square end-to-end dimensions are the same as the dimensions of the freely rotating model. In the general case, if all the rotational states available to the polymer chain are equally probable, the authors choose to call this the "unrestricted" chain $(\bar{r}_u^2)$. For a real chain with these rotational states, when experimentally determined values of $\bar{r}_0^2/nl^2$ are compared to $(\bar{r}_u^2/nl^2)$ (which here equals $\bar{r}_{0f}^2/nl^2$), a direct indication of the conformational order of the polymer chain (thus, the potential energy difference between the trans and gauche conformations) is obtained.

If a real polymer chain does not assume staggered conformations then:

$$\langle \cos \phi \rangle \neq 0$$
$$\langle \sin \phi \rangle = 0 \text{ for states symmetrically disposed}$$
$$\text{about the } trans \text{ position}$$
$$\langle \sin \phi \rangle \neq 0 \text{ for unsymmetrically disposed states}$$

Here the dimensions of the "unrestricted" chain are not equivalent to the dimensions of the freely rotating chain. Thus, comparisons made of $\bar{r}_0^2$ with $\bar{r}_{0f}^2$ are not fruitful. We propose that $\bar{r}_0^2$ be compared to the "unrestricted" dimensions, $\bar{r}_u^2$, so a more meaningful analysis of conformational order in the polymer chain can be obtained.

Experimental evidence for the complete delineation of the potential energy versus rotational angle function is difficult to obtain. Evidence for preferred rotations can be deduced from x-ray analysis of crystalline polymers, infrared spectra, and dipole moment measurements, but data on the less preferred states are relatively unavailable. Recently, Liquori et al.[7] calculated rotational potential curves for several simple polymer chains considering only interactions of non-bonded atoms. Approximate functions were used to describe the interactions between pairs of nonbonded

---

* For a chain model having a continuum of rotational states,

$$\langle \cos \phi \rangle = \int_0^{2\pi} e^{-u(\phi)/kT} \cos \phi \, d\phi \Big/ \int_0^{2\pi} e^{-u(\phi)/kT} \, d\phi$$

where $\mu(\phi)$ is the rotational potential energy function.
For a chain model consisting of a finite number of discrete rotational states,

$$\langle \cos \phi \rangle = \sum_{i=1}^{n} P_i \cos \phi_i \Big/ \sum_{i=1}^{n} P_i$$

where P_i is the probability that the chain assumes the ith rotational state.

atoms and the most stable helical conformations were calculated. The most preferred rotational states for each polymer considered were predicted with surprising accuracy, and unpreferred states appeared at rotational angles not previously suspected.

In the following section, values of $\bar{r}_u^2$ will be calculated for four polymer chains. For the polydimethylsiloxane chain, the rotational states used are justified from experimental work and Liquori's calculations for the similar polymethyleneoxide chain. States used for the polyethylene, isotactic polypropylene, and the polyisobutylene chains are those determined from x-ray diffraction and additional states predicted by Liquori.

THE POLYDIMETHYLSILOXANE CHAIN

Experimental evidence exists which substantiates the presence of *trans*, *gauche r*, *gauche l* in the siloxane polymer chain. Existence of *gauche r* and *gauche l* states have been demonstrated by the electron diffraction studies of Yokoi,[8] which showed octamethylcyclotetrasiloxane to have a cradle form resulting from the sequence of conformational states, $g_r, g_r, g_l, g_l, g_r, g_r, g_l, g_l$. Existence of the *trans* state and further evidence for the *gauche* states was given also by Damaschun[9] in an x-ray diffraction study of a dimethylsiloxane polymer filled with 35% aerosil and vulcanized. The study showed this polymer chain to have a helical structure with the sequence of conformations, t, g_r, g_l, t, g_l, g_r.

The *cis* conformation in the dimethylpolysiloxane chain is indicated by the planarity of the six-membered ring, hexamethylcyclotrisiloxane. The planarity of this ring has been demonstrated by x-ray[10, 11] and electron[12] diffraction studies. Results of these investigations are summarized in Table I.

Experimental evidence for the appearance of hexamethylcyclotrisiloxane during the equilibrium polymerization of octamethylcyclotetrasiloxane to polydimethylsiloxane is given by Hartung and Camiolo.[13]
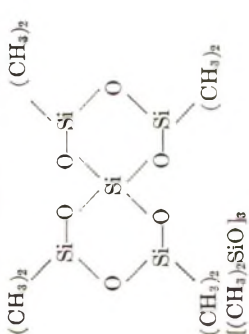
Thus, considering these four states, the condition for unrestricted rotation in the polydimethylsiloxane chain is $P_t = P_c = P_{\theta_r} = P_{\theta_l} = 0.25$; therefore, $\langle \sin \phi \rangle = 0$, $\langle \cos \phi \rangle = 0.25$. The unrestricted chain dimension can be calculated for a chain of this type via eq. (3), where θ_1 and θ_2 are the supplements of the alternating valence angles of the chain.

$$
\frac{\bar{r}_u^2}{nl^2} = \frac{(1 - \cos \theta_1)(1 - \cos \theta_2)}{(1 - \cos \theta_1 \cos \theta_2)} \frac{(1 - \langle \cos \phi \rangle)}{(1 + \langle \cos \phi \rangle)}
\tag{3}
$$

Rotational angle data necessary for calculating $\bar{r}_u^2/nl^2$ are given in Table II.

In Table III, values for experimentally determined $\bar{r}_u^2/nl^2$, and calculated values of $\bar{r}_u^2/nl^2$ and $\bar{r}_{0f}^2/nl^2$ are listed. Of particular interest are the ratios $\bar{r}_0^2/\bar{r}_u^2$ and $\bar{r}_0^2/\bar{r}_{0f}^2$ given in the last two columns.

TABLE I

Compound	Si—O, A.	<OSiO	<SiOSi	Comments
	1.64 ± 0.03	109 ± 4°	130 ± 4°	(Si—O)₃ ring reported to be planar[a]
[(CH₃)₂SiO]₃	1.61	104°	136°	Ring reported to be planar[b]
[(CH₃)₂SiO]₃	1.66 ± 0.04	115 ± 5°	125 ± 5°	Ring reported to be planar[c]

[a] Data of Roth and Harper.[10]
[b] Data of Peyronel.[11]
[c] Data of Aggarwal and Bauer.[12]

TABLE II
Data for the Calculation of Unrestricted Dimensions

Polymer	Angles at which rotational states occur	$\langle \sin \phi \rangle$	$\langle \cos \phi \rangle$
Polydimethyl-siloxane	0°, 60°, 180°, 300°	0	0.250
Polyethylene	60°, 90°, 180°, 270°, 300°	0	0
Isotactic polypropylene	ϕ_1: 60°, 80°, 183°, 200°, 260°, 298°	−0.069	−0.162
	ϕ_2: 62°, 100°, 160°, 177°, 280°, 300°	+0.069	−0.162
Polyisobutylene	45°, 85°, 155°, 160°, 200°, 205°, 275°, 315°	0	−0.263

TABLE III
Comparison of Experimental and Calculated Polymer Dimensions

Polymer	Chain bond length, A.	Chain bond angle	$\bar{r}_0^2/nl^2$	$\bar{r}_u^2/nl^2$	$\bar{r}_{0f}^2/nl^2$	$\bar{r}_0^2/\bar{r}_u^2$	$\bar{r}_0^2/\bar{r}_{0f}^2$
Polydimethyl-siloxane	1.65	θ_1 = 109.5 θ_2 = 142.5	7.23[a]	2.55	4.26	2.83	1.70
Polyethylene	1.54	110°	6.55[b]	2	2	3.28	3.28
Isotactic polypropylene[c]	1.54	114°	7.35[d]	3.25[e]	2.37	2.26	3.10
Polyisobutylene	1.54	114°	7.45[f]	4.06	2.37	1.83	3.14

[a] Data of Flory et al.[14]

[b] Data of Hoeve.[3]

[c] The equation developed for isotactic chains is:

$$\bar{r}^2/nl^2 = \frac{(1 + \cos \theta)(1 - \langle \cos \phi_1 \rangle^2 - \langle \sin \phi_1 \rangle^2)}{(1 - \cos \theta)(1 + \langle \cos \phi_1 \rangle^2 + \langle \sin \phi_1 \rangle^2)}$$

[d] Data of Kinsinger.[15]

[e] Data of Lifson.[16]

[f] Data of Flory.[4]

DISCUSSION OF RESULTS

1. Polydimethylsiloxane

In the polydimethylsiloxane case, the inclusion of the *cis* state in the model results in a higher ratio of $\bar{r}_0^2/\bar{r}_u^2$ than $\bar{r}_0^2/\bar{r}_{0f}^2$. This higher value indicates that (a) the *cis* state has a low probability, and/or (b) the *trans* state has a higher probability than previously suspected, and/or (c) certain states tend to propagate themselves leading to increased conformational order. Until further experimental information is available, a choice of one or more of the above as the correct explanation would be speculative.

2. Hydrocarbon Polymers

a. Polyethylene. Liquori's calculations for polyethylene predict two rotational states at 90° and 270° which were previously unsuspected. However, these additional states do not contribute to the dimensions of the "unrestricted" model since the sin 90° = 1, sin 270° = −1, and

$\cos 90° = 0$, $\cos 270° = 0$. Hence, the "unrestricted" dimensions remain identical to the freely rotating dimensions.

b. Isotactic Polypropylene. Due to the asymmetric nature of this chain, two different rotational angle functions are necessary. Liquori calculates six states for each of these.

c. Polyisobutylene. Liquori's calculations predict eight statistically independent rotational states. A significant feature of this chain is the absence of a *trans* state. Here, the symmetry of the chain causes the two rotational angle functions $u(\phi_1)$, $u(\phi_2)$ to be equal. As a result of Liquori's model which considers first and higher neighbor interactions, of the 8^2 possible pairs of rotational states, only twelve are energetically feasible:

$$\phi_1 = 85°, \phi_2 = 85°$$
$$\phi_1 = 155°, \phi_2 = 45°$$
$$\phi_1 = 45°, \phi_2 = 155°$$
$$\phi_1 = 205°, \phi_2 = 85°$$
$$\phi_1 = 160°, \phi_2 = 160°$$
$$\phi_1 = 85°, \phi_2 = 205°$$
$$\phi_1 = 275°, \phi_2 = 155°$$
$$\phi_1 = 155°, \phi_2 = 275°$$
$$\phi_1 = 200°, \phi_2 = 200°$$
$$\phi_1 = 205°, \phi_2 = 315°$$
$$\phi_1 = 315°, \phi_2 = 205°$$
$$\phi_1 = 275°, \phi_2 = 275°$$

Calculation of $\bar{r}^2/nl^2$ for models assuming statistically independent pairs of rotational states in the polyisobutylene chain will be made in a later publication.

The ratios of $\bar{r}_0^2/\bar{r}_{0f}^2$ for these three hydrocarbon chains infer that each has approximately the same conformational order or "stiffness." Comparison of $\bar{r}_0^2/\bar{r}_u^2$, however, clearly indicates that these three polymers are not equivalent. As stated previously, several possibilities will lead to high ratios of $\bar{r}_0^2/\bar{r}_u^2$. In this case, argument (1a) does not apply, because no *cis* state is available. Hence, the larger ratios imply higher population of the *trans* conformation and/or a higher degree of conformational order. The crystal structure of polyethylene and isotactic polypropylene reveal *trans* as a preferred conformation and larger values of $\bar{r}_0^2/\bar{r}_u^2$ imply retention in solution of some structural integrity from the crystalline state. Furthermore, the order of the ratios $(\bar{r}_0^2/\bar{r}_u^2)$ polyethylene $>$ isotactic polypropylene $>$ polyisobutylene is qualitatively consistent with Flory's theory of crystallization of semiflexible polymer molecules from dilute solutions.[17] The low value of 1.83 for polyisobutylene reflects this polymer's inability to crystallize from dilute solution.

As a final note, when more refined experimental and theoretical techniques are developed for delineation of the rotational potential energy function, more realistic values of $\bar{r}_u^2/nl^2$ can be easily calculated.

References

1. The number of excellent papers in this field far exceeds the limitations of space. A comprehensive discussion of many models is available in M. V. Vol'kenstein, *Configurational Statistics of Polymer Chains*, Publishing House, Academy of Sciences, U.S.S.R., Moscow, 1959.

2. Flory, P. J., C. A. J. Hoeve, and A. Ciferri, *J. Polymer Sci.*, **34**, 337 (1959).

3. Hoeve, C. A. J., *J. Chem. Phys.*, **35**, 1266 (1961).

4. Flory, P. J., *Principles of Polymer Chemistry*, Cornell Univ. Press, Ithaca, N. Y., 1953, p. 415.

5. Benoit, H., *J. Chim. Phys.*, **44**, 18 (1947).

6. Taylor, W. J., *J. Chem. Phys.*, **16**, 257 (1948).

7. De Santis, P., E. Giglio, A. M. Liquori, and A. Ripamonti, *J. Polymer Sci.*, **A1**, 1383 (1963).

8. Yokoi, M., *Bull. Chem. Soc. Japan*, **30**, 100 (1957).

9. Damaschun, G., *Kolloid-Z.*, **180**, 65 (1962).

10. Roth, W. L., and D. Harper, *Acta Cryst.*, **1**, 34 (1948).

11. Peyronel, G., *Atti Accad. Nazl. Lincei, Rend., Classe Sci. Fis., Mat. Nat.*, **15**, 402 (1953); *ibid.*, **16**, 78, 231 (1954).

12. Aggarwal, E. H., and S. H. Bauer, *J. Chem. Phys.*, **18**, 420 (1950).

13. Hartung, H. A., and S. M. Camiolo, papers presented to the Division of Polymer Chemistry, 141st National Meeting, American Chemical Society, Washington, D. C., March 1962.

14. Flory, P. J., L. Mandelkern, J. B. Kinsinger, and W. B. Schultz, *J. Am. Chem. Soc.*, **74**, 3364 (1952).

15. Kinsinger, J. B., private communication.

16. Lifson, S., *J. Chem. Phys.*, **29**, 80 (1958).

17. Flory, P. J., *Proc. Roy. Soc. (London)*, **A234**, 60 (1956).

Résumé

Les auteurs proposent qu'une chaîne polymérique ayant des états rotationnels également probables mais discrets soient appelés chaînes à rotation non restreinte. Ce modèle n'est équivalent à celui du modèle à rotation libre que dans des conditions bien spécifiques. A l'heure actuelle, il est de coutume de comparer les distances moyennes carrées entre extrémités de chaînes "non-perturbées" des polymères $(\bar{r}_0^2/nl^2)$ avec les valeurs correspondantes calculées au départ des modèles à rotation libre des chaînes polymériques. Toutefois la comparaison de $(\bar{r}_0^2/nl^2)$ à la dimension du modèle équivalent à rotation non-restreinte $(\bar{r}_u^2/nl^2)$ est une meilleure mesure de la rigidité de chaîne ou d'ordre conformationnel. Des calculs ont été effectués pour le polydiméthylsiloxane, le polyéthylène, le polypropylène isotactique et le polyisobutylène. On discute de la signification de $\bar{r}_0^2/r_u^2$ pour ces polymères.

Zusammenfassung

Die Autoren schlagen vor, eine Polymerkette mit gleich wahrscheinlichen, aber diskreten Rotationszuständen eine Kette mit "unbeschränkter" Rotation zu nennen. Dieses Modell ist dem "frei rotierenden" Modell nur unter spezifischen Umständen äquivalent. Es ist gegenwärtig üblich ungestörte quadratische Mittelwerte der End-zu-Enddimensionen von Polymeren $(\bar{r}_0^2/nl^2)$ mit den entsprechenden, aus dem frei rotierenden Modell einer Polymerkette berechneten Werten zu vergleichen. Der Vergleich von $(\bar{r}_0^2/nl^2)$ mit den äquivalenten Dimensionen des Modells mit "unbeschränkter" Rotation $(\bar{r}_u^2/nl^2)$ bildet jedoch ein besseres Mass für "Kettensteifigkeit" oder Konformationsordnung. Berechnungen für Polydimethylsiloxan, Polyäthylen, isotaktisches Polypropylen und Polyisobutylen werden durchgeführt. Die Bedeutung von r_0^2/r_u^2 für diese Polymeren wird diskutiert.

Competing Side Reactions in the Polymerization of α-Olefins by Ziegler-Natta Catalysts

A. D. KETLEY and J. D. MOYER, *W. R. Grace & Company, Washington Research Center, Clarksville, Maryland*

Synopsis

The polymerization of 3-methylbutene-1 by $TiCl_3$–$Al(C_2H_5)_3$ catalysts in dilute solution above 80°C. yields a polymer which is contaminated with polyethylene. By using tagged aluminum alkyl, this polyethylene was shown to arise almost wholly by displacement of ethylene from the alkyl by the monomer. This side reaction was shown to be a general one in the polymerization of α-olefins other than propylene at elevated temperatures. Analysis of the gas phase above the reaction showed also that some decomposition of the monomer occurs under these conditions.

INTRODUCTION

The polymerization of 3-methylbutene-1 by the system $TiCl_3$–$Al(C_2H_5)$ normally yields a highly isotactic, crystalline polymer with a melting-point of 300°C.[1,2] We have found, however, that when the polymerization is carried out in dilute solution in an inert solvent or at temperatures in excess of 80°C., the poly-3-methylbutene-1 is mixed with polyethylene which is present either as homopolymer or block copolymer. The source of this polyethylene is most reasonably ascribed to polymerization of ethylene which has been displaced from triethylaluminum by 3-methylbutene-1. Such a situation has been previously described in the polymerization of propylene by $TiCl_3$–$Al(C_2H_5)_3$ in which ethylene is claimed to be incorporated in the polymer.[3–5] It has been suggested that isotacticity is thus reduced and that, for this reason, the replacement of triethyl aluminum by tripropylaluminum leads to higher stereoregularity in the polymer.[6]

In the case of 3-methylbutene-1, side reactions can compete much more with the normal polymerization since this monomer is polymerized much more slowly by $TiCl_3$–$Al(C_2H_5)_3$ than is propylene. We have attempted first to determine, in the work reported here, whether the ethylene incorporated in the product does arise solely by displacement from the aluminum alkyl or whether other reactions such as concurrent, catalytic decomposition of the monomer play a part. Also we have tried to obtain some knowledge of the kinetics of the displacement reaction under polymerization conditions, that is, in the presence of $TiCl_3$. Finally we have determined, qualitatively, the degree of importance of these side reactions in the polymerization of other α-olefins by $TiCl_3$–$Al(C_2H_5)_3$.

RESULTS AND DISCUSSION

Figure 1 shows the infrared spectrum of poly-3-methylbutene-1 prepared by polymerization of bulk monomer at 60°C. with $TiCl_3$–$Al(C_2H_5)_3$. This spectrum has no absorption at 721 cm. characteristic of long-chain methylene groups.[7] There is, however, a very strong absorption at 760 cm^{-1} which we had previously assigned to the ethyl group.[7] The presence of this band has never before been noted in a α-olefin polymer which was known not to contain ethyl groups. It is not a crystallinity band since it is present in the molten polymer. We have, at present, no explanation for this absorption.
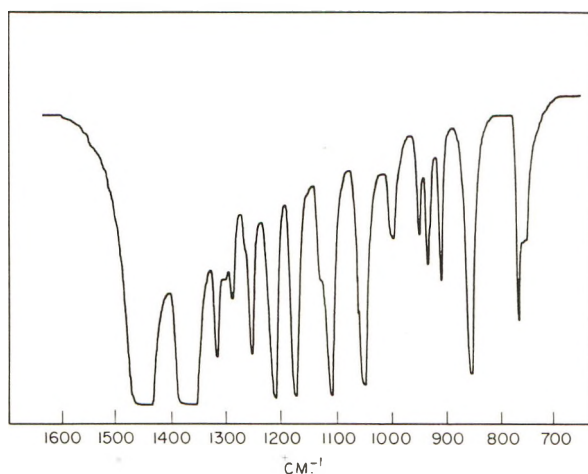

Fig. 1. Infrared spectrum of product from bulk polymerization of 3-methylbutene-1 at 60°C. Run 3-292B.
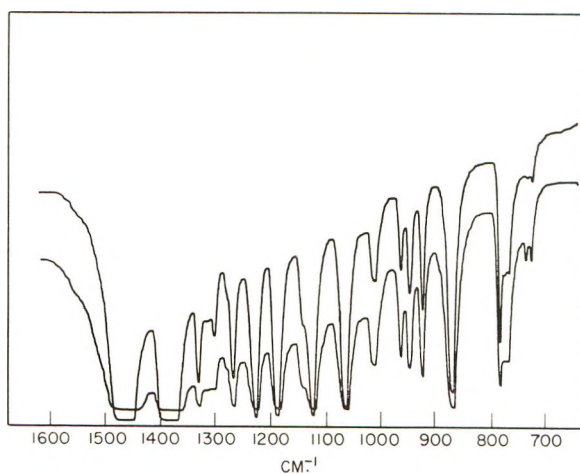

Fig. 2. Infrared spectrum of product from polymerization of 3-methylbutene-1 in cyclohexane at 60°C. Run 3-286A.
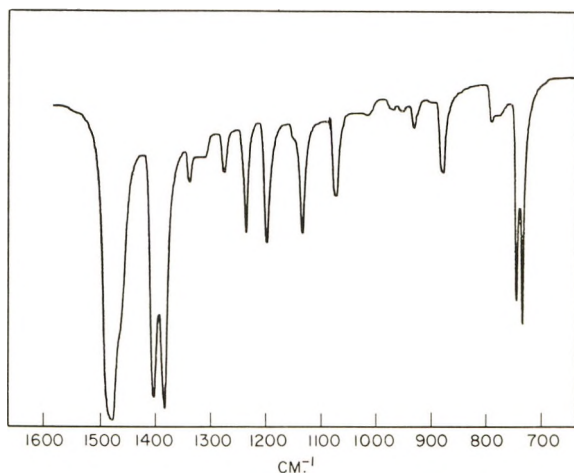
Fig. 3. Infrared spectrum of product from polymerization of 3-methylbutene-1 in cyclo-hexane at 120°C.   Run 3-286B.
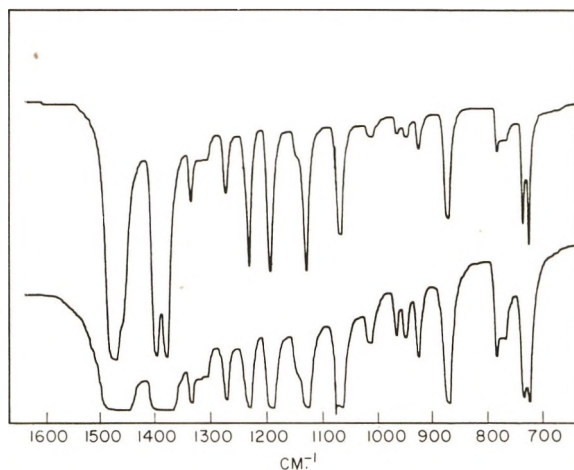
Fig. 4. Infrared spectrum of product from polymerization of 3-methylbutene-1 in cyclo-hexane at 90°C.   Run 3-286C.

Figures 2-4 show infrared spectra of the polymers prepared under the conditions shown in Table I.

TABLE I

Run No.[a]	TiCl$_2$, mole/l.	Al(C$_2$H$_5$)$_3$, mole/l.	Temp., °C.	3-Methyl-butene-1, ml.	Cyclo-hexane, ml.	Conversion, %
3-286A	0.20	0.20	60	25	75	16.7
3-286C	0.20	0.20	90	25	75	11.7
3-286B	0.20	0.20	120	25	75	8.7

[a] All runs were carried out for 3 hr.

All show marked absorptions at 721 cm.$^{-1}$ with, in each case, the band at 724 cm.$^{-1}$ due to the crystallization of long methylene chains. X-ray data on these polymers confirm the presence of crystalline polyethylene. The ethylene must therefore be present substantially either as homopolymer or as long blocks rather than as random copolymer with 3-methylbutene-1.

Evidence for Displacement of Ethylene from Triethylaluminum

The displacement of an olefin from an aluminum alkyl by another olefin is a well known and exhaustively studied reaction which will go to completion if the displaced olefin can be removed from the system. Ziegler has shown, for example, that propylene is evolved when triisopropylaluminum is boiled with 2-ethylhexene-1.[8] The reaction is first-order in triisopropylaluminum and zero-order in the olefin and proceeds at about the same rate when 2-ethylhexene-1 is replaced by styrene. However, the rate of decomposition of aluminum triethyl is rather slow; Ziegler has reported a half-life of 10 days at 120°C. It is somewhat surprising, therefore, that even at 60°C. the 3-methylbutene-1 polymer produced in 3 hr. should be considerably contaminated with polyethylene.

That the polyethylene does arise primarily from ethylene displaced from triethylaluminum is shown definitely by running reactions with C^{14}-labeled aluminum alkyl (Table II).

TABLE II

Run No.[a]	TiCl$_3$, mole/l.	Al(C$_2$H$_5$)$_3$, mole/l.[b]	Temp., °C.	Time, hr.	Conversion, %	Polymer activity, μ c./mg.	Polyethylene (by C^{14} assay), wt.-%
1200-11B	0.20	0.40	120	5	6.8	1.55 × 10^{-3}	61
1067-42A	0.20	0.40	120	36	15.4	7.2 × 10^{-4}	28
1200-11A	0.20	0.40	60	5	5.0	5.4 × 10	2

[a] All runs using 25 ml. 3-methylbutene-1 in 75 ml. cyclohexane.

[b] Al(C$_2$H$_5$) assayed as 1.54 μc./ml. (see experimental section).

The total activity in both the samples prepared at 120°C. is about 1.7 μc., while the total activity of the Al(C$_2$H$_5$)$_3$ used is about 6 μc. It appears, therefore, as if one ethyl group per triethylaluminum has been replaced rapidly while further displacement is slow.

Natta has polymerized propylene with TiCl$_3$ and C^{14}-labeled Al(C$_2$H$_5$)$_3$.[11] The presence of activity in the polymer has been cited as evidence that polymerization is initiated by ethyl groups on the aluminum alkyl. Al-(C$_2$H$_5$)$_3$-C^{14} has also been used to measure chain transfer of growing chains with the alkyl.[12] Since the presence of crystalline polyethylene has been observed in our case, the C^{14} incorporation could not have been wholly due to initiation or transfer reactions. Unless displacement of ethylene C^{14} from Al(C$_2$H$_5$)$_3$ by monomer can be completely ruled out the results quoted by Natta are somewhat ambiguous. However, it will be shown later that

even for an extreme case, no spectral evidence for the presence of polyethylene could be found when propylene was polymerized. Nevertheless, it does seem likely that at least some displacement takes place since we have shown that at 70°C., C^{14}-labeled ethylene will slowly react, with $Al(C_2H_5)_3$ to give active aluminum alkyl (see experimental section).

When triethylaluminum is replaced by triisobutylaluminum, no polyethylene is observed in the infrared spectra of polymers prepared at 60, 90, and 120°C. These spectra are identical to that of poly-3-methylbutene-1 prepared in bulk at 60°C. Although displacement may take place in this case also, the displaced olefin, isobutylene, is not polymerized by the $TiCl_3$–AlR_3 system. Curiously, whereas with triethylaluminum the system becomes progressively less active with increasing temperature (Table I) this is not so with triisobutylaluminum, which shows the same activity (in grams polymer/gram catalyst/hour) at 90°C. as at 60°C. Whether the loss in activity and formation of ethylene are connected in the $Al(C_2H_5)_3$ case we do not know. It is interesting to note, however, that the first-order rate constants for 3-methylbutene-1 polymerization in Table III are constant under conditions where no polyethylene is observed in the infrared but fall sharply when polyethylene is present.

TABLE III

Run No.	$TiCl_3$, mole/l.	$Al(C_2H_5)_3$, mole/l.	Temp., °C.	3-Methyl-butene-1, mole/l.	K_1 hr.$^{-1}$	Poly-ethylene infrared
3-348	0.07	0.07	60	4.4	3.4	—
3-360	0.07	0.07	60	3.5	3.5	—
3-348D	0.07	0.07	60	2.2	3.1	—
3-348B	0.07	0.07	60	1.5	3.2	—
3-363	0.07	0.07	60	0.7	2.1	+

Table IV shows relative amounts of polyethylene formed in a given time for a number of different reaction conditions. These values were estimated from the infrared spectra as described in the experimental section. These results suggest that the rate of polyethylene formation shows a first-order dependence on triethylaluminum concentration but little or no dependence on $TiCl_3$ concentration. Although the order with respect to 3-methylbutene-1 has not been checked, it must be less than the order of poly-3-methylbutene-1 formation, since, as shown in Table III,

TABLE IV

Run No.	$TiCl_3$, mole/l.	$Al(C_2H_5)_3$, mole/l.	Temp., °C.	3-Methyl-butene-1, mole/l.	K_1, hr.$^{-1}$	Relative polyethylene
3-376	0.07	0.07	90	2.2	1.4×10^{-2}	1.0
3-384	0.07	0.04	90	2.2	1.3×10^{-2}	2.4
3-388	0.14	0.14	90	2.2	1.5×10^{-2}	2.6

polyethylene is observed only as the monomer concentration is decreased. Since the poly-3-methylbutene-1 formation is first-order, the formation of polyethylene is presumably zero-order in 3-methylbutene-1. This agrees with the unimolecular decomposition of triethylaluminum as the rate-determining step followed by fast polymerization of the resulting ethylene:

$$Al(C_2H_5)_3 \xrightarrow{\text{slow}} Al(C_2H_5)_2H + C_2H_4 \xrightarrow{\text{fast}} -CH_2-_n$$
$$\downarrow C_5H_{10}$$
$$Al(C_2H_5)_2(C_5H_{11})$$

The evidence thus far suggests that the above is the only route by which polyethylene is formed. However, when the gas above the reaction vessel is analyzed by gas chromatography, ethylene and ethane are found, as expected, but also considerable concentrations of propylene and propane, the former in particular. We have shown that the monomer is completely free from these materials. We have shown, further, that when the $Al(C_2H_5)_3$ used is decomposed by acid, no propylene or propane is evolved—in other words, no tripropylaluminum is present. From the reactants present, then, the only possible source of propylene would seem to be decomposition of the monomer into propylene and ethylene. We have no theories as to how such a decomposition can come about, nevertheless, there is some evidence that it does, indeed, take place. This is presented in the next section. However, since there is no evidence for polyethylene in the infrared spectra of polymers prepared with triisobutylaluminum, this reaction, if indeed it does occur, must be of small significance.

Monomers Other Than 3-Methylbutene-1

Figures 5 and 6 show infrared spectra of 3,3-dimethylpentene-1 polymerized in bulk with $TiCl_3–Al(C_2H_5)_3$ at 60°C. and vinylcyclohexane polymer-

Fig. 5. Infrared spectrum of product from polymerization of bulk 3,3-dimethylpentene-1 at 60°C. Run 3-277.
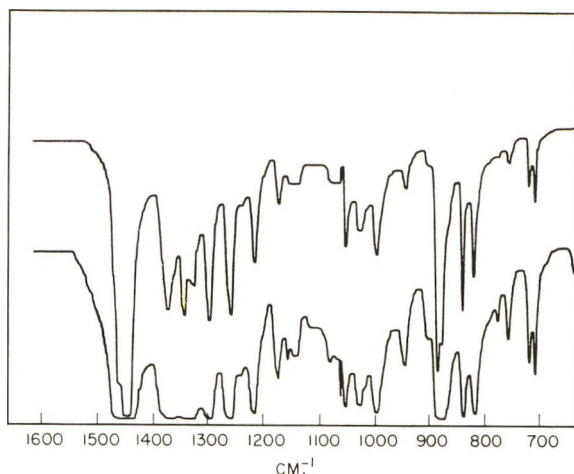
Fig. 6. Infrared spectrum of product from polymerization of vinylcyclohexane at 80°C. Run 3-283.

ized by the same catalyst at 80°C. in 25% solution in cyclohexane, respectively. Both show considerable polyethylene incorporation; in fact, the same general results have been obtained with vinyl-cyclohexane as with 3-methylbutene-1. The relative ease with which monomers displace ethylene from triethylaluminum under these conditions appears to be: 3-methylbutene-1 = vinylcyclohexane > 3,3-dimethylheptene-1 = 3,3-dimethylbutene-1 >, butene-1, = pentene-1, hexene-1, heptene-1, octene-1. Propylene, even at low pressures (5 psi) and high temperatures (190°C.), gave only polypropylene and no evidence at all for polyethylene.

Analysis of the gas phase in the cases of the linear olefins showed only ethylene and ethane present when the monomer had an even number of carbon atoms but propylene when the number was odd. This, again, suggests that some "unzipping" of the olefin takes place. No evidence for the presence of isobutylene could be found, however, in the case of 3,3-dimethylbutene-1.

EXPERIMENTAL

Materials

3-Methylbutene-1 was Matheson C. P. grade. It was stored at −20°C. over CaH_2 before use. Impurities boiling below the monomer, as measured by gas chromatography, were negligible.

3,3-Dimethyl-1-butene was obtained as a research sample from Sinclair Petrochemicals Inc. It was washed with water to remove any inhibitor and dried over solid KOH. Before use it was distilled over sodium through a 50-cm. column and a cut b.p. 43.0–43.5°C. taken.

3,3-Dimethyl-1-pentene was obtained from Sinclair and treated as described above. A fraction B.P. 77.5–78.0°C. was used.

Vinylcyclohexane was practical grade obtained from Matheson, Coleman and Bell. After water washing and drying it was distilled over sodium through a microdistillation apparatus. A fraction boiling at 125.0°C. at 755 mm. was used.

4-Vinylcyclohexene was also obtained from Matheson, Coleman and Bell. It was purified in the same way as vinylcyclohexane. Material boiling at 127.5°C. at 763 mm. was used.

$TiCl_3$ was obtained from Stauffer; HA grade was used.

Triethylaluminum was obtained pure from Ethyl Corp. and diluted to 25% before use with n-heptane.

Triisobutyl aluminum was obtained as a 25% solution in n-heptane from Ethyl Corp.

Cyclohexane was pure grade from Phillips Petroleum. It was dried over silica gel before use.

Preparation of $Al(C_2H_5)_3$-C^{14}

A 1-mc. quantity of ethylene-1,2-C^{14} (New England Nuclear) was transferred to an evacuated 5-liter steel bomb, equipped with valving and a pressure gauge, and diluted with 8 atm. of Phillips research grade ethylene. This was then connected to another cylinder, previously purged with ethylene, containing 119.5 g of triethylaluminum, diethylaluminum hydride mixture (Ethyl Corp. analysis: 38.5% diethylaluminum hydride). This latter cylinder was placed in a constant temperature bath at 70°C. and allowed to remain there until the pressure in the ethylene cylinder remained constant (approximately 24 hr.).

A known volume of this material was then syringed into a flask through a rubber septum and frozen in liquid nitrogen. The flask was connected to a Nuclear Chicago Model GW-1 wet oxidation and transfer apparatus. Concentrated sulfuric acid was then added to the flask. The liquid nitrogen bath was then removed and the mixture allowed to warm-up. The evolved gases were collected in a 250-ml. ionization chamber which was then brought to atmospheric pressure by flushing nonactive ethylene through the reaction flask. The chamber was transferred to a Dynacon vibrating reed electrometer (Nuclear Chicago Corp.) and the current across the chamber due to the applied potential measured. This current is proportional to the C^{14} concentration.[9] The system was calibrated against 1 ml. of N.B.S. C^{14} standard Na_2CO_3 solution (0.0338 c./g.) which was decomposed with acid as described above.

$Al(C_2H_5)_3$-C^{14} prepared in this way gave consistently higher activities than would be expected from the Et_2AlH content of the mixture. That this was due to a displacement reaction was shown by taking nonradioactive 100% triethylaluminum and allowing it to equilibrate with 100 psi ethylene-C^{14} (138 μc./mole) for 36 hr. at 70°C. Ethylene was then removed and the $Al(C_2H_5)_3$ pumped at high vacuum for 2 hr. to remove dissolved ethylene. The $Al(C_2H_5)_3$ remaining had an activity of 0.15 μc./ml.

Counting of Polymer Samples

Polymer samples were oxidized in the wet-oxidation and transfer apparatus by a variation of the method of Van Slyke and Folch.[10]   The CO_2 evolved was collected in the ionization chamber, brought to atmospheric pressure with nonactive CO_2, and the C^{14} content measured as described in the previous section.

Preparative Runs

Preparative runs were carried out in Fischer-Porter aerosol bottles fitted with plug valves and magnetic stirrers.   Monomer, solvent, $TiCl_3$, and aluminum alkyl were added in that order to the bottles in a nitrogen filled dry bag and then the plug valves closed.   The bottles were then transferred rapidly to an oil bath thermostated at the desired temperature.   At the completion of the run an isopropanol–HCl quench solution was syringed into the bottles.   The polymer was filtered, washed with further isopropanol, and dried at 60°C. in a vacuum oven.

Kinetic Runs

Kinetic runs were also carried out by Fischer-Porter aerosol bottles. In these cases the plug valves were fitted with long copper water-cooled condensers to prevent loss of 3-methylbutene when aliquots were taken from the bottles.   At various times during the reaction the bottles were quickly taken from the thermostat baths, shaken vigorously, inverted and the plug valve opened and an aliquot was run carefully into a graduated cylinder.   The aliquot was then quenched and the polymer filtered and cleaned up in the usual way.   After drying, the polymer samples were carefully weighed.   Rate constants were then calculated from t versus log $(a - x)$ plots.

Per Cent Polyethylene from Infrared Spectra

Polymer samples were run as KBr pellets.   Relative amounts of polyethylene in the samples were obtained from the values of the ratios of the band heights of the 721 cm.$^{-1}$ methylene rocking vibration of polyethylene to the 1375 cm.$^{-1}$ methyl vibration of poly-3-methylbutene-1.

Gas Chromatography

Samples were collected either by flushing some of the gas from the reactor dead-space through mass-spectrometer bombs or by collecting the gas in evacuated Fischer-Porter aerosol tubes.   Gas chromatography was carried out with a Perkin-Elmer Model 154C vapor fractometer with 6 ft. $AgNO_3$/diethylene glycol and 12 ft. di-n-butyl maleate columns at room temperature.

References

1. Montecatini and K. Ziegler, Belg. Patent 549,891 (July 28, 1956).

2. Reding, F. P., and E. R. Walter, *J. Polymer Sci.*, **37**, 555 (1959).

3. Montecatini and K. Ziegler, Belg. Patent 538,782 (June 6, 1955).

4. Montecatini and K. Ziegler, Austral. Pat. Appl. 9651/55 (June 6, 1955).

5. Montecatini and K. Ziegler, Fr. Pat. 1,138,290 (June 12, 1957).

6. *Linear and Stereoregular Addition Polymers*, N. Gaylord and H. Mark, Interscience, New York, 1959, p. 129.

7. Harvey, M. C., and A. D. Ketley, *J. Appl. Polymer Sci.*, **5**, 247 (1961).

8. Ziegler, K., W. R. Kroll, W. Larbig, and O. W. Stendel, *Ann.*, **629**, 53 (1960).

9. Tolbert, B. M., *AEC Report*, UCRL 3499.

10. Van Slyke, D. D., and J. Folch, *J. Biol. Chem.*, **136**, 509 (1940).

11. Natta, G., G. Pajaro, L. Pasquon, and V. Stellacci, *Atti Accad. Nazl. Lincei Rend. Classe Sci. Fis. Mat. Nat.*, [8], **24**, 479 (1958).

12. Natta, G., L. Pasquon, E. Giachetti, and G. Pajaro, *Chim. Ind. (Milan)*, **40**, 267 (1958).

Résumé

La polymérisation du 3-méthylbutène-1 sous l'action du catalyseur TiCl$_3$-Al(C$_2$H$_5$)$_3$ en solution diluée au-dessus de 80°C fournit un polymère, contaminé de polyéthylène. En utilisant de l'alcoyl-aluminium marqué, on a démontré que ce polyéthylène provient du déplacement de l'éthylène des groupes alcoyles par le monomère. On a montré que cette réaction secondaire a toujours lieu dans la polymérisation des alpha-oléfines autres que le propylène, à haute température. Une analyse de la phase gazeuse au dessus du mélange réactionnel a démontré qu'une certaine décomposition du monomère a lieu dans les conditions opératoires réalisées.

Zusammenfassung

Die Polymerisation von 3-Methylbuten-1 mit einem TiCl$_3$-Al(C$_2$H$_5$)$_3$-Katalysator liefert in verdünnter Lösung oberhalb 80°C ein Polyäthylenhältiges Polymeres. Durch Verwendung eines markierten Aluminiumalkyls konnte nachgewiesen werden, dass dieses Polyäthylen fast völlig durch Verdrängung des Äthylens aus dem Alkyl durch das Monomere entsteht. Diese Nebenreaktion tritt allgemein bei der Polymerisation von α-Olefinen, mit Ausnahme von Propylen bei erhöhter Temperatur ein. Eine Analyse der Gasphase über dem reagierenden System zeigte, dass auch eine gewisse Zersetzung des Monomeren unter diesen Bedingungen stattfindet.

Behavior of Polymer Solutions in the Velocity Field with Parallel Gradient.   III. Molecular Orientation in Dilute Solutions Containing Flexible Chain Macromolecules

RACHELA TAKSERMAN-KROZER, *Institute of General Chemistry. Department of Technical Physics, Warszawa-Żoliborz, Poland*

Synopsis

The orientation of flexible, coiled, chain macromolecules in the velocity field with parallel gradient has been analyzed on the basis of the subchain model. It has been found that the axial orientation factor in the steady state depends only on the velocity gradient q, diffusion constant D, and molecular dimensions. The internal viscosity of macromolecule has no influence upon the steady-state orientation factor. The relation describing the time dependence of the orientation factor have also been derived.

Introduction

In the previous papers[1,2] some hydrodynamic properties of polymer solutions containing rigid, ellipsoidal particles when subject to uniaxial drawing (velocity field with parallel gradient) were analyzed. In this and the following paper,[3] relations will be derived describing the orientation and intrinsic viscosity of solutions of statistically coiled chain macromolecules flowing in the velocity field with parallel gradient.

Definition of Molecular Model

The analyzed system is a dilute, monodisperse polymer solution. To describe the behavior of a flexible chain macromolecule the subchain model has been chosen, which permits one to allow for hydrodynamic interactions between individual parts of the long chain and effects of limited flexibility ("internal viscosity" of the macromolecule). According to this model, the macromolecule is considered to be composed of N Gaussian subchains, each subchain involving n statistical (Kuhn) segments of length a (Fig. 1). The interaction between macromolecule and liquid (resistance of flow) is thought to be localized in the $(N + 1)$ junction points of the subchains.

Anisotropy of the System and Axial Orientation Factor

The optical anisotropy may be described with an aid of a tensor of polarizability. Kuhn and Grün[4] have calculated the polarizabilities of a
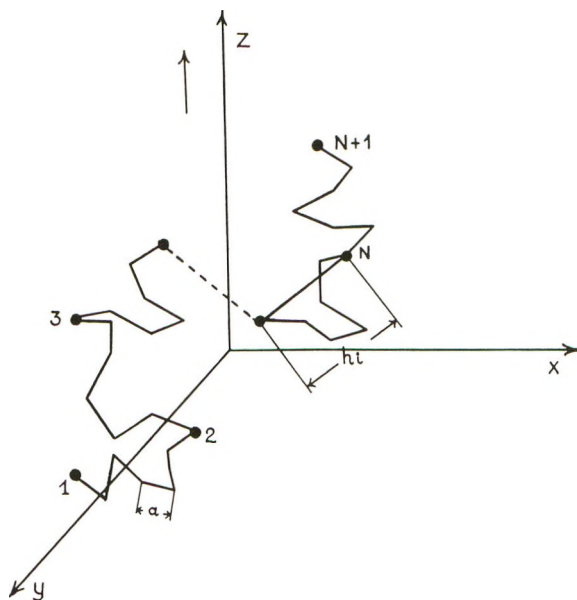
Figure 1.

single statistical chain (elastic dumbbell, Kuhn model), which may be considered to be a single subchain in the present treatment. Let $\gamma_{1,i}$ be the polarizability component along the vector $\mathbf{h}_i$ joining the two ends of the ith subchain, and $\gamma_{2,i} = \gamma_{3,i}$ polarizability components perpendicular to that vector. According to Kuhn and Grün, in the Gaussian approximation (small extensions):

$$\gamma_{1,i} = n(\alpha_1 + 2\alpha_2)/3 + 2(\alpha_1 - \alpha_2)/h_i^2/5na^2$$

$$\gamma_{2,i} = n(\alpha_1 + 2\alpha_2)/3 - (\alpha_1 - \alpha_2)/h_i^2/5na^2 \tag{1}$$

where α_1, α_2 are the main polarizabilities of the statistical segment. The difference between polarizability components parallel and perpendicular to the vector $\mathbf{h}_i$ amounts to:

$$\gamma_{1,i} - \gamma_{2,i} = {}^3/_5(\alpha_1 - \alpha_2)h_i^2/na^2 \tag{2}$$

The expression (2) is valid for small extensions only. For large deformations, the Gaussian statistics should be replaced by another one; in the region of large extensions better approximation gives an inverse Langevin function $\mathcal{L}^*$:

$$\alpha_{1,i} - \alpha_{2,i} = n(\alpha_1 - \alpha_2)[1 - (3h_i/na)/\mathcal{L}^*(h_i/na)] \tag{3}$$

The present paper will involve only Gaussian approximation.

The polarizability of the whole macromolecule is a sum of contributions from N subchains. Expressed in the fixed-in-space coordinates x, y, z the average polarizability of the total system, $\overline{\mathbf{P}}$ may be written as:[5]

$$\bar{P} = (N + 1)[n(\alpha_1 + 2\alpha_2)/3 - (\alpha_1 - \alpha_2)/5]E + [3(\alpha_1 - \alpha_2)/5na^2]$$

$$\begin{pmatrix} \langle x^T A x \rangle & \langle x^T A y \rangle & \langle x^T A z \rangle \\ \langle y^T A x \rangle & \langle y^T A y \rangle & \langle y^T A z \rangle \\ \langle z^T A x \rangle & \langle z^T A y \rangle & \langle z^T A z \rangle \end{pmatrix} \quad (4)$$

where **x**, **y**, **z** are vectors in the $(N + 1)$-dimensional space of the individual junction points of subchains.

A is a matrix:

$$A = \begin{pmatrix} 1 & -1 & 0 & 0 & \ldots & 0 & 0 \\ -1 & 2 & -1 & 0 & \ldots & 0 & 0 \\ 0 & -1 & 2 & -1 & \ldots & 0 & 0 \\ \multicolumn{7}{c}{\ldots\ldots\ldots\ldots\ldots\ldots\ldots} \\ 0 & 0 & 0 & 0 & \ldots & 2 & -1 \\ 0 & 0 & 0 & 0 & \ldots & -1 & 1 \end{pmatrix} \quad (5)$$

For the liquid flowing in the velocity field with parallel gradient $V(-qx/2, -qy/2, qz)$ the difference of average polarizabilities ΔP in the direction of z (unique axis) and x, y amounts to:

$$\Delta\bar{P} = 3(\alpha_1 - \alpha_2)/5na^2[\langle z^T A z \rangle - \langle x^T A x \rangle] \quad (6)$$

The amount of streaming birefringence is proportional to the difference $\Delta\bar{P}$ (anisotropy of polarizability) and the concentration of the macromolecules in the solution. As in the previous paper,[1] the average degree of orientation will be described with an aid of a dimensionless axial orientation factor f, i.e., the ratio of average anisotropy of polarizability of the system, to that anisotropy of polarizability which the same system would possess if all the macromolecules were ideally extended and aligned parallel with the direction z:

$$f = \Delta\bar{P}/\Delta P_{id} = {}^3/_5[\langle z^T A z \rangle - x^T A x]/Nn^2a^2 \quad (7a)$$

Factor f expressed in spherical coordinates is:

$$f = {}^3/_5 \sum_{i=1}^{N} \langle h_i^2(1 - {}^3/_2 \sin^2\theta_i)\rangle/Nn^2a^2 \quad (7b)$$

The last formula is consistent with expressions given in our previous papers for rigid particles[1,6] and by Ziabicki for single Kuhn chains.[6]

Axial Orientation Factor in Steady Flow

The analysis of motion of a flexible chain in the velocity field with parallel gradient is the subject of another work.[7] The basis for calculation of the distribution function ψ is the equation of diffusion:

$$\partial\psi/\partial t = q/2(\partial\psi/\partial x)^T x + q/2(\partial\psi/\partial y)^T y - q(\partial\psi/\partial z)^T z$$

$$+ \sum_{u = x,y,z} \{D(\partial/\partial u)^T H(\partial\psi/\partial u) + \sigma(\partial\psi/\partial u)^T H A u + \sigma\psi(\partial/\partial u)^T H A u$$

$$+ \psi\rho[\partial/\partial u)^T H A \dot{u} d + \rho(\partial\psi/\partial u)^T H A \dot{u} d\} \quad (8)$$

where

$$\sigma = 3D/na^2$$

and D is the translational diffusion constant, q is the velocity gradient ρ is the ratio of internal to external friction coefficients, and $\mathbf{H}$ is the matrix of hydrodynamic interactions. After Kirkwood and Riseman:[8]

$$\mathbf{H} = \mathbf{T} + \mathbf{E}$$

where

$$\mathbf{T} = \begin{pmatrix} 0 & 1 & 2^{-1/2} & \cdots & N^{-1/2} \\ 1 & 0 & 1 & \cdots & (N-1)^{-1/2} \\ \cdots\cdots\cdots\cdots\cdots\cdots\cdots\cdots\cdots\cdots\cdots\cdots\cdots \\ N^{-1/2} & (N-1)^{-1/2} & (N-2)^{-1/2} & \cdots & 0 \end{pmatrix} \qquad (9)$$

$\mathbf{E}$ is the unit matrix, and $\psi\,(x_0, y_0, z_0, x_1, \ldots, z_N t)$ is the distribution function of subchains. It has been shown[7] that in the steady state $(\partial\psi/\partial t = 0)$ all the terms in eq. (8) involving the ratio ρ drop out because the deformation rate of a macromolecule in steady flow is zero. To obtain the solution, eq. (8) was transformed into the normal coordinates (cf. Zimm[5]) u, v, w. After transformation, the equation for diffusion for the steady state reads:

$$\sum_{i=1}^{N} \left\{ -3qw_i/2 + \sum_{\xi=u,v,w} [Dv_i(\partial^2\psi/\partial\xi^2) + (\sigma\lambda_i + q/2)\xi_i(\partial\psi/\partial\xi_i)] + 3\sigma\lambda_i\psi \right\} = 0 \quad (10)$$

and for $q = 0$ (solution at reset):

$$\psi_0 = \text{const. exp}\left\{ -\sigma/2D \sum_{i=1}^{N} \mu_i(u_i^2 + v_i^2 + w_i^2) \right\} \qquad (11)$$

The coefficients λ_i, μ_i, ν_i, as related to diagonalization of matrices $\mathbf{HA}$, $\mathbf{A}$, and $\mathbf{H}$ have been calculated for free-draining coils by Zimm:[5]

$$\lambda_i = \pi^2 i^2/N^2$$
$$\mu_i \approx \lambda_i$$
$$\nu_i \approx 1 \qquad (12)$$

The orientation factor in normal coordinates is:

$$f = \sum_{i=1}^{N} 3\mu_i/5Nn^2a^2[\langle w_i^2 - u_i^2 \rangle] \qquad (13)$$

The averaging of expressions u_i^2 and w_i^2 was accomplished directly in eq. (10) by multiplication of all terms by u_i^2 or w_i^2 and integration over the whole space.* This yielded

* This averaging may also be accomplished on the basis of the distribution function ψ written explicitly:[7]

$$\psi = 1/\pi^{3N/2} \prod_{i=1}^{N} [(\sigma\mu_i/2D)^{3/2}(1 + q/2\sigma\lambda_i)(1 - q/\sigma\lambda_i)] \exp\left\{ \sum_{i=1}^{N} (-\sigma\mu_i/2D) \right.$$
$$\times [(1 + q/2\sigma\lambda_i)(u_i^2 + v_i^2)] - [1 - (q/\sigma\lambda_i)w_i^2]\Big\}$$

$$\langle u_i^2 \rangle = D \nu_i / (\sigma \lambda_i + q/2) \tag{14}$$

$$\langle w_i^2 \rangle = D \nu_i / (\sigma \lambda_i - q) \tag{15}$$

Putting eqs. (14) and (15) into eq. (13) yields:

$$f_{st} = 9qD/5Nn^2a^2 \sum_{i=1}^{N} \lambda_i / (\sigma \lambda_i - q)(2\sigma \lambda_i + q) \tag{16}$$

It may be noted that the orientation factor in the steady state does not depend on the internal viscosity of macromolecules. For $q = 0$ we obtain $f_{st} = 0$, which might be expected regarding the physical sense of the orientation factor. The asymptotical value of f for q approaching infinity may not be calculated from our Gaussian approximation. The Gaussian model superposes a limit on the maximal velocity gradient:

$$q_{max} \ll \sigma \lambda_1$$

For the estimation of q_{max} we will express the product $\sigma \lambda_1$ through the intrinsic viscosity at zero gradient $[\eta]_0$. As will be shown in a subsequent paper:[3]

$$[\eta]_0 = 3RT/2M\eta_0\sigma \sum_{i=1}^{N} 1/\lambda_i = RTN^2/4M\eta_0\sigma \tag{17}$$

where M is molecular weight, T is absolute temperature, R is the gas constant, and η_0 is the viscosity of the solvent.

Taking into account eqs. (12) and (17) the condition for the maximal gradient may be written in the form:

$$q_{max} \ll \pi^2 RT/4M\eta_0[\eta]_0$$

For instance, for a polystyrene with $M = 200,000$, solvent viscosity $\eta_0 = 1$ cpoise, and $T = 300°K$. we have:

$$q_{max} \ll 3 \times 10^4 \text{ sec.}^{-1}$$

It may be noted that the parallel velocity gradient usually occurring in fiber-spinning or liquid jet problems does not exceed 10^2sec.^{-1}.

We will now introduce the symbols:

$$\bar{m} = M/L$$

$$\alpha = q/D$$

$$\beta = \alpha[\eta]_c\bar{m}$$

where $\bar{m}$, the molecular weight per unit length of extended chain, is a polymer constant.

It has been shown by Rouse[9] that for large N, $[\eta]_0$ approximately does not depend on the way in which the macromolecule is divided into subchains. Consequently, the parameter β and all the quantities expressed only by β are also (approximately) independent of N.

Therefore we may write the orientation factor in the form:

$$f_{st} = (s/p)(32\beta/5\pi^3) \sum_{i=1}^{N} i^2/(i^2 - 32\beta/3\pi^3)(2i^2 + 32\beta/3\pi^3) \quad (18)$$

where p is the degree of polymerization and s is the number of monomer units per statistical chain segment.

In a similar way, the axial orientation factor may be calculated for the more simple molecular elastic dumbbell model (Kuhn model). The equation of diffusion for this case in steady flow with a parallel velocity gradient reads:

$$(qx/2)(\partial\psi/\partial x) + (qy/2)(\partial\psi/\partial y) - qz(\partial\psi/\partial z) + D\Delta\psi + \sigma[3\psi$$
$$+ x(\partial\psi/\partial x) + y(\partial\psi/\partial y) + z(\partial\psi/\partial z)] = 0 \quad (19)$$

In the case of elastic dumbbells, the distribution function $\psi(x, y, z)$ determines the probability density of finding one dumbbell end in the region $dx\,dy\,dz$, the other one being fixed in the origin of the coordinate system. For this model according to eq. (19):

$$\langle x^2 \rangle = D/(\sigma + q/2)$$
$$\langle z^2 \rangle = D/(\sigma - q) \quad (20)$$

and
$$f_{st} = (s/p)(9D/5n^2a^2)[1/(\sigma - q)(2\sigma + q)] \quad (21)$$

or
$$f_{st} = (s/p)(16\beta/15\pi)[1/(1 - 16\beta/9\pi)(2 + 16\beta/9\pi)] \quad (22)$$

In Figure 2 the expressions $(f_{st}\,p/s)$ are plotted versus β for both molecular models. It is evident that the both curves are of similar shape, the dif-
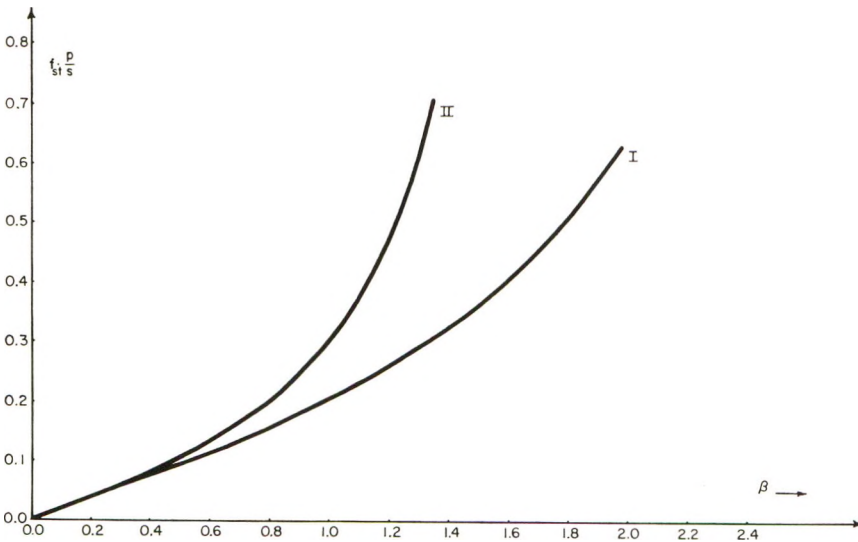

Fig. 2. Steady-state orientation factor vs. parameter β for flexible chain macromolecules: (*I*) subchain model; (*II*) elastic dumbbells (Kuhn model).
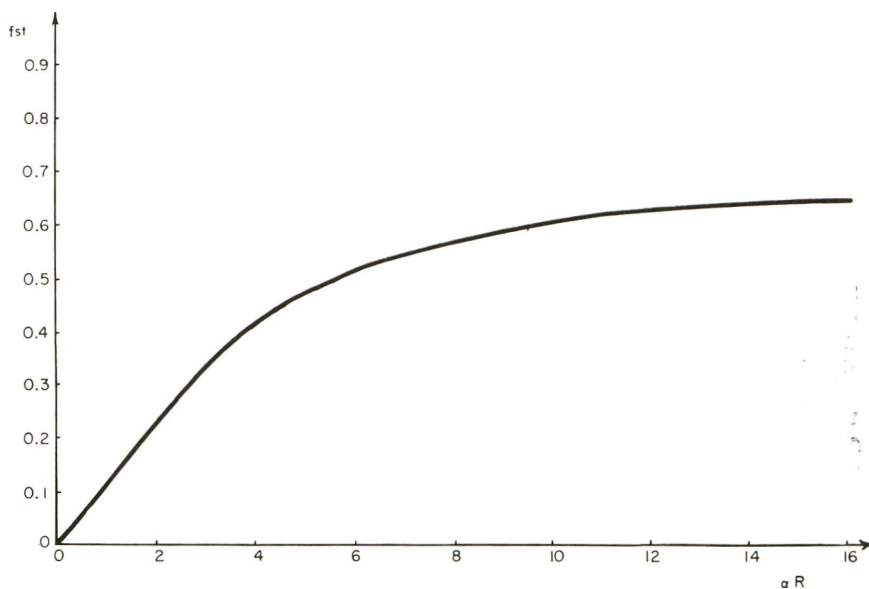
Fig. 3. Steady-state orientation factor vs. parameter αR for rigid ellipsoidal particles (after Takserman-Krozer and Ziabicki[1]).

ferences being quantitative rather than qualitative. An analogous relation f_{st} versus (αR) for rigid ellipsoids is shown in Figure 3.

A comparison of Figures 2 and 3 makes it evident that the orientation factor for flexible chains increases more rapidly with velocity gradient (parameter β) than that for rigid particles (parameter αR). The differences in the shape of the characteristics $f_{st}-(\alpha R)$ and $(f_{st}p/s)-\beta$ are due to deformability of chain macromolecules. For rigid, undeformable ellipsoids, the orientation factor depends only on the average angle θ between the axes of the ellipsoids and the direction of flow. The orientation change produced by an increase of velocity gradient is, however, less effective when this angle is smaller; hence $f_{st}-q$ (or $f_{st}-\alpha R$) characteristic is convex. For flexible, deformable chains, the orientation factor depends not only on the average orientation angle, but also on the degree of extension h/L. The change of orientation factor with increasing velocity gradient q (or parameter β) is affected by two opposite agents: it increases with deformation ratio h/L and decreases with decreasing orientation angle θ, the former effect being evidently stronger, as shown by the concave $f_{st}-\beta$ characteristic.

It may be noted that analogous differences in orientational behavior between rigid and flexible macromolecules have been found by other authors[10] in the velocity field with perpendicular gradient.

Time-Dependent Orientation Factor

In order to obtain the time-dependence of the axial orientation factor, the averages of the terms u_i^2 and w_i^2 were obtained on the basis of the non-

steady-state diffusion equation. The calculations were carried out for the case with zero internal viscosity ($\rho = 0$):

$$\partial\psi/\partial t = \sum_{i=1}^{N} \{(q/2)u_i(\partial\psi/\partial u_i) + (q/2)v_i(\partial\psi/\partial v_i) - qw_i(\partial\psi/\partial w_i)$$
$$+ \sum_{\xi = u,v,w} [Dv_i(\partial^2\psi/\partial\xi_i^2) + \sigma\lambda_i(\psi + (\xi_i\partial\psi/\partial\xi_i))]\} \quad (23)$$

From eq. (23) we obtained:

$$\langle u_i^2 \rangle = Dv_i/(\sigma\lambda_i + q/2) + C_{1,i}\exp\{-(2\sigma\lambda_i + q)t\}$$
$$\langle w_i^2 \rangle = Dv_i/(\sigma\lambda_i - q) + C_{2,i}\exp\{-(2\sigma\lambda_i - 2q)t\} \quad (24)$$

$C_{1,i}$ and $C_{2,i}$ (the integration constants) can be determined from corresponding initial conditions.

We assume that at time $t = 0$, a velocity field with constant gradient q is instantly switched on. Since our molecular model involves Hookean elasticity, at $t = 0$ an instant deformation of macromolecules must occur. This deformation may be calculated from the force balance equation:

$$(3kT/na^2)\lambda_i u_{i(t=0)} = -kT(\partial \ln \psi_0/\partial u_i) + fu_i^{\circ} \quad (25)$$

where: $-kT(\partial\ln\psi_0/\partial u_i)$ is the force arising from Brownian motions related to the distribution at rest ψ_0, and fu_i° is the force of friction between the solvent and the macromolecule at rest.

From eq. (25) the initial values of u_i and w_i are found to be:

$$u_{i,t=0} = u_i^{\circ}(1 - q/2\sigma\lambda_i)$$
$$w_{i,t=0} = w_i^{\circ}(1 + q/\sigma\lambda_i) \quad (26)$$

and the average squares are:

$$\langle u_i^2 \rangle_{t=0} = (na^2/6)[1 - (q/2\sigma\lambda_i)]^2$$
$$\langle w_i^2 \rangle_{t=0} = (na^2/6)[1 + (q/\sigma\lambda_i)]^2 \quad (27)$$

Equations (27) set our initial conditions, and therefore:

$$C_{1,i} = [na^2(2\sigma\lambda_i - q)^2(2\sigma\lambda_i + q) - 48D\sigma^2\lambda_i^2]/[24\sigma\lambda_i(2\sigma\lambda_i + q)]$$

$$C_{2,i} = [na^2(\sigma\lambda_i + q)^2(\sigma\lambda_i - q) - 6D\sigma^2\lambda_i^2]/[6\sigma\lambda_i(\sigma\lambda_i - q)] \quad (28)$$

Such a treatment, though following logically for the assumed model, does not describe the real behavior of a macromolecule at times near approaching zero, since actually the deformation is not instant. With the conditions of eq. (27), the nonsteady-state orientation factor results:

$$(p/s)f(t) = (p/s)f_{st} + 3/5na^2 \sum_{i=1}^{N} [C_{2,i}\exp\{-(2\sigma\lambda_i - 2q)t\}$$
$$- C_{1,i}\exp\{-(2\sigma\lambda_i + q)t\}] \quad (29)$$

or, expressed in terms of β:

$$(p/s)f(t) = (p/s)f_{\mathrm{st}} + (3/5na^2) \sum_{i=1}^{N} \big([(i^2 + 32\beta/3\pi^3)^2/6i^4$$

$$- i^2/3(i^2 - 32\beta/3\pi^3)] \exp\{-(t/\tau_i - 2qt)\} - [(2i^2$$

$$- 32\beta/3\pi^3)^2/24i^4 - 2i^2/3(2i^2 + 32\beta/3\pi^3)] \exp\{-(t/\tau_i + qt)\}]\big) \quad (30)$$

The time dependence is characterized by two constants, the smaller of which may be used as a measure of the rate of settlement the steady state. The time of settlement the steady state $t_{u,i}$ is then:

$$t_{u,i} = 1/(2\sigma\lambda_i - 2q) \quad (31)$$

For $q = 0$ we obtain the relaxation time τ_i of the system

$$\tau_i = 1/2\sigma\lambda_i \quad (32)$$

independent of the parameters characteristic for the velocity field (q). It may be noted that the value of τ_i according to eq. (32) is identical with that found by Zimm[5] for the case of flexible chains flowing in the velocity field with perpendicular velocity gradient.
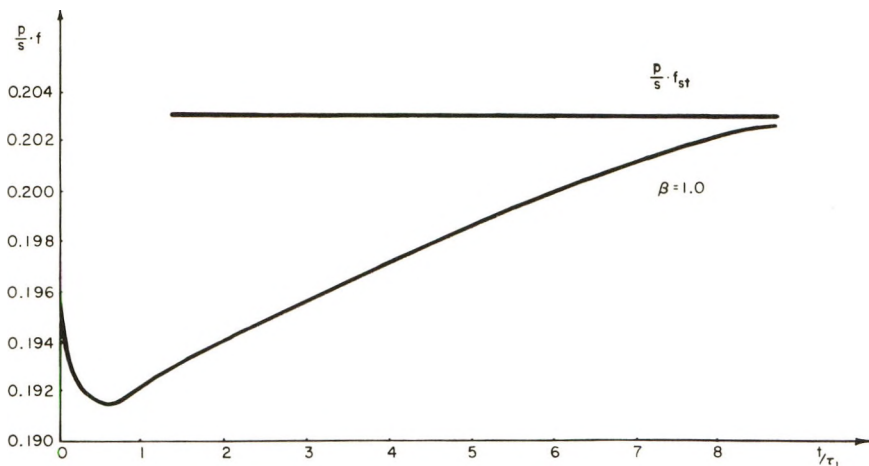

Fig. 4. Orientation factor vs. time for flexible chain macromolecules (subchain model) for a constant value of β ($\beta = 1.0$).

In Figure 4 the nonsteady-state orientation factor (fp/s) has been plotted versus (t/τ_1). The shape of this characteristic, a saturation curve with an asymptote $(fp/s)_{(t\to\infty)} = (f_{\mathrm{st}}p/s)$, is similar to that found previously for rigid ellipsoids. The minimum observed in Figure 4 near $t = 0$ apparently has no physical significance and arises from the above-mentioned model inconsistency.

References

1. Takserman-Krozer, R., and A. Ziabicki, *J. Polymer Sci.*, **A1**, 497 (1963).
2. Takserman-Krozer, R., and A. Ziabicki, *J. Polymer Sci.*, **A1**, 507 (1963).
3. Takserman-Krozer, R., *J. Polymer Sci.*, **A1**, 2487 (1963).
4. Kuhn, W., and H. Grün, *Kolloid Z.*, **101**, 248 (1942).
5. Zimm, B., *J. Chem. Phys.*, **24**, 269 (1956).
6. Ziabicki, A., *J. Appl. Polymer Sci.*, **2**, 24 (1959).
7. Takserman-Krozer, R., to be published.
8. Kirkwood, J. G., and J. Riseman, *J. Chem. Phys.*, **16**, 565 (1948).
9. Rouse, P. E., *J. Chem. Phys.*, **21**, 1272 (1953).
10. Peterlin, A., in *Physik der Hochpolymeren*, Vol. II, H. A. Stuart, Ed., Springer Verlag, Berlin-Göttingen-Heidelberg, 1953, p. 535.

Résumé

On a étudié l'orientation des chaînes flexibles et pelotées de macromolécules dans un champs de vitesse à gradient parallèle. L'étude se basait sur le modèle à parties de chaînes. On trouve que le facteur d'orientation axial dans l'état d'équilibre dépend uniquement du gradient de vitesse q, de la constante de diffusion D et des dimensions moléculaires. La viscosité interne des macromolécules n'a pas d'influence sur le facteur d'orientation à l'état d'équilibre. On a également développé les équations donnant la relation tempsfacteur d'orientation.

Zusammenfassung

Eine Analyse der Orientierung biegsamer, verknäuelter makromolekularer Kettenmoleküle im Geschwindigkeitsfeld mit parallelem Gradienten wurde durchgeführt. Die Analyse basierte auf dem Subkettenmodell. Es zeigt sich, dass der axiale Orientierungsfaktor im stationären Zustand nur vom Geschwindigkeitsgradienten q, der Diffusionskonstanten D und den Moleküldimensionen abhängt. Die innere Viskosität des Makromoleküls hat auf den Orientierungsfaktor für den stationären Zustand keinen Einfluss. Beziehungen für die Zeitabhängigkeit des Orientierungsfaktors wurden ebenfalls abgeleitet.

Behavior of Polymer Solutions in the Velocity Field with Parallel Gradient.   IV. Viscosity of Dilute Solutions Containing Flexible Chain Macromolecules

RACHELA TAKSERMAN-KROZER, *Institute of General Chemistry, Department of Technical Physics, Warszawa-Żoliborz, Poland*

Synopsis

The intrinsic viscosity of dilute solutions containing flexible chain macromolecules flowing in a velocity field with parallel gradient has been analyzed.   It has been found that the viscosity at rest is three times the value of the shearing viscosity.   The viscosity increases monotonically with velocity gradient (steady flow) and with time (at constant gradient).   On the basis of the results of this and previous papers, general features of the dynamic behavior of dilute polymer solutions flowing in the velocity field with parallel gradient have been discussed.

In the preceding paper[1] an analysis was given of the molecular orientation as observed in dilute solutions with flexible, coiled chains, subjected to uniaxial drawing.   The Gaussian subchain system was chosen as a model for description of the behavior of macromolecules.   The aim of the present paper is to analyze the rate of dissipation of energy accompanying such a flow and the dependence on velocity gradient and time of the intrinsic viscosity of solutions.

Intrinsic Viscosity of Polymer Solution in the Velocity Field with Parallel Gradient

The change of solution viscosity due to the motion of a macromolecule is proportional to the rate of dissipation of energy combined with this motion.   The rate of dissipation of energy depends on the force with which the flow is distorted due to the presence of the macromolecule.   Such distortions have been calculated by Burgers.[2]   For the considered velocity field with parallel gradient, i.e.,

$$\mathbf{V}^0(-qx/2, -qy/2, qz)$$

the formula for the intrinsic viscosity reads:

$$[\eta] = (-N_A/M\eta_0 q^2)\,\langle\mathbf{F}\cdot\mathbf{V}^0\rangle \qquad (1)$$

where N_A is Avogadro's number, M is molecular weight, η_0 is the solvent viscosity, q is the velocity gradient, and $\mathbf{F}$ is the force of interaction between the macromolecule and solvent.   According to the assumed model,

this interaction (resistance of flow) is considered to be localized in the $(N + 1)$ junction points between the individual subchains. The components of the interaction force $\mathbf{F}$ are given by eq. (2):

$$\mathbf{F}_x = -kT\nabla_x \ln \psi - (3kT/na)^2\mathbf{Ax} - f\mathbf{A\dot{x}}_d \tag{2}$$

where ψ is the distribution function of $(N + 1)$ junction points in the macromolecule, $\mathbf{A}$ the tensor is

$$\mathbf{A} = \begin{pmatrix} 1 & -1 & 0 & 0 & \ldots & 0 & 0 \\ -1 & 2 & -1 & 0 & \ldots & 0 & 0 \\ 0 & -1 & 2 & -1 & \ldots & 0 & 0 \\ \hdotsfor{7} \\ 0 & 0 & 0 & 0 & \ldots & -1 & 1 \end{pmatrix} \tag{3}$$

f_i are the coefficients of internal friction of the macromolecule, and $\mathbf{x}$, $\mathbf{y}$, $\mathbf{z}$ are vectors in the $3(N + 1)$-dimensional space corresponding to the coordinates of all junction points. The distribution function ψ satisfies the equation of diffusion:

$$\partial\psi/\partial t = (q/2)(\partial\psi/\partial\mathbf{x})^T\mathbf{x} + (q/2)(\partial\psi/\partial\mathbf{y})^T\mathbf{y} - q(\partial\psi/\partial\mathbf{z})^T\mathbf{z}$$
$$+ \sum_{u=x,y,z} \{D(\partial/\partial\mathbf{u})^T\mathbf{H}(\partial\psi/\partial\mathbf{u}) + \sigma(\partial\psi/\partial\mathbf{u})^T\mathbf{HAu} + \sigma\psi(\partial/\partial\mathbf{u})^T\mathbf{HAu}$$
$$+ \psi\rho(\partial/\partial\mathbf{u})^T\mathbf{HA\dot{u}}_d + \rho(\partial\psi/\partial\mathbf{u})^T\mathbf{HA\dot{u}}_d\} \tag{4}$$

where D is the translational diffusion constant, $\sigma = 3D/na^2$, and $\mathbf{H}$ is the tensor connected with the hydrodynamic interactions between the individual subchains.[1] The transformation into the normal coordinates,[3] $\mathbf{u}$, $\mathbf{v}$, $\mathbf{w}$ yields for intrinsic viscosity $[\eta]$ and force $\mathbf{F}$:

$$[\eta] = -(N_A/M\eta_0 q^2) \langle \mathbf{F}_u\dot{\mathbf{u}}^0 + \mathbf{F}_v\dot{\mathbf{v}}^0 + \mathbf{F}_w\dot{\mathbf{w}}^0 \rangle \tag{5}$$

$$F_{u_i} = -kT\nabla_{u_i} \ln \psi - (kT\sigma\mu_i/D)u_i - f_i\mu_i\dot{u}_{d,i} \tag{6}$$

In eqs. (4)–(6) ρ_i denotes the ratio of the internal friction coefficient to the external friction coefficient:

$$\rho_i = f_i/f = f_iD/kT$$

Putting the force components from eq. (6) into eq. (5) and taking into account the velocity components expressed in normal coordinates:

$$\dot{u}_i^0 = (-q/2)u_i$$
$$\dot{v}_i^0 = (-q/2)v_i \tag{7}$$
$$\dot{w}_i^0 = qw_i$$

we obtain $[\eta]$ in the form:

$$[\eta] = (N_AkT/M\eta_0 q) \sum_{i=1}^{N} \Big\{ \int_{-\infty}^{+\infty} [w_i(\partial\psi/\partial w_i) - (v_i/2)(\partial\psi/\partial v_i)$$
$$(-u_i/2)(\partial\psi/\partial u_i)]dV + (\sigma\mu_i/D) \int_{-\infty}^{+\infty} \psi[w_i^2 - 1/2(u_i^2 + v_i^2)]dV$$
$$+ (f_i\mu_i/kT) \int_{-\infty}^{+\infty} \psi(\dot{w}_{d,i}\cdot w_i - 1/2\dot{v}_{d,i}\cdot v_i - 1/2\dot{u}_{d,i}\cdot u_i)dV \Big\} \tag{8}$$

Since

$$\lim_{u_i, v_i, w_i \to \infty} \psi = 0$$

the first integral in eq. (8) becomes zero. Moreover, for the considered velocity field:

$$u_i = v_i$$

and

$$\dot{u}_{d,i} = \dot{v}_{d,i}$$

and we obtain finally:

$$[\eta] = (3N_A kT/na^2 M \eta_0 q) \sum_{i=1}^{N} \{ \mu_i \int_{-\infty}^{+\infty} \psi(w_i^2 - u_i^2) dV$$

$$+ (\rho_i \mu_i / \sigma) \int_{-\infty}^{+\infty} \psi(\dot{w}_{d,i} \cdot w_i - \dot{u}_{d,i} u_i) dV \} \quad (9)$$

Intrinsic Viscosity in Steady Flow

It has been shown in our previous works[4] that in steady flow with parallel velocity gradient, the deformation rate of a macromolecule is equal to zero:

$$\dot{u}_{d,i} = \dot{w}_{d,i} = 0$$

Therefore, in the equation of diffusion, eq. (4), and the formula for intrinsic viscosity, eq. (9), all the terms involving the ratio ρ_i in the steady state drop out. In the preceding paper[1] it was shown that the average values of u_i^2 and w_i^2 for steady-state conditions are:

$$\langle u_i^2 \rangle = D\nu_i/(\sigma\lambda_i + q/2) \quad (10)$$

$$\langle w_i^2 \rangle = D\nu_i/(\sigma\lambda_i - q) \quad (11)$$

Thus, the intrinsic viscosity in steady flow is:

$$[\eta]_{st} = (9N_A kTD/na^2 M \eta_0) \sum_{i=1}^{N} \lambda_i/(\sigma\lambda_i - q)(2\sigma\lambda_i + q) \quad (12)$$

The coefficients λ_i, μ_i, ν_i, connected with the diagonalization of matrices **H, A,** and **HA** have been calculated by Zimm[3] for the case of small hydrodynamic interactions:

$$\lambda_i = \pi^2 i^2/N^2$$

$$\mu_i \approx \lambda_i \quad (13)$$

$$\nu_i \approx 1$$

For $q = 0$ (solution at rest),

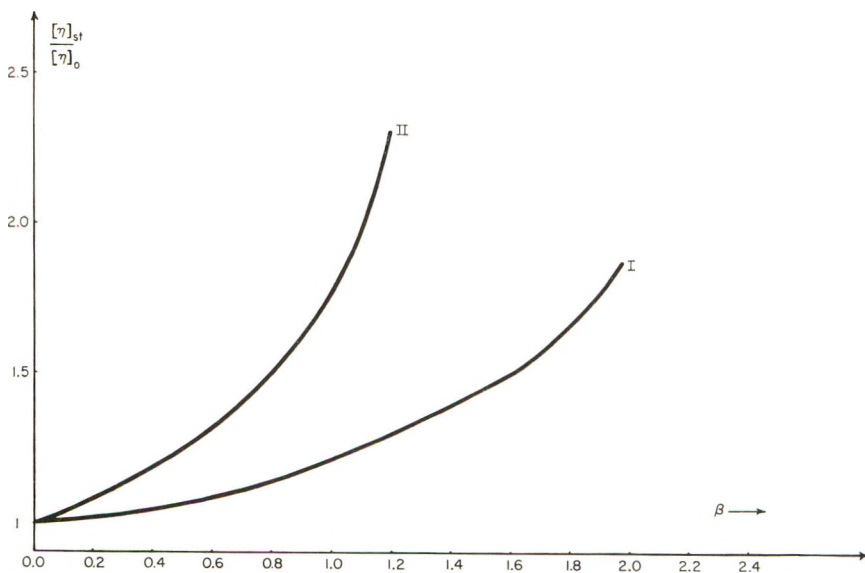$$[\eta]_0 = N_A kTna^2/2M\eta_0 D \sum_{i=1}^{N} 1/\lambda_i$$

Fig. 1. Steady-state intrinsic viscosity vs. parameter $\beta = \bar{m} \alpha [\eta]_0$ for flexible chain macromolecules: (I) subchain model; (II) elastic dumbbell (Kuhn model).

This value differs from that given by Zimm[3] for steady laminar flow (velocity field with perpendicular gradient) by a factor of 3. This result is not unexpected, since for the assumed incompressible liquid (Poisson coefficient $\mu = 0.5$) the "traction viscosity" should be three times that of the ordinary, shearing viscosity.

By introduction, as in the preceding paper,[1] of the new variable β we obtain:

$$[\eta]_{st} = (RTna^2/M\eta_0 D) \sum_{i=1}^{N} i^2/[i^2 - (32\beta/3\pi^3)][2i^2 + (32\beta/3\pi^3)] \quad (14)$$

The relation given in eq. (14) is independent of the way in which the macromolecule is divided into the subchains.[1]

The relation $[\eta]_{st}/[\eta]_0$ versus β as calculated from ten terms of the series of eq. (14) was plotted in Figure 1. In the same figure there is shown the relation $[\eta]_{st}/[\eta]_0$ versus β for the more simple Kuhn model (elastic dumbbell), equivalent to a single subchain. It is quite evident, that the steady-state intrinsic viscosity increases monotonically with velocity gradient for both molecular models.

Time-Dependent Intrinsic Viscosity

The time dependence of intrinsic viscosity will be analyzed for velocity with constant gradient $q = $ constant.

An instant switching-on of the velocity field is accompanied by corresponding changes in the degree of orientation and deformation of macro-

molecules.[1] The variation of the structure of flowing solution leads to a definite variation of intrinsic viscosity. This variation may be calculated by use of the functions $\langle u_i^2 \rangle$ (t) and $\langle w_i^2 \rangle$ (t) obtained through averaging of u_i^2 and w_i^2 values through the time-involving equation of diffusion:[1]

$$\langle u_i^2 \rangle = D\nu_i/(\sigma\lambda_i + q/2) + [na^2(2\sigma\lambda_i - q)^2(2\sigma\lambda_i + q)$$
$$- 48D\sigma^2\lambda_i^2] \exp\{-(2\sigma\lambda_i + q)t\}[24\sigma\lambda_i(2\sigma\lambda_i + q)] \quad (15)$$

$$\langle w_i^2 \rangle = D\nu_i/(\sigma\lambda_i - q) + [na^2(\sigma\lambda_i + q)^2(\sigma\lambda_i - q)$$
$$- 6D\sigma^2\lambda_i^2] \exp\{-(2\sigma\lambda_i - 2q)t\}/[6\sigma\lambda_i(\sigma\lambda_i - q)] \quad (16)$$

where t is the time measured from the switching-on of the velocity field.

We will denote the relaxation time by

$$\tau_i = 1/2\sigma\lambda_i$$

Therefore, the time-dependent viscosity amounts to:

$$([\eta] - [\eta]_{st})/[\eta]_0 = (12\sigma/na^2N^2q) \sum_{i=1}^{N} \Big([na^2(\sigma\lambda_i + q)^2(\sigma\lambda_i - q)$$
$$- 6D\sigma^2\lambda_i^2] \exp\{-(2\sigma\lambda_i - 2q)\ t\}/6\sigma\lambda_i(\sigma\lambda_i - q) \quad (17)$$
$$- [na^2(2\sigma\lambda_i - q)^2(2\sigma\lambda_i + q) - 48D\sigma^2\lambda_i^2] \exp$$
$$\{-(2\sigma\lambda_{i+q})t\}]/24\sigma\lambda_i(2\sigma\lambda_{i+q})\Big)$$

or, expressed in terms of the variable β:

$$([\eta] - [\eta]_{st})/[\eta]_0 = (9\pi/8na^2\beta) \sum_{i=1}^{N} \Big([(i^2 + 32\beta/3\pi^3)^2/6i^4$$
$$- i^2/3(i^2 - 32\beta/3\pi^3)] \exp\{-(t/\tau_i) + 2qt\} - [(2i^2 - 32\beta/3\pi^3)/24i^4$$
$$- 2i^2/3(2i^2 + 32\beta/3\pi^3)] \exp\{-(t/\tau_i) - qt\}\Big) \quad (18)$$

For a given velocity gradient q, the intrinsic viscosity changes from the value:

$$[\eta]_{t=0} = (3RT/2M\eta_0) \sum_{i=1}^{N} (1/\sigma\lambda_i)[1 + (q/4\sigma\lambda_i)] \quad (19)$$

to the steady-state viscosity η_{st}.

The initial value $[\eta]_{t=0}$, eq. (19), is not equal to that expected for solution at rest $[\eta]_0$, eq. (13). This is the consequence of the assumption that the velocity field, when switched on, brings about an instantaneous, elastic deformation of macromolecules.[1] This is also the origin of the minimum observed in the viscosity–time characteristic near $t = 0$ (Fig. 2).

The relaxation time and time for settlement of the steady flow are equal to those found in considering molecular orientation.[1]

The relation $[\eta](t)/[\eta]_0$, is plotted against (t/τ_1) in Figure 2. The shape of this characteristic is similar to the limiting curve found for the
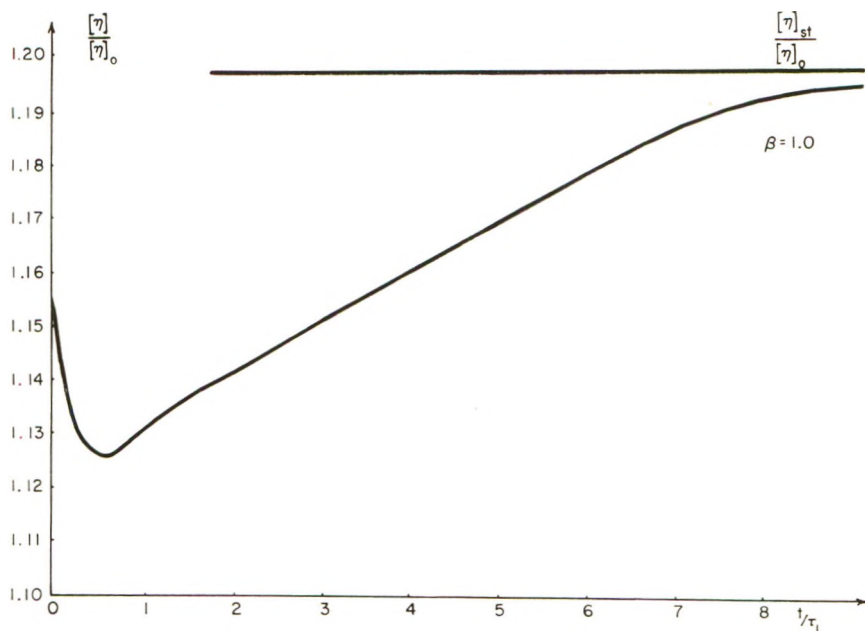
Fig. 2. Intrinsic viscosity vs. time for subchain model for a constant value of β ($\beta = 1.0$).

orientation factor. The asymptotical value $[\eta]_{t \to \infty}$ is equal to that for the steady flow $[\eta]_{st}$.

Discussion

It is evident from the presented results that the intrinsic viscosity of dilute solutions containing flexible, coiled chains subject to uniaxial drawing (velocity field with parallel gradient) is a monotonically increasing function both of velocity gradient (steady flow) and of time (velocity gradient constant).* It was shown that such an increase of viscosity occurs when the macromolecule is assumed to be a simple elastic dumbbell (Kuhn model) as well as when a more complex subchain model, allowing for hydrodynamic interactions between the individual parts of the macromolecule, and the internal viscosity was considered (Fig. 1). Similar behavior was predicted for dilute solutions of rigid ellipsoids flowing in the velocity field with parallel gradient.[5]

Quite different viscosity–velocity gradient relations were found experimentally and theoretically predicted for laminar flow (velocity gradient perpendicular to the direction of flow). For solutions of rigid ellipsoids[6] intrinsic viscosity decreases with velocity gradient; for flexible chains without internal viscosity (models of Kuhn or Zimm[3]) the steady-flow viscosity does not depend on q. The consideration of finite internal viscosity[7] or anisotropy of hydrodynamic interactions[8,9] leads to a decrease of viscosity with q.

---

* The minimum observed in Figure 2 has probably no physical significance, since it results from some inconsistencies in the assumed molecular model.[1]

The reason for the difference in behavior of polymer solutions in the two velocity fields is a kind of deformation.   In the velocity field with perpendicular velocity gradient (shearing) there are two factors affecting the rate of dissipation of energy (and viscosity) in opposite directions. An increase of spatial orientation leads to decreasing number of macromolecules binding the parallel layers of the laminar stream, and, in consequence, to a decrease of viscosity of such a solution.   The effective extension of a macromolecule due to periodic stretching and compressing stresses causes an increase of viscosity.

For ideally flexible (internal viscosity equal to zero) chain macromolecules, because of their high deformability, the above two effects compensate one another and the solution viscosity remains constant.   An increase of internal viscosity causes the orientational effect to prevail over the deformational one and the viscosity to fall with increasing velocity gradient. In the extreme case (rigid, nondeformable particles, e.g., ellipsoids) the only effect is orientation, and the intrinsic viscosity strongly decreases with q.[6]

In the velocity field with parallel gradient (uniaxial drawing) these two factors affect the solution viscosity in the same direction.   Both the orientation and deformation (extension) of the macromolecule lead to an increase of stream velocity difference near the ends of the macromolecule. With increasing orientation and/or extension, the macromolecule binds the parts of stream with greater velocity difference and distorts the flow more intensively.   The increase of viscosity predicted in our theory is due to the corresponding changes of orientation and deformation of macromolecules with velocity gradient and time.[1]

Conclusions

Results of this and the previous papers concerning the hydrodynamic behavior of flexible[1] or rigid macromolecules[5,10] make it possible to draw out some general conclusions on the dynamic behavior of dilute polymer solutions in the velocity field with parallel gradient.   In the considered velocity field, the motion of both rigid and deformable macromolecules is aperiodic, and the macromolecules tend to some positions of stable equilibrium.   The time required to settlement of such an equilibrium depends on the relaxation time of the system.

For rigid ellipsoids this is the relaxation time is

$$\tau = 1/6D$$

For flexible chains it is

$$\tau = N^2 na^2/6\pi^2 i^2 D$$

The time of settlement of the steady-state depends also on the velocity gradient-to-diffusion constant ratio α and factors connected with dimensions and character of macromolecules.

Since in steady-state flow with parallel velocity gradient the orientation and deformation rates are zero,[4] the distribution function does not depend

on the dynamic flexibility (internal viscosity) of macromolecules. The properties of solutions arising from the distribution (optical anisotropy, viscosity, etc.) are thus independent of internal viscosity.

The relation between optical anisotropy and velocity gradient is similar in both velocity fields. There is also similar change in the shape of dynamooptical characteristics when rigid particles are replaced by flexible, coiled chains.

A specific feature of the behavior of dilute polymer solutions in the velocity field with parallel gradient is an increase of viscosity with velocity gradient (steady flow) and with time (velocity gradient constant). An opposite change occurs in the case of field with perpendicular velocity gradient.

Our results are evidence for the fact, that some dynamic properties of dilute polymer solutions are determined by the kind of deformation (velocity field). Therefore, the considerations concerning the process of shearing may not be used to explain the effects of uniaxial drawing and vice versa

References

1. Takserman-Krozer, R., *J. Polymer Sci.*, **A1**, 2477 (1963).
2. Burgers, J. M., *Second Report on Viscosity and Plasticity*, New York, 1938.
3. Zimm, B., *J. Chem. Phys.*, **24**, 269 (1956).
4. Takserman-Krozer, R., to be published.
5. Takserman-Krozer, R., and A. Ziabicki, *J. Polymer Sci.*, **A1**, 507 (1963).
6. Peterlin, A., *Physik der Hochpolymeren*, H. A. Stuart, Ed., Vol. II, Springer Verlag, Berlin-Göttingen-Heidelberg, 1953, p. 535.
7. Cerf, R., *J. Polymer Sci.*, **23**, 125 (1957).
8. Čopic, M., *J. Chem. Phys.*, **23**, 440 (1956).
9. Ikeda, Y., *J. Phys. Soc. Japan*, **12**, 378 (1957).
10. Takserman-Krozer, R., and A. Ziabicki, *J. Polymer Sci.*, **A1**, 497 (1963).

Résumé

On a analysé la viscosité intrinsèque de solutions diluées contenant des chaînes de macromolécules flexibles, s'éioulant dans un champs de vitesses à gradient parallèle. On a trouvé que la viscosité au repos a une valeur de trois fois la viscosité de cisaillement. La viscosité augmente selon un premier ordre en fonction du gradient de vitesse/courant stationnaire et en fonction du temps/à gradient constant. En se basant sur les résultats de cette publication ainsi que des précédentes, on discute de l'allure du comportement dynamique de solutions diluées de polymère s'eioulant dans un champs de vitesse avec gradient parallèle.

Zusammenfassung

Eine Analyse der Viskositätszahl verdünnter Lösungen von biegsamen makromolekularen Kettenmolekülen beim Fliessen im Geschwindigkeitsfeld mit parallelem Gradienten wurde durchgeführt. Es wurde gefunden, dass die Viskosität im Ruhezustand den dreifachen Wert der Scherungsviskosität besitzt. Die Viskosität nimmt monoton mit dem Geschwindigkeitsgradienten (stationäres Fliessen) und mit der Zeit (bei konstantem Gradienten) zu. Auf Grundlage der Ergebnisse der vorliegenden und früherer Mitteilungen wurden die allgemeinen Züge des dynamischen Verhaltens verdünnter Polymerlösungen beim Fliessen im Geschwindigkeitsfeld mit parallelem Gradienten diskutiert.

BOOK REVIEWS

N. G. Gaylord, Editor

Physik der Kunststoffe, Werner Holzmüller and Kurt Altenberg, Editors.   Akademie-Verlag, Berlin, 1961.   xvi + 652 pp.

Plastics constitute a very large, interesting, and industrially important class of macromolecular materials, and the physics of plastics is to a considerable extent identical with the physics of macromolecular materials of other types.   It is concerned, for example, with the physical aspects of the polymerization and degradation of polymers, the effects of radiation on polymers and other macromolecules, macromolecular structures, and the application of physical methods to the study of their structures and properties in solution.   More than half of the volume under review deals with these subjects, in a manner which would be equally appropriate in a treatise dealing with the physics (or physical chemistry) of any other class of macromolecular materials.

On the other hand, the chapters of this book dealing with mechanical, thermal, electrical, and optical properties and with testing methods are definitely oriented toward plastics.

The quality of the treatment is uniformly high.   Fundamental relationships and useful generalizations are skillfully presented, usually in mathematical form but without detailed derivations.   The choice of subject matter is excellent and the allotment of space to the chosen subjects well balanced.   Experimental data for individual plastics are introduced only when they serve to illustrate important points in the text.

The reviewer knows of no other book where this whole field is so adequately covered. He is glad to recommend it to all interested in the field who do not consider the fact that it is written in German too great a problem.

In addition to the editors, the following scientists have contributed to this volume: K. Bethge, M. Dietze, P. Jung, S. Kästner, H. Krönert, G. Langhammer, H. G. Pohl, E. Schlosser, H. Tautz, and G. Wilke.

Maurice L. Huggins

Stanford Research Institute
Menlo Park, California

Advances in Petroleum Chemistry and Refining, Vol. IV, John J. McKetta, Jr., Editor. Interscience Publishers, Inc., New York, 1961. vi + 585 pp. $20.00.

With each additional volume, the Advances in Petroleum Chemistry and Refining series becomes broader in scope and takes on more value.   With the expanding interest of the refiner in petrochemicals and the growing importance of monomers and polymers among such chemicals, the series offers many topics that will interest the polymer chemist.   The topics in Volume IV include the techniques of purifying petroleum gases, the preparation of raw materials useful for polymer production, the application of statistical methods to process operation, the action of heterogeneous catalysts, and a description of the new types of elastomers.

Because of the sensitivity to impurities of many polymerization catalysts, especially the newer heterogeneous ones, monomers usually must be very pure.   The techniques used in gas adsorption to remove and concentrate gasoline, butanes, and propane from natural gas by means of solid-bed adsorbents can be extrapolated to monomer purifica-

tion. By similar processes moisture also can be removed from gaseous monomers. Details of these techniques are described. Furthermore, an entire chapter is devoted to molecular sieves. These synthetic zeolites are most valuable for such treatments. The discovery, properties, and manufacture of molecular sieves receive attention. The description of process equipment and process design for utilizing molecular sieves is accurate. The use of molecular sieves as catalysts or catalyst supports is ignored, despite their potential for catalyzing general chemical reactions and polymerization.

The preparation of petrochemicals such as nitriles and amines, aromatics, and mono- and diolefins via catalytic dehydrogenation leads to products suitable as raw materials for polymers. The various methods of preparing acrylonitrile and methacrylonitrile are compared. An entire chapter is devoted to the preparation and separation of aromatics which are sources of styrene and acids for polyester formation. In the chapter on catalytic dehydrogenation, data on dehydrogenation equilibria and a detailed description of the Houdry process for butadiene production are given.

The chapter on statistical methods is a useful introduction and bibliographic source for those not familiar with the application of these methods to design of an efficient pattern for experimentation. A detailed guide for setting up process models and for increasing the efficiency of process development is given. Of more importance are the details on a method of process operation that gives information on process improvement without interfering with productive capacity. To those interested in process development, whether of petroleum, petrochemical, or polymerization processes, this review can be a valuable introduction to the application of such techniques.

Because of the utility of solid petroleum catalysts for production of linear polyethylene and olefin copolymers, the chapter reviewing the preparation, properties, and utility of such catalysts for cracking and re-forming will interest polymer chemists despite the lack of specific information on their application to the preparation of high polymers. Of special interest is the discussion of dual-function re-forming catalysts. The acidity function promotes isomerization, while the electron-defect properties assist the dehydrogenation. Such electron-defect properties also play an important role in polymerization. Control of the number and type of defects, while minimizing the acidity function, will improve control of the polymerization process and of the properties of the polymer or copolymer prepared with such catalysts.

Specifically for the polymer chemist, a timely review of the new type of elastomers is included. The bibliography allows the reader to obtain more specific information for further exploration of the interesting aspects of this expanding field in which polymers and petroleum chemistry are so closely associated.

Herbert N. Friedlander

17840 Tipton Avenue
Homewood, Illinois